

RWTHedition

RWTHAACHEN
UNIVERSITY

Barbara Linke

Life Cycle and Sustainability of Abrasive Tools

 Springer

RWTHedition

Series editor

RWTH Aachen University, Aachen, Germany

More information about this series at <http://www.springer.com/series/7858>

Barbara Linke

Life Cycle and Sustainability of Abrasive Tools

 Springer

Barbara Linke
Department of Mechanical and Aerospace
Engineering
University of California Davis
Davis, CA
USA

ISSN 1865-0899

ISSN 1865-0902 (electronic)

RWTHedition

ISBN 978-3-319-28345-6

ISBN 978-3-319-28346-3 (eBook)

DOI 10.1007/978-3-319-28346-3

Library of Congress Control Number: 2015960222

© Springer International Publishing Switzerland 2016

This work is subject to copyright. All rights are reserved by the Publisher, whether the whole or part of the material is concerned, specifically the rights of translation, reprinting, reuse of illustrations, recitation, broadcasting, reproduction on microfilms or in any other physical way, and transmission or information storage and retrieval, electronic adaptation, computer software, or by similar or dissimilar methodology now known or hereafter developed.

The use of general descriptive names, registered names, trademarks, service marks, etc. in this publication does not imply, even in the absence of a specific statement, that such names are exempt from the relevant protective laws and regulations and therefore free for general use.

The publisher, the authors and the editors are safe to assume that the advice and information in this book are believed to be true and accurate at the date of publication. Neither the publisher nor the authors or the editors give a warranty, express or implied, with respect to the material contained herein or for any errors or omissions that may have been made.

Printed on acid-free paper

This Springer imprint is published by SpringerNature

The registered company is Springer International Publishing AG Switzerland

Grinding tools are the most up-to-date and at the same time the least known tools for processing. [MOSE80]

Acknowledgments

This thesis was written mainly during my time as postdoc researcher at the Werkzeugmaschinenlabor (WZL) at the RWTH Aachen University, and at the Laboratory for Manufacturing and Sustainability (LMAS) at the University of California Berkeley. The research on the life cycle engineering of abrasive tools was funded by the Deutsche Forschungsgemeinschaft (DFG, German Research Foundation) through the project LI1939/3-1. Thank you to the DFG for the support and the opportunity to study abroad.

I thank Prof. Klocke from the bottom of my heart for mentoring me during my time as research associate at his institute and beyond. Grinding technology, detailed research, and teaching are our shared passion. Prof. Klocke trusted all the while that pursuing an academic career would be the right way for me to go. Thank you for being such a great mentor to me and for introducing me to the international research community!

Professor Dornfeld earns my deepest gratitude for hosting me in his laboratory and providing me with excellent opportunities for networking. I learned so much from his visionary yet applied research on sustainable manufacturing.

Thank you to Prof. Karpuschewski for being a role model and inspiring me to pursue an international research fellowship. I am also grateful for his advice on this thesis.

Dr. Busch was one of my closest discussion partners and a very great help. I thank him wholeheartedly. Many thanks also to Dr. Sigwart and Mr. Noichl from Tyrolit; Dr. Hall and Dr. Arcona from Saint-Gobain Abrasives Norton; Prof. Vollstädt and Dr. List from Vollstaedt-Diamant; Dr. Bot-Schulz and Dr. Pähler from Saint-Gobain Abrasives; Dr. John Barry from E6; Dr. Magg from Tesch; Mr. Danner from Elbe Schleifmittel; and Dr. Paul and Dr. Michels from Wendt. I am thankful for all the insights into how companies secure the sustainability of their abrasive tooling systems. Thank you to Prof. Aurich for the inspiring cooperation on the CIRP keynote paper on sustainability in abrasive processes.

I am thankful for all the technical help from my former faithful student assistants Seamus Laprell and Janis Thiermann, and guest researchers Sabine Mannebach, Zhiwei Zhang, and Gero Corman. Sabine Ms. Mannebach conducted the case study on CBN and corundum tools thoroughly.

Many thanks to Prof. Garret O'Donnell, Trinity College Dublin, Dr. Markus Weiss, Tyrolit, Benjamin Doebbler, Werkzeugmaschinenlabor (WZL) at the RWTH Aachen University, and Maria Celeste Castillo, University of California Davis for reviewing the thesis thoroughly.

I am thankful for the cordial atmosphere at the Aachener Schleifer Group and at the UC Berkeley LMAS. I would like to thank Dr. Bernd Meyer, Dr. Michael Duscha, Guido Kochs-Theisen, Peter Ritzerfeld, Dr. Dirk Friedrich, Dominik Schluetter, Dr. Holger Groening, Dr. Moneer Helu, Dr. Margot Hutchins, and Dr. Daeyoung Kong, just to name a few of all the great laboratory members at both institutions.

Last, but not least I am grateful for the support and encouragement by my husband Andor and my daughters Kira and Kim, by my parents, my sister Annika, my extended family, and best friends.

Contents

1	Introduction	1
2	Abrasives	7
2.1	Corundum	8
2.1.1	Chemistry, Types and Characteristics of Corundum	8
2.1.2	Manufacture of Corundum by Electrofusing	12
2.1.3	Manufacture of Corundum by Sintering	15
2.1.4	Manufacture of Corundum by Sol-Gel Process	16
2.1.5	Performance of Corundum	17
2.2	Silicon Carbide	19
2.2.1	Chemistry, Types and Characteristics of Silicon Carbide	19
2.2.2	Manufacture of Silicon Carbide	22
2.2.3	Performance of Silicon Carbide	23
2.3	Diamond	24
2.3.1	Chemistry, Types of Diamond and Performance	24
2.3.2	Natural Diamond Genesis	28
2.3.3	Artificial Synthesis of Diamonds	29
2.3.4	Performance of Diamonds	31
2.4	Cubic Boron Nitride	32
2.4.1	Chemistry, Types and Characteristics of CBN	32
2.4.2	Synthesis of CBN	34
2.4.3	Performance of CBN	36
2.5	Other Types of Abrasives	36
2.5.1	Natural Abrasives	36
2.5.2	Boron Carbide (B ₄ C)	37
2.6	Grit Post-Processing	37
2.6.1	Crushing	37
2.6.2	Heat Treatment	37
2.6.3	Chemical Processes	37
2.6.4	Electrostatic Processes	38

2.7	Grit Coatings	38
2.7.1	Non-metallic Coatings	38
2.7.2	Metallic Coatings	38
2.7.3	Purpose of Coatings	39
2.8	Grit Characteristics	42
2.8.1	Grit Size	42
2.8.2	Shape, Morphology	43
2.8.3	Hardness and Temperature Hardness	44
2.8.4	Toughness, Breaking Behavior.	44
2.8.5	Thermal, Electric and Magnetic Properties.	45
2.8.6	Distribution of Characteristics Within Batch	46
2.9	Methods for Grit Selection and Analysis.	46
2.9.1	Grit Size Selection	46
2.9.2	Grit Shape Selection and Analysis	50
2.9.3	Toughness and Breaking Behavior Analysis	52
2.9.4	Analysis of Residual Stress via Polarisation Microscopy	53
2.9.5	Magnetic Susceptibility Selection and Analysis	53
2.9.6	Other Analyses	54
2.9.7	Evaluation of Grit Analysis and Sorting Techniques	54
2.10	Sustainability Dimensions to Abrasive Grits	56
2.10.1	Technological Dimension	56
2.10.2	Economic Dimension	57
2.10.3	Environmental Dimension	58
2.10.4	Social Dimension	60
2.10.5	Sustainability Model for Abrasive Grits	60
3	Bonding Systems	63
3.1	Resin Bonds	65
3.1.1	Chemistry and Types of Resin Bonds	65
3.1.2	Manufacturing of Resin Bonds	68
3.1.3	Fillers in Resin Bonds	71
3.1.4	Performance of Resin Bonds	72
3.2	Vitrified Bonds	73
3.2.1	Chemistry and Types of Vitrified Bonds	73
3.2.2	Manufacturing of Vitrified Bonds	74
3.2.3	Performance/Grit Retention	79
3.3	Metallic Multi-layer Bonds	80
3.3.1	Chemistry and Types of Metallic Bonds for Multi-layer Abrasive Tools	80
3.3.2	Manufacturing of Metallic Bonds by Infiltration.	81
3.3.3	Manufacturing of Metallic Bonds by Sintering.	82
3.3.4	Performance of Metallic Multi-layered Bonds	83

- 3.4 Metallic Single-layer Bonds. 83
 - 3.4.1 Chemistry and Types of Metallic Bonds 83
 - 3.4.2 Manufacturing of Electroplated Bonds 84
 - 3.4.3 Manufacturing of Brazed Bonds. 87
 - 3.4.4 Performance of Metallic Single-layered Bonds. 88
- 3.5 Other Bonding Types and Hybrid Bonds 89
 - 3.5.1 Rubber 89
 - 3.5.2 Shellac Bonds 89
 - 3.5.3 Other Bonds 90
- 3.6 Sustainability Dimensions to the Bonding System 90
 - 3.6.1 Technological Dimension 90
 - 3.6.2 Economic Dimension 92
 - 3.6.3 Environmental Dimension 92
 - 3.6.4 Social Dimension 94
 - 3.6.5 Sustainability Model for Bonding Systems 95
- 4 Abrasive Tool Types 97**
 - 4.1 Grinding Wheels 97
 - 4.1.1 Shapes 98
 - 4.1.2 Special Grinding Wheel Types. 100
 - 4.2 Coated Abrasive Tools 103
 - 4.2.1 Manufacturing 104
 - 4.2.2 Abrasive Grits 106
 - 4.3 Honing Tools 107
 - 4.4 Polishing Tools 107
 - 4.4.1 Abrasives for Polishing. 108
 - 4.4.2 Binding Materials for Pastes 109
 - 4.4.3 Counterparts 110
 - 4.5 Lapping 110
 - 4.5.1 Abrasives for Lapping 111
 - 4.6 Tools for Abrasive Sawing 111
 - 4.6.1 Wires with Bonded Grits. 112
 - 4.6.2 Wires with Loose Abrasives 112
 - 4.6.3 Inner Diameter Saw 112
 - 4.7 Other Methods with Free Abrasives 112
 - 4.7.1 Crushing. 112
 - 4.7.2 Free Abrasive Machining 113
 - 4.7.3 Abrasive Blasting. 113
 - 4.8 Tool End of Life 113
 - 4.8.1 Shelf Life and Transport. 114
 - 4.8.2 Disposal 114
 - 4.8.3 Recycling of Abrasive Tools 115
 - 4.8.4 Conclusion and Sustainability Model for Tool End
of Life 116

5 Grinding Wheel Macro-design—Shape, Body, and Qualification . . . 119

- 5.1 Body Concepts 119
 - 5.1.1 Body Shapes—Stresses and Special Design
for High-Speed Applications 120
 - 5.1.2 Body Materials 123
 - 5.1.3 Layout and Reinforcements of Cut-off Wheels 126
- 5.2 Clamping and Balancing 127
 - 5.2.1 Flanges 127
 - 5.2.2 Balancing Methods 128
- 5.3 Tool Qualification 130
 - 5.3.1 Tool Hardness and Tool Elasticity 131
 - 5.3.2 Tool Breakage 134
- 5.4 Sustainability Dimensions to the Grinding Wheel Macro
Design 135
 - 5.4.1 Technological Dimension 135
 - 5.4.2 Economic Dimension 135
 - 5.4.3 Environmental Dimension 135
 - 5.4.4 Social Dimension 136
 - 5.4.5 Sustainability Model for Grinding Wheel
Macro-design 136

6 Grinding Wheel Micro-design—Abrasive Layer and Wear 139

- 6.1 Abrasive Layer Composition 140
 - 6.1.1 Volumetric Composition 140
 - 6.1.2 Porosity 142
 - 6.1.3 Secondary Grits 144
- 6.2 Cutting Edge Density 144
 - 6.2.1 Definitions 144
 - 6.2.2 Measuring, Replicating and Modeling of the Tool
Topography 150
- 6.3 Tool Wear Effects 152
 - 6.3.1 Macro Effect—Tool Profile Loss 152
 - 6.3.2 Micro Effect—Sharpness Loss 154
 - 6.3.3 G-Ratio 155
- 6.4 Tool Wear Mechanisms 158
 - 6.4.1 Wear Types 158
 - 6.4.2 Grit Surface Wear 160
 - 6.4.3 Grit Splintering or Breakage 162
 - 6.4.4 Grit-Bond-Interface Wear 163
 - 6.4.5 Bond Wear 163
 - 6.4.6 Clogging of the Abrasive Layer 163
- 6.5 Tool Conditioning 165
 - 6.5.1 Overview on Conditioning Principles 165
 - 6.5.2 Dressing with Diamond Tools 165

6.5.3	Dressing Parameters	167
6.5.4	Dressing of Superabrasive Tools	170
6.6	Sustainability Dimensions to Grinding Wheel Micro-Design and Wear	170
6.6.1	Technological Dimension	170
6.6.2	Economic Dimension	171
6.6.3	Environmental Dimension	171
6.6.4	Social Dimension	172
6.6.5	Sustainability Model for Tool Use Phase.	172
7	Sustainability of Grinding Tools	173
7.1	Life Cycle Engineering	174
7.1.1	Environmental Aspects—Life Cycle Assessment (LCA)	174
7.1.2	Social Life Cycle Assessment (SLCA)	176
7.1.3	Life Cycle Costing (LCC).	177
7.1.4	Sustainability Indicators	179
7.2	Life Cycle Inventory of Grinding Processes.	179
7.2.1	Evaluating Sustainability of Unit Processes	179
7.2.2	Input-Output Streams of Grinding	180
7.3	Axiomatic Grinding Process Model	184
7.3.1	Methodology	185
7.3.2	Grinding Process Model	187
7.3.3	Matrixes from Axiomatic Model	205
7.3.4	Case Study on Grit Size Choice.	212
8	Sustainability Case Studies	215
8.1	Case Study on Conventional Abrasives Versus Superabrasives for Vitriified Bonded Tools	215
8.1.1	Scope and Method	215
8.1.2	Energy of Raw Materials	216
8.1.3	Manufacturing Energy of a Vitriified Bond	217
8.1.4	Manufacturing Energy of the Steel Body for Superabrasive Wheels.	220
8.1.5	Embodied Energy in Grinding Tools	221
8.2	Case Study on Comparing Hard Turning and Grinding	224
8.3	Leveraging Abrasive Machining.	224
8.3.1	Case Study on Speed-Stroke Grinding with High Grinding Wheel Speeds	225
8.3.2	Leveraging Example for Gear Grinding.	225
9	Future Prospectives	227
9.1	Market Trends for Abrasive Tools and Grit Material	227
9.2	Innovative and More Sustainable Tools.	230
9.2.1	Future Requirements.	230

- 9.2.2 Developments in Tool Design 230
- 9.2.3 Options for Tool Manufacturers 234
- 9.3 Conclusion on Abrasive Tool Sustainability 236
- Literature 237**

Symbols and Abbreviations

This list of symbols and abbreviations is not exhaustive. The symbols in equations are described in the text.

Uppercase Letters

ACGIH	American Conference of Governmental Industrial Hygienists (–)
Al ₂ O ₃	Corundum/alumina/aluminum oxide (–)
ANSI	American National Standard Institute (–)
AVV	Verordnung ueber das Europaeische Abfallverzeichnis (–)
BFA	Brown fused alumina (–)
CBN	Cubic boron nitride (–)
CO ₂ PE!	Cooperative effort on process emissions in manufacturing (–)
CVD	Chemical vapor deposition (–)
DC	Direct current (–)
DIN	Deutsche Industrie Norm (German Institute for Standardization) (–)
EWC	European Waste Catalog (–)
FEPA	Federation of European Producers of Abrasives (–)
G	G-ratio, grinding ratio (mm ³ /mm ³)
HIP	Hot isostatic pressing (–)
HK	Knoop hardness (HK)
HMIS	Hazardous Materials Identification System (–)
HPHT	High pressure high temperature (–)
IARC	International Agency for Research on Cancer (–)
LCA	Life cycle assessment (–)
LCC	Life cycle costing (–)

LCI	Life cycle inventory (-)
MCD	Mono-crystalline diamonds (-)
MMBtu	Million British thermal unit (MMBtu)
NO _x	Nitrogen oxides (-)
OSHA	Occupational Safety and Health Administration (-)
PCBN	Polycrystalline CBN (-)
PCD	Polycrystalline diamond (-)
PEL	Permissible exposure limits (-)
PM	Particulate matter (-)
PVD	Physical vapor deposition (-)
Ra	Average surface roughness (μm)
REACH	Registration, Evaluation, Authorization and restriction of CHEMicals (-)
Rq	Root-mean-square surface roughness (μm)
SI	International System of Units (-)
SiC	Silicon carbide (-)
SLCA	Social life cycle assessment (-)
TLV	Threshold limit values (-)
UPLCI	Unit process life cycle inventory (-)
VOC	Volatile organic compounds (-)

Lowercase Letters

ct	Carat = 0.2 g (ct)
m	Mass (kg)

Greek Letters

μ	Friction coefficient (-)
λ	Thermal conductivity (W/m °C)
ρ	Density (g/cm ³)
ω	(1/s)
η	Viscosity of the settling medium [g/(s cm)]

Conversions

The units are kept as in the original reference. Here are the conversions to SI units and SI derived units.

Dimensions	1 inch = 1 in. = 25.4 mm
Energy	1 kWh = 3,600,000 J
	1 MMBtu = 1,055,870,000 J
	1 kcal = 4184 J
Force	1 kp = 9.80665 N
	1 lb = 4.4482216152605 N
Knoop hardness	HK = 1 kg _f /mm ² = 9,806,650 Pa
Power	1 W = 1 N m/s = 1 J/s
	1 MVA = 1 MW = 1 MJ/s
Pressure	1 atm = 101,325 Pa
	1 bar = 100,000 Pa
	1 psf = 47.88020833333 Pa
Temperature	(°F - 32) * 5/9 = °C
	K - 273 = °C

Chapter 1

Introduction

Das 21. Jahrhundert fñhrt die Menschheit an ihre natuerlichen Grenzen. [...] Welche Moeglichkeiten haben die Unternehmen des produzierenden Gewerbes, durch effizientere Technologien sowohl Kosten als auch Ressourceneinsatz und Emissionen zu reduzieren? [...] An die Stelle von «maximaler Gewinn aus minimalem Kapital» muss «maximaler Gewinn aus minimalen Ressourcen treten». [FHG08]

Translation: “The 21th century leads humanity to its natural limits. [...] What options do manufacturing companies have to reduce costs, resource use and emissions through more efficient technologies? [...] «Maximum profit from minimum capital» needs to be replaced by «maximum profit from minimum resources».” [FHG08].

Looming shortages of resources and energy induce a growing importance of sustainability in manufacturing. In the long run, the manufacturing paradigm has to shift from non-sustainable mass production to a sustainable environmentally conscious one [UMED12]. Furthermore, producers will have higher responsibility for the product life cycle in the future. Manufacturers may have to manage various legislative restrictions on product ingredients [e.g. the European REACH initiative (Registration, Evaluation, Authorization and restriction of Chemicals)] [UMED12]. In addition, customers increasingly demand greener products, which leads to more competition in the sustainability and manufacturing of the products. The World Commission on Environment and Development, also known as the Brundtland Commission, coined the definition of sustainable development as meeting the needs of the present without compromising the ability of future generations to meet their own needs [UN87].

Abrasive processes, also called machining with geometrically undefined edges, represent a key technology with high performance, process stability, and quality tolerances. Abrasive processes are applied in nearly every production, even if this includes the manufacturing of the mold. Abrasive processes are also core technologies in developing new energy systems as well as in improving efficiency of existing products. Nevertheless, the consideration of sustainability aspects in abrasive machining is just arising, but has a high recognition by the industry [OLIV09].

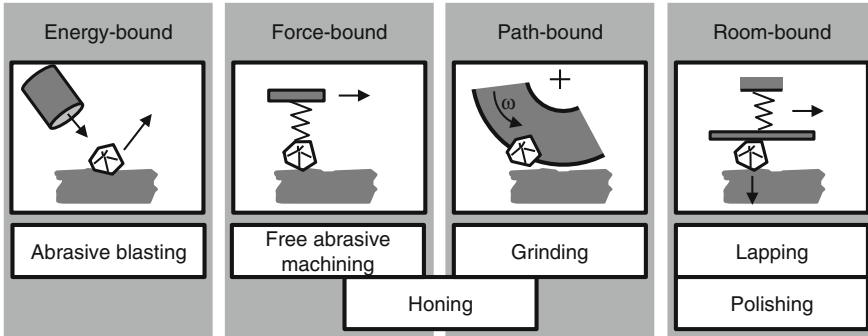


Fig. 1.1 Grit engagement principles after [KLOC09]

Abrasive processes use grits to remove material. The engagement physics of grit and workpiece can be energy-bound, force-bound, path-bound, or room-bound grits (Fig. 1.1). Except for the energy-bound principle, all processes use abrasive tools consisting of abrasive grits in a bonding or a slurry paste. The abrasives should be harder than the workpiece material to form chips. Splintering of dull grits leads to self-sharpening and can be forced by proper abrasive grit design. In the case of path-bound grits, bonding has to hold the grits until they are too blunt, then relieve them and expose new sharp grits. The pores in a bonded or coated tool are important to supply cooling lubricant and remove chips from the contact zone. The abrasive layer might be attached to a body or backing material. All components and their composition affect the sustainability of the abrasive tools and abrasive processes. This work focusses on grinding tools.

The advantages and problems of abrasive tools arise from their often undefined cutting edge shapes, edge orientation, and number. Due to the high number of active cutting edges in the grinding tool, grinding is advantageous as it is not ruined by failure of a single cutting edge, like cutting [WERN73, p. 67]. However, the choice of an appropriate abrasive type is difficult because the interaction between abrasive grit, workpiece material, and the machining result is fairly unknown [LUDE94, p. 1].

In 1968, Malkin stated that “the main difficulty encountered by the grinding engineer is the choice of the grinding wheel best-suited for a given work” [MALK68]. This statement is still true today. The design of grinding tools holds the dilemma of providing either a cheap, mass-produced product versus an expensive, customized product. The range of machinable workpiece materials for a certain wheel has to be balanced against the tool performance. In addition, the possible workpiece geometries depend on the flexibility of the tool, e.g. the dressability of conventional wheels against pre-profiled superabrasive tools. As consequence, a mass produced tool can be used for several applications, but will never be as effective as a tool designed for one special purpose.

Several milestones in the development of abrasive grit materials and bonding systems, and the refinement of the tool components and manufacturing processes

have led to large improvements in process performance (Fig. 1.2). The life of the grinding tool is intertwined with the life of the product produced by grinding (Fig. 1.3). Similar to the manufactured product, an abrasive tool life has four phases: raw material extraction, manufacturing, use, and end of life. The use phase coincides with the machining process of another product. This thesis will discuss all life cycle phases of a grinding tool.

Abrasive tool compositions and manufacturing techniques are widely company proprietary and development is still in progress. As the design process of a grinding tool relies on the expertise of the tool manufacturer, it is often not a transparent procedure to the customer. Therefore, it is hard to comprehend considerations on sustainability. This thesis summarizes publicly available knowledge and unveils how it relates to sustainability.

Traditionally, sustainability has been viewed in three categories or pillars: economy, environment, and society. However, this is not sufficient because it

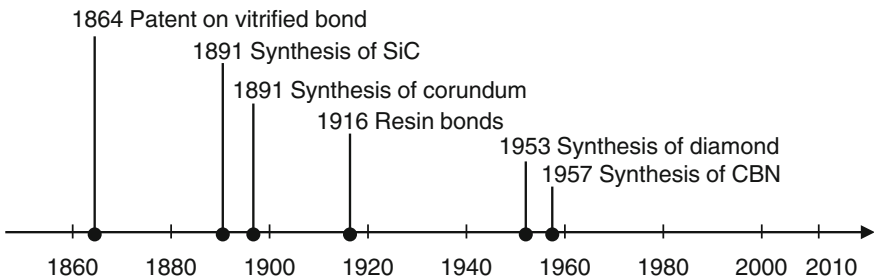


Fig. 1.2 Some milestones in the development of grinding tools

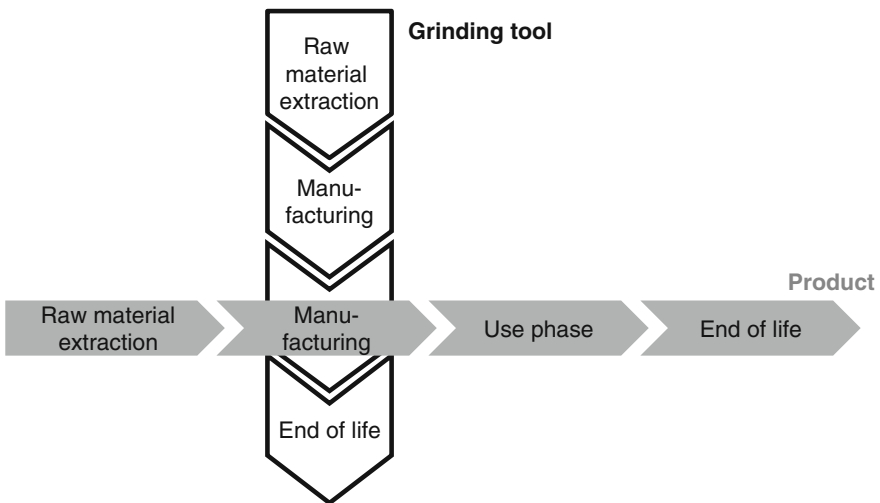


Fig. 1.3 Life cycle perspective of grinding tools and ground products

disregards many decisions heavily based on technological considerations. For example, choice of grit size does not translate easily into one of the traditional three pillars of sustainability but depends on part surface roughness which is a technological factor. Therefore, in this work sustainability for abrasive tools is viewed under the following four aspects:

- Economics in terms of productivity and costs
- Environment in terms of energy use, materials use, waste, recyclability, emissions, etc.
- Society in terms of worker safety, health, and education
- Technology in terms of feasibility, workpiece quality, best practice, performance

This thesis revises the state of the art of research and common practice in the field of abrasive tooling systems for fine machining applications. Despite the diverse technical terms used in the literature, this thesis uses uniform terms.

Life cycle considerations and sustainability aspects in grinding are trend-setting perspectives, which are discussed in this thesis for the first time comprehensively throughout. All Chaps. 2–5 end with an interim model on technological, economic, environmental, and social sustainability.

Chapter 2 “Abrasives” analyzes the grit materials including their chemical composition, chemical and physical properties, material processing, and abrasive process performance. The knowledge of grit materials is crucial to understand the life cycle of abrasive tools holistically—where do the materials come from, how are they processed and what performance do they imply for the abrasive tool.

In a similar way, the bonding system defines tool performance and the tool manufacturing route. Therefore, Chap. 3 “Bonding Systems” explains different bond types, their ingredients, processing, and resulting tool performance.

Different abrasive applications need distinct tool designs as described in Chap. 4 “Abrasive Tool Types”. There is hardly ever only one perfect tool type, but tools can be used interchangeably affecting process performance and product quality. Moreover, the tool type affects the tool end of life significantly in terms of recyclability, re-use, or disposal.

The implications of the tool design and tool fixture specific to grinding tools are discussed in Chap. 5 “Grinding Wheel Macro-design—Shape, Body, and Qualification”. The shape and material of the tool affect its manufacture, raw materials, its use and end of life. In addition, the tool microstructure as explained in Chap. 6 “Grinding Wheel Micro-design—Abrasive Layer and Wear” changes tool performance and tool manufacture. The structure defines the tool topography that interacts with the workpiece surface and the wear phenomena, and affects sustainability since the grinding tool needs to be consumed during its use phase. Lower wear might yet lead to lower energy efficiency of the grinding process. Tool conditioning is an important method to adjust and regenerate tool profile and topography.

Having introduced the main factors of tool design, this knowledge needs to be tied back to sustainable grinding technology. Therefore, Chap. 7 “Sustainability of Grinding” first explains methods of Life Cycle Engineering (Life cycle

assessment (LCA), Life cycle costing (LCC), Social life cycle assessment (SLCA), and Sustainability Indicators). Then a generic life cycle inventory of grinding processes is gathered to show the state of the art in grinding process sustainability. In addition, a new approach to understand and dissect grinding processes is explained and applied. This so called axiomatic grinding process model visualizes how process setup and tool design are connected to traditional quality indicators and newer sustainability indicators.

Chapter 8 “Sustainability Case Studies” then uses the concepts from the former chapter to discuss several examples: Vitrified bonded grinding wheels with corundum and CBN are compared with regard to their manufacturing strategies and energies; Hardturning and grinding are more or less favorable in terms of sustainability depending on the criteria. The example of leveraging gear grinding focuses on how the manufacturing process can improve the product performance towards higher overall energy efficiency, even if the gear grinding procedure consumes more energy. In a similar way, speed stroke grinding can improve product quality through a more sophisticated manufacturing process.

The final Chap. 9 “Future Prospectives” explains the actual market situation for grit material and introduces new abrasive tool concepts with potentially higher sustainability. All interim models from Chaps. 2 to 5 are combined to a generic model allowing for final conclusions on abrasive tool life cycle and sustainability.

The aims of this work are to

- Educate students and tool users on abrasive tools,
- Help tool manufacturers to emphasize sustainability in tool manufacturing,
- Help tool users to evaluate sustainability in tool use.

Chapter 2

Abrasives

Look at this small grit, this tiny grain, so small one must rub hundreds of them between finger and thumb to feel their sharpness. Insignificant little grits and easily slighted in our sophisticated technological world, but without this small fragment of abrasive, transformed, when viewed under a microscope, into jagged heroic blocks - without these small grits ours might still largely be an agricultural society and the conquest of space merely a dream. With these grits are grinding wheels made. [LEWI76, p. 3]

The main task of the abrasive grits is to conduct material removal that arises from chip formation, surface shattering, or pressure softening. In most applications, the grits have to be harder than the machined workpiece material. Moreover, abrasive grits need a high toughness and thermal and chemical resistance for a sustainable tool life. In addition, appropriate fracture behavior of the grits enables tool self-sharpening and results in efficient machining processes. A wide variety of abrasive materials is used in abrasive processes (Fig. 2.1).

Tool performance is defined by the grit material. It affects economic, technological, environmental and social sustainability of the tool and the abrasive process. Since grit materials compose a large portion of the tool volume, the raw material processing defines embodied energy, resource intensity, labor intensity, etc. which are indicators of tool sustainability.

Though there are still some applications with natural materials, most abrasive grits are made of synthesized materials [KLOC09]. Over the years, a large variety of trade names for abrasive grits have arised, sometimes leading to confusion [MARI04, p. 371].

The following review focuses on the prominent abrasive grit types used for grinding and honing tools. These abrasive grits can be subdivided into so called conventional abrasives [corundum (Al_2O_3) and silicon carbide (SiC)] and superabrasives (cubical boron nitride (CBN) and diamond). Superabrasives stand out by their higher hardness and wear resistance.

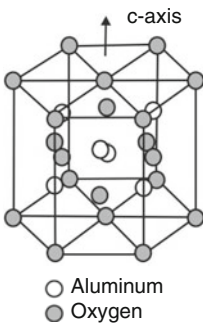
Abrasive blasting	Grinding Honing	Lapping	Polishing
silicon carbide (SiC) corundum (Al ₂ O ₃)			
diamond			
boron carbide (B ₄ C) quartz (SiO ₂) garnet	cubic boron nitride (CBN)	boron carbide (B ₄ C) chromium oxide	pumice beryllium oxide (BeO) chrome oxide (Cr ₂ O ₃) iron oxide (Fe ₂ O ₃) garnet (X ₃ Y ₂ (SiO ₄) ₃) emery quartz (SiO ₂)
		Soft abrasives: quartz (SiO ₂) garnet emery	Soft abrasives: kaolin chalk barite (barium sulfate) talc tripoli Vienna lime

Fig. 2.1 Common grit types in abrasive machining

2.1 Corundum

2.1.1 Chemistry, Types and Characteristics of Corundum

Corundum is crystalline aluminum oxide, Al₂O₃, and also known as alumina. Al₂O₃ is also the active element in the natural abrasive material emery [LEWI76, p. 9] and in the gemstones sapphire and ruby. Aluminum oxide occurs in at least five modifications, α-Al₂O₃, β-Al₂O₃, γ-Al₂O₃, δ-Al₂O₃, and ε-Al₂O₃. The technologically most important modification is the rhombohedral crystalline α-Al₂O₃, being the basis for corundum (Fig. 2.2). The proportion of covalent atom bonds to



Density	3.97 g/cm ³	[MÜLL01]*
Hardness Knoop	21 - 24 GPa	[MÜLL01]*
Fracture toughness	2.2 MPa m ^{1/2} (3.8 MPa m ^{1/2} for sol-gel-corundum)	[KLOC02]
Melting temperature	2,027 °C	[SALM07]
Thermal stability	Up to 1750 °C	[MÜLL01]
Thermal conductivity	35 W/ m K	[ROWE09]

*after 3M, GE, Norton, Treibacher

Fig. 2.2 Basic properties of α-corundum, picture source [BOTS05]

ionic atom bonds is 40–60 % [MÜLL01, p. 25]. The cubic form γ -Al₂O₃ (clay, German “Tonerde”) is the basis for vitrified bonds and other ceramic products.

Industry applies several corundum types with different chemical composition and manufacturing routes:

- Molten or fused corundum, such as
 - Brown corundum (also known as brown fused alumina, BFA, semi-friable corundum, regular corundum),
 - White corundum (also known as pure white alumina),
 - Pink corundum,
 - Ruby corundum (also known as red alumina),
 - Zirconium corundum (also known as alumina zirconia),
 - Mono crystalline corundum (also known as single crystal alumina),
 - Micro crystalline corundum,
 - Hollow sphere corundum (also known as bubble alumina)
- Sintered corundum
- Sol-Gel corundum

Table 2.1 gives the chemical composition of several types of molten corundum.

2.1.1.1 Shape, Morphology

Corundum appears as polycrystalline material and is broken down to the desired grit sizes. The size of the single crystals within the larger abrasive grits depends on the manufacturing route. Pink corundum appears as blocky grits with sharp edges and an average crystal size of 750 μm [WASH12b]. Zirconium corundum can have much smaller crystal sizes down to 10–12 μm [WASH12b]. Sol-gel corundum is known for the very fine crystals below 500 nm, enabling a very distinctive fracture behavior [ENGE02, p. 7].

2.1.1.2 Toughness, Breaking Behavior, Friability, Hardness

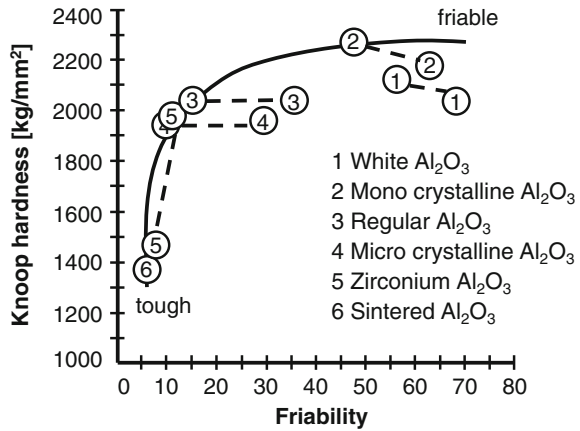
The different corundum types have a broad bandwidth of hardness and friability from 1300 to 2300 HK and a friability index between 5 and 75 (Fig. 2.3). Contents of Cr₂O₃ and TiO₂ increase the toughness, whereas Na₂O contents are disadvantageous, because Na₂O induces the softer β -11Al₂O₃·Na₂O [TYRO03b].

Corundum is considered to be the softest of the four main abrasives for grinding tools with a Knoop hardness of 2100–2400 kg_f/mm² for the purer molten corundum types, down to around 1600 kg_f/mm² or less for zirconium corundum (Fig. 2.3) [KLOC09, p. 27]. The compressive strength of Al₂O₃ is around 569 N/mm² [MERB03, p. 6].

Table 2.1 Chemical composition of typical molten corundum for grinding applications [TYRO03b, WASH12b]

	Al ₂ O ₃ (%)	Na ₂ O (%)	Cr ₂ O ₃ (%)	TiO ₂ (%)	SiO ₂ (%)	Fe ₂ O ₃ (%)	Others (%)	Hardness (HK)
Brown corundum	96.1			2.70	0.67	0.11		2090
White corundum	99.8	0.2						2000–2160
Pink corundum	99.5	0.2	0.25–0.3		0.05	0.03		2160
Ruby corundum	97.4	0.2–0.26	2.1–2		0.01	0.08		2150
Mono-crystalline corundum	99.3	<0.09		0.3–0.6				
Zirconium corundum (40 %)	59–60	≤0.03		0.15–0.3	≤0.35	≤0.15	39–40 % ZrO ₂ 0.6–0.8 % Y ₂ O ₃	1600–1700
Zirconium corundum (25 %)	75	0.08		0.1	0.3	0.3	23 % ZrO ₂	1450

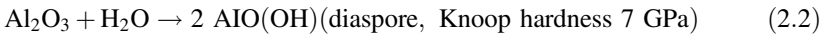
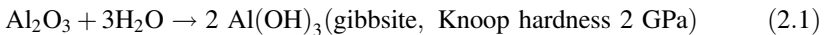
Fig. 2.3 Hardness and friability for several corundum abrasives, grit size 12 mesh [LEWI76, p. 12, WINE12]



Polycrystalline corundum experiences increasing toughness and hardness when the crystal grain sizes get smaller [KLOC03, KREL95]. Presumably, the yield stresses from dislocations lead to micro cracks at the grain boundaries, which increase the toughness [EVAS90].

2.1.1.3 Temperature Stability, Chemical Reactions

Corundum (α -Al₂O₃) and water (H₂O) can result in gibbsite (Al(OH)₃, Eq. 2.1) or diaspore (AlO(OH), Eq. 2.2) [LUDE94, p. 77]. The reaction to the relatively soft gibbsite in Eq. 2.1 is likely at temperatures from 0 to 300 °C and pressures up to 1000 bar [LUDE94, p. 79].

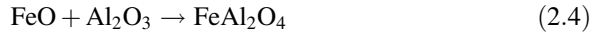


Kumagai and Kamei found heavy attrition wear at the corundum grits when grinding titanium and titanium alloys [KUMA84]. A possible reaction for machining of titanium and titanium alloys with corundum is shown in Eq. 2.3 [KUMA84].



In the grinding contact between corundum and steel, an iron spinel FeO·Al₂O₃ can form [KLOC09, KIRK74]. This happens according to the reaction 2.4, after the chip surface has oxidized to FeO [LAUE79, p. 59]. Iron spinels can form an interim

layer between corundum grits and chip adhesions, which are more likely to adhere onto the spinel than onto bare corundum [LAUE79, p. 68 f.].



2.1.1.4 Thermal Conductivity, Electric and Magnetic Properties

Corundum has the comparatively lowest thermal conductivity of the common abrasives with $\lambda = 6 \text{ W/m } ^\circ\text{C}$ for brown corundum [KLOC09, p. 27]. This leads to a comparatively higher heat flux into the workpiece compared to heat flux into the grit material during grinding [BRIN82, p. 128].

2.1.2 *Manufacture of Corundum by Electrofusing*

Molten corundum, such as regular, white or pink corundum, is produced by electrofusion from bauxite. Charles B. Jacobs developed the method, which worked at temperatures above $2200 \text{ }^\circ\text{C}$, in 1897 [LEWI76, p. 9, MARI07, p. 76, JACO00]. In 1904, Aldus C. Higgins of the Norton Company introduced the Higgins furnace, an arc oven, which is still used today [MARI07, p. 76]. Besides this stationary electric furnace type, the worldwide trend switches to the tilt pour furnace type [NN00]. The tilt pour furnace typically has a higher throughput and more consistency in brown fused alumina quality [NN00].

The Higgins furnace consists of a metal shell on a heavy metal hearth (Fig. 2.4). [MARI07, p. 76, HIGG04]. The shell builds the crucible and can be moved up and down relative to the electrodes, which are inserted into the raw materials. An arc builds between the electrodes through the processed material. The shell and bottom are water-cooled.

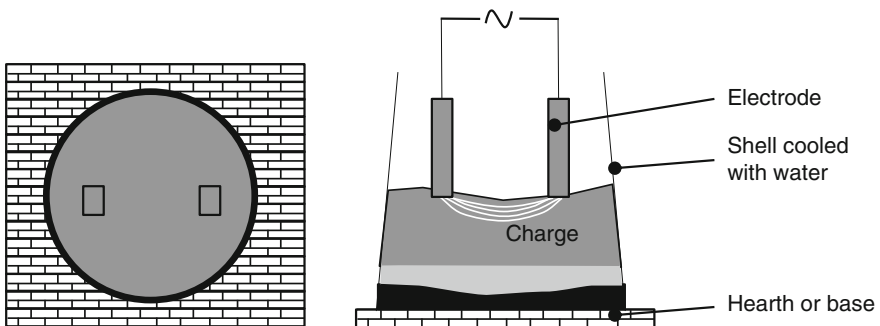


Fig. 2.4 Cross-section of a Higgins furnace for corundum production after [TYRO03b, MARI07, p. 76, HIGG04]

Melting times depend on the applied method and the furnace size (block furnace/Higgins furnace 15–24 h, tilting furnaces 3–5 h) [KLOC05a, p. 23]. The subsequent cooling and solidification of the molten mass also depends on the oven size (4–20 tons weight) and can take up to 14 days [ENGE02, p. 6, KLOC05a, p. 24]. The size of the corundum crystals depends on the block size and cooling rate and can range from 0.2 mm to several millimetres [ENGE02, p. 6].

The cooling procedure happens either through the billet method or the tilting method. In the billet method, a huge block of up to 20 tons cools down slowly in air, which takes up to 10–14 days, and large crystals are formed. In the tilting method, the molten mass cools in flat casting pans. Fine crystals result from the quicker cooling.

The main raw material, bauxite ($\text{Al}_2\text{O}_3 + \text{SiO}_2 + \text{TiO}_2 + \text{Fe}_2\text{O}_3$), is an impure aluminum oxide found in nature. The name refers to Les Baux in France where it was first quarried [LEWI76, p. 9]. Natural Bauxite contains 80–90 % alumina with impurities such as 2–5 % TiO_2 , and Fe_2O_3 , $\text{Fe}(\text{OH})_3$, silicic acid, $\text{Al}(\text{OH})_3$, and aluminum oxide hydrates [KLOC05a, p. 23, MARI07, p. 76]. Before fusion, the bauxite is either calcinated or purified by the Bayer-process.

The pre-processed bauxite is fused with carbon from coke or coal, metallic iron, and other additives. Carbon reduces the impurities in the bauxite to the elemental state, and the iron unites with the reduced impurities. The compound of impurities solidifies as a magnetic mass, so called button, at the furnace bottom [LEWI76, p. 9].

Changes in the ingredients or in the fusion procedure result in several different types of fused or molten corundum as follows: **Brown and semi-friable corundum** is made from calcinated bauxite (Fig. 2.5) [KLOC05a, p. 23, LEWI76, p. 9]. The calcination process takes place at about 950 °C and dehydrates the bauxite [LEWI76, p. 9]. Around 80 % calcined bauxite, 16 % iron and 4 % coke are used [KLOC09, p. 21]. The fusion of 1 ton of of brown corundum needs around 2.2 MVA [JACK07, p. 24].

White corundum is produced from relatively pure raw materials, in particular from >99 % pure alumina (Fig. 2.6) [MARI07, p. 77]. These pure clays of Al_2O_3

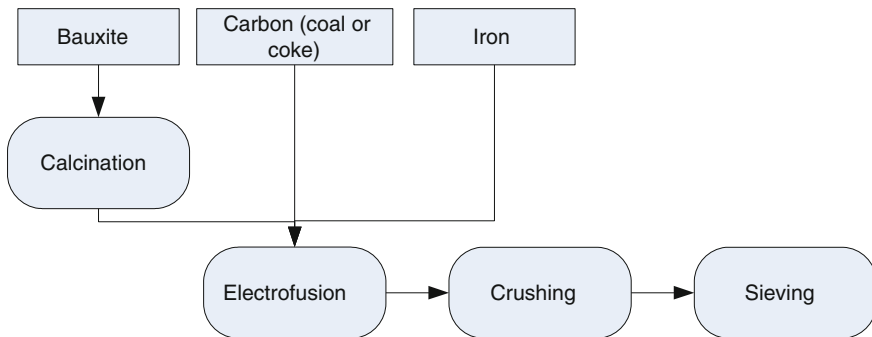


Fig. 2.5 Production of brown corundum after [JACK11, p. 22]

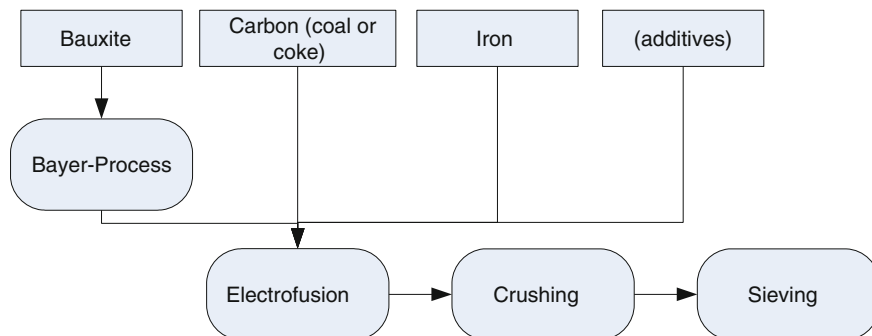


Fig. 2.6 Production of white, pink or ruby corundum after [JACK11, p. 22]

are produced from Bauxite by the Bayer-method [KLOC05a, p. 23]. Fusion of 1 ton of white corundum needs around 1.5 MVA [JACK07, p. 24]. Due to a small amount of sodium oxide, this grit type is friable and “cool cutting” [LEWI76, p. 10].

Pink corundum and **ruby corundum** are made like white corundum, but chromium oxide Cr_2O_3 is added in amounts of 0.3 or 2 % respectively to the fusion process (Fig. 2.6) [KLOC05a, p. 27]. The chromium oxide is built into the Al_2O_3 crystal structure. Additions of vanadium oxide give a green corundum abrasive [LEWI76, p. 10].

Mono-crystalline corundum is produced like white corundum, but iron sulphide is added besides coke to the molten mass, so that a pure, mono-crystalline aluminium oxide forms in a ferrous sulphide matrix [KLOC05a, p. 27, TYRO03b]. The Na-content is beneficially low [TYRO03b]. The sulphidic matrix is crushed and treated with water so that the monocrystalline corundum grits are washed out [MALK08, p. 23]. The crystal structure is defectless and, therefore, a higher toughness than conventionally molten corundum is obtained [ENGE02, p. 6]. In addition, no high crushing forces are used to acquire the grits [MALK08, p. 23]. Environmental complications accompany the process [TYRO03b].

A more or less regular, spherical form characterizes **hollow sphere corundum** [KLOC05a, p. 27 f.]. It can be obtained from different manufacturing routes. One way is to melt the raw materials in an electric arc oven and pour the material out of the furnace through a high-pressure air stream [HAUE07]. The molten stream transforms into smaller particles, which cool while flying through the air. Surface tension forces the particles into spheres. The exterior of the spheres cool quicker than the inside, so that material shrinks away from the sphere center and leaves an open core [HAUE07]. The high cooling rate results in a fine-crystalline structure [HAUE07]. The air stream velocity controls the sphere size between 5 mm to 100 μm [HAUE07].

Zirconium corundum is generated through adding of up to 40 % zirconium dioxide ZrO_2 to the fusion process and a subsequent chill casting [WASH12b]. During solidification, eutectic structures of Al_2O_3 and ZrO_2 are formed [KLOC05a,

p. 27]. Mechanical load or heating of up to 700 °C induces a transformation of the zirconium oxide from the tetragonal into the monocline phase. Herein, the oxide volume increases and micro-cracks build inside the abrasive grit, which inhibit cracks under load [ENGE02, p. 7]. The wear mechanism of zirconium corundum can be influenced by the content of ZrO_2 to a certain degree. A decreasing ZrO_2 content results in falling toughness and the breakage of bigger grit particles as a consequence, but the tendency towards larger wear areas by abrasion is also diminished [LUDE94, p. 99]. Zirconium corundum grits cannot be used in vitrified bonds because the sintering process with temperatures above 900 °C leads to destruction of the abrasives by volumetric change [ENGE02, p. 7].

2.1.3 Manufacture of Corundum by Sintering

Sintered corundum is a family of grains produced from unfused alumina by sintering processes [JACK11, p. 29]. The aim of sintering is to form a solid ceramic body of $\alpha-Al_2O_3$ with a regular, fine-crystalline structure [KLOC05a, p. 25]. This structure is supposed to have a good wear resistance in the abrasive grinding process [KLOC05a, p. 25]. Different manufacturing methods exist based on raw or purified bauxite.

2.1.3.1 Sintering of Bauxite

Sintering of bauxite is one process method (Fig. 2.7). Raw bauxite, water, binders, and pressing auxiliary agents are mixed and the resulting compound is extruded and cut into short cylinders [KLOC05a, p. 25, JACK11, p. 29]. The cylinders are then sintered in rotary kilns at temperatures of 1350–1500 °C [JACK11, p. 29]. The impurities in the bauxite act as auxiliary sintering agents [JACK11, p. 29]. This manufacturing procedure results in a homogeneous, fine-crystalline grit structure with increased toughness [ENGE02]. The extruded long corundum particles are also known as “Spaghetti corundum” [ENGE02, p. 6].

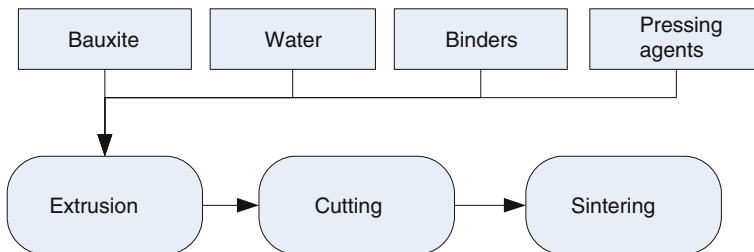


Fig. 2.7 Production of sintered corundum from bauxite after [JACK11, p. 29]

2.1.3.2 Sintering of Fused Corundum

Sintered corundum can be also produced from fused corundum, which is crushed and sintered with auxiliary agents such as glass phase agents [KLOC05a, p. 25].

2.1.4 Manufacture of Corundum by Sol-Gel Process

Sol-Gel corundum is produced by the sol-gel procedure and a subsequent pressure-less sintering procedure (Fig. 2.8) [KLOC05a, p. 25]. The crystal sizes are below 500 nm [ENGE02, p. 7]. Growth inhibitors or nucleating agents themselves can still be present in the sol-gel corundum grits.

Bauxite is purified by the Bayer process and then transformed through the Ziegler process into boehmite, which is γ -aluminum oxide hydroxide (γ -AlOOH) [JACK11, p. 29]. Powdered boehmite (γ -AlOOH) is transformed into a clear sol by mixing with water. Modifying agents are added, such as grain growth inhibitors (MgO , ZrO_2 , TiO_2 , lanthanum and other noble earths) or nucleating agents (Al_2O_3 or Fe_2O_3) [KLOC03]. Adding the nucleating agents is called seeding. Sol-gel corundum can either be produced with or without seeding [KOMAO7].

Then a peptisator, being nitric acid (HNO_3) in most cases, is added. Agglomerates are dissolved and the sol is stabilized. The boehmite is now finely dispersed and homogeneously distributed. After adding of a diluted acid or nitrate solution, the sol reacts to a gel including dehydration and polymerisation. The gel is rolled into thin layers or lines and dried at about 80–100 °C. The resulting solid and brittle body is milled and sieved if necessary. Heating at about 450–550 °C for

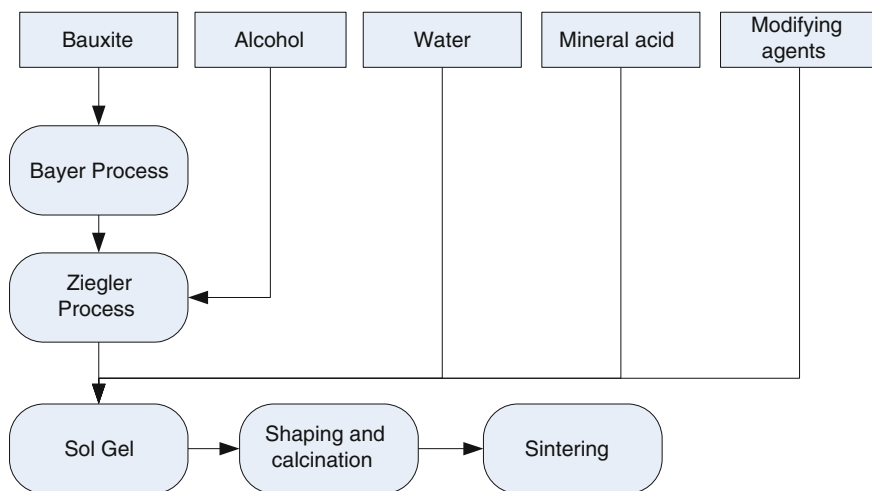


Fig. 2.8 Production of sol-gel corundum [LUDE94, JACK11, p. 35]

about 16 h transforms the boehmite grits into $\gamma\text{-Al}_2\text{O}_3$. During this so called calcination, nitrogen (NO_x) and water are set free. Afterwards, the $\gamma\text{-Al}_2\text{O}_3$ is sintered pressure-less for about 30 min. Generally, seeded sol-gel material is sintered at 1300–1400 °C, nonseeded sol-gel at temperatures that are about 100 °C higher [ENGE02, p. 11, KLOC05a, p. 26, KOMA07]. With additional extrusion processes, needle-shaped, extruded sol-gel corundum is manufactured with aspect ratios of 8:1 [MARI07, p. 113].

2.1.5 Performance of Corundum

All corundum types have individual performance profiles. Various mechanisms to increase grit toughness take effect in the different corundum grits [LUDE94, p. 74 ff].

2.1.5.1 Molten Corundum

Pure white corundum is one of the hardest, but most friable corundum grit types and is used most in vitrified grinding wheels for precision grinding processes [MARI07, p. 77]. The low sodium content of pure white corundum deters tool breakdown from cooling lubricant attack [MARI07, p. 77].

Zirconium corundum undergoes a martensitic phase, which increases the toughness transformation and depends on the process load (see Sect. 2.1). This can be an advantage, but this mechanism needs a certain load level [LUDE94, p. 77].

2.1.5.2 Comparison of Sintered Corundum and Molten Corundum

The most dramatic differences in performance occur between the grinding behavior of molten and sintered corundum. The introduction of sintered corundum led to tremendous tool life enhancements.

The higher wear resistance and larger material removal rates of micro crystalline corundum compared to molten corundum results not only from the higher toughness of the abrasive material but also from the specific wear behavior [MÜLL01, p. 122 f., UHLM97]. Sintered corundum types consist of small crystals, which wear by breakout [LUDE94, p. 74]. The longer crystal boundaries that have to be broken lead to higher grit toughness. The specific wear mechanisms are based on micro-crystalline fracture, so that only small particles break out of the sol-gel corundum grits and establish a self-sharpening effect [MÜLL01, p. 122 f., UHLM97]. However, this micro-crystalline fracture only appears above a certain load. Below this minimum load, corundum grits wear mainly by surface flattening (Fig. 2.9) [MÜLL01, p. 122 f., UHLM97]. The right process design, e.g. working with high material removal rates, is crucial for an efficient, sustainable process.

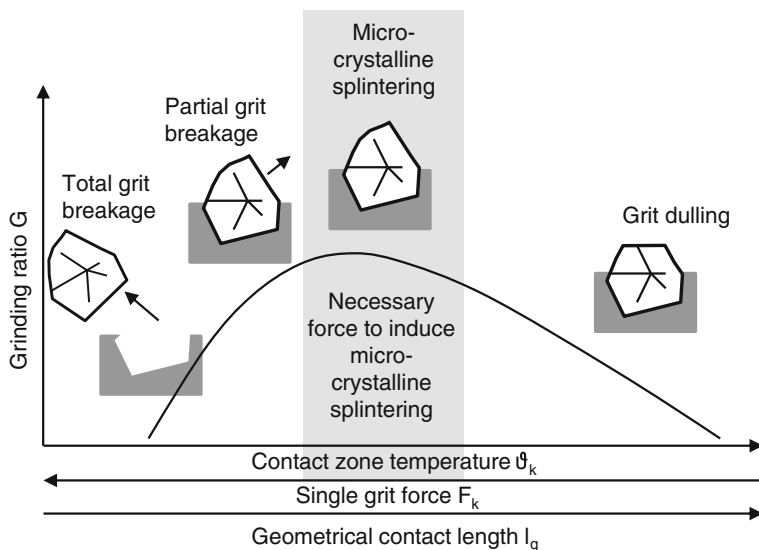


Fig. 2.9 Wear behavior of sol-gel corundum depending on the single grit load, after [UHLM97]

Another mechanism is the presence of cavities in the abrasives [LUDE94, p. 76]. They act like hindrances and split cracks in smaller micro cracks. Furthermore, comparatively long crystals with high tear strength (whiskers) in a tough matrix can increase grit toughness [LUDE94, p. 76]. The crystals are pulled out off the matrix during crack propagation. This leads to a zipper effect, which absorbs the crack energy.

The high aspect ratio of extruded sol-gel corundum results in a low packing density of these grains of only 30 % by volume [MARI07, p. 113]. So grinding tools of very high porosity can be manufactured for high performance processes where pores get clogged easily. Vitrified grinding wheels with this grit type are on the market with an interlinked porosity of 65–70 % and they prove to be well suited for high efficiency grinding with low process heat [MARI07, p. 113, WEBS04].

2.1.5.3 Comparison of Sol-Gel Corundum and Molten Corundum

In the beginning, sol-gel corundum was used as the solitary abrasive grit type in grinding tools (percentage of 100 %). However, its toughness led to excessive grinding forces. Today typical blends are 50, 30 and 10 % of sol-gel corundum with white corundum or mono-crystalline corundum as secondary grits [KLOC03, MARI04, p. 378, MÜLL01]. In 2003, sol-gel corundum was about 15–20 times more expensive than pure white corundum [KLOC03].

Furthermore, the usage of sol-gel corundum in vitrified bonds was limited by the sintering temperatures of the bond. Temperatures above 1200 °C result in aggregation of the micro-crystals, which reduces the efficiency of the abrasive grits. Therefore, low-fired bonds were developed resulting in spreading of sintered corundum grinding tools [KLOC03].

Compared to superabrasives, sol-gel corundum has much lower production costs. Therefore, it can be used in solid body grinding tools instead of thin abrasive layers. As a consequence, the sol-gel corundum tools can be reprofiled more often and are flexible for different workpiece profiles [KLOC03].

Sol-gel corundum wears by favorable micro splintering when a minimum load is exceeded (Fig. 2.9) [MÜLL01, ENGE02]. Especially for high material removal rates, sol-gel corundum has a higher performance than conventional abrasives, but is less expensive than CBN. Thus, the full potential of sol-gel corundum evolves only at high cutting speeds and high material removal rates. Sol-gel corundum shows a quasi stationary cutting performance even at higher grit load until the break-down of the abrasive layer. Therefore, high surface qualities are possible at shorter machining times [KLOC03].

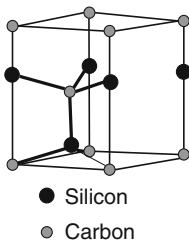
In applications with low process loads, sol-gel corundum grinding tools have only minor advantages in performance and wear resistance against conventional abrasives [KLOC03, MÜLL01, p. 123]. In fact, sol-gel corundum grinding tools have to be applied at high process loads to maximize their potential [KLOC03, MÜLL01, p. 123]. Sol-gel corundum showed much lower radial wear and a higher maximum specific material removal rate than pure white corundum at high load or cutting speeds (e.g. $v_c = 63\text{--}125$ m/s) [KLOC03].

In single grit scratching tests, a highly viscous oxide layer formed on the grit edge of sol-gel corundum [KLOC02]. This oxide layer presumably reduces the strain energy between the workpiece and the abrasive grit, so that friction coefficient and grit wear are decreased [KLOC02].

2.2 Silicon Carbide

2.2.1 *Chemistry, Types and Characteristics of Silicon Carbide*

Silicon carbide, also known as carborundum and SiC, is used as abrasive material in its hexagonal form, α -SiC (Fig. 2.10) [MALK08, p. 24]. It is composed of 70.05 wt % Si and 29.95 wt% C [LIET08]. Each C atom is surrounded by four Si atoms and vice versa. The proportion of covalent atom bonds to ionic atom bonds is 90–10 % [MÜLL01, p. 25]. Silicon carbide occurs in two modifications: cubic β -SiC and α -SiC (mostly hexagonal and rhombohedral).



Density	3.21 g/cm ³	[LIET08]
Hardness Knoop	24 - 26 GPa	[MÜLL01]*
Fracture toughness	3.1 MPa m ^{1/2}	[MÜLL01]*
Thermal stability	Up to 1500 °C	[MÜLL01]*
Thermal conductivity	100 W/ m K	[ROWE09]

*after 3M, GE, Norton, Treibacher

Fig. 2.10 Basic properties of α -silicon carbide, picture source [PRES08]

Silicon carbide was the first abrasive to be synthesized. Two main types of silicon carbide are characterized by their color:

- Green silicon carbide has higher purity and is mainly used for precision grinding [TYRO03b].
- Black silicon carbide has higher toughness and is used for rough grinding operations [TYRO03b].

The chemical composition is shown in Table 2.2.

2.2.1.1 Shape, Morphology

Pure α -SiC is colorless, but inclusions of nitrogen in the crystal lattice give a green or yellow color [LIET08]. Aluminum or boron gives a blue-black color [LIET08].

2.2.1.2 Toughness, Breaking Behavior, Friability, Hardness

SiC has a Knoop micro hardness between 21 and 29 GPa in general and SiC abrasive grits between 24–26 GPa [LIET08, MÜLL01]. The impurities in black SiC do not seem to affect grit toughness negatively [LEWI76, p. 8]. Green SiC has a slightly higher friability than black SiC [LEWI76, p. 8, TYRO03b]. The compressive strength of SiC is around 2943 N/mm² [MERB03, p. 6].

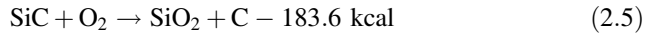
Table 2.2 Composition of SiC green and SiC black [TYRO03b, KLOC05a]

	SiC (%)	C (%)	Si (%)	Fe (%)	others
SiC green	99.3–99.6	0.05–0.5	0.01–0.3	0.01–0.1	N contents of 10 ⁻⁴ to 10 ⁻³ %
SiC black	98.8–99.3	0.15–0.4	0.1–0.4	0.01–0.5	With parts of Al or Al ₂ O ₃

2.2.1.3 Temperature Stability, Chemical Reactions

SiC is resistant to organic solvents, alkalis, acids, salt solutions, and even aqua regia and fuming nitric acid [LIET08]. Nevertheless, SiC undergoes several reactions with oxygen, such as a passive oxidation of pure SiC above 600 °C and an active oxidation above 1000 °C [LIET08]. Presser and Nickel as well as Moser discuss more potential reactions of SiC [PRES08, MOSE80, p. 142 ff].

In abrasive machining, Komanduri and Shaw describe the oxidization of SiC with oxygen at high temperatures to SiO₂ (Eq. 2.5) [KOMA76b]. This exothermic reaction produces SiO₂ layers [PRES08]. The layers are removed mechanically in the grinding process [KOMA76b].



SiC is inclined to react with oxygen above temperatures of 800 °C and when in contact with metals (Eq. 2.6) [LUDE94, p. 31].

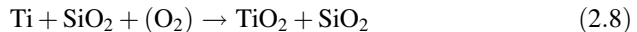


Reactions of SiC with Fe are also suspected (Eq. 2.7) [LUDE94, p. 31]. Molten iron dissolves SiC, forming iron carbide and iron silicide [LIET08].



When grinding cobalt alloys with silicon carbide grits, Komanduri and Shaw found diffusion of silicon into the workpiece material and formation of metal silicides. In addition, carbon from the grit material diffused into the work material and formed unstable metal carbides such as Ni₃C and Co₃C [KOMA76b].

SiC proves to be a good abrasive material for machining titanium and titanium alloys, despite the possible reactions in Eqs. 2.8 and 2.9 [KUMA84].



2.2.1.4 Thermal Conductivity, Electric and Magnetic Properties

The thermal conductivity of silicon carbide is comparatively high for a ceramic material with around 100 W/mK [ROWE09]. Silicon carbide is a semiconductor with a broad energy band gap with a resistivity between 0.1–10¹² Ω cm depending on purity [LIET08].

2.2.2 *Manufacture of Silicon Carbide*

Silicon carbide (SiC) cannot be found in nature in sufficient quality for technical applications [TYRO03b]. For the use as abrasive, SiC is molten from quartz sand in resistance furnaces by a process that was invented by Edward Goodrich Acheson in 1891 on an industrial scale [MOSE80, p. 119]. Originally, Acheson had intended to synthesize diamond. After finding the compound of carbon and alumina from the synthesis process, he called the material “carborundum” [PRES08].

The raw materials are silicon dioxide (SiO₂) in the form of white quartz sand with a purity of 97–99.5 % SiO₂, and petroleum coke (C) (Fig. 2.11) [LEWI76, p. 8, STAD62, p. 25]. Both materials are ground to particle sizes of 1–2 mm [STAD62, p. 25]. In addition, sawdust and salt are inserted. The sawdust carbonizes during the reaction process and leaves pores, through which the resulting carbon monoxide (CO) can escape (Eq. 2.10) [STAD62, p. 25]. The salt turns impurities such as aluminum or iron to chlorides. An example composition of raw materials is 53 % quartz, 40 % coal, 5 % sawdust, and 2 % salt [KLOC09, p. 34].

Commonly, resistance furnaces are used. The furnace is half filled with the raw material mixture (Fig. 2.12). A central core of petroleum coke, nut-coal or graphite is inserted in the middle of the furnace [LEWI76, p. 8, STAD62, p. 25]. The rest of the quartz, coke, sawdust mixture is put on top. At each end of the oven are electrodes [LEWI76, p. 8]. The central core conducts the electric current and acts as resistor. At a voltage of for example 240 V the current heats the furnace to the reaction temperature of around 2000 °C [STAD62, p. 25]. Coke and sand react after Eq. (2.10) to hexagonal α -SiC [LUDE94]. It has to be noted that SiC production inherently produces CO emissions. The resistor core can be straight or zig-zag-shaped [MOSE80, p. 123].



At higher temperatures the core resistance drops and the reaction mass begins to conduct, so that the applied voltage and power input have to be controlled [LEWI76, p. 8, STAD62, p. 25]. The voltage is reduced so that the furnace has a constant power consumption of for example 1000 or 3000 kW [STAD62, p. 25].

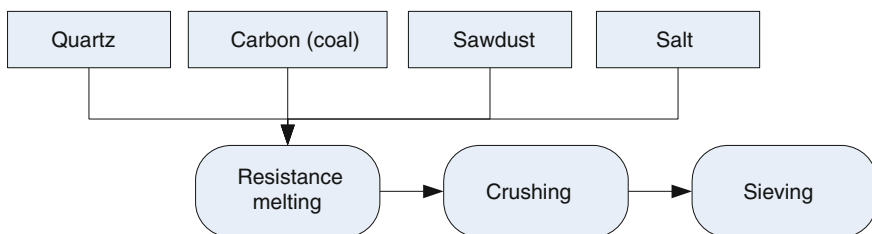


Fig. 2.11 Production of silicon carbide

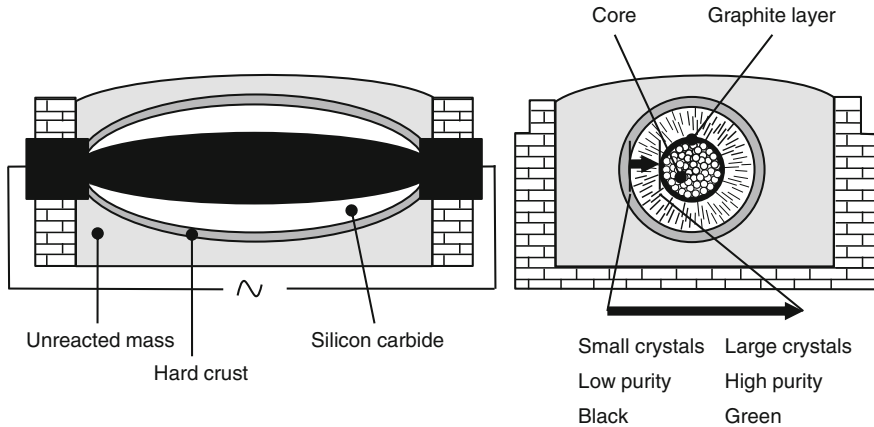


Fig. 2.12 Cross-section of a resistance furnace for silicon carbide production after [STAD62, p. 25; TYRO03b, BORC07, p. 49 ff]

The energy per kg of α -SiC produced is around 8 kWh/kg [TYRO03b]. The reaction ends after 36–40 h and results in several reaction products (Fig. 2.12).

After cooling and stripping the furnace walls, unreacted mass is obtained that can be used for further reactions [LEWI76, p. 8]. The ingot of silicon carbide is surrounded by a hard crust consisting of salt and silicon carbide dioxide. The crystals in the silicon carbide layer increase in size and purity from outside to inside; also, the color of the crystals shifts from black to green [STAD62, p. 25]. Graphite from decomposed SiC surrounds the electrode core [LIET08].

Different grades of pureness, toughness, and color can be produced depending on the process control [LEWI76, p. 8]. Like in corundum production, the material blocks are crushed and milled to the according size (see Sect. 2.6 “Grit Post-Processing”).

Waste from the manufacturing process is unreacted coke and partly reduced “firesand”, which can be returned to the furnace [MALK08, p. 24 f.]. In some furnaces, the gases from the reaction are collected and used for energy production [LIET08].

2.2.3 Performance of Silicon Carbide

SiC reacts heavily with many Al_2O_3 containing vitrified bonds leading to grit damage [TYRO03b]. Therefore, special bond types for SiC are applied.

Silicon carbide is known for wearing mainly by splintering in the medium FEPA size ranges. Instead of steady and slow wear by adhesions, abrasion or chemical mechanisms, SiC wears by breaking into bigger grit particles. In contrast, the tougher mono-crystalline corundum can sustain dynamical and sudden loads better,

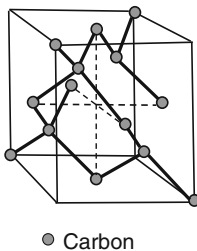
like present in grinding of hardened bearing steels. Additionally, SiC wears dominantly anisotropic depending on the loaded crystal plane. Nevertheless, the wear behavior enables good self-sharpening abilities of the tool. Under small process loads such as for small chip thicknesses, SiC wears by tribochemical mechanisms, likely oxidation and silicization [LUDE94, p. 71].

2.3 Diamond

2.3.1 Chemistry, Types of Diamond and Performance

Carbon forms several allotropes: hexagonal graphite, diamond in the cubic zinc blende structure, non-graphitic carbon, and the cage-like fullerene (C_{60}), discovered in 1985 [JAEG10]. Diamond is the hardest material in nature and very resistant against compaction. This is due to the dense packing of the carbon atoms, their regular, symmetrical order, and the energy rich covalent atom bonds [SEN02, TOLA68].

The crystal unit cell of diamond consists of eight carbon atoms (Fig. 2.13). Four of these ($8 \cdot 1/8 + 6 \cdot 1/2$) define a cubic area-centered lattice. The left four atoms are positioned on the centers of the eighth dice and build a second cubic area-centered lattice that is displaced in the direction of the body diagonal with a quarter of its length [HÜTT72]. The lattice constant of diamond is $a = 0.355 \text{ nm}$. Every carbon atom in diamond is surrounded tetrahedrally by four atoms, in which the angle between two neighboring atoms amounts consistently to 109.5° and the distance is 1.5445 \AA [HOLL95, HÜTT72, MORT87]. These angles originate from the geometrical crystal structure due to the sp^3 -hybridization: when one of the $2s$ -electrons is lifted into the empty p -orbit from the basic state ($1s^2 2s^2 2p^2$). From three p -orbitals and one s -orbital four new similar orbitals are generated. The four hybrid orbitals push each other away, so that the orbitals are directed into the edges of a regular tetrahedron [HOLL95, MORT87].



Density	3.53 g/cm ³	[ROWE09]
Hardness Knoop	65 GPa	[ROWE09]
Fracture toughness	3 - 3.7 MPa.m ^{0.5}	[GRAN12]
Thermal stability	500 – 700 °C	[GARD88]
Thermal conductivity	600 – 2,000 W/m K	[ROWE09]

Fig. 2.13 Basic properties of diamond

Several diamond materials are used in abrasive tools today [MARIO4]:

- Natural diamond grits,
- Synthetic diamond grits,
- Synthetic mono-crystalline diamond logs (MCD),
- Synthetic poly-crystalline diamonds in Co-matrix as logs or plates (PCD) and
- Chemically disposed diamonds without binder as logs or plates (CVD).

2.3.1.1 Shape, Morphology

The diamond crystal structure belongs to the cubic system and is expected to grow in the octahedron form [MOOR85]. This can be explained by crystal growth through atoms adhering to the surface, so that facets are built. The slowest-growing facets will dominate the crystal morphology. In the case of diamond, these are the octahedral planes in ideal growth conditions. Nevertheless, structure, purity, and morphology of diamonds depend on the growth circumstances [FIEL79, WEDL77]. Crystal morphology of synthetic diamonds ranges from a perfect cube to a perfect octahedron (Fig. 2.14). Synthetic diamonds appear often as cubooctahedrons with $\{100\}$ - and $\{111\}$ -planes [FIEL79, TOLA68]. Natural diamonds occur commonly as octahedrons or rhombic dodecahedrons, but often they are distorted, their edges rounded or their surfaces convex [FIEL79, MARIO4].

Nitrogen atoms are the most common impurity in diamond material. Since 1934, diamond has been classified into two main groups: type I (up to 0.25 % of nitrogen) and type II (nitrogen-free) according to their nitrogen content [FIEL79, LENZ86]. 98 % of all diamonds belong to type I and 99 % of the natural diamonds are classified as type Ia, where nitrogen appears as small platelets. Nearly all synthetic diamonds belong to type Ib with finely-dispersed nitrogen inclusions. In the crystal structure, the nitrogen atoms substitute carbon atoms at isolated spots. This leads to a changed light absorption and the diamonds appears yellowish [EPPL94, LENZ86].

2.3.1.2 Toughness, Breaking Behavior, Friability

The density of atom bonds in the different diamond planes defines hardness and cleavage behavior (Fig. 2.15) [BRUN62, FIEL79]. The octahedral plane (111) is the main cleavage plane [FIEL81, LENZ86]. This can be explained by the lower toughness and, therefore, smaller necessary breakage energy along this plane



Fig. 2.14 Crystal morphology of diamond [BAIL98]

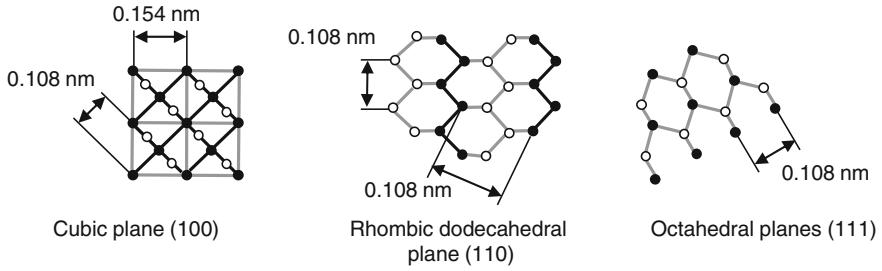


Fig. 2.15 Density of carbon atoms in different diamond planes after [LINK07, p. 16]

[TELL00, WILK62]. However, cleavage occurs also along the planes (211), (110), and (322) [FIEL79]. Similar mechanisms decide on the lapping behavior of the diamond grits. The smaller the bonding density in a crystal plane is, the easier the material removal. The (110) plane can be machined best via lapping, followed by the (100) plane and (111) as most difficult to machine [BOUW99, YUAZ03].

Natural and synthetic diamond grits show different breakage behavior. Natural diamond collapses in several breakage events; synthetic grits, however, fail with one breakage event [HIMM90]. Grit structure, types and occurrence of crystal growth defects define the breakage behavior [BENE03].

2.3.1.3 Hardness

Diamond density is about 3.52 g/cm^3 depending on pureness. Diamond hardness and toughness are determined by crystal purity, regardless of size, shape, and genesis [BENE03]. The hardness of single crystal diamond is anisotropic depending on the crystal orientation (Fig. 2.16). This results from the different distances of the carbon atoms in different crystal planes. The highest density of atom bonds occurs in the octahedral plane (111), which results in the highest hardness [TOLA68]. The cubic plane (100) is the softest direction [TOLA68]. In the (110) plane the hardness is as high as 123 % of the hardness in the (111) plane, in the (100) plane even 138 % [KLOC05a].

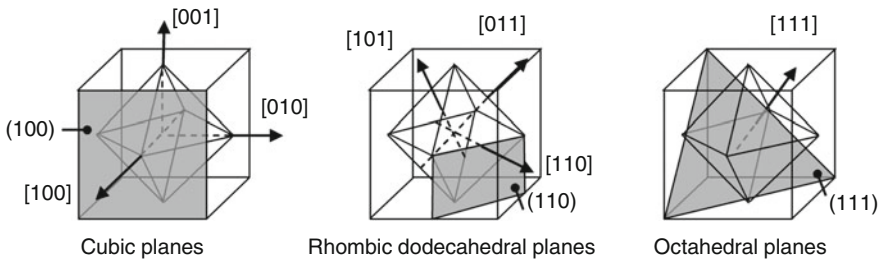


Fig. 2.16 Crystal structure of diamond after [HÜTT72, LINK07, p. 16]

Hardness and cleavage behavior are not only defined by the crystallographic structure but also by the occurrence of structural defects and diamond purity [BRUN62, WILK91]. Smaller grits are commonly tougher than bigger diamonds because they have fewer and smaller defects and inclusions [FIEL79, WILK91].

Synthetic diamonds often contain metal inclusions of the catalysts [YIN00]. All crystal defects like substituted atoms, atoms between lattice sites, or lattice vacancies are imperfections of diamond structure and enable micro-splintering [ODON76]. In addition, macroscopic inclusions can act as initial points for crack growth.

2.3.1.4 Temperature Stability, Chemical Reactions

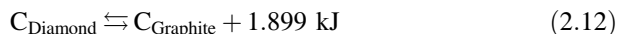
At room temperature, diamond is nearly inactive regarding chemical reactions. At temperatures above 800 °C, diamond burns to carbon dioxide with air oxygen (Formula 2.11) [HOLL95, MARI04]. Depending on the grit size, the specific surface area, and the grit crystal type, reactions with oxygen occur even already at 500–700 °C [GARD88].



Diamond performs further reactions with different groups of carbide builders [GARD88, WEDL77]:

- Transition elements of the 8th group and the metals Mn, Cr, Ta, and Nb compose carbides with diamond.
- Strongly electro-positive elements like Ca build stable carbides with an ionic bond.
- Further carbide builders like Si, B, Al, etc. form covalent bonds with carbon.

A commonly known transition of diamond is the so called graphitization. The carbon atoms in diamond are activated by the sp^3 -hybridization, so that diamond is meta stable at room temperature and atmospheric pressure. Furthermore, diamond has more energy than graphite (Formula 2.12) [HOLL95, HÜTT72, UHLM01a]. However, the activation energy for the phase transition to the stable modification of graphite is so high, that graphitization rather does not occur at room temperature [EVAN62, WILK91]. When diamond is heated above 1800 K in an inert environment, graphite is formed in a slightly exothermic reaction, which is called true graphitization [FIEL79, HOLL95, WILK91]. In the presence of oxygen, the diamond surface graphitizes already at temperatures of 900 K [FIEL79].



2.3.1.5 Thermal Conductivity

At room temperature, diamond is the material with the highest known temperature conductivity, which can reach up to 2100 W/(m K) depending on crystal purity [SEN91]. Furthermore, diamond exhibits a low electric conductivity, which can increase significantly with Boron assembled into the diamond crystal structure. In oxygen atmosphere, diamond has a low friction coefficient of $\mu = 0.05\text{--}0.1$ with most materials, including diamond itself [MARI04].

2.3.1.6 Electric and Magnetic Properties

Electric and magnetic conductivity of diamond depends on the inclusions [YIN00]. In particular, catalyst inclusions in synthetic diamonds change the electric and magnetic behavior, which can negatively affect electroplating processes or enable to align the abrasive grits on grinding belts or wheels.

2.3.2 Natural Diamond Genesis

Diamond forms only at high pressures and temperatures. Its natural genesis is assumed to happen in depths from 100 to 300 km beneath earth's surface at temperatures above 1200 °C and pressures above 50,000 bar [EPPL94]. It can be distinguished between primary deposits where diamond is located within parent rock and secondary sources where diamond is accumulated in rivers, in the sea, or in dunes by erosion [EPPL94]. However, the source of diamond has a main influence on the chemical and physical properties. Bigger natural diamond grits are mechanically broken down to smaller grits [FIEL81]. Grit suppliers and tool manufacturers sort natural diamonds and treat their surface to work best in different bonding systems and machining applications. Natural diamonds, especially high-quality diamonds for jewelry are closely related to social sustainability in two ways: Mining practices are to be reviewed and diamonds might be used to feed conflicts.

Natural polycrystalline diamonds are known as carbonado, ballas, boart, framesite, stewartite, etc. They occur in various different structures. Since the synthesis of fragile diamond was invented, the importance of fragile natural diamond for manufacturing technology has decreased.

Jewel industry uses the "4 C's" to appraise diamond grits, i.e. the criteria carat (weight), clarity (purity), color, and cut. In fine machining, however, grit morphology, purity, and size are most important. In natural diamonds, inclusions of minerals can be found, which were present at diamond genesis. Possible contaminations are SiO₂, MgO, FeO, Fe₂O₃, Al₂O₃, TiO₂, graphite, etc. [MARI04]. Cracks in diamonds can also be of natural origin, e.g. from geological mechanical load [LENZ86].

2.3.3 Artificial Synthesis of Diamonds

2.3.3.1 Monocrystalline Diamonds

The first artificial diamond synthesis was conducted by the Swedish company ASEA with a six-anvil press in February 1953 [TOLA68, WEDL77]. In 1955, company GE followed with the synthesis in a belt press and in 1958 company De Beers [MARI04].

Graphite can be transformed to diamond directly at temperatures above 1800 K and pressures above 60 kbar (Fig. 2.17) [WILK91]. However, the use of appropriate catalysts can reduce the temperature-pressure-range significantly. Metals of the 8th main group (nickel, cobalt, iron, et al.) enable synthesis even at pressures of 5–8 GPa and temperatures of 1500–2100 K [ODON76, YIN00]. This method takes advantage of the fact that graphite solves easier in metal than diamond. Graphite is also less thermodynamically stable within the working range. As consequence, carbon precipitates as diamond from the supersaturated metal carbide solution [HOLL95, MARI04].

The belt press consists of a hollow cylinder of tungsten or carbide with two anvils moving in vertical direction (Fig. 2.18 left). The high pressure high temperature (HPHT) chamber forms inside the hollow cylinder. Shrunk-on steel rings compress and pre-load the cylinder and anvils [LUND68]. Graphite as reaction mass is put into the HPHT chamber and coated concentrically with pyrophyllite, which is an aluminum silicate and isolates the reaction mass [LUND68]. The anvils are pressed

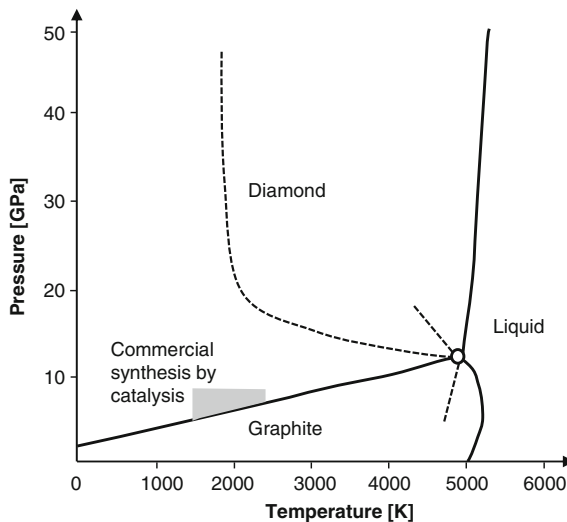


Fig. 2.17 Pressure-temperature diagram of carbon [BUND96]

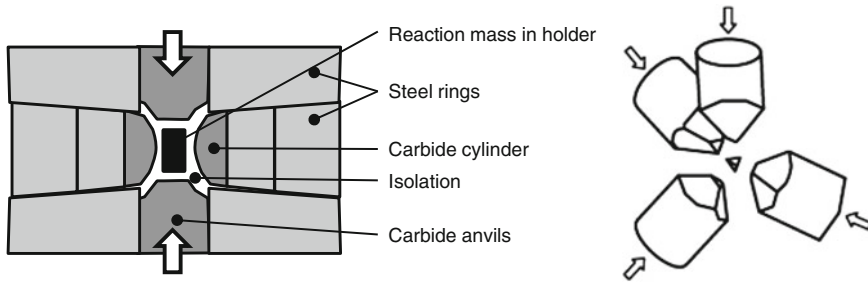


Fig. 2.18 Presses for diamond production, *left* belt-press [HALL60, KOMA01, LUND68, KHVO08, COES71], *right* anvil press [KHVO08]

together and generate the needed high pressure. Pyrophyllite creeps through the press joints and seals them enlarging the internal pressure in the reaction chamber [LUND68]. Resistor elements in the chamber walls generate the high temperatures needed for diamond synthesis [LUND68]. State of the art belt-presses reach a pressure of 8–10 GPa [KHVO08].

Today, another press type, the six anvil press, is widely used. It has the advantage of reaching higher pressures of 20–30 GPa in relatively large chamber volumes (around 10 mm³) (Fig. 2.18 right). In Russia, diamond synthesis is conducted in chambers of a toroid and lentic type with even higher pressures. [KHVO08]

Quick temperature and pressure changes during diamond synthesis can force segregation of many diamond seeds. They will interfere during growth so that polycrystalline and irregularly grown diamonds develop [ODON76, PIRA03]. Before industrial use, synthetic and natural diamonds are often broken mechanically or prepared with acid to change their surface [TOLA68]. Whereas natural diamond must be crushed before use in grinding tools, diamond synthesis produces abrasive particles in appropriate size for abrasive applications [METZ86, p. 38].

2.3.3.2 More Synthesis Methods

Besides a direct transformation of graphite into diamond and the most common synthesis technique with molten catalyst, there are more synthesis methods [WEDL77]. These are Shock Wave Synthesis, growth from carbon melt and chemical diamond deposition from gas phase (Chemical vapor deposition, CVD). During CVD synthesis, carbon-containing gas like methane is disintegrated in presence of hydrogen at 2000 °C or in plasma sparks. At normal pressure, the dissolved products condense on appropriate areas. Graphite seeds are hydrated quickly to methane, but diamond seeds grow faster than they are decreased by hydrogenation [HOLL95]. The resulting diamond layer is polycrystalline.

2.3.4 Performance of Diamonds

2.3.4.1 Grinding Tools

After the successful synthesis of diamond, natural diamond in grinding tools was replaced more and more by synthetic diamond [NOTT80]. The first commercially available synthetic diamond in 1955 was friable and polycrystalline, arising presumably from a lack of control in the early days of diamond synthesis [DYER79]. However, this type of grit had advantageous self-sharpening abilities not displayed by natural diamond.

Today, grinding tools of resin bond consist mostly of friable diamond, such as natural diamonds of lesser purity or synthetic diamonds with defined defects. In metallic bonds, cubic diamond grits with high toughness are applied. Naturally, a grinding wheel with blocky diamonds has lower wear rates than a tool with friable grits; in contrast, the grinding forces are higher due to the higher friction between flat grit areas, workpiece, and chips [WIMM95, BAIL99].

Diamond wears because of diffusion and graphitization during grinding of ferrous materials with low carbon content [KOMA76]. The diamond turns to graphite in the surface layers, which is accelerated by oxygen as catalyst [KOMA76]. Then the carbon diffuses from graphite into the ferrous material.

Research is ongoing on engineered wheels with defined grit patterns or CVD diamonds as abrasive layer (see Sect. 9.2 “Innovative and More Sustainable Tools”).

2.3.4.2 Honing Tools

Other than in grinding, diamond has far fewer limitations when machining steel by honing. This can be explained by the low cutting speeds, cooling and lubrication conditions in honing, which tend to suppress the reaction between diamond and workpiece materials with carbon affinity [KOPP81].

2.3.4.3 Dressing Technology

Natural diamonds of high purity are commonly used in dressing tools [ODON76, KAIS97, SEN02]. In addition, synthetic diamond logs are common in dressing technology. Mono-crystalline diamonds (MCD) have the advantage of keeping their geometry despite of wear [COEL00, LIER02]. Depending on their orientation, only the properties of one crystal plane are present. In polycrystalline diamonds (PCD), the single diamond crystals are arranged in a Co-matrix, so that the hardness anisotropy of each crystal is equalized. PCD logs are quasi isotropic and have no preferred direction of mechanical properties [LIER02, SEN02]. Sometimes dressing tools with PCD logs are called “geometrically defined dressing tools” because of

their uniform wear behavior [MINK88]. The second polycrystalline dressing log material CVD diamond consists of diamond micro-crystals that grew together without binder [MARI04].

2.3.4.4 Diamond Powder

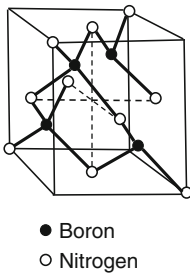
Micron diamond powder is widely used in suspension for lapping and polishing, as fine abrasive in bonded tools, and as loose abrasive in die stone production, gem stone polishing, and jewel bearing manufacture [HERB81]. Smaller grits have normally higher toughness, due to their lower number of defects [FIEL81]. Diamond performance is determined by grit shape, type, number of inclusions, cracks, and structural defects [SEN91]. Grit surface roughness and grit morphology define bonding adherence [BAIL02]. Diamonds are etched to roughen their surface or are coated with metallic deposits to optimize bonding retention [MARI04].

2.4 Cubic Boron Nitride

2.4.1 Chemistry, Types and Characteristics of CBN

The invention of the superabrasive cubic boron nitride (CBN) is linked closely to the synthesis of artificial diamond. CBN has the same crystal structure as diamond (cubic zinc blende structure), but the carbon atoms are replaced by the elements boron and nitrogen (Fig. 2.19 left). Boron nitride (BN) appears in forms isostructural to carbon: hexagonal α -BN similar to graphite, diamond-like β -BN, γ -BN in the wurtzite structure, and others [GREI06, HAUB02].

In CBN and diamond each of their atoms is bonded to four others in a perfect tetrahedrally alignment (bond angle $109^\circ 28'$). In CBN, each nitrogen atom is bonded to four boron atoms and vice versa. Cubic boron nitride has predominantly covalent bonds with a small degree of ionic bonding because boron and nitrogen are dissimilar atoms [BAIL98].



Density	3.47 g/cm ³	[MÜLL01]*
Hardness Knoop	42 - 45 GPa	[MÜLL01]*
Fracture toughness	3.7 MPa m ^{1/2}	[MÜLL01]*
Thermal stability	Up to 1200 °C	[MÜLL01]*
Thermal conductivity	240 – 1,300 W/m K	[ROWE09]

*after 3M, GE, Norton, Treibacher

Fig. 2.19 Basic properties of cubic boron nitride

2.4.1.1 Shape, Morphology

As cubic boron nitride is less symmetric than diamond due to the alternation between boron and nitrogen, its morphology is more complex. In CBN, four of the octahedral (111) faces are terminated with boron and four with nitrogen. If the growth rates of the two types of octahedral faces are equal, an octahedron will result (Fig. 2.20 left). If one face type grows to the exclusion of the other, then a tetrahedron will form. Therefore, the morphology of CBN can vary between cubic and octahedral like diamond and between octahedral and tetrahedral (Fig. 2.20 right) [BAIL98]. The synthesis conditions adjust the CBN morphology to a certain range. Nitrogen dominated CBN particles appear red brown colored.

2.4.1.2 Toughness, Breaking Behavior, Friability, Hardness

Diamond has four cleavage planes, whereas CBN has six. All are {110}, one of which is indicated in Fig. 2.21. Young's modulus is accounted to 4500 kg/mm² [HAUB02]. The compressive strength of CBN is around 7063 N/mm² [MERB03,

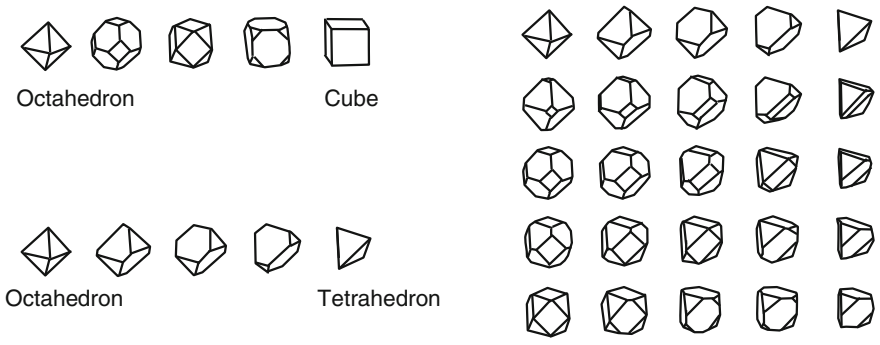


Fig. 2.20 Left crystal morphology; right morphology of CBN [BAIL98]

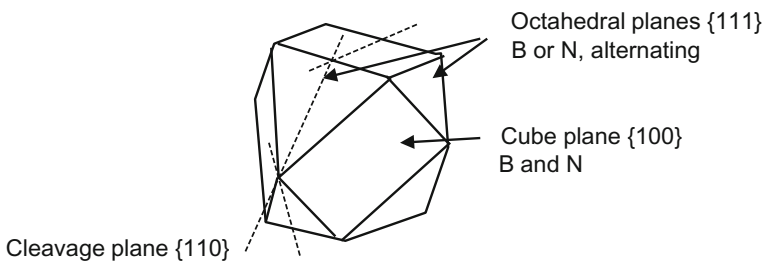


Fig. 2.21 Typical CBN crystal [BAIL98]

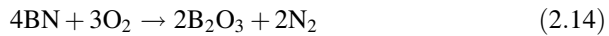
p. 6]. The Knoop hardness is around 4700 HK, so that CBN is the second hardest mineral compared to diamond [GREI06].

2.4.1.3 Temperature Stability, Chemical Reactions

In air, CBN is stable up to 1400 °C [GREI06]. When grinding titanium, CBN shows attrition wear and fractures [KUMA84]. A possible reaction for machining of titanium and titanium alloys with CBN is shown in Eq. 2.13 [KUMA84].



CBN is covered with boron oxide, B_2O_3 , in dry air at temperatures of 1200 °C (Eq. 2.14). In grinding, this layer has supposedly a wear-inhibiting effect [KLOC09, p. 36].



Hydrolysis of CBN occurs above a temperature of 1000 °C (Eq. 2.15) [KLOC09, p. 36, MOSE80, p. 166]. It is presumed that this reaction needs longer contact times than present in grinding and is therefore not relevant for this technology [KLOC09, p. 36].



2.4.1.4 Thermal Conductivity, Electric and Magnetic Properties

Pure CBN is colorless and a good electrical insulator, but doping with Li_3N , Be, Si, C, or P changes color, conductivity, and toughness [GREI06]. The electrical resistivity of CBN varies between 10^{10} – 3.3×10^{13} Ω m at room temperature [HAUB02].

The thermal conductivity ranges from 240 to 1300 W/m K [ROWE09, HAUB02]. This high thermal conductivity is caused by phonons and not electrons like in metals [HAUB02].

2.4.2 Synthesis of CBN

The first synthesis of cubic boron nitride was conducted in 1957 [KLOC05a, p. 35, WENT60]. Direct conversion of hexagonal BN into CBN without any catalyst is possible at pressures up to 18 GPa (Fig. 2.22) [BUND63]. However, the direct conversion is not used on an industrial scale [HAUB02]. In the industrial synthesis, the cubic boron nitride crystals are produced from boron and nitrogen in a HPHT

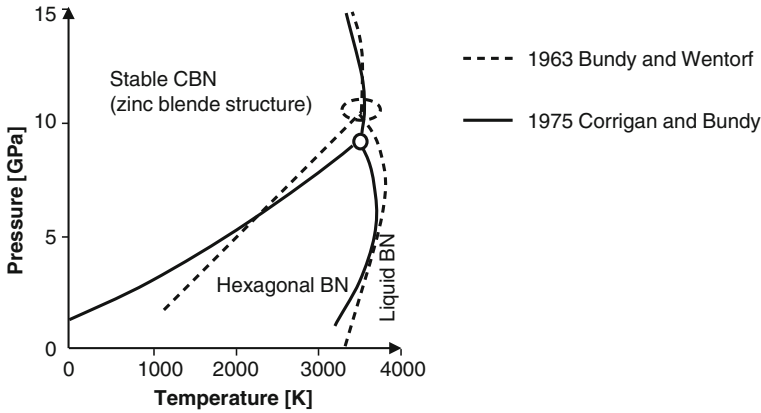


Fig. 2.22 Pressure-temperature phase diagram for boron nitride, after [HAUB02, BUND63, CORR75]

process with the help of a catalyst. The catalyst has the function of a solvent with different solubilities for CBN and hexagonal BN [HAUB02]. The hexagonal, graphitic BN is used as raw material and the catalyst metal can be elemental metal, such as Mg, Ca, Sn, Li, Ba, and a catalyst compound that decomposes to the catalyst metal or catalyst metal nitride, in particular Li_3N [WENT60].

The first synthesis processes used Li_3N catalysts and applied pressures of 4–6 GPa at temperatures between 1400 and 1700 °C [GREI06, WENT61]. Later, the use of the compound $\text{Ca}_3\text{B}_2\text{N}_4$ was investigated to gain highly pure CBN material [GREI06, ENDO81]. Today, the pressures are still between 4 and 6 GPa and the temperatures between 1300 and 1600 °C [CERA10].

First, the hexagonal α -BN reacts with the molten metals to nitrides (such as Li_3N) and to elemental boron (Eq. 2.16). Then the nitride reacts with hexagonal α -BN to a eutectic mixture. The cubic form CBN crystallizes when it becomes the stable phase depending on pressure and temperature (see Fig. 2.22).



Hexagonal boron nitride is produced by the pyrolysis, i.e. the thermochemical composition, of boron chloride ammonia (BCl_3NH_3) at room pressures and temperatures (Eq. 2.17) [MARI07, p. 93].



The synthesized material is cleaned in acid baths to dissolve the residues of the synthesis process [KLOC05a, p. 36]. Sieving or further treatment can narrow down the quality of the abrasives. In general, CBN is produced with closer shape tolerances than diamond.

2.4.3 Performance of CBN

In the first years of CBN at the market, it was seen as competitor to diamond. However, CBN proved soon to be an ideal complement for machining of hard to machine ferrous materials [JUCH78]. In addition, CBN has advantages in its higher thermal stability over diamond. In the beginning, CBN was bonded in metal or resin bonds, however, vitrified bonds featured the intrinsic advantages of CBN best. The first vitrified bonded tool needed additional profiling processes [STUC88, p. 113]. With newer bondings, now the dressing process with diamond dressing tools provides a sharp grinding wheel topography in one conditioning process.

Thermally induced damage with CBN tools is less of a problem compared to conventional abrasives [MALK08, p. 215; MALK85]. Not only are the specific grinding energies normally smaller for CBN grinding, but the abrasive grit material CBN has also a much higher thermal conductivity (e.g. 35 times bigger than that of corundum) [MALK08, p. 215 f.]. The comparably lower heat flux into the work-piece results in smaller tensile stresses and even favorable compressive stresses at the surface [BRIN82, p. 128].

CBN proves especially useful in high-speed grinding operations. The wear resistance of CBN is much higher than for conventional abrasives, so that CBN grinding wheels excel with G-ratios up to 1000× higher for steel grinding compared to Al_2O_3 tools [JACK11, p. 9 f.].

In honing tools, the usage of CBN instead of diamond enables the use of emulsion instead of oil lowering the cleaning costs for workpieces [JUCH78].

2.5 Other Types of Abrasives

2.5.1 Natural Abrasives

Before the development of appropriate grit synthesis methods, natural abrasives were used. Today, some natural materials are still used for polishing applications. The disadvantages of natural abrasives are their lower strength with the exception of natural diamond, as well as the non-reproducible grit quality [KLOC09, p. 17].

Quartz (silica, SiO_2) includes the abrasives flint and tripolite with impurities of iron oxide (FeO) and titanium dioxide (TiO_2) [KLOC09, p. 18]. Natural corundum has an Al_2O_3 content of 80–95 % [KLOC09, p. 18]. Emery consists of 37–70 % Al_2O_3 plus iron oxide Fe_2O_3 , which can be considered as abrasive material itself [LEWI76, p. 8]. Garnet includes a group of minerals with similar crystal structure and is composed as $\text{X}_3\text{Y}_2(\text{SiO}_4)_3$. Most garnet grits for abrasive applications is from almandite ($\text{Fe}_3\text{Al}_2(\text{SiO}_4)_3$) [MENA00].

2.5.2 Boron Carbide (B_4C)

Boron carbide (B_4C) is used as polishing, lapping, blasting, and grinding media for hard materials, in particular cemented carbide and fine ceramics [GREI06, KOMA97]. B_4C is produced by different methods, such as carbothermic reduction of boric oxide B_2O_3 or magnesiothermic reduction of boric oxide B_2O_3 [GREI06].

2.6 Grit Post-Processing

2.6.1 Crushing

Especially for conventional abrasives, crushing and milling are applied to change the size and shape of the abrasive grits [KLOC05a, p. 24]. For this purpose, jaw crushers, roll mills (roll crushers), gyratory crushers, ball mills, or pipe mills are utilized [LIET08]. Crushing with rollers can create needles in extreme cases; crushing with impact mills (hammer mills) produces cubical, blocky grits; crushing with roll mills causes grit splintering [MARI07, p. 79]. The crushing and milling processes are always carried out so that the abrasive grits remain sharp-edged [STAD62, p. 7].

Abrasion of the crushing equipment cannot be avoided [LIET08]. Steel equipment is preferred because the abraded particles can be removed by magnetic separators [LIET08].

2.6.2 Heat Treatment

Heat treatment in general increases toughness in conventional abrasives [SCHT81]. However, the grit toughness in one-phase systems such as white corundum and SiC is not affected much, whereas regular corundum shows a larger toughness increase at temperatures up to 1350 °C [SCHT81]. Heat treatment takes place at temperatures of 1100–1400 °C in an oxide containing, oxidizing atmosphere. The cracks and flaws created by the crushing process anneal and the containing TiO_2 converts [MARI07, p. 79, TYRO03]. Above 1350 °C grit toughness is rapidly decreased [SCHT81]. During heating, regular corundum changes its color from dark brown to dark blue and grey [SCHT81].

2.6.3 Chemical Processes

The abrasives are processed chemically with acids and water damp to obtain wanted size, shape, and purity. SiC is washed with alkali or acid to remove adhesions of silicon, metals, metal compounds, graphite, dust, and SiO_2 [LIET08].

Diamonds undergo an etching process to roughen their surface [MARI04]. Some abrasives like white corundum undergo special treatments only for marketing aspects, such as washing with acid to remove remaining particles from crushing processes. These remainings would otherwise lead to unwanted grinding tool discoloration.

2.6.4 *Electrostatic Processes*

Electrostatic methods separate sharp-edged grit shapes from blocky grits [MARI07, p. 79].

2.7 Grit Coatings

Grit coatings are either non-metallic or metallic coatings; the first ones being mostly applied to conventional grits.

2.7.1 *Non-metallic Coatings*

Grit coatings based on silane (SiH_4) are applied onto conventional grits to enhance retention in resin bonds and to resist interactions with the cooling lubricant [KLOC05a, p. 25, JACK11, p. 27, WASH12b, UAMA09]. Silane coating includes mixing of grits and silane solution, then the silane treated grits are cured [SETH11]. Dispersed silicon dioxide is either mixed directly with the grits or applied to the grits in a suspension [KUNZ91].

Red iron oxide coatings are ceramically bonded to the grit in an electronically controlled high temperature heat treatment [WASH12b]. Red iron oxide coatings protect grit surface areas and link well with resin or rubber bonds [JACK11, p. 27, WASH12b]. Corundum grits for cutoff wheels are sometimes coated with red iron oxide [MARI07, p. 79].

Ceramic coatings based on Al_2O_3 basis are also available for phenolic resin bonded tools [FACT12]. Their advantage is the high coating hardness.

2.7.2 *Metallic Coatings*

Metal coatings (also called claddings) came up in the mid 1960s for diamond grits in resin bonded wheels [DYER79]. The metallic coatings were in weight equal or exceeded the weight of the diamond grit [DYER79]. Earlier attempts with very thin

metallic coatings, primarily in metal bond wheels, had not been successful [DYER79].

Diamond in resin bonded tools, in particular for grinding cemented carbides, are usually coated with nickel comprising about 55 % by weight of the grit and coating [MALK08, p. 25, DYER79]. The optimum percentage of nickel coating does not change significantly with the grit size [DYER79].

2.7.2.1 Manufacture of Metallic Coatings

Grit coatings are applied by various technologies, such as chemical vapor deposition (CVD), physical vapor deposition (PVD), electroless coating, electrolytic wet chemical methods, or dry deposition (Table 2.3) [KOMP05, [FARK72]. The different coating processes lead to certain chemical signatures, coating morphologies, and effects on the grit material [KOMP05].

Several layers can be applied sequentially; for example, the diamond is coated with a Ti layer by electroplating, electroless plating or PVD processes first, then a Ni-coating is applied by electroplating [CAVE75]. An additional heating process induces the formation of alloys between the layers and the substrate [CAVE75]. The coated grains can additionally be etched to enhance grinding performance in resin bonded wheels [SEAL70].

The tool manufacturer has to control the tool production process carefully, because grit coatings change the grit weight and grit size. Therefore, the theoretical and real grit concentrations differ. Measuring of coating weight for diamond and CBN grains is also introduced in the FEPA 62/93 standard [MENA00].

2.7.3 Purpose of Coatings

Grit coatings are applied for various reasons, such as grit retention in the bonding, grit protection, grit alignment, or heat transfer during the tool manufacturing process or tool use. One coating can have several useful purposes, which are described in the following.

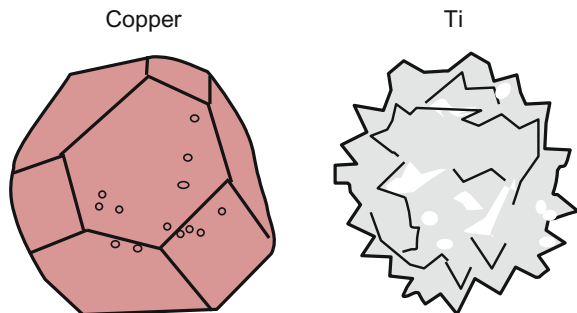
2.7.3.1 Grit Retention in the Bond

Grit morphology and grit surface define grit retention in the bonding matrix [BAIL02]. The metal nodules of coatings enlarge the effective grit surface and increase the roughness of the grit leading to a better mechanical grip (Fig. 2.23) [METZ86, p. 42, YEGE86]. In addition, the coating changes the wettability of the coated grit by the bond ingredients [METZ86, p. 42]. Especially for diamonds in resin bonds, metal coatings form a more cohesive connection with the bond than uncoated diamond surfaces [DYER79].

Table 2.3 Metal grit coating methods

Coating method	Processing temperature (°C)	Coating types	Bonding and example applications	Reference
Electroless coating—the abrasive grits are immersed in a metal alloy solution with reducing agents	<100	Ni, Cu, Ag alloys, thick layer	Phenolic and polyimide resin bonds for carbide and cermet grinding	[KOMP05]
Electrolytic coating, electroplating—the abrasive grits are wired as cathode; the metal to be deposited is the anode.	<100	Thick layer	Phenolic and polyimide resin bonds for carbide and cermet grinding, bronze saw tools for tile trimming and stone polishing	[KOMP05]
Physical vapor deposition (PVD)	~ 500	Elemental metals, such as Ti, W, thin, 2–10 μm layer	Unproven utility in metal bonds	[KOMP05]
Chemical vapor deposition (CVD)	600–800	On diamond: Carbides of transitional metals, on CBN: Metal nitride or boride, thin, 2–10 μm layer	Metal bond saws for reinforced concrete sawing, stone or rock-drilling; glass grinding wheels; ferrous material honing stones	[KOMP05]
Dry deposit method—grits are mixed with metal powder until they are covered, then the covered grits are heated	350–1000	Transition metals		[FARK72]

Fig. 2.23 Schematic appearance of two common grit coatings



In the manufacturing of vitrified bonded tools, chemical reactions between superabrasives and the bond likely occur leading to sufficient grit retention. In resin or metal bonds chemical reactions between grit and bond are less likely. Therefore, grit coatings are applied on superabrasives to allow chemical alloying between coating and bonding and to enhance grit retention [KOMP05]. For metal bonds, common coatings for Ni-, Co- or Fe-based bonds consist of Ti; for bronze-based bondings Cr is used as grit coating material [MARI04].

2.7.3.2 Grit Protection During Tool Manufacturing

Coatings on diamond grits enable the tool manufacturer to choose an inexpensive bond material with iron, which otherwise would shorten the diamond life time [KOMP05]. In addition, elevated tool manufacturing temperatures can be applied [KOMP05].

2.7.3.3 Grit Alignment During Tool Manufacturing

Grits for coated tools are coated to enhance their electrostatic properties. A grinding belt passes through an electrostatic field so that each grit is polarized and aligns with the field. [UAMA09]

2.7.3.4 Grit and Bond Protection During Tool Use—Heat Transfer

In resin bonds, coatings work as a heat sink absorbing temperature peaks during grit-workpiece contact and prevent the resin bond from burning up [DYER79]. In particular, diamond with its high thermal conductivity transfers the grinding heat fast to the resin mass, which might burn. Grit coatings disperse the heat first into the coating and thermal stresses of the bonding can be reduced [METZ86, p. 42]. The grinding processes can be more efficient due to the coating's ability to act as heat sink [HERB81]. Büttner [BÜTT68, p. 82] described one example for the heat insulating effect of nickel-phosphor coating on diamond grits in resin bond.

Metal coatings transport the process heat from the grit into the wheel bonding. The life time of heat sensitive diamond grits increases. Copper coating is a more conductive metal layer than nickel alloy for specialized bonds, so that there are some applications where copper coated diamond in resin bonds works well for grinding tungsten carbide [NOTT76].

2.7.3.5 Grit Protection During Tool Use—Grit Coherence

New coatings based on silicon dioxide or silane are modified to have hydrophilic or hydrophobic properties [KUNZ91, SETH11]. The coatings repel infiltration of

cooling lubricant between grit and bond and therefore protect the resin bond [KLOC05a, p. 25, MARI04, p. 377]. Corundum grits can be coated with silane to optimize their performance in some resin bonds. Coated abrasive tools for example can fail if water separates the backing material from the bond [SETH11].

Another advantage of coatings is a more controlled breakdown behavior of the abrasive grits [HERB81]. Metal coatings envelope friable grit particles and retain their integrity even if parts are removed by impacts in the abrasive process [DYER79].

2.8 Grit Characteristics

The characteristics of the abrasive grits are important variables controlling the process. Evaluating the characteristics is a complex problem due to the non-uniform grit geometry [BREC73]. The grit properties are influenced by the chemical composition, crystal structure, grit size, and much more. Unfortunately, many properties for ideal process performance are contradictory, such as toughness and hardness. Furthermore, tool manufacturing is affected substantially by the grit properties. Grit properties have always to be balanced between optimal properties for tool use and for tool manufacturing. The following discussion of grit characteristics aims to clarify the difficulties in the choice of abrasives.

2.8.1 Grit Size

2.8.1.1 Effect on Tool Performance

In bonded abrasive tools, grit size in combination with grit concentration influences the number of cutting edges (Sect. 6.2 “Cutting Edge Density”). As consequence, the undeformed chip thickness during grinding is affected [WERN71]. Grinding tools with smaller grit sizes commonly cause higher machining forces and shorter tool life. [LINK15]

Grit size is also connected to grit toughness. Smaller single-crystal grits, especially superabrasives, are commonly tougher because of fewer defects [FIEL81]. Conventional abrasives expose higher toughness because they are often broken down from larger grits [MALK08, p. 21].

Oversize particles in lapping and polishing can have negative effects on workpiece quality. In lapping, the stock removal rate drops as abrasive size is reduced. One reason for this are the wear particles between the workpiece and lapping plate, which perform as non-abrasive load carriers and interfere with the cutting action. A second explanation is that smaller abrasive particles lead to increased workpiece material displacement rather than cutting action. A third explanation is that the lapping plate embraces smaller particles to a bigger extent and limits the cutting action. [DAVI74]

2.8.1.2 Effect on Tool Production

Tool production is affected by grit particle size and size distribution [BENE10]. The mold packing density can be increased by mixing different sizes of grit and bond material [WEBS04]. The finer material will fill spaces between larger grit sizes and affect the homogeneity of the abrasive layer.

2.8.2 Shape, Morphology

Synthesis conditions and post-processing steps (such as crushing) influence grit shape and morphology. For diamond grits, the shape correlates well with grit toughness and grit performance [LIEB96, GESU00]. There are several measurable characteristics to describe the shape of abrasive grits, such as ellipticity or roundness (see Sect. 2.9.2 “Grit Shape Selection and Analysis”). However, one value is not sufficient to classify a grit explicitly and the single values differ for different grit morphologies.

2.8.2.1 Effect on Tool Production

Grits for bonded tools should expose a rough surface to provide mechanical adherence in the bonding [DYER79]. For the production of bonded tools, abrasives of a given size and shape have a limiting natural packing density that can be reached by shaking and pressing. Coarser and blockier grits have a higher packing density than finer and less symmetrically shaped grits [MALK08].

2.8.2.2 Effect on Tool Performance

The shape itself is less important than the breakage behavior and the number of cutting edges. This relates to the chip thickness, process forces, and workpiece roughness. The sharpness of a cutting edge defines the engagement into the workpiece, the proportion of elastic or plastic deformation and chip forming. Many grinding models for superabrasive grits work with simplified grit geometries like balls, ellipsoids, or octahedrons [DOMA06, HEIN09b, KOSH03]. For CBN grits, octahedrons give realistic simulation results [YEGE86]. Metallic grit coatings change the grit surface and support bond retention, especially in resin and vitrified bonded grinding wheels (Sect. 2.7 “Grit Coatings”).

In the same way, grit shape, size, size distribution, and breakdown characteristics are important variables for process control in abrasive processes with loose abrasives [DAVI74].

2.8.3 *Hardness and Temperature Hardness*

The hardness of abrasives is defined in terms of the static indentation hardness as determined by Knoop or Vickers hardness test [MALK08]. Chip formation needs a high degree of grit hardness and toughness [KLOC05a]. Moreover, cutting edge sharpness over a longer period is affected by the grit hardness and wear resistance. There is no direct physical relation between hardness and toughness, but commonly harder abrasive grains are more friable [MALK08].

Jackson gives the rule of thumb that a grit has to be at least 20 % harder than the workpiece to be suitable as abrasive [JACK11, p. 9]. He regards hardness as the key factor in controlling attritious grit wear (see Sect. 6.4.2 “Grit Surface Wear”). In addition, hardness can change with the temperature, meaning temperature hardness has to be also considered in tool use [JACK11, p. 9].

2.8.4 *Toughness, Breaking Behavior*

Today, grits are available in a large range of toughness suitable for many applications [MARIO4, p. 347]. Hard and friable abrasives are generally applied in precision grinding, whereas tough, large grits are more suitable for heavy-duty grinding [MALK08]. Grit types for resin bonds are usually more friable than for bronze bonding [BÜTT68, p. 73].

Toughness is the resistance of a material against breakage and crack propagation and is often measured under dynamic conditions [LINK15]. Higher toughness implies that the grit is less likely to fracture when engaging the workpiece. The breaking or fracture behavior describes how the grits break, i.e. breakout of large or small particles, leaving a rough surface with many cutting edges or a smooth surface with only one cutting edge (see Sect. 2.1.5 “Performance of Corundum”). Jackson and Davim introduce the term friability as inverse term of fracture toughness [JACK11, p. 11]. The sum of toughness and friability, both in [N], accounts to 100 [SCHT81]. The “toughness index” is one industrial measure [VOLL12]. Temperatures during grinding can induce grit defects that change the grit breaking behavior, so “temperature toughness index” is another useful measure. The “friability index” is a measure for the loss of abrasive material by splintering [JACK11, p. 11].

On the one hand, grits that are too tough for a special application will become dull and increase friction. This leads to unnecessary thermal damage of the workpiece material and the danger of process vibrations. On the other hand, too friable grits wear away quickly resulting in short tool life and possibly form errors. As optimum, the grits should have a controlled breakdown behavior, so that they regenerate sharp cutting edges and the tool works in the so called self-sharpening mode.

Conventional grits are usually produced by crushing of coarser material resulting in fewer surface defects and in less friable grits [BREC73, MALK08]. In the same

way, smaller diamond grits are commonly tougher because of fewer structural defects [FIEL81]. The toughness of conventional abrasives can be changed through the sintering temperature of the grinding tool [SCHT81].

Natural and synthetic diamond grits show different breakage behavior. Natural diamond collapse with several breakage events, synthetic grits, however, fail with one breakage event [HIMM90].

2.8.5 Thermal, Electric and Magnetic Properties

2.8.5.1 Effect on Tool Production

High sintering temperatures over 1300 °C can occur in manufacturing of vitrified bonded tools. In particular, diamond features low thermal wear resistance in air, which forced manufacturers to develop special low-temperature sintered bonds and to apply inert atmospheres [LINK15].

Electric and magnetic properties are important for electro-plated bonds because they affect the deposition of the galvanic bond on grit and tool body [LINK15]. In particular, synthetic diamonds contain metallic inclusions, mostly of ferromagnetic character [YIN00]. For the tool manufacturing process, it is therefore necessary to separate between magnetic and non-magnetic grits.

2.8.5.2 Effect on Tool Performance

In the use phase of abrasive grits, the most important thermal properties are the thermal conductivity, the point of softening under load, and the melting point [KLOC05a, p. 34]. Thermal conductivity describes the material's ability to level temperature differences. The grits will be loaded with a nearly punctiform heat source at the cutting edges during chip formation. With high thermal conductivity, the heat will distribute quickly along the grit volume.

For corundum, the temperature conductivity decreases rapidly with increasing temperature [KLOC05a, p. 34 f., COES71]. For high temperatures, it can be expected that the heat load concentrates more and more on the cutting edge leading to heat peaks. Thermal stresses inside the grit increase, being intensified by the simultaneously increasing thermal expansion coefficient. Thermal stress can occur between grit and bonding for strongly distinct thermal expansion coefficients [KLOC05a, p. 34 f.]. In synthesized diamonds, the thermal expansion of the metallic inclusions can induce grit fracture [MARI07].

High chemical resistance is desired for the grits when they interact with the air, cooling lubricant, or workpiece material. Chemical reactions could weaken the grit and need to be avoided also at higher pressures and temperatures [KLOC05a, p. 19].

2.8.6 *Distribution of Characteristics Within Batch*

Grit characteristics in a batch appear always in a range. A narrow distribution of characteristics allows a good predictability for the later tool performance [DYER79]. Abrasive layers should be homogeneous to have constant performance during lifetime and no imbalance during tool rotation. Grit density and grit size are related to the number of cutting edges in a bonded abrasive tool [YEGER86].

In the case of grit sizes, the use of a wider range facilitates the wheel manufacture, because it becomes easier to pack the abrasive grits tightly together in molding the wheel [MALK08]. Control of grit size and size distribution lowers the danger of high rejection rates [BENE10]. Grit size distribution is defined as the percentage of particles of different size in the defined grit size range.

2.9 Methods for Grit Selection and Analysis

2.9.1 *Grit Size Selection*

2.9.1.1 *Sieving*

The size distribution of abrasive grits is adjusted by sieving for coarser grits and sedimentation for finer grits [KLOC05a, p. 27, MARI07]. Sieving is the simplest method to separate particles and works with sieves of defined mesh sizes [SALM07, p. 132]. Sieving can be performed manually or automatically on dry or wet batches.

Several national and international standards exist to define the size ranges (Tables 2.4 and 2.5). It has to be noted that most standards define the grit sizes as a range and not as single values. European standards are mainly based on DIN ISO 8486-1 and the so called FEPA standard from the European Federation of Abrasives Producers (FEPA) [KLOC05a, p. 28]. As example, the FEPA standard ranges from the largest grit size F4 (diameter 3 mm) to the finest F1200 (diameter 3 μm).

Most standards define conventional abrasives by a pair of numbers corresponding to the mesh size of two sieves [ANSI01]. The mesh size is given in number of meshes per linear inch. The lower number is the mesh number, through which the grit just passes, while staying on the sieve with the upper number mesh size (Eq. 2.18) [MARI07].

$$\text{ANSI, FEPA conv.} = [\text{mesh per inch upper sieve}/\text{mesh per inch lower sieve}] \quad (2.18)$$

Superabrasive grits are commonly defined by the mesh size, through which the grit will just pass, given in micrometer (Eq. 2.19) [MARI07, KLOC05a].

Table 2.4 International standards for grit sizing for bonded tools [MENA00, BENE10, MARI07, ANSI01]

Norm	Grit type and size		Sizing method
ANSI B74.12	Conventional grits, in particular fused Al ₂ O ₃ , SiC	Macrogrits	Sieving
ANSI B74.10 [ANSI77]		Microgrits	
DIN ISO 8486-1 [DIN97]		Grit sizes F4–F220	Sieving
DIN ISO 8486-2 [DIN97]		Grit sizes F230–F1200	Sedimentation
FEPA 42-1:2006		Macrogrits F4–F220	
FEPA 42-2		Microgrits	
ISO R565-1990 and DIN 848-1988	Superabrasives		
FEPA 61/97		Macrogrits	
FEPA 60/77		Microgrits	
ANSI B74.16		Macrogrits	
ANSI B74.20 [ANSI81]	Diamond grits	Microgrits (powder)	Microscopical

Table 2.5 International standards for grit sizing for coated abrasives [MENA00, ANSI01]

Norm	Grit type and size	Sizing method
FEPA 43/93	Microgrits and macrogrits	
ISO 6344 (part 1 and 2)	Macrogrits, P12–P220	
ISO 6344 (part 3)	Microgrits, P240–P2500	
ANSI B74.18-1984 [ANSI84]	Al ₂ O ₃ , SiC, garnet, size 220–12 Flint, size 220. 180. 150 Emery, fine–extra coarse Flint, extra fine–extra coarse	Sieving
	Al ₂ O ₃ , SiC, garnet, flint, size 600–240	Sedimentation

$$\text{FEPA superabrasives} = [\text{size of mesh hole through which grit just passes in microns}] \tag{2.19}$$

The size definition by mesh implies no absolute value, but rather a size band. The tolerances, i.e. the permitted particles with sizes above and below the defining band, are based on the total weight. Consequently, the proportion or number of finer particles to coarser ones within a given size is not fixed [ENGL03]. This leads to variations in number of particles per carat and average grit size within a specified size. Therefore, abrasive tool performance can fluctuate.

2.9.1.1.1 Sieving Procedure

Each grit size has a set of five sieves of metal wire cloth with decreasing mesh size, e.g. defined by ISO 3310 [DIN97]. The reason for the five sieve setup is to simulate the actual mass when using the sieves for test grading [ANSI01]. The sieves are arranged with the roughest sieve above and the finest below it, on a cup. The aperture size decreases technically by a factor of $\sqrt{2}$ in the stack of sieves [MALK08, p. 12]. A certain mass of a representative grit probe is put onto the top sieve. After a certain time on a test-sieving machine (defined by ISO 9284 or ANSI B74.12) the amount of particles on each sieve is weighted [ANSI01].

As example, the total probe volume of a F10 grit sample has to pass sieve 1 (mesh size 3.35 mm) (Fig. 2.24). Sieve 2 (mesh size 2.36 mm) can be passed fully, but a maximum of 20 % mass can be withheld. On sieve 3 (mesh size 2 mm) a minimum of 45 % probe mass has to retain, but 100 % may have passed sieve 2. The combination of sieve 3 and 4 (mesh size 1.7 mm) has to hold a minimum of 70 % of the total weight, so sieve 4 has to retain the difference, i.e. a maximum of 25 %. There are no definitions for the finest sieve 5 (mesh size 1.4 mm), but only 3 % of probe mass is allowed to pass sieve 5 and to be collected in the bottom cup.

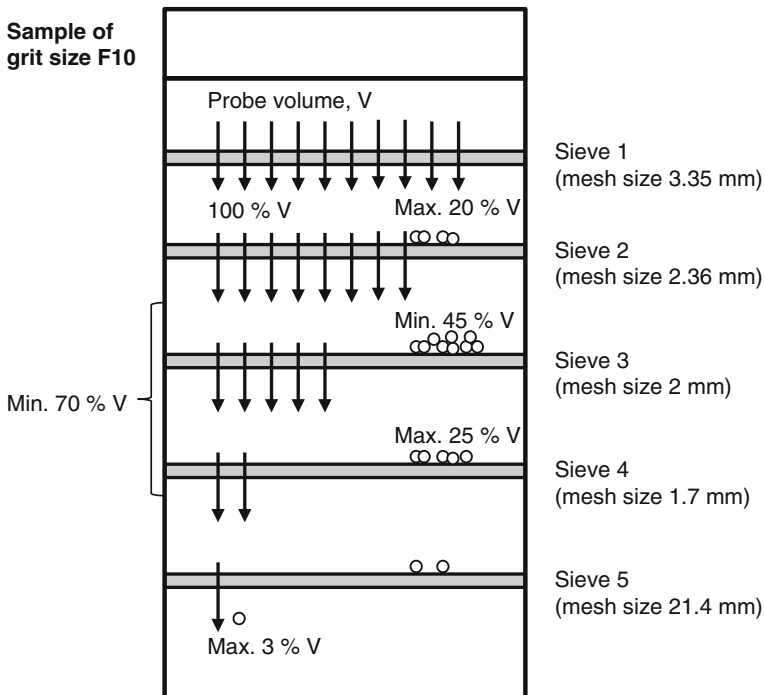


Fig. 2.24 Example for mesh sizing [DIN97]

Metrological variances are considered in percentage deviations of 3 to 4 % of retained probe mass [DIN97, ANSI01].

2.9.1.2 Sifting

Sifting is a separating procedure where the falling particles are exposed to a contrary flow [SALM07, p. 134]. If the flow rate meets the falling velocity of a certain particle size, these particles hover. Smaller particles stay in the flow, coarser particles decant.

One method is to suspend the particles in an aerosol beam and measure the movement time of the particles between two points of known distance apart [UAMA09]. If a fluid is used as medium, the process is called elutriation [SALM07, p. 137]. Air forms the medium for wind sifting and the time of flight defines the mass and grit size.

2.9.1.3 Sedimentation

Stokes' law can be used for evaluating the particle size distribution (Eq. 2.20) [ANSI77]. Sedimentation or Stokesian methods work with a stationary medium and the particles are in free fall [SALM07, p. 138]. Sedimentation methods are usually used for grading finer grit, such as in ANSI B74.10 [ANSI77].

$$\text{Stokes' law for small spheres } v = \frac{2 \cdot g \cdot r^2 \cdot (p - d)}{9\eta} \quad (2.20)$$

- v settling velocity in (cm/s)
- g gravity acceleration in (980 cm/s²)
- r effective particle radius in (cm)
- p density of the particles in (g/cm³)
- d density of the settling medium in (g/cm³)
- η viscosity of the settling medium in [g/(s cm)]

The FEPA 43 and DIN ISO 8486-2 standards define a calibrated US-Sedimentometer. The water in the sedimentation tube should be thermally controlled. In an automated system, light barriers can measure the sedimentation height per time [TOPA10]. This data is then used to calculate the particle size distribution with Stokes' law. Another method is to apply abrasive grits in a carrier medium onto the surface of a rotating fluid ring.

Stokesian methods work best for spheres. Flat particles and needles experience a greater drag per unit mass than spheroidal particles. As consequence, they settle in a viscous medium as fast as smaller round particles and will therefore cause oversizes in the grading. Especially for fine finishing operations such as lapping and polishing, these oversizes can ruin the workpiece quality. [DAVI74]. Overall, irregular, less

blocky grit shapes can present severe problems in size grading [HERB81]. In addition, sedimentation can be a very time consuming method (more than 24 h for very fine particles) [UAMA09]. The operator has to constantly tap the settling tube during the test to insure even packing and level settling [UAMA09].

2.9.1.4 Counting Methods

Counting methods work for single particles or on their projection [SALM07, p. 140]. A common procedure for counting abrasive grits is laser granulometry. Herein, a mixture of loose samples in a fluid medium flows through a ring. Laser light leads to different shadowing effects depending on the grit size. Commonly, three proportions of different grit sizes are measured, i.e. grit sizes of 10 % of biggest and of smallest grit proportion of the complete grit mixture and the size, which is 50 % of sample, in total 10, 50, 90 % [HORI10].

Especially for coarse diamond grits, the number of particles per carat (PPC) is an important characteristic. Coarser diamonds with high purity are used in electroplated tools, rotary dressing tools or as so called “saw grits” in saw blades, circular saws, drill bits, wire saws, and milling tools, e.g. for stone cutting or drilling operations. Since PPC may vary if the average grit size is defined by the sieving method, significant variations in tool performance can occur [ENGL03]. Therefore, the number of particles per carat offers an additional measure for the consistency of the diamond batch [LIST08]. The PPC value can be obtained directly by weighing and counting or indirectly by two-dimensional digital image processing [LIST08].

2.9.1.5 Other Methods

Several more methods for particle size characterization exist, such as laser light diffraction, dynamic light scattering, photon correlation spectroscopy, Brownian motion turbidity, etc. [BENE10].

The size of microgrits can be analyzed by their electrical resistance as defined in the ANSI standard B74.10-2001 [UAMA09]. The underlying principle is that a particle causes a change in the strength of the current proportional to the particle volume [UAMA09]. Problems, however, arise for irregular grit shapes, which will be graded with finer sizes than by sedimentation methods.

2.9.2 Grit Shape Selection and Analysis

2.9.2.1 Picture Analysis

Picture analysis is based on a two-dimensional projection of the grit, e.g. via back light microscopy or film scanners, or on a picture, e.g. by transmitted light

microscopy or scanning electron microscopy. Picture analysis has some restrictions. The equipment defines the minimum grit size that is measurable. In addition, the grit placement interferes with the measured results. For example, when the grits are dispersed on the scanner plate, the probability of grits to fall on certain grit planes varies.

Picture analyses work mostly on a two dimensional projection of the abrasive grits. Figure 2.25 gives an example for different measurement values from a two-dimensional picture, such as maximum and minimum grit diameter, grit circumference, and grit cross-sectional area in the projection plane. Some shape characteristics are derived in comparison with a coextensive circle, i.e. a circle with the same area as the projected grit (Fig. 2.25).

Equations 2.21 [LIEB96] and 2.22 [LIEB96, SCHI02] define shape factors indicating grit roundness. The ratio in Eq. 2.23 is another characteristic for the roundness or compactness [PIRA03, LIST06]. The grit ellipticity can be evaluated by Eq. 2.24 [GESU00, SCHI02]. Further characteristics are derived from the proportion of convex parts in the grit perimeter [LIST06].

$$\text{Max. grit diameter/diameter of coextensive circle} \tag{2.21}$$

$$\text{Grit perimeter/perimeter of coextensive circle} \tag{2.22}$$

$$4\pi \text{ grit area}/(\text{grit perimeter})^2 \tag{2.23}$$

$$\text{Max. grit diameter/min. grit diameter} \tag{2.24}$$

Two methods to define the particle size are possible, such as the grit's largest dimension or the average of the maximum grit dimension and the largest dimension rectangular to it [DAVI73, DAVI74, BENE10]. Taking a round grit, both values are similar. For an elongated grit, the largest dimension is much bigger than the average dimension calculated by the second method. Thus, the greater the deviations from the ideal blocky shape, the bigger the difference of both measurement methods. One

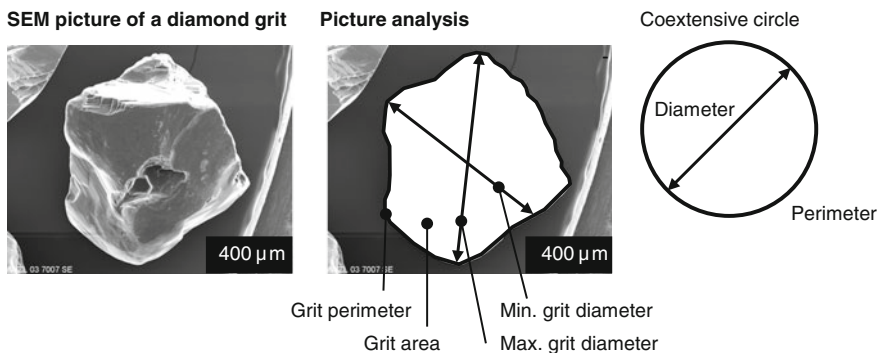


Fig. 2.25 Example for picture analysis of a grit

method for grit size analysis of micron powder recommended by FEPA is to take the smallest circle, which circumscribes the particle [HERB81].

2.9.2.2 Packing Density

Packing density or bulk density depends on grit size and shape. For example, equidimensional shapes pack to a higher bulk density than flat shapes [MENA00]. The packing density is a rather simple but effective measure for the dominant grit shape of a batch, if grit size and size distribution are known [MALK08, SCHAT81].

Measurement procedures for the packing density of conventional abrasive grits are defined in ISO 9136, parts 1 and 2, or ANSI B74.4 [MENA00]. ANSI B74.17 specifies the packing density for superabrasives [MENA00]. One method is to determine the weight of grits required to fill a cylinder of known volume when the grits are allowed to flow through a funnel and fall from a fixed height [ANSI92]. The packing density is given in (kg/l), (g/l) or (g/cm³) [SCHAT81, ANSI92].

2.9.2.3 Shape Sorter

The shape sorter, also called vibration table (German “Rütteltisch”) consists of an inclined table, which by oscillating causes the abrasive grits to move up or down depending on their shape. Boxes at the edge of the table collect the different shape fractions. Diamonds are sorted from cubic crystals and cubooctahedrons to broken particles of irregular shapes, such as needle-like crystals or platelets. The principle works only for batches of the same grit size range [VOLL10, LINK15].

2.9.3 Toughness and Breaking Behavior Analysis

2.9.3.1 Friatest

Manufacturers of superabrasives evaluate the grit fracture behavior by impact strength tests, so called friability test or friatester [ODON76, MARI04]. A grit sample with a defined weight and a steel ball are encased in a capsule, which is then shaken with a defined cycle number [VOLL12]. The impact load breaks a portion of the grits. The percentage of the non-destroyed grits is defined as toughness index (TI) [VOLL12]. The friability index (FI) defines the number of cycles needed to break 50 % of the grits [VOLL12]. Diamond grit manufacturers qualify their grits by room temperature toughness (TI) and thermal toughness after heating (TTI), for example at 1000 °C [MARI07]. [LINK15]

In general, the friability characteristics do not have a sufficient correlation to the grit performance and more research is needed. Another problem of the friability test method is that several characteristics intermingle in the test results.

2.9.3.2 Single Grit Toughness Test

The single grit breakage test enables a particle related description of grit strength. This method is based on the maximum force to break a particle, measured along one axis [VOLL03a, VOLL03b]. Some systems allow combining a two-dimensional picture analysis of grit size and grit shape, and measurement of the specific breakage force. In the procedure, a single grit is positioned between two anvils, which are pressed together with increasing, pneumatic force until the grit brakes [LIST06]. The maximum uniaxial force needed to break the particle is measured. The force divided by the grit area defines the breakage strength.

Diamonds with a diameter of 250 μm can have average breakage strength of 5000 N/mm^2 , so that the pressing forces have to be sufficiently high [LIST06]. The single grit fracture test has similarities to the real grinding process, where the normal forces are higher than the tangential forces.

Benea and Griffin introduced a strength testing method for micron powder [BENE03b].

2.9.4 Analysis of Residual Stress via Polarisation Microscopy

Polarisation microscopy can detect stresses inside of transparent single-crystals, which is in particular important for monocrystalline diamond for jewelery [KLEB98, LENZ86]. Lattice defects in the crystals result in interference patterns and are recorded in double refraction pictures [MALZ00]. The results can be improved by embedding the grits into material with the same refractive index so that light refractions are avoided at the grit surface and only the internal refractions due to lattice defects appear.

2.9.5 Magnetic Susceptibility Selection and Analysis

ANSI B74.19 presents a test method to determine the magnetic content of conventional abrasive grits [MENA00, ANSI90]. A standardized magnetic analyzer is used on a sample size of 150 g. Its two coils, one as a reference, one for the sample, are excited with an odd frequency AC source (390 Hz) [ANSI90]. The unbalance is measured and translated to the relative magnetic content of the sample [ANSI90]. Other analyzers on the market work with 80 Hz excitation and are mobile [VOLL11a].

A sorting process for magnetic and non-magnetic grits can be based on lifting one sort of grits from a drum or a belt with a magnetic force higher than the grit gravity force [VOLL11b]. A related task is to recover abrasives from blasting material containing magnetic, metallic particles [DREN97].

2.9.6 Other Analyses

Grit hardness is usually tested by a Knoop micro indenter test [SCHT81, MENA00]. By means of an electrostatic separator, particles with conductive surfaces can be selected. Capillarity is a measure for the wettability of abrasive grits [UAMA09, SCHT81]. Capillarity gives an indication of grit cleanliness and is particularly important for aqueous glues for coated abrasive tools [UAMA09]. The test procedure foresees to fill glass tubes with the grit sample and measure the capillarity height of water [SCHT81, ANSI64].

Several chemical analyses are in practice, such as atomic absorption, emission spectroscopy, and X-ray fluorescence [MENA00]. Silicon carbide can be heated in a 27 % potassium hydroxide solution for 9 h to detect free silicon dioxide [SCHT81]. Other chemical analyses are based on classical wet methods, such as FEPA 46/93, ISO 9285, and ANSI B74.14 for fused aluminum oxides and ISO 9286, FEPA 45/93, and ANSI B74.15 for silicon carbides [ANSI86, MENA00].

2.9.7 Evaluation of Grit Analysis and Sorting Techniques

The sorting method affects the variance of grit characteristics in a batch. This has a direct correlation to tool manufacturing and tool performance. One has to be aware that variances in the process chain add up. A narrow distribution band of grit characteristics defines the tool performance more precisely. This potentially leads to highly efficient and well balanced abrasive processes. Low scrap rates and high product quality are important for sustainable manufacturing technologies. However, the sorting method to obtain the narrow band might be more expensive. Additionally, a broad grit size distribution can facilitate tool manufacturing by lower mold pressure and higher packing density. Both, selection method and tool manufacturing affect the tool price.

Uniformity of the grit batch is a useful characteristic for the quality of grit selection; however, the overall quality of the batch has to be judged according to the application. Novikov et al. [NOVI08] describe a calculation method for uniformity, which allows assessing powder uniformity from diverse characteristics. Uniformity can be improved during the abrasive grit production, at the stage of grit selection, and by grit sizing [NOVI10].

In Table 2.6 the most important analysis and selection methods are compared. Criteria are the applicability for superabrasives or conventional grits, use as selection method, or non-destructive method. Some methods are only applied for macrogrits or for powders. In addition, measurement methods can be characterized by the following criteria [BENE10]:

- Accuracy = closeness of the measured value to the true value,
- Precision = variation in repeated measurements,

Table 2.6 Comparison of grit analysis and sorting methods, na = not applied, + = yes, - = no [LINK15]

Method	Characteristics	Apt for conv. grits?	Apt for superabrasives?	Selection /sorting method?	Non-destroying method?	Other comments
Sieving	Size	+	+	+	+	Size is important for mold pressure, macrogrits
Granulometry	Size			-	+	
Sedimentation / Stokesian Methods	Size			+	+	Used for microgrits
Picture analyses	Size, shape	+	+	-	+	Only applicable for macrogrits, processing time
Shape sorter	Shape (toughness)	-	+	+	+	Avoid electrostatic
Packing density	Shape	+	+	-	+	Combined with sieving
Friatest	Toughness	+	+	-	-	
Single grit breakage tests	Toughness	+	+	-	-	
Magnetic separator	Magnetic susceptibility	na	+	+	+	Magnetic inclusions
Magnet susceptibility analyzer	Magnetic susceptibility		+	-	+	
Electrostatic separator	Electric conductivity	na	+	+	+	Adjusted grit direction
Polarisation microscopy	Stresses in single crystals	-	+	-	+	

- Reproducibility = variation between different instruments, operators and sample preparation,
- Resolution = minimum detectable differences between features,
- Upper and lower limits.

These criteria were not evaluated in Table 2.6 because they differ for the equipment and are in constant development. Future research should focus on the effort per sorting method and the achievable tool performance and productivity. This could be connected to the sustainability analysis in Chap. 7 “Sustainability of Grinding”.

2.10 Sustainability Dimensions to Abrasive Grits

2.10.1 *Technological Dimension*

Table 2.7 summarizes the most important grit characteristics in grinding technology. In general, the grit type is chosen with regard to the machined material and the grit size is defined by the desired workpiece quality. The individual performance profiles of the grit types can be visualized in radar charts [HELL11].

The abrasive material should be harder than the machined material. In general, corundum and CBN are used for long-chipping, ductile materials, whereas silicon carbide and diamond are used for short-chipping, brittle materials or titanium alloys [KLOC09, HELL11, LINK12b]. Superabrasives are chosen in particular for the higher precision or higher performance applications due to their low wear rate and ability to achieve close size tolerances [ROWE09, LINK12b]. The reactivity of diamond with transition metals such as nickel and iron limits the use of diamond to machine these metals, especially steels. However, there are some applications with ferrous materials where diamond is the tool material of choice, e.g. honing of cast iron [MARI07]. Diamond covers many applications formerly conducted by SiC [JUCH78].

The higher thermal conductivity of superabrasives compared to conventional abrasives can reduce grinding temperatures drastically [ROWE09, LINK12b]. For a specific application, the use of corundum could lead to unfavorable tensile stresses in the part surface layer, whereas CBN could produce favorable compressive stress [BRIN82, BRIN04b]. However, there is a common understanding that the surface finish is rougher with CBN grits than with conventional wheels [LINK12b]. It is believed that sharper and more pointed cutting edges lead to earlier chip formation and shallower initial depth [MALK08]. CBN grits have typically chip angles between -60° and -70° and have sharper cutting edges than conventional abrasives [FERL92, p. 31].

Table 2.7 Relevant properties of abrasives for tool manufacturing and use [MALK08, KLOC05a, JUCH78, MÜLL01, GRAN12]

	Diamond	CBN	SiC	Al ₂ O ₃
Main elements components	≈100 % C	≈43.6 % B ≈56.4 % N	≈97 % SiC	95–99 % Al ₂ O ₃
Crystal structure	Cubic	Cubic	Hexagonal	Hexagonal
Manufacture of abrasives	HPHT-synthesis	HPHT-synthesis	Melting in resistance furnace	Melting in arc furnace or sintering or sol-gel procedure
Density (g/cm ³)	3.52	3.48	3.22	3.8–3.98
<i>Effect on tool performance</i>				
Chemical reaction relevant to tool use [JUCH78]	Chemical reaction with non carbon saturated steels above 875 K	Possible chemical reaction with water above 1075 K	Chemical reaction with ferrous materials	Chemically neutral
Knoop hardness (HK)	7000–8000	4700	2400–3000	1600–2160
Thermal stability up to K	1173	1643	1573	2273
Thermal conductivity (W/m K)	600–2100	200–700	55	6
Fracture toughness K _{IC} (MPa m ^{1/2})	3–3.7	3.7	3.1	2.7–4.3
<i>Effect on tool production</i>				
Chemical affinities relevant to tool manufacture [JUCH78]	Chemical reaction with oxygen above 1075 K	Heat-resistant up to 1375 K	Chemical reaction with flux like boron acid, water glass, above 975 K	Chemically neutral
Melting point (°C)	≈3700 °C at 130 kbar (triple point)	≈3200 °C at 105 kbar (triple point)	≈2830 °C	2040 °C

2.10.2 Economic Dimension

The fusion of corundum began at the Niagara Falls using cheap hydro-electric power. Today China has huge capacities for producing fused corundum, and Eastern Europe, India, South Korea, and South America are growing manufacturers in the world production of fused corundum [JACK11, p. 27]. Low cost energy has become an important factor for the competitiveness of corundum producers, as well as furnace capacity, and low costs of raw material sourcing [JACK11, p. 27]. Similar challenges apply for manufacturers of all abrasive grit types.

Today, tool producers can choose between several grit toughnesses amongst one grit type [MARI04, p. 347]. A high toughness does not necessarily lead to the longest grit life. On the one hand, grits which are too tough for a special application will become dull and increase friction. This leads to unnecessary thermal influence and process vibrations. On the other hand, too friable grits wear away quickly resulting in short tool life and possible form errors.

The tool user can choose between conventional and superabrasive grits, which both generate highly efficient grinding wheels. The decision has to consider the grit properties in the abrasive layer on the one hand. For example, superabrasives have higher raw price costs than conventional abrasives, but also a better wear resistance leading to higher efficiency of superabrasives. On the other hand, the production environment has to be taken into account. For example, the usage of CBN can be very cost-effective in serial and mass production with appropriate machine tools. In contrast, in small and middle-size companies, flexible production with conventional tools follows the trend towards product diversification and stock reduction.

The price of grinding tools is strongly influenced by the price of the grit material, accounting for up to 50 % of CBN tools. The grit price increases with the pressure during the production process, the length of the process, and the overall energy consumed (Fig. 2.26 left). Although diamond synthesis needs very high pressures, the process happens only in several minutes. In contrast, corundum synthesis takes hours or even days and needs therefore power longer. Grit costs and hardness, which indicates wear resistance against abrasive wear, shows some correlation (Fig. 2.26 right).

2.10.3 Environmental Dimension

The ecological hazard of abrasive grits themselves is minor (Table 2.8 left), but some problems arise from the grit production emissions and waste. Emissions from the production of conventional abrasive grits are likely to consist primarily of particulate matter (PM), and carbon monoxide (CO) from the furnaces [EPA94].

In the sintering process of SiC from quartz and coal (with salt and sawdust as auxiliary materials), a considerable amount of greenhouse gas CO₂ is produced

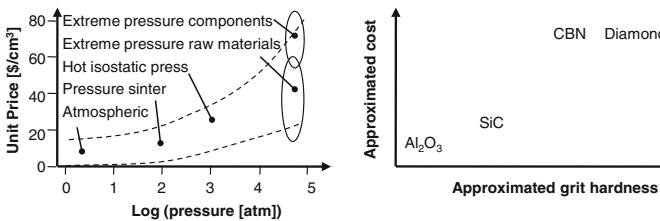


Fig. 2.26 Economic correlations for abrasive grits, *left* price and manufacturing pressure [LUCE13], *right* price and hardness [UAMA09]

Table 2.8 Examples for information the material safety data sheets [WASH12]

	Known ecological information	Chemical safety assessment
Emery	–	Irritant (eye, respiratory system)
Boron carbide	Low order of aquatic toxicity, low potential for bioaccumulation	Harmful (oral, inhalation) suspect reproductive hazard
Zirconia corundum	Low potential for bioaccumulation	Irritant (skin, eye, respiratory system)
Brown corundum	Low potential for bioaccumulation	Irritant (skin, eye, respiratory system), suspect carcinogen (inhalation—repeated exposure only)
White corundum	Low potential for bioaccumulation	–
Silicon carbide	Low potential for bioaccumulation	Irritant (skin, eye, respiratory system)

(Eq. 2.10). Salt and sawdust are likely to produce chlorides and volatile organic compounds (VOC) [EPA94]. Moreover, the SO₂ and dust in the waste gases cause pollution [LIET08]. Furnaces collect and trap the reaction gases, so that CO can be purified and used [LIET08]. The gases can be desulfurized so that elemental sulfur is obtained as well [LIET08].

The production of corundum is likely to emit fluorides, sulfides, and metal constituents of the raw materials. Sol-gel processing of sol-gel corundum emits NO_x [EPA94].

The re-processing steps of conventional abrasives like cleaning and refinement also use diverse acids and complex machinery. Grit crushing emits PM [EPA94]. Also in the synthesis process of superabrasives, metallic catalysts and refractories remain as waste material. Moreover, metallic grit coatings are common to improve retention and heat-flow in resin and vitrified bondings, but may involve hazards in their production.

Because of the different synthesis routes for the different grit types, the energy consumption to produce a gram of abrasives is different (Table 2.9). Furthermore, the energy consumption per machined part material will be different due to the different wear resistances (see Sect. 8.1 “Case Study on Conventional Abrasives vs. Superabrasives for Vitrified Bonded Tools”).

Solid or chemical waste from grit production processes needs to be classified and may be treated as hazardous waste. Some manufacturing approaches re-use scrap material. For example, one grit manufacturer fuses recycled aluminum oxide into high quality fused aluminum oxide, so that a completely closed loop process is possible recycling 100 % of the spent material [WASH12]. In another example, grit producers invented a process using alumina/zirconia/silica scrap, because zirconia for the production of zirconium corundum has a high cost [ASHL96]. By adding a reducing agent, the silica content of the final abrasive grit can be kept below 0.8 % by weight [ASHL96].

Table 2.9 Environmental material data (* estimated data) [GRAN10]

	Embodied energy, primary production (estimated) (MJ/kg)	CO ₂ footprint, primary production (estimated) (kg/kg)	Water usage (estimated) (l/kg)	Raw materials
SiC	*70.2–77.6	6.25–6.91	*33.5–101	Si and carbon are plentiful
Al ₂ O ₃ (99.5 % purity)	49.5–54.7	2.67–2.95	29.4–88.1	Al ₂ O ₃ is one of the most plentiful chemical compounds in the earth's crust
H-BN	120–133		126–139	

2.10.4 Social Dimension

Mining for raw materials is known for having many physical, chemical, biological, ergonomic and psychosocial occupational health hazards [DONO04]. In addition, the processing of grits can be harmful to workers. For example, the emissions from melting corundum from bauxite in electric arc furnaces can lead to a lung disease known as corundum smelters lung, bauxite worker's lung, or bauxite fibrosis (German "Korundschmelzerlunge") [KONE94, p. 473].

The abrasive grits and powders themselves can create nuisance dust, which can cause respiratory tract irritation, coughing, and shortness of breath. Human skin and eyes can be harmed by mechanical, abrasive action of the grits (Table 2.8 right). In particular, mining and processing of silica, or sandblasting operations with silica are tied to respiratory diseases [MADL08, DONO04]. The protection of workers in these applications is crucial.

2.10.5 Sustainability Model for Abrasive Grits

Raw material extraction, manufacturing, and choice of abrasive grits for later processing and use affect different stakeholders. The grit manufacturer is mostly concerned with the following aspects:

- The **grit price** depends on raw material availability, raw material price, local energy costs, labor costs as well as equipment costs and maintenance.
- The **location** defines energy and material availability, labor and energy costs, and logistics.
- **Hazards to the environment and the workers** need to be reduced and evaluated by local regulations.

Most important aspects for the tool manufacturer are as follows:

- The **grit price** affects the later tool price strongly, up to 50 % in the case of CBN.
- **Grit availability and quality** defines the constancy of tool quality.

The tool user is concerned about

- **Technology**, in particular how the abrasive grit material interacts with the workpiece material and how the tool wears in the use phase.
- The **tool price** is affected by the grit price and important for the tool user's competitiveness.

Society worries about

- **Mining hazards** from emissions and particulate matter to the local community and to the workers.

Chapter 3

Bonding Systems

After thousands of years of manual grinding with stones, the first synthetic grinding tools were known in the beginning of the 19th century. [COLL88, p. 894]

The grit material performs the main abrasive cutting action and has been discussed in the previous chapter. However, grits alone cannot maintain a sustainable process with sufficient workpiece quality. One method is to bond the grits together by a bonding system that has to fulfil several tasks as follows [KLOC05a, MARI04]:

- Provide sufficient grit retention without untimely grit pullout,
- Provide sufficient strength to transfer machining forces and centrifugal forces,
- Allow controlled bond erosion to expose new cutting edges,
- Offer enough pore space to transport chips and cooling lubricant,
- Provide adequate heat conductivity and thermo-shock resistance,
- Provide chemical resistance against cooling lubricant.

Bonded grits form either grinding wheels or grinding belts (see Sects. 4.1 “Grinding Wheels” and 4.2 “Coated Abrasive Tools”). As consequence of the complex requirement profile on the tools, maximum grit retention capability is not synonymous with high performance in the abrasive process [MARI04].

Several bonding systems have evolved for grinding tools and will be discussed in this chapter. As contrasting method, the abrasive grits can also be applied as loose abrasives, which will be described in Sects. 4.4 “Polishing Tools”, 4.5 “Lapping”, and 4.7 “Other Methods with Free Abrasives”.

The most important bonding systems for grinding wheels are resin bonds, vitrified bonds, and metallic bonds (multi-layer or single-layer) (Fig. 3.1). Besides the primary ingredients, there are fillers, separator agents, auxiliary components, or even secondary abrasives in the bonding composition to modify the abrasive tool. All ingredients need to be considered in their life cycle from raw material extraction to end of life.

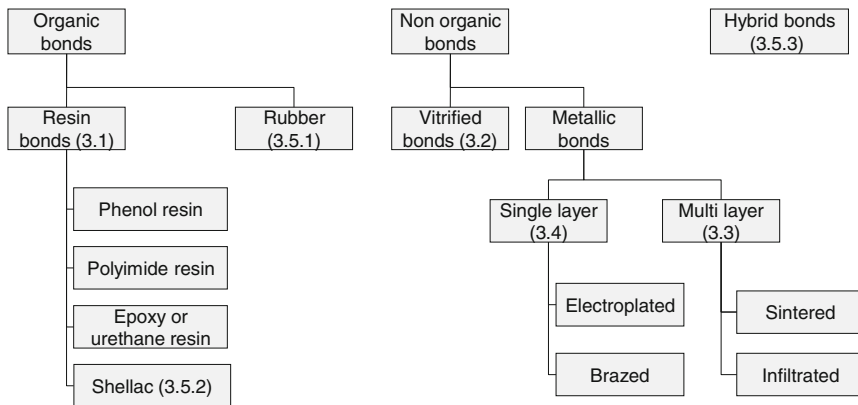


Fig. 3.1 Grinding tool bonds after [KLOC09]

Grinding tools with resin, vitrified and multi-layer metallic bond systems pass through similar manufacturing steps, such as mixing, forming, pressing, heat treatment, and post-processing [TYRO03]. All tool manufacturing processes include additional auxiliary steps such as raw material quality control, weighing, intermediate control steps, sieving, stocking, etc.

The homogeneous distribution of abrasive grits, bonding material and pores inside the abrasive layer is crucial for a constant process performance. A non-uniform distribution of the abrasive material leads to an uneven material removal process and respectively to a change in average chip thickness. This results in varying loads affecting the generated workpiece surface as well as the wear behavior of the grinding wheel that decreases process sustainability [KLOC05c].

Variations in the manufacturing process of tools cannot be totally avoided. However, it is important to control the deviation of the quality parameters per single production step so that the final product stays within the acceptable quality ranges [KLOM86, p. 12].

In contrast to conventional grinding tools, superabrasive tools are commonly built from an abrasive layer applied to a carrier, so called body (see Sect. 4.1 “Grinding Wheels”). The abrasive layer is fixed to the body either as ring or as straight or curved segments for larger diameters (commonly above 200 mm wheel diameter). Like conventional grits, superabrasives can be held by resin and vitrified bonds. Resin and vitrified bonds, however, have to be adapted to the chemistry and performance of superabrasives. Metallic bonds have particular importance for superabrasive grits and are nearly exclusively used for this grit type.

3.1 Resin Bonds

3.1.1 Chemistry and Types of Resin Bonds

A resin bonded grinding wheel consists of abrasive grits in a resin bond with or without fillers (Fig. 3.2). This wheel type has commonly a low porosity compared to vitrified bonded tools.

Resins are viscous liquids capable of hardening. They are polymers, i.e. large molecule chains composed of monomers. Monomers are substances with the elements C, H, O, N, Cl, S, or F, from which oligomers (“resins”) are synthesized [GARZ00, p. 109]. These are then transformed to crosslinked, insoluble polymers in a second step, called curing, which optionally involves heat, catalysts, fillers, or pressure [GARZ00, p. 109].

Resin bonds for abrasive tools consist of single resins or a resin combination with or without fillers (see Sect 3.1.3 “Fillers in Resin Bonds”). The resin itself is typically manufactured by esterification or soaping of organic compounds. Filler material has not only the task to reinforce the bonding in toughness, heat resistance, strength, and breakage safety, but also to support the grinding process as secondary abrasive [COLL88]. Silicates, sulfides, halogenides increase the bonding strength and wear resistance and hinder the oxidative degradation of the resin [KREB06]. In cut-off wheels, the resin bond is additionally enforced by body materials of glass fiber, linen cloth, etc. (see Sect. 4.2 “Coated Abrasive Tools”).

Resin bonds can be divided into three classes based on strength and temperature resistance [KLOC05a, p. 43, MARI07, p. 119, COLL88, p. 896 f., ROWE09, p. 41, MENA00]:

- Phenolic resin,
- Polyimide and polyamide resin, and
- Epoxy or urethane resin, often called plastic bonds.

3.1.1.1 Phenolic Resin

Phenolic resin bonds, in particular phenol-formaldehyde resin bonds, are the most common resin bonds; tools made of this bonding type represent the largest market segment for conventional wheels after vitrified tools [KREB06, KLOC05a, p. 65, MARI07, p. 119]. Originally, this bond type was known as bakelite and for this



Fig. 3.2 Structure of a resin bonded tool

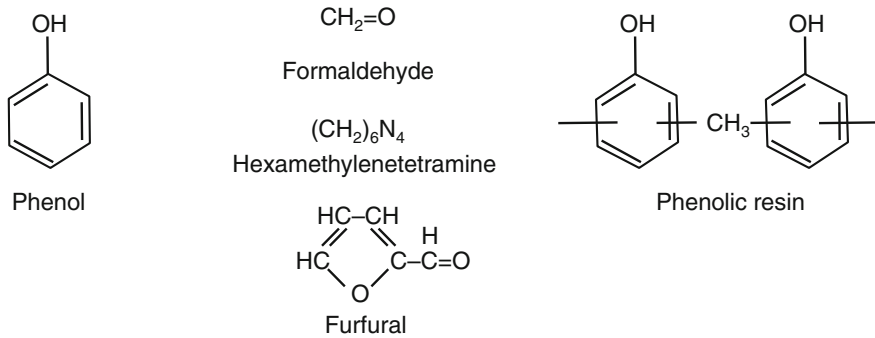


Fig. 3.3 Structures of phenol, relevant aldehydes, and phenolic resin [GARZ00, p. 8, 14, 21, HARR89]

reason retains the letter “B” in many wheel specifications [MARI04, p. 413, GARZ00, p. 318]. In comparison to other resins, phenolic resin is less expensive and easier to mold [ASAM10, p. 310].

Phenolic resins are obtained by the reaction of phenol and aldehyde [GARZ00, p. 3, 111]. Phenols are aromatic compounds with the hydroxyl group bonded to the aromatic nucleus (Fig. 3.3) [GARZ00, p. 3]. The phenol synthesis is commonly done by the cumene process, an oxidation process of cumene (isopropylbenzene) and air to cumene hydroperoxide, which is cleaved to phenol and acetone [GARZ00, p. 5, 8]. Safety is a critical aspect for plant design and operation, because the oxidation takes place close the flammability limit and cumene hydroperoxide is an unstable material [GARZ00, p. 8].

Relevant aldehydes for bond production of abrasive tools are formaldehyde, furfural, and hexamethylenetetramine. Formaldehyde is a hazardous chemical with potential eye, nose and throat irritation above a certain concentration (Fig. 3.3) [GARZ00, p. 14]. Hexamethylenetetramine, also called hexamine, is a common hardener in phenolic resin bonds [KREB06, HARR89] (Fig. 3.3). Basic oxides such as calcium oxide or magnesium oxide are curing accelerators in phenolic resins [GARZ00, p. 321].

The mode of catalysis and molar ratio of phenol and aldehyde result in a resin that is either of resole type or novolak type [GARZ00, p. 24]. Resoles are easily cured by acid, base, or thermal conditions; novolaks are cured with formaldehyde from hexamethylenetetramine, solid resoles, or other methods [GARZ00, p. 61]. Resoles occur either as solid resole, resole solution or aqueous resole; novolaks appear as solid resins, novolak solutions, aqueous novolak dispersions, and powder resins with hexamethylenetetramine [GARZ00, p. 122]. For the manufacturing of abrasive tools, aqueous resole and powder novolak are the most important forms [GARZ00, p. 122].

The phenolic resin bond for grinding wheels contains liquid (resole) and powdered (novolak), straight and modified phenolic resins, powdered resins with wetting agents, or low melting phenolic resin combined with powdered phenolic

resin [GARZ00, p. 323]. Various modifications with epoxy resins, rubber, polyvinyl butyral, etc. are possible [GARZ00, p. 325]. Furthermore, phenolic resin bonds for superabrasives are enhanced by SiC grits and solid lubricants [METZ86, p. 54].

Phenolic resins are cured at around 150–200 °C through polycondensation [KREB06, MARI04, p. 413]. Gardziella et al. give detailed compositions of the single liquid and powdered resins used for the production of abrasive tools [GARZ00, p. 324 and 326].

3.1.1.2 Polyamide and Polyimide Resin

Polyimides are polymers with a noncarbon atom of nitrogen in one of the rings in the molecular chain (Fig. 3.4) [HARP03, p. 432 f.]. Polyamide-imide are members of the same polymer family and contain aromatic rings and nitrogen linkages (Fig. 3.4) [HARP03, p. 432 f.].

Polyamid and polyimide bondings have a higher toughness, thermal resistance and elasticity than phenol resin bondings [KLOC05a, p. 66]. Polyimide bonds have 5 to 10 times the toughness of phenolic bonds and can withstand temperatures of 300 °C for 20 times longer [MARI07, p. 121]. However, the higher price reduces the use of this bonding system type to special applications and to superabrasives [MARI07, p. 121]. Polyimide resin is a dominant bond type for high-production carbide grinding especially for flute grinding [MARI07, p. 121] or for cut-off grinding under cooling lubricant.

3.1.1.3 Epoxy or Urethane Resin

Epoxy or urethane wheels are the softest of resin bonded wheels. With conventional abrasives, they are popular for double disc and cylindrical grinding. However, for

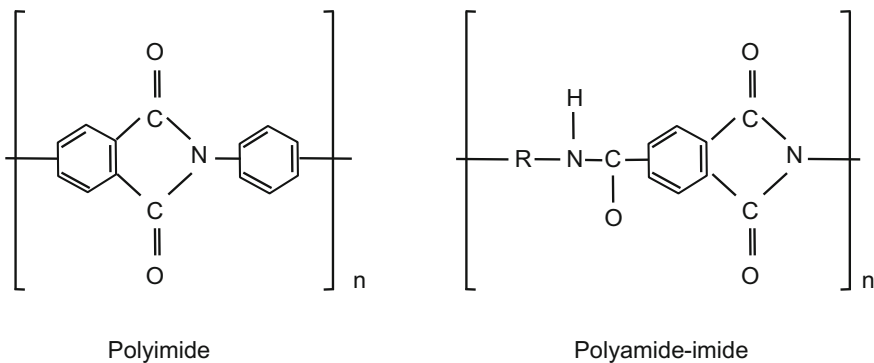


Fig. 3.4 Structures of polyimide and polyamide-imide [HARP03, p. 432 f.]

superabrasives, epoxy or urethane bonds appear to be limited to micron diamond grain applications for the glass and ceramics industries [MARI04, p. 413].

Epoxy resins are characterized by their epoxide group which consists of oxirane rings ($-\text{CH}_2-\text{O}-\text{CH}_2-$) [HARP03, p. 161 f., 388]. The epoxy resin then is hardened with a fluidic hardener to a polymer [KLOC05a, p. 63, COLL88].

3.1.2 Manufacturing of Resin Bonds

Resin bonded grinding tools are manufactured via mixing, pressing and hardening at temperatures up to 200 °C (Fig. 3.5) [COLL88]. Resins consist normally of the two main components resin and hardener. Mixing both parts results in the reactive resin material. During hardening, the resin's viscosity rises and a duroplastic material is generated.

3.1.2.1 Mixing and Molding

Mixing is often done in several steps, wet mixing, dry mixing, and final mixing (Fig. 3.5). In the wet mixing step, abrasive grits and liquid resins or furfural, a wetting agent, are combined [COLL88, GARZ00, p. 328 f.]. The abrasive grits will be coated so that the powder resins and fillers will cleave easier onto the grit surface. Wetting agents also improve the aggregation of grits. In addition, the abrasive tool can be handled in its raw, so called "green" state [TYRO03, A2, p. 6, COLL88].

Powder resin on phenol basis and fillers are mixed dry before they are combined with the wet mixture composed of abrasives and wet resins. Additives are included to support the mixing process by improving the pourability and storage life of the

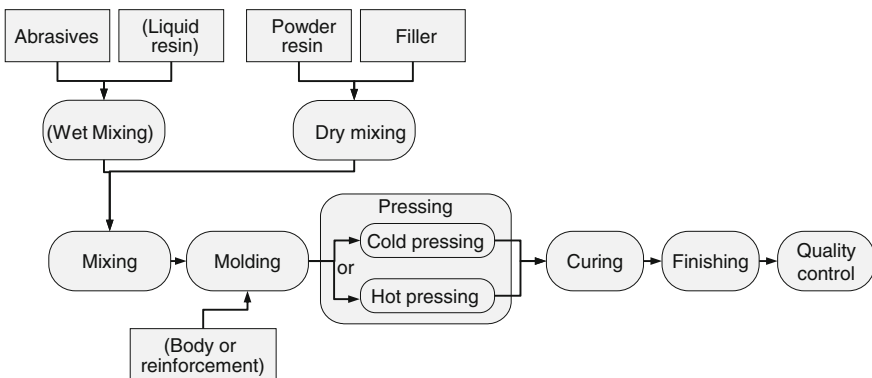


Fig. 3.5 Manufacturing of resin bonded tools after [GARZ00, ASAM10, KLOC09, TYRO03]

mixture and reducing the clumping tendency [GARZ00, p. 326 f.]. Examples for additives are powdered additives, silica and derivatives [GARZ00, p. 327]. The mixing process is continued until a homogenous, pourable mixture emerges [COLL88]. Dust is a safety issue during handling of powder resins. Therefore, antidusting agents can be useful additives to minimize dust [GARZ00, p. 327]. Before pressing, body material such as glass cloth for cut-off wheels or aluminum bodies for superabrasive wheels can be imbedded [KREB06].

3.1.2.2 Pressing

The bond and grit mixture can be either cold pressed and hardened in a furnace or hot pressed and hardened on a press with a heating plate. Figure 3.6 shows an example setup for pressing an abrasive layer onto a grinding wheel body. Conventional wheels are either hot or cold pressed and hardened at 140–200 °C [COLL88, p. 896 f., MENA00]. Most superabrasive wheels and dense, low porosity wheels are produced by hot pressing at 160–175 °C [MENA00, GARZ00, p. 338]. In the case of superabrasive wheels with a diameter below 200 mm, the abrasive layer can be pressed directly onto the tool body [KLOC09]. Epoxy or urethane bonds are casted or joggled in molds where they are hardened at temperatures of 20–80 °C [KLOC05a, p. 63, COLL88].

Cold pressing is done on hydraulic presses with compression strength of 15–30 N/mm² [GARZ00, p. 330, KLOC09, p. 54]. Pressing time ranges from 5–50 s and depends on the dimensions and shape of the abrasive tool, grit size, mixture plasticity and distribution [GARZ00, p. 330]. In hot pressing, the pressing times are determined to be about 30–60 s per millimeter of wheel thickness [GARZ00, p. 338].

The pressing process works either on a defined volume or with a defined pressure [COLL88]. The internal friction and friction with the mold walls lead to a deviation in particle density and therefore tool hardness (Fig. 3.7) [TYRO03b]. Density deviations can be overcome by two-anvil presses or superimposed oscillations in the pressing process, which was successfully proven for vitrified bonded tools [BEHR11].

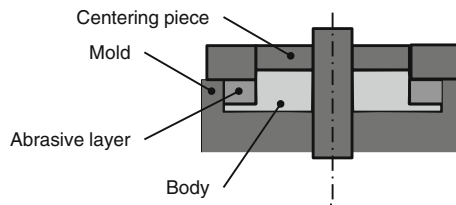
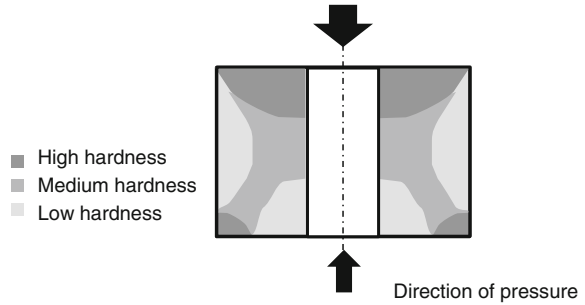


Fig. 3.6 Pressing of resin bonded tools

Fig. 3.7 Schematic theoretical hardness deviation in a pressed grinding wheel [TYRO03b]



3.1.2.3 Curing

The hardening process has to follow a defined temperature program (examples given in Fig. 3.8). Several chemical processes happen during curing depending on the actual temperature [COLL88, GARZ00, p. 331]:

- 70–80 °C: The resin bond starts to flow and to transform into a fused mass. Water in the phenol resin evaporates and the resin hardens under this separation of water [COLL88]. Water can drain off well in porous tools [ESCH05].
- 110–120 °C: The hexamethylenetetramine decomposes and induces the hardening process of the fused powder resin (Fig. 3.9). Gas is liberated, particularly ammonia (NH_3). [COLL88, GARZ00, p. 331]
- 170–180 °C: The structure finally hardens and the crosslinking of the phenol resin takes place [COLL88]. Overcuring should be avoided because overcured tools exhibit reduced strength [GARZ00, p. 331].
- 180–200 °C: Benzylamin structures split and result in new ammonia generation (Fig. 3.9). The resin bond becomes brittle, but also thermally more stable [COLL88].

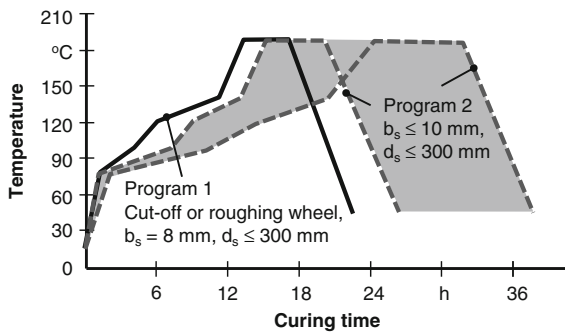


Fig. 3.8 Example temperature profiles for curing of resin bonded tools after [COLL88], for two wheel widths, b_s , and similar wheel diameters, d_s

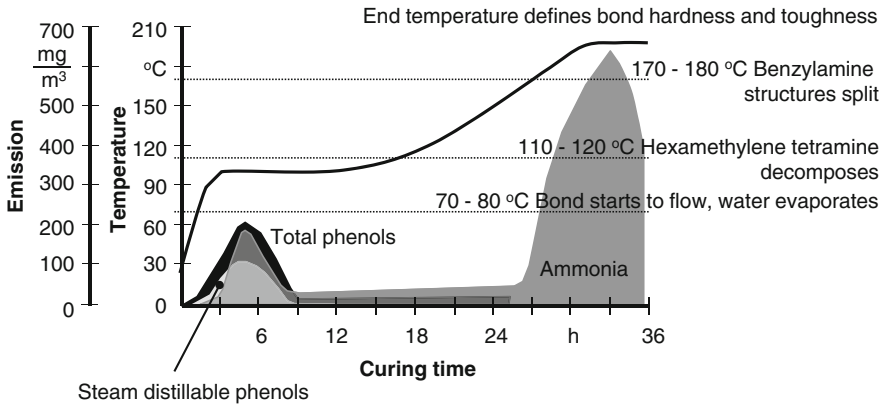


Fig. 3.9 Temperature profile and emissions for curing of a resin bonded tool [COLL88, GARZ00]

- The final temperature level (165–170, 175–180, or 185–195 $^{\circ}\text{C}$) affects the final tool properties (hardness, toughness, brittleness) considerably [GARZ00, p. 332].

Curing can also happen dielectrically with radio frequency and microwave heating [MENA00, HARI83]. These methods need the existence of a significant electrical loss factor, which is common with phenolformaldehyde resin [HARI83].

3.1.3 Fillers in Resin Bonds

Fillers in resin bonds have several tasks in both manufacturing phase and grinding operation: They induce porosity, reinforce bond properties, change aesthetics, and more [FRAC10]. Common fillers in resin bonded grinding tools are cryolite (Na_3AlF_6), pyrite (FeS_2), zinc sulfide (ZnS), lithopone (ZnSbBaSO_4), potassium fluoroborate and potassium chloride (KAlF_4 , K_3AlF_6), potassium sulphate (K_2SO_4), and mixtures of these materials (KCl) [COLL88, p. 897, GARZ00, p. 321, HICK91]. The toxic materials antimony trisulfide (Sb_2S_3) and lead chloride (PbCl_2) were used in the past, but are substituted by special iron halides and others [GARZ00, p. 321]. The percentage of fillers and resin bond varies with the grinding tool hardness and density (Table 3.1).

In the manufacturing phase, fillers can induce porosity [FRAC10]. Basic oxides, such as CaO and MgO , are fillers that accelerate the hardening process [COLL88, p. 897]. However, CaO should only be applied to grinding tools for dry grinding operations, because CaO fillers can hydrate and transform into CaCO_3 in contact with cooling lubricant [COLL88, p. 897 f.].

In the grinding process, fillers reinforce the bonding in toughness, heat resistance, strength, and burst resistance or they support the grinding process as

Table 3.1 Common resin and filler content percentage in grinding wheels [COLL88, p. 897, GARZ00, p. 323]

	Abrasive grit content (w%)	Resin content (w%)	Filler content (w%)
Hard and dense grinding wheels	65–95	12–18	8–20
Medium hardness grinding wheels		8–12	3–8
Soft grinding wheels		5–8	0–3

secondary abrasive [COLL88, p. 897, GARZ00, p. 321]. Glass chips reinforce wheels around the inner diameter [ASAM10, p. 317]. Fine metal powder of high thermal conductivity can be introduced into the bond to improve the tool's heat absorption in the machining process [HERB80]. An example is fine silver powder, mesh size 325 or finer [NN74]. In addition, fine silicon carbide grits act as bond strengtheners [HERB80].

Fillers in the form of solid lubricants introduced into the bond formulation resulted in the following functional characteristics [HERB80]:

- Reduced friction at the wheel/workpiece interface,
- Fewer loading of the wheel by grinding swarf,
- Preserved sharpness of the abrasive grits.

An example is provided by organic dryfilm lubricant of polytetrafluoroethylene (PTFE) type for wheels with a mesh size of 325 or finer [NN74]. In other applications, the lubricants FeS_2 and K_2SO_4 improved grinding quality and versatility [HICK91]. Finely divided graphite can improve the performance in dry grinding [NN74]. Cryolite (Na_3AlF_6) melts at about 950 °C and prevents wheel clogging by metal [COES71, p. 158 f.]. However, it acts as solvent for Al_2O_3 grits [COES71, p. 159]. The resin bond of grinding belts that will be used in very basic media has to be additionally stabilized [COLL88, p. 916]. Fillers can change the tool aesthetics when they act as coloring agents [FRAC10].

3.1.4 Performance of Resin Bonds

Resin bonds have comparably high elasticity. Therefore, this bond type is selected for wheels that are subject to impacts, sideways load, sudden loads, or high cutting speeds. Typical applications are cut-off or roughing operations. In addition, resin bonds work well for finishing processes to achieve high surface quality. Bond elasticity, however, might have a negative effect on dimensional accuracy [COLL88].

Resin bonded wheels are easy to profile, but do not achieve a high enough grit protrusion through profiling. Therefore, they need an extra sharpening process.

In the grinding process, only workpiece materials that set back the bond will lead to a sufficient self-sharpening effect. Appropriate materials are brittle materials, for example in the application of carbide tool grinding.

Dense grinding tool surfaces are achieved with fine abrasive grit sizes. Large grits and metallic grit coatings improve grit retention in resin bonding systems. Some filler materials, such as CaO, should not be exposed to water [COLL88, p. 897 f.].

Furthermore, resin bonds are sensitive to heat. They start to degrade at temperatures above 200 °C and grit coatings help to dissipate the grinding heat. Resin bonded wheels have limited shelf lifetime and should be used within two years [KREB06]. The polycondensation process that hardens the bond resins does not lead to complete hardening so that the strength of resin bonds can change due to atmospheric or chemical exposure [KREB06].

3.2 Vitrified Bonds

3.2.1 Chemistry and Types of Vitrified Bonds

Vitrified bonds consist of silicates (red and white clay), kaolin (also known as white clay, $\text{Al}_2\text{Si}_2\text{O}_5(\text{OH})_4$), field spar (KAlSi_3O_8 – $\text{NaAlSi}_3\text{O}_8$ – $\text{CaAl}_2\text{Si}_2\text{O}_8$), quartz (also known as silicon oxide, SiO_2), and frits, i.e. pre-molten bonding components [BEYE04, HADE66, PADB93, JACK11, p. 92]. The bond is sintered at temperatures above 800 °C and results in a structure where the grits are enclosed by the bond (Fig. 3.10). The bond bridges between grits leave room for pores. Due to the high sintering temperatures, reactions between grits and bond are likely (Sect. 3.2.3 “Performance/Grit Retention”). In contrast to resin and metallic bonds, vitrified bonds have a significant amount of pores.

Vitrified bonds vary in their appearance due to the proportion of ingredients and sintering conditions. The two bond type extremes are melted bonds and sintered bonds [KLOC09, KREB06, TYRO03b]:

- Melted or fusible bonds are glassy bonds with a high amount of glass phase [JACK95]. They result from a high proportion of clay and frits as raw materials. Melted bonds melt totally, flow around the grits and react with the grit surface [HELL94]. The frits enhance the melting properties of the bond resulting in higher grit retention at lower firing temperatures [KREB06].



Fig. 3.10 Structure of a vitrified bonded tool

- Sintered bonds occur as porcelain bond type with a small amount of the glass phase. A high proportion of feldspar and a low amount of frits leads to this bond type. The grits are only “glued” together by the partially molten bonding. The proportion of bond and the firing temperatures are comparatively high [KREB06]. Nevertheless, this bond type is used for critical grinding operations with low forces and for silicon carbide tools [KREB06]. High glass contents can decompose the silicon carbide grits [KREB06].

3.2.2 Manufacturing of Vitrified Bonds

First, the bond components and abrasives are mixed and filled into a mold, either by a casting process in the case of clayey bonds or by a molding process (Fig. 3.11). Pressing compacts the material and produces the so-called “green body” which can be handled. The green body is dried and sintered. After that, the grinding wheel will be finished and undergoes quality control.

3.2.2.1 Mixing

The proportion of grit, bond and pore volume defines the structure and hardness of a grinding tool (see Sect. 6.1 “Abrasive Layer Composition”). The right amount of bond components and grits are weighted and mixed. Even if the various ingredients have different size, density, form, and weight it has to be controlled that the mixture is homogenous and without agglomerations, so that the final abrasive tool has a homogeneous cutting edge distribution [BOTS05, p. 23]. Furthermore, the mixing process must not demix the components, induce changes in the mixture, or produce heat [TYRO03].

In the first step, the coarse particles are made sticky by mixing them in for example a water dextrose solution [MESP91, TYRO03]. The fine components are added afterwards and stick to the prepared coarse components [MESP91, TYRO03].

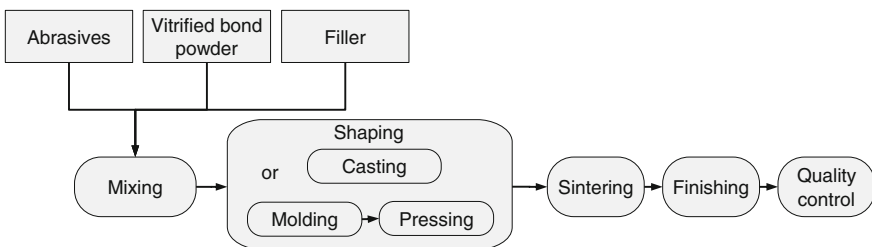


Fig. 3.11 Manufacturing of vitrified bonded tools after [KLOC09, TYRO03]

The lubrication has to be controlled to avoid aggregation [BOTS05, p. 23]. Aqueous phenolic resin binders are one example for temporary binders [HUZI00].

A common mixer type is the planetary mixer [MESP91]. As ingredients might change their viscosity and react chemically during this process an adequate mixing time is also of great importance [MESP91]. Standard mixing times of up to one hour are therefore quite common. To enhance tool quality, vitrified bondings can be granulated and sieved after mixing.

3.2.2.2 Casting

Casting is applied for bonds with high clay content. The casting process is more expensive and therefore being replaced by molding processes [KLOC09].

3.2.2.3 Molding and Pressing

Most vitrified bonded tools are manufactured by molding. In the past, the mixture was formed into the mold manually; today fully or partially automated systems supply and disperse the mixture into steel molds. The mixture has to be filled into the mold homogeneously and without demixing, which is done by conveyor belts, vibrating trough, or other supply systems. The filling height is leveled with sheets. Molding gets more complicated for complex grinding tools such as wheels with different layers for crankshaft grinding, different hardness areas for raceway grinding, or large width for centerless grinding [TYRO03].

The pressing process defines the density distribution and thus the specific characteristics of the component [BEHR11]. The pressure is an important factor for tool quality and commonly not published. Today, computer controlled hydraulic presses between 500 kN to 45 MN are in use [TYRO03]. Commonly, the target volume, not the target pressure, controls the pressing process. Segments for superabrasive wheels are pressed with hydraulic or pneumatic presses or by hand at comparatively low pressures (max. 50 N/mm²).

Inevitable friction between the dies, molds, and powder leads to density gradients, (Fig. 3.7), which can result in sintering distortions and inhomogeneous material properties [BEHR11]. Additives like paraffin, polysaccharide, silicon oil, wax, and polyethylene emulsions lubricate the mixture and therefore support the pressing process [BOTS05, p. 25]. Oscillations of about 60 Hz can be superimposed to the pressing process and enhance the density distribution [BEHR11]. Expensive two-die presses can be substituted.

Hot pressing is used for high density tools [KLOC09, p. 59]. Hot pressing of diamonds in vitrified bond produces wheels of low porosity. Using graphite molds enables higher sintering temperatures in the hot pressing process. However, as the graphite molds are of low strength, the process has to be heated above regular sintering temperatures to limit pressing pressures [MARI04, p. 418]. As consequence, the bonds are densified with less than 2 % of open porosity.

3.2.2.4 Drying

In the drying or debinding process, the water from the temporary binders is expelled [TYRO03]. The drying process is conducted in a special drying furnace or in the sintering furnace during the general heat-up period. The drying temperature depends on tool ingredients, composition, and application and ranges usually between 200 to 600 °C.

3.2.2.5 Sintering Process

In the sintering process, the bond components melt and flow around the abrasive grits. Bonds with a large amount of clay melt at higher temperatures; bonds with more frit content melt at lower temperatures [MALK08, p. 27]. The mechanisms of melting, wetting, resolidification, and forming of bonding bridges between grits are highly complex [BOTS05, MOSE80].

The bond mixture is formed into non-uniform glass of complex composition including several ceramic bond minerals that form during the sintering process [JACK11, p. 83, 85]. Jackson studied the vitrification behavior of sintered and fusible bonds for conventional grinding wheels [JACK95]. Bot-Schulz analyzed the chemical reactions and sintering mechanisms for varying bonding composition for white corundum and Sol-Gel-corundum [BOTS05]. If the bond contains MgO, mullite ($3\text{Al}_2\text{O}_3 \cdot 2\text{SiO}_2$), cordierite ($2\text{MgO} \cdot 2\text{Al}_2\text{O}_3 \cdot 5\text{SiO}_2$), and spinel ($\text{MgO} \cdot \text{Al}_2\text{O}_3$) are formed during devitrification [JACK11, p. 83 ff]. If the bond contains CaO, anorthite ($\text{CaO} \cdot \text{Al}_2\text{O}_3 \cdot 2\text{SiO}_2$) and mullite ($3\text{Al}_2\text{O}_3 \cdot 2\text{SiO}_2$) can form [JACK11, p. 83 ff].

One problem in manufacturing of vitrified bonded tools is the shrinkage after melting and sintering. A higher amount of abrasives and secondary abrasives reduces the shrinkage, but might have a negative effect on the grinding tool performance. Pore builders that burn leave voids, which sometimes collapse during the sintering shrinkage and counter the purpose. New approaches to reduce sintering shrinkage are to use fired clay (“grog”) or crushed firebricks in sizes between 30–200 µm. Cerium oxide, andalusite, sillimanite, willemite, or a combination thereof serves the same purpose. [HUZI12]

Several chemical processes happen during sintering [BOTS05, 25 f.]:

- 20–600 °C: Free and bound water dissolves. The temporary binders burn out. Quartz (SiO_2) changes volume at 573 °C. Gas pressure and volumetric shrinkage lead to high internal stresses in the tool.
- 600–900 °C: Carbonates, organic material, chemically combined water in the clay, and other volatile materials drive out.
- Furthermore, chemical reactions between grits and bond are possible.

The sintering temperature must not harm the abrasive grits by inducing unwanted oxidization or other chemical reactions. The bondings for CBN and diamond have to fuse together under lower forming pressures and vitrification

temperatures than for conventional grits [JACK07]. Because CBN is thermally more stable than diamond, CBN grits can be used with a wider range of vitrified bonds [MALK08, p. 26]. Special coatings protect CBN grits from chemical reactions above 800 °C with the water and alkali in most frits [MALK08, p. 27]. For diamond wheels, a non-oxidizing atmosphere is applied to enable a sintering temperature higher than the diamond oxidation temperature of around 700 °C.

Different furnace types are used depending on application and batch size. Continuous furnaces, also called tunnel furnaces or traveling kiln, are often used for the mass production of conventional grinding wheels and can be 70 m long. Periodic hood-type furnaces are used for smaller batch sizes. In general, about 80 % of the inner furnace volume can be used for producing products. Additional accessories enable special gas atmospheres in the furnace or pressure control. Furnaces are heated by electrical energy, with gas or oil [KLOC09]. Gas furnaces are usually cheaper but they cannot be used for all processes.

The temperature distribution is not constant along the furnace cross-section. Temperature fluctuations inside the furnace should not exceed ± 10 °C. A smaller range enhances process capability. Tools properties can depend on their position on the kiln car [RAMM74].

The temperature curve has to be controlled precisely. The rate of heating, peak temperature, and isothermal soaking time define the grinding wheel properties [JACK95, p. 82]. The temperature profile consists of a heating, soaking and cooling phase. The total time can be 100 h [TYRO03]. For example, corundum wheels in a tunnel furnace are heated up to 1260 °C over 1 to 2 days, held for about 12 h at the maximum temperature, then slowly cooled down [MALK08, p. 27]. The cooling process has to be carefully controlled to avoid thermal stresses or cracking of the wheels [MALK08, p. 27]. The cooling process can take weeks for very large wheels [MALK08, p. 27].

3.2.2.6 Frits

Frit is a generic term for a material that is generated by blending minerals, oxides, and other inorganic compounds, heating to at least melting temperature, cooling, and pulverizing [HAY90]. An example frit production process is given as follows: Melting of the ingredients above 1150 °C, holding at the temperature for 4 h, cooling down in water, crushing, and pulverizing of the material. A glass is an amorphous substance without significant crystal formation [HOLL95]. In thermodynamics, glass is defined as frozen, undercooled fluid. All substances that were molten and cooled down appropriately follow this definition. The quick cooling results in the formation of crystal seeds during solidification, but the time is too short for the crystallization process.

Frits for the manufacturing of grinding wheels consist commonly of boron silicates or magnesium glass [BOTS05]. In addition, frits also contain TiO₂, feldspar, borax, quartz, soda ash, red lead, zinc oxide, whiting, antimony trioxide, sodium silicofluoride, flint, cryolit, and boric acid [HAY90]. In producing grinding tools,

frits act as flux agents and change the properties of the vitrified bond, for example by lowering the sintering temperature [JACK11, p. 92].

Frit manufacturers characterize their products by melting behavior (temperatures for beginning of fusion, melting, and sintering) and thermal expansion. A hot stage microscope analyzes the melting behavior.

3.2.2.7 Flux Agents

Siliceous clay with low melting point is considered as 'flux agent' and minimizes the surface tension at the interface between bond and abrasive grit [JACK07]. Lithium for example is one of the most expensive flux agents, but can decrease softening and melting point, viscosity, as well as heat expansion coefficient [BOTS05].

3.2.2.8 Porosity Builders

In vitrified bonded wheels, the natural packing of the abrasive particles leaves certain porosity [DAVS04]. Additional pore builders produce higher porosity when they sublime or burn off during the sintering process. Pore builders are typically either hollow particles or fugitive materials [MARIO7]. Hollow particles such as hollow ball corundum, glass beads, or mullite maintain a stronger wheel structure [MARIO7]. Conventional fugitive pore builders include nut shell powder, sugar, starches, polymeric materials, plast granulat, naphthalene, ceralith (from rye groats), wax balls, etc. [DAVS04, HUZ12]. Fugitive pore formers allow flexible pore shapes and sizes [MARIO7].

Naphthalene is a fugitive pore builder, which boils at 218 °C [GEST12]. Because naphthalene is regarded as carcinogenic, tool manufacturers attempt to substitute it with natural components, supercritical CO₂, liquid CO₂, or other materials [GEST12, DAVS04].

Other substances that build pores during the tool production are often organic such as wood shavings, salt, etc. Variations in pore distribution can lead to non-uniform tool shrinkage in the manufacturing process, especially for tools produced at high temperatures. This is a result of two factors. On the one hand, the effective thermal expansion coefficient of a composite body depends on the relative contents of the various components. On the other hand, denser zones with fewer pores undergo a more thorough sintering action with stronger contraction. To minimize discontinuities in the abrasive layer, the mixture of pore builder and the other ingredients should be well blended. [YARN69]

One problem of pore builders can be carbon residues [DAVS04]. Possible defects in the grinding tool arise from swelling, slumping, off-gassing, or collapsing of pores during sintering shrinkage [DAVS04, HUZ12].

3.2.2.9 Finishing

Connecting body and abrasive layer for superabrasives is explained in Sect. 5.1 “Body Concepts”. Conventional grinding wheels are machined to achieve the final dimensions and tolerances. Superabrasive tools are near-net-shape and need less effort if any.

3.2.3 Performance/Grit Retention

The first vitrified bonded wheels were considered as inappropriate for large temperature variations because the bond was not elastic enough to withstand thermal expansion differences within the tool [KING86, p. 87]. Certain bond elasticity is important to equalize the volumetric expansion of the abrasive grits induced by the grinding process heat [STAD62, p. 51]. Vitrified bonds are thermally highly stable. However, Stade reports about molten beads of vitrified bond in the grinding debris [STAD62, p. 51].

Grit retention in vitrified bonds is partially mechanical because the bond encloses the grits. In addition, the bond often reacts chemically with the grit surface. For example, the vitrified bond dissolves the grit surface in corundum wheels [JACK11, p. 62]. For CBN, the early vitrified bonds were just transferred from conventional applications and happened to be so reactive that they dissolved the CBN into the bond and converted it into boric oxide [MARI04, p. 419]. However, the bond composition was changed over the years so that well dressable CBN bond systems became state of the art [MARI04, p. 419]. CBN grits can be coated to avoid chemical reactions between CBN grits and alkali or water present in most glass frits at temperatures above 800 °C [MALK08, p. 26].

Diamond, however, does not show significant chemical bonding with the components of a vitreous bond [MARI04, p. 418]. Retention of diamond grits is mostly mechanical. However, diamond is reactive with oxygen at temperatures above 650 °C. Therefore, diamond wheels must be fired at low temperatures or in inert or reducing atmosphere [MARI04, p. 418]. However, titanium based coatings on diamond or CBN grits have a protective function during the sintering process.

Reaction layers between the vitrified bond and corundum white or sol-gel corundum consists from bond and grit material and can be adjusted by the sintering process. The characteristics of the layer affects grit retention. Sol-gel corundum grits expose thicker reaction layers than white corundum due to microcrystalline structure and higher number of grit boundaries. [KLOC06a]

The first vitrified bonded CBN grinding wheels needed separate profiling and sharpening processes [STUC88]. However, this problem has been overcome by new bonding compositions. Today, vitrified bonded grinding wheels are easy to

profile and sharpen in one step. The dressing mechanisms are mainly grit breakage, grit splintering, bonding breakage, grit break-out off the bonding, and grit deformation [MARI04, WIMM95, MINK88, MESS83, KLOC08b]. Linke found that the dressing forces likely induce cracks or support crack propagation in the tool bond, so that the abrasive layer is weakened by the dressing process [LINK07]. However, hot pressed vitrified bonded wheels are difficult to dress and need a separate sharpening process similar to resin and metal bonded wheels [MARI04, p. 418].

3.3 Metallic Multi-layer Bonds

Metallic bonds are either multi-layered (produced by sintering or infiltration) or single-layered (produced by electroplating or brazing) [MARI07]. They are only applied to superabrasive grits because conventional grits wear too quickly to use the bonding strength to full capacity.

3.3.1 *Chemistry and Types of Metallic Bonds for Multi-layer Abrasive Tools*

Metallic multi-layered bondings consist of various alloys such as copper/tin-bronze (Cu/Sn), cobalt-bronze (Co/Cu), tungsten carbides (W/WC) or alloys from the iron-copper-tin-system (Fe/Cu/Sn) [KLOC09, STOC86]. Common Cu/Sn alloys have a ratio of 85:15 or 80:20 Cu to Sn with fillers and additional alloys [MARI07, p. 122]. The binder needs to have good wettability for the abrasive grits.

Iron and iron consisting metals may cause undesired reactions with diamond grits [STOC86]. Diamond tools for stone drilling and sawing use bond systems based on tungsten, tungsten carbides, or cobalt alloys [STOC86, WEIS08]. Besides high wear resistance and toughness, tungsten builds an advantageous, small interface layer of tungsten carbide with the diamond grits [STOC86]. Therefore, the bond retention is not only mechanical but also chemical. Moreover, auxiliary metal powders on the basis of cobalt, nickel, copper, iron, and mixtures of copper-nickel-zinc, copper-zinc and copper-manganese optimize bond retention [STOC86].

Metallic bonds have strong grit retention and are wear resistant against the chips of brittle, short-chipping materials. The high hardness becomes a disadvantage in tool conditioning. Nevertheless, metallic bonds can be modified to be brittle and dressable, for example increasing the Sn content or adding Ag embrittles bronze bondings [MARI07, p. 122]. Co increases wear resistance.

3.3.2 Manufacturing of Metallic Bonds by Infiltration

Metallic bonding by infiltration is used mainly for dressing rollers and special applications [KLOC09]. Infiltrated bonds are also used for superhard honing sticks (bronze, Co-bonding), stone drilling crowns, or saws.

Grits, bond, and fillers are either mixed and filled into the die or the grits are fixed first onto the bottom of the die form and the matrix powder is added afterwards (Figs. 3.12 and 3.13). After then adding a defined amount of hard solder and flux (often copper, nickel or zinc alloys), the die form is heated in continuous ovens with inert gas or by induction [KLAU76, STOC86]. The solder has a relatively low melting point. Therefore, the molten solder penetrates the matrix powder by capillary forces. The resulting matrix is strong and highly wear-resistant [KLAU76]. The tool body can be connected to the abrasive layer simultaneously by brazing. Subsequent to the heating process, pressure can be applied to further influence the tool characteristics [STOC86] (Fig. 3.12).

The melting point of the solder defines the temperature of the infiltration process. Infiltration of copper-based solder takes place at 1000–1250 °C [YOUN66]. Die forms are made of graphite. This material has several tasks [KLAU76]:

- Prohibiting wetting of the die form with solder by its non-adhesive behavior,
- Building an air gap between die form and produced tool by different thermal expansion,

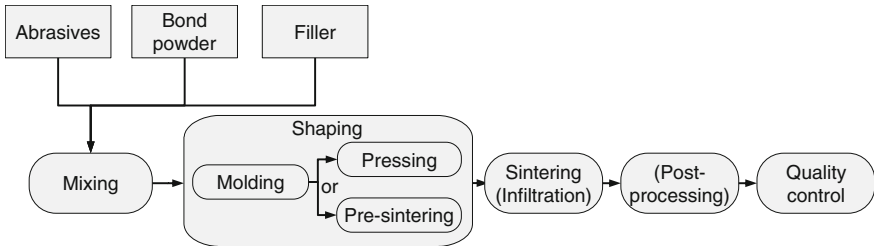


Fig. 3.12 Manufacturing of metal bonded tools by infiltration after [KLOC09, STOC86, KLAU76]

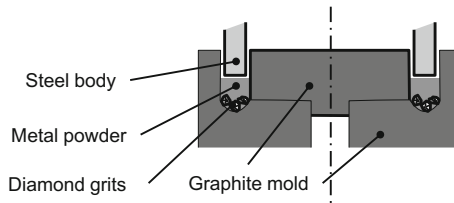


Fig. 3.13 Manufacturing of diamond crowns with infiltration method [YOUN66]

- Being multi-usable because of the two above described properties,
- Binding oxygen from the atmosphere and building of CO/CO₂-atmosphere as oxidization protection for diamond grits.

The appropriate choice of the graphite die material is important for a stable manufacturing process as reactions between tool bonding ingredients and graphite matrix can occur [KLAU76]. Graphite for the infiltration process should be easily machinable, be free of cracks and have low porosity, so no solder flows into the die material itself and destroys it. The generation of carbides between graphite and matrix powder ingredients can be suppressed by coating of the die form before each infiltration process. Coating materials can be e.g. Al₂O₃-powder and alcohol or natural graphite and glycol [KLAU76].

3.3.3 Manufacturing of Metallic Bonds by Sintering

Sintered bonds are produced by mixing of metal powder and abrasive grits, molding, either hot pressing or cold pressing, and sintering (Fig. 3.14). In exceptional cases, the metallic powder is mixed with an organic binder (paraffin oil and/or wax granule). This binder helps to produce a green compact, which can be handled, and vaporizes in the sintering process [STOC86]. The binder also leaves pore space, which might be infiltrated with a soldering agent.

In the cold pressing method, the green compact is taken out and sintered in a melting oven under inert gas atmosphere [STOC86]. Sintering takes place with or without form [STOC86]. Iron or steel compacts are sintered at 1100 °C [YOUN66]. Bronze bondings are easy to process and press and they are sintered at temperatures between 500–700 °C gesintert.

In the hot pressing method, the mixture is compressed under additional heat directly in the graphite form. Three heating types, namely inductive heating, indirect and direct resistance heating, can be used in hot pressing [DRFR05].

The cold pressing procedure allows the application of fast, mechanical pressing methods as well as sintering at neutral or reduced atmosphere in melting ovens.

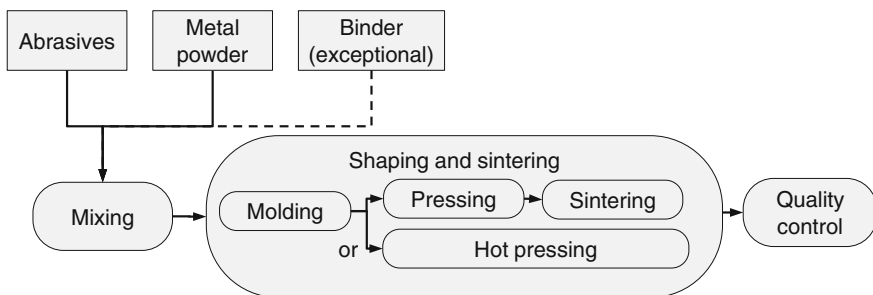


Fig. 3.14 Manufacturing of sintered metal bonded tools after [KLOC09, STOC86]

Hydrogen or other inert gases provide an oxygen-free surrounding, which is important for the protection of diamond grits at higher sintering temperatures. The hot pressing procedure is a one step operation and, therefore, a time-effective process with good quality control [STOC86].

Hot isostatic pressing is a competing method for traditional hot pressing [DRFR05]. Onishi et al. produced highly porous wheels from hot isostatic pressing (HIP) of 73 w% of cast-iron or iron powder, 25 w% of diamond grits and 2 w% of wax [ONIS97]. In this procedure, the material was pressed first, presintered to remove the wax, and HIP processed.

Porosity in sintered metal bonded tools is achieved by vaporizing fillers and adjusted pressing pressure. Porosity in bronze bonding is gained from adding carbon, e.g. up to 20 V% in diamond cup grinding wheels [BÜTT68, p. 74].

3.3.4 Performance of Metallic Multi-layered Bonds

Metallic bonds provide high grit retention and low wear during grinding. However, a copper bonding might smear during grinding. Metallic bonds might have low porosity, so that fillers in the bond are added for lubrication during grinding.

Metallic bonded tools are difficult to condition mechanically [WEGE11]. Electro physical and electro chemical processes can be applied due to the electrical conductivity of the metallic bond and are used in many different set-ups [WEGE11]. Klink examined the electro discharge and electro chemical dressing of different metallic bond compositions (Cu-bronze, Fe-bronze, Co-bronze) [KLIN09]. Ohmori and Nakagawa invented the Electrolytic In-process Dressing (ELID) method [OHMO90]. The cast iron fiber bonding of a diamond grinding wheel is anodized to generate grit protrusion [OHMO90]. ELID has advanced a lot and is possible when applied to grinding wheels with cast iron bonding, hybrid metal-resin bonding, and bronze bonding [BIFA99, ITOH98, WEGE11, KLIN09].

Porous metallic wheels can be conditioned by crushing, i.e. inducing bond breakage by high dressing forces [HESS03]. Crushing commonly takes place at dressing speed ratios of $q_d = +1$, which means there is no relative speed between the dressing tool and the grinding wheel in the contact point. For example, crushing replicates fine threads into brittle bronze bonding [KLOC82].

3.4 Metallic Single-layer Bonds

3.4.1 Chemistry and Types of Metallic Bonds

Single layer metallic bonds have a layer height of only the average grit size and a high grit protrusion of 20–70 % of the grit diameter. Because of the high grit

performance, single layered wheels are limited to superabrasives. The metallic single-layer bonds are produced by electroplating, brazing, or electroless plating processes:

- Electroplated wheels—The production takes place at room temperature. The most common bond type for single layer bonds is nickel bonding deposited in an electroplating process. Electroplated CBN wheels were important for the successful development of high efficiency deep grinding (HEDG) [ROWE09].
- Brazed wheels—The production happens at temperatures of up to 1000 °C [MARI04, p. 415]. Strongly wetting solders like titanium containing material, Ni–Cr–Bo–Si-alloys or others are used.
- Electroless plating process—Nickel/phosphor-alloys can be chemically deposited [KLOC09, p. 61]. Chemically precipitated bonds are of higher strength than electroplated bonds and can have a more even coating thickness, but the equipment is more expensive, processing temperatures are higher and the bond is more brittle [KLOC09, p. 61].

3.4.2 Manufacturing of Electroplated Bonds

Electroplating is based on the cathodic metal deposition from a watery electrolyte (Fig. 3.15). A metallic layer can only be deposited on a workpiece, if there are enough electrons to discharge the metal ions within the watery solution. Depending on the origin of the electrons, a distinction is drawn between chemical metal deposition (without external voltage source) and electrochemical metal deposition (with external voltage source) [KLOC07, p. 187]

The body material of grinding tools needs to be electrically conductive, at least in the area to be coated [KLOC09, p. 60]. Common materials are steel, e.g. C15, C45 or alloyed steel, hardened ball bearing steel (100Cr6), aluminum, or bronze/brass if the application does not allow for a magnetic material [BOLD02]. Before electroplating, the body has to be prepared carefully and the areas that

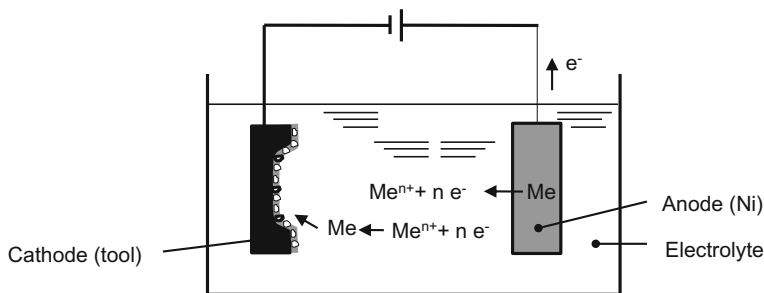


Fig. 3.15 Electroplating process after [KLOC07, p. 188, BOLD02]

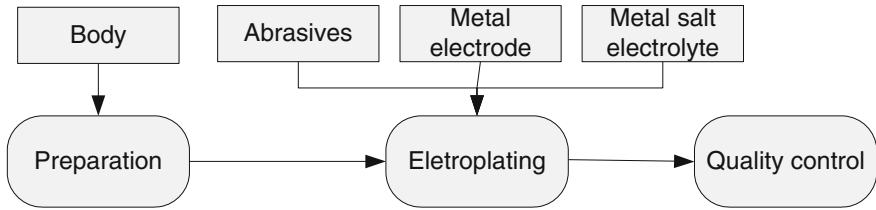


Fig. 3.16 Manufacturing of electroplated tools

should not be plated need to be painted (Fig. 3.16) [METZ86, p. 63]. The surface needs to be degreased and oxide layers need to be removed [KLOC07, p. 196]. Aluminum alloys need special treatment to remove oxide layers and activate the surface layer for better chemical bonding [KLOC07, p. 196].

The body is covered with superabrasive grits and placed into the electrolytic bath [KLOC09, p. 60]. The area to be coated needs to be surrounded by a sufficient amount of grits, which can present a big amount of fixed capital [METZ86, p. 63]. The bath consists of a watery solution of metal salts from the deposited metal, such as Ag, Co, Cu, Ni, Au salts [BOLD02, KRAF08]. In general, the anode consists of the bond material and the tool body acts as cathode. The direct current (DC) voltage leads to precipitation of Ni at the tool body. After the initial bonding of the grits, the excessive grits are removed and the process is continued until the desired plating depth is reached [KLOC09, p. 60]. The first bonding phase needs a motionless bath; the second phase of layer growth can work with higher power and bath circulation [KLOC07, p. 197]. The plating depth leaves about 50 % of the grit exposed (Fig. 3.17) [MARI04, p. 415].

Typical superabrasive grits are strong, well-formed and blocky with well-defined cutting edges [NOTT80]. Disadvantageous process parameters or grit choice can lead to faulty tools. If the operating current density is too high, overplating, spikes, or nodules in the space between the grits occur and the grit protrusion shrinks [NOTT80, CHAT90]. Handling and disposal of the electrolytic baths and metals used underlies strict regulations (see Sect. 3.6.3 “Environmental Dimension”).

Profile accuracy of electroplated tools with a single layer of grits depends on the grit size distribution as well as concentricity and profile precision of the body [KLOC07, p. 196]. The grit size defines the minimum concave profiles [KLOC07, p. 197].

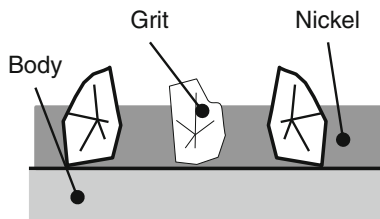


Fig. 3.17 Structure of an electroplated layer after [MARI04, p. 416]

Because of electric field concentration, edges and corners can be hard to coat evenly [KLOC07, p. 197]. To get a more even precipitation of Ni the throwing power of the electrolyte might be modified or the anode shape might bear the reverse profile of the wheel profile.

The metallic body of the abrasive tools can be re-used and re-coated, if the abrasive layer is removed. This can be done by an unsoldering process, so called stripping (see Sect. 4.8.3 “Recycling of Abrasive Tools”).

3.4.2.1 Manufacturing of Dressing Rollers

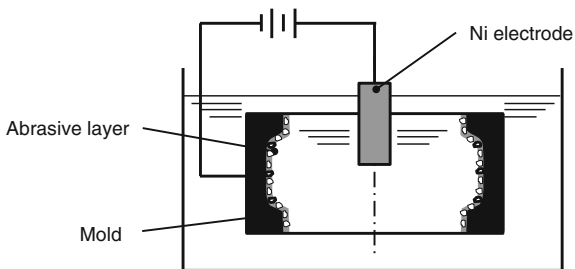
Diamond dressing rollers are important electroplated tools. They are used for profiling and sharpening of grinding tools (Sect. 6.5 “Tool Conditioning”). Diamond dressing rollers are either produced with a direct method or a reverse method [MINK99, YEGE86, KLOC09, p. 140]. In the direct method, the diamond grits are fixed stochastically on a profiled body. Therefore, the size deviation of the grits defines the geometrical envelope [KLOC09, p. 140].

The reverse method works with lost molds that have the negative profile of the dressing roller [LIER01]. The diamonds are either scattered or hand-set onto the profile area. The grits are then bonded together by electroplating or infiltration methods and the abrasive layer is fixed on the body.

Figure 3.18 displays the reverse centrifugal method for electroplating. The reverse centrifugal method works with a Ni-rich electrode to improve the coverage of the grits and a graphite mold. The process is relatively slow. The geometrical envelope of the dressing tool is not defined by the grits but by the mold. The concave profile elements of the mold define the maximum grit diamond size. Diamond rollers with highest packing density manufactured by the reverse method have the highest importance in industrial applications [KLOC09].

The German term “Diamantierung” summarizes diamond pattern, grit type, and bonding method. Manufacturers specify dressing tools by either the concentration of diamond grits in carat per cm^3 or by the number of diamond grits per cm^2 [MERZ94]. Profile rollers with a large diamond grit size or small diamond grit concentration generate high effective grinding wheel surface roughnesses [MERZ94, SCHM68]. Similar tendencies are obtained for form rollers [MERZ94, STUF96]. High grit

Fig. 3.18 Reverse centrifugal method for manufacturing dressing tools



concentration decreases the load on the single dressing grit, increasing dressing tool life [WIMM95]. However, the higher dressing tool costs might be unprofitable.

Hand-set diamond patterns can vary along the profile of a dressing roller. For example, the shoulder of a profile roller is equipped with bigger diamond grits in a smaller concentration than the face area [KLOC87]. The profile roller can then generate the grinding wheel shoulder with a higher surface roughness and the danger of thermally induced workpiece damage is minimized.

3.4.3 Manufacturing of Brazed Bonds

Brazing is a soldering process at higher temperatures. The grits are held mechanically and chemically in the bond. Therefore, the grit exposure can be higher than for electroplated wheels leading to bigger chip space (Fig. 3.19) [MARI04, p. 416 f.]. Chemically bonded grits allow for even thinner bonding layers than electroplated grits [CHAT90]. This has advantages of higher chip storage space and achievable material removal rate.

The wheel body material acts as substrate for the brazing process and has to be cleaned before [DING05]. The solder, also known as braze material, is deposited on the body (Fig. 3.20). This can be done by spreading the solder as powder. The abrasive grits are either deposited along with the solder or fixed temporarily before the brazing takes place. Brazing is done at temperatures of up to 1000 °C; the solder builds up around the grits and puts them under tensile stress when cooling [MARI04, p. 416 f.]. The mechanisms within the brazing process include complex

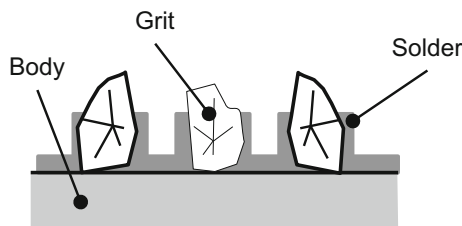


Fig. 3.19 Structure of a brazed layer after [MARI04, p. 416, DING05]

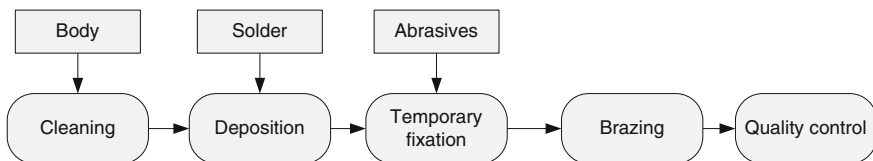


Fig. 3.20 Manufacturing of brazed bonded tools after [CHAT94, DING05]

steps, such as dissolution of the substrate, diffusion of elements, formation of reaction products, and wetting phenomena [DING05].

In the case of diamond, conventional brazing often results only in mechanical retention. Therefore, vacuum soldering is applied [BENZ91]. Using metals such as titanium, zircon, niob, or tantal in the solder enable carbide forming and therefore chemical grit retention. Because of the high oxygen affinity of these metals, the soldering process must be conducted in inert gas atmosphere or in high vacuum [BENZ91].

For CBN, high temperature metal alloys, for example based on Ni/Cr, are used [MARI04, p. 416]. Density and distribution pattern of the CBN grits define the performance of a brazed grinding tool [CHAT94]. Research on Ag–Cu–Ti alloy solders for CBN grinding wheels shows that reaction layers of TiN and TiB₂ can form [DING05]. These layers are key factors in achieving a strong bond between the CBN grits and the steel body of the grinding wheel.

3.4.4 Performance of Metallic Single-layered Bonds

In general, electroplated wheels have just one layer of abrasive grits. Therefore, tool life can be a major determining factor and grit strength is of major relevance. The range of characteristics available in diamond grit types is considerably wider for metal bonds than for use in other bonding systems. Often high strength crystalline diamond types are used. Abrasives that are more friable at lower loads are chosen for surface finish operations. [BAIL99]

The typical wear behavior of an electroplated grinding tool is not based on grit pull-out. Preferably, the grits undergo progressive chipping which maintains sufficient cutting action of the tool [BAIL99]. The worn surface, however, has minimal grit protrusion and the top surfaces of the grits are rough [BAIL99]. The achieved surface roughness Rt amounts to around 10 % of the abrasive grit size for a new electro-plated tool; with tool wear (running-in) Rt amounts to around 5 % [BOLD02].

Electroplated grits are held mechanically, brazed grits are held mechanically and chemically. In comparison to an electroplated CBN grinding wheel, a brazed CBN tool may offer higher grit protrusion and a stronger grit-bond adhesion [CHAT94]. The solder is able to establish a strong joint between the grit, solder, and the metal substrate of the wheel body as a result of chemical affinities [DING05]. Regular grit distribution can overcome loading problems from clustered grits in a random grit distribution [CHAT94].

A major improvement in performance for single-layered metallic bonds was achieved by the so called “Touch dressing” method in the mid 1980s [FERL92, p. 9]. Small depths of dressing cut level the protruded grit tops, so that the surface roughness of the grinding wheel is decreased, its profile accuracy improves, and the grinding process stability rises [STUC88]. Electroplated tools can be cleaned with a sharpening stone or ultrasonic bath [BOLD02].

3.5 Other Bonding Types and Hybrid Bonds

3.5.1 Rubber

Rubber bonds are another type of organic bonds [ROWE09, p. 42]. Rubber bonds were once prominent for grinding of bearings and cutting tools, but today are mainly used for cut-off wheels and control wheels in centerless grinding [MALK08, p. 29]. Rubber bonded tools are manufactured by mixing of grits with synthetic rubber or vulcanized natural rubber and sulphur, then rolled into sheets with the required thickness, and cutting out the desired shape (Fig. 3.21). Thin wheels are then directly vulcanized under pressure at 150–275 °C. In the case of thick wheels, the sheets are first stacked to the final wheel width and then vulcanized [MALK08, p. 29].

3.5.2 Shellac Bonds

Shellac bonding is another type of organic bonds [ROWE09, p. 42]. The first commercial use dates back to watchmaking applications in England in 1880, but it is also said that shellac bonds have been in use by Tamils longer before [LEWI76, p. 23]. Shellac bonds were once used for flexible cut-off wheels, but today are applied commonly to fine finishing of mill rolls, camshafts, and cutlery [MALK08, p. 29]. A further application is razor blade grinding [COLL88, p. 869 f.].

Shellac is a natural resin based on abietic acid derivatives [COLL88, p. 869 f.]. Insects swarming Cassum or lac trees in India exude shellac and its availability and properties depend on the weather conditions and species [MARI04, p. 413]. Shellac bonded tools are made by mixing grits with shellac, shaping under pressure in heated molds, and baking at temperatures of up to ca. 150 °C [MALK08, p. 29, COLL88, p. 869 f.]. Thinner wheels are consolidated on the mold by a steel roller; thicker wheels are baked several hours in quartz sand [LEWI76, p. 23].

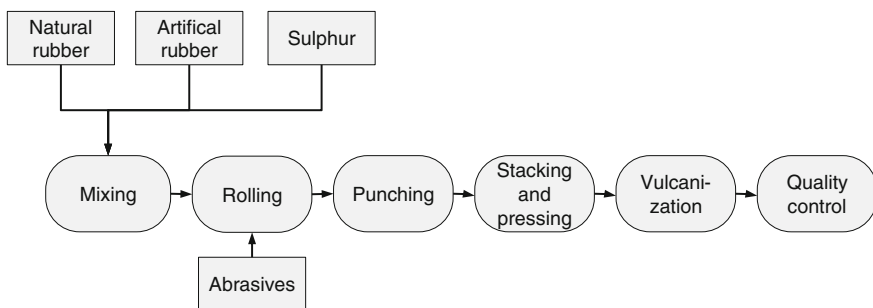


Fig. 3.21 Manufacturing of rubber bonded tools after [KLOC09]

3.5.3 Other Bonds

Oxychloride bonds were popular about a hundred years ago, but are used today only for disk grinding [MALK08, p. 29]. Oxychloride bonded wheels have excellent cool cutting abilities under dry grinding conditions [LEWI76, p. 23]. Oxychloride is formed as cement by cold-setting from the oxide and chloride of magnesium, i.e. magnesium oxide and an aqueous solution of magnesium chloride [MALK08, p. 29, LEWI76, p. 23].

Silicate bonds consist mainly of liquid glass and enable a grinding process with low temperatures, but silicate bonded tools wear quickly [BORK92, p. 38]. This bond type can be manufactured at lower temperatures (about 600 K) and in shorter cycles (10 - 30 h) than vitrified bonds [MALK08, p. 29, BORK92, p. 38]. Silicate bonded tools are produced by mixing grits with sodium silicate, compacting in a mold, drying, and baking [MALK08, p. 29, BORK92, p. 38].

Magnesite bonds consist of magnesium oxychloride from MgO and MgCl₂ solution [COLL88, p. 896]. The tools are formed by pounding or pressing, then dried and hardened in the mold at room temperature via formation of Mg(OH)₂ with stored MgCl₂. This bond type is only seldomly used, for example for the grinding of knives and files [COLL88, p. 896]. Magnesite bonds have to be marked with an expiration date, which is at maximum one year after the manufacturing date [DIN07].

Hybrid bonds of a resin and a metallic phase are generally used for superabrasive tools [UPAD09]. The metallic phase can be either a filler or a binding component to enhance grit retention depending on specification or manufacturing conditions [METZ86, p. 54]. In the 1970s, a hybrid bond from interpenetrating bronze and epoxy resin was invented and is used for the grinding of carbide cutting tools [CHAL72, UPAD09]. The porous metal bond is manufactured by cold pressing and sintering; the resin component is vacuum casted to infiltrate the pores [CHAL72, UPAD09]. Another composition of a hybrid bonding consists of bronze and polyimide phases [UPAD09].

3.6 Sustainability Dimensions to the Bonding System

3.6.1 Technological Dimension

Bond composition and structure define the self-sharpening ability of the tool and process stability. The main bonding systems for grinding tools are resin, vitrified and metallic bonds (Table 3.2). Each type has a huge variety in its specifications, manufacturing, and ingredients. For polishing and lapping processes also different kinds of slurry or pasteous binders exist, described in Sects. 4.4 and 4.5.

The bond composition has to enable strong grit retention, optimum grit protrusion, and optimum self-sharpening abilities. The tool manufacturer has to find

Table 3.2 Overview on bonds after [COLL88, p. 869 f.]

Bonding type	Chemistry	Manufacturing	Use
Resin bonds	Thermoset macro molecules (Duroplast) of crosslinked phenol, epoxy, or urethane resins	Dry mixture process with liquid resin and powder resin, hot or cold pressing, hardening in oven at 140–200 °C; or wet processing with two component system of resin and hardener, hardening in mold at 20–80 °C	Insensitive against impact, shock, and lateral pressure; high toughness; high cutting speeds and material removal rates possible for cut-off and roughing operations; high elasticity enables finishing operations with high surface quality
Vitrified bonds	Aluminum silicates of kaoline, quartz, feldspars and glass frits as fluxing agents	Casting or forming with temporarily binders and pressing, sintering process at 1000–1300 °C	High porosity; good resistance against cooling lubricants; cool cutting; wet and dry grinding
Sintermetallic bonds	Metals of steel, bronze, carbide powder	Sintering after pre-compressing in oven with reduced atmosphere, then pressing at high temperatures	High toughness; often used for diamond and CBN to machine hard and brittle material
Rubber bonds	Natural and synthetic caoutchouc	Mixture of vulcanization agent and grits between rolls, punching out of tools, hot pressing and vulcanization	Thin cut-off wheels of up to 0.05 mm thickness; precision grinding tools; control wheels for centerless grinding

Table 3.3 Mechanical properties for most utilized bonds after [MARI04, METZ86, p. 51]

Bonding type	Brinell Hardness (HB)	Rupture strength (N/mm ²)	Elasticity modulus (N/mm ²)
Resin bonds	228	7.21	1196.24
Vitrified bond	380	8.57	4133.41
Sintermetallic bond	278	14.29	5460.65

the appropriate compromise between hardness and erosion resistance [STOC86]. In the past, resin bonded wheels were preferred over vitrified bonded tools for working at higher speeds. This was due to the higher tensile strength of resin bonded wheels, but this limitation has been overcome [WHIT72]. Example mechanical properties of resin, vitrified and metallic bonds are shown in Table 3.3.

3.6.2 Economic Dimension

The type of bonding is decided by the application and technological performance and not so much by tool price. Nevertheless, the costs for a grinding tool are mainly impacted by the costs of the ingredients and processing costs. The ingredients' prices result from raw material extraction and material processing. Many raw materials in vitrified bonding systems are still obtained from natural resources because of the lower price, although synthetic materials ensure better constant quality [BOTS05, p. 14].

The heat treatment processes in tool manufacturing are major cost factors within the processing costs. Table 3.4 shows examples for different heat treatment processes indicating the varying energy demands for producing different bond types.

Reproducibility of bonded abrasive tools not only depends on the process stability influenced by machines and workers but also on environmental factors like air humidity, raw material wetness, etc. On a larger scale, this affects the number of faulty grinding tools and variability in grinding performance.

In grinding cost calculations, the user not only considers the acquisition costs of abrasives tools, but in addition, the costs for auxiliary processes such as conditioning and tool change (see Sect. 7.1.3 "Life Cycle Costing (LCC)"). The conditioning costs can vary widely depending on the choice of the bonding system.

3.6.3 Environmental Dimension

In Europe, the chemicals in the grinding tools have to be classified by REACH, the European Community Regulation on Chemicals and their Safe Use standards [ECHA12]. In the U.S., OSHA (Occupational Safety and Health Administration) and EPA (Environmental Protection Agency) have developed the OSHA Occupational Chemical Database [OSHA12b].

Bond ingredients might be health endangering, such as Li, CaO, B₂O₃ in vitrified bonds (Table 3.5) or heavy metals in metallic bonds (Table 3.6). However, substituting these risky ingredients might reduce the residuals intensity and direct hazards from these materials, but indirectly this might lead to higher tool manufacturing costs.

Table 3.4 Examples for heat treatment processes [TYRO03]

Bonding type	Heat treatment	Maximum temperature T_{\max} (°C)	Processing time t_{ges} (h)
Resin bonds	Curing/hardening	190	24
Vitrified bond	Sintering	1250	100
(Sinter) Metallic bond	Sintering	800	0.25

Table 3.5 Ecological and safety information on ingredients for vitrified bonding; hazardous materials identification system (HMIS) from 0 (no/minimum hazard)—4 (severe risk) [GEST12, SIGM12, NPCA02]

	Known ecological information	Chemical safety assessment
Calcium oxide, CaO	Low hazard to waters	Skin irritation, category 2 Serious eye damage, category 1 Specific target organ toxicity (single exposure), category 3; may cause respiratory irritation
Boron trioxide B ₂ O ₃	Hazardous waste Low hazard to waters	Reproductive toxicity; may damage fertility or the unborn child (category 1B)
Lithium oxide, Li ₂ O	–	Causes severe skin burns and eye damage (corrosive), category 3
Magnesium oxide, MgO	Low hazard to waters	–
Potassium oxide, K ₂ O	Low hazard to waters	Can react dangerously with water
Silicon dioxide, SiO ₂	–	Carcinogenic category 1 (silicosis)
Sodium oxide, Na ₂ O	Hazardous waste Low hazard to waters	Skin corrosion, category 1B; causes severe skin burns and eye damage Reacts violently with water
Naphthalene, C ₁₀ H ₈	Hazardous waste Severe hazard to waters	Carcinogenicity, category 2 Acute toxicity, category 4, oral

Pore builders are important fillers in bonded grinding tools. The prominent chemical naphthalene (Table 3.5) is hazardous to workers and the environment. Ongoing attempts to substitute naphthalene, e.g. with renewable material, indicate the problem to find a solution with technological similar results [DAVS04].

Particulate matter (PM) might occur from handling of loose abrasive grits and bond components [EPA94]. Heat treatment processes such as curing of resin bonded tools or sintering of vitrified bonded tools emit the main emissions in grinding tool production, in particular volatile organic compounds (VOC) or products of combustion, such as CO, CO₂, NO_x, SO_x, and PM [EPA94].

During the manufacturing of resin bonded tools, emissions form from formaldehyde and phenol. These emissions can be reduced to follow air standards by thermal after-burning [COLL88, p. 916]. However, investment and energy costs for the after-burning systems are relatively high and not feasible for small and medium sized companies, who will likely use absorption methods with activated-carbon filters [COLL88, p. 917].

Metal bonded abrasive tools are produced by infiltration, sintering, brazing, chemical or electroplating processes. The following basic principles can be applied for disposing the electrolytic baths [KLOC07, p. 192 f.]:

Table 3.6 Ecological and safety information on ingredients for metallic bondings [GEST12, UNIT09b]

		Exposure guidelines	Chemical Safety Assessment
Cu	Sintered bond (bronze), Solder in infiltrated bond	Exposure guideline for Cu dust: 1 mg/m ³ by OSHA PEL and ACGIH TLV	–
Co	Sintered bond (bronze)	Exposure guideline for Co: 0.1 mg/m ³ (as dust or fume) (OSHA PEL), 0.02 mg/m ³ (ACGIH TLV)	Cobalt exposure can cause skin irritation and skin sensitization Cobalt can cause skin and/or respiratory sensitization Cobalt is classified as group 2B carcinogens by IARC
Fe	Sintered bond	Exposure guideline for iron oxide: 10 mg/m ³ (fume) (OSHA PEL), 5 mg/m ³ (respirable) (ACGIH TLV)	–
Ni	Electroplated bond, Solder in infiltrated bond	Exposure guideline for Ni: 1 mg/m ³ (OSHA PEL), 1.5 mg/m ³ (inhalable fraction) (ACGIH TLV)	Nickel exposure can cause an allergic dermatitis Nickel can cause skin and/or respiratory sensitization Nickel is classified as group 2B carcinogens by IARC
Sn	Solder in infiltrated bond	Exposure guideline for Sn: 2 mg/m ³ (OSHA PEL, ACGIH TLV)	–

- Transformation of toxic substances in non-toxic chemical compounds,
- Transformation of all organic products into CO₂, water, and N₂,
- Transformation of all heavy metal compounds into an insoluble form,
- Neutralization of all solutions, or
- Avoidance of additional saline load from the waste water treatment.

Table 3.7 shows data on embodied energy, CO₂ and water usage in the primary production of epoxies and phenolics for resin bonds and Ni, Cu, and WC for metallic bonds. Reserves and recyclability are important for the future availability of these materials.

3.6.4 Social Dimension

The workers need to be protected during handling of potentially dangerous bond ingredients (Tables 3.5 and 3.6). Furthermore, the electrolytic baths in producing single layer metal bonded tools need to be maintained carefully to keep workers and local communities safe. Naphthalene as pore builder is discredited and might also affect worker health.

Table 3.7 Environmental material data (*estimated values) [GRAN10]

	Embodied energy, primary production (MJ/kg)	CO ₂ footprint, primary production (kg/kg)	Water usage (l/kg)	Reserves and recyclability
Epoxies	105–130	4.22–4.56	*107–322	*3.7–3.8 Mt
Phenolics	85.9–95	2.83–3.12	*94–282	*251–255 Mt
Ni and alloys	127–140	*7.89–8.82	*134–512	63–65 Mt, Can be recycled
Cu and alloys	65–80	4.9–6.74	*149–535	470–490 Mt Can be recycled
WC	82.4–91.1	4.44–4.9	47.8–144	

3.6.5 Sustainability Model for Bonding Systems

The bond material is chosen with technological, economic, environmental and social considerations. The raw material supplier is mostly concerned with the following aspects:

- **Bond and raw material price** depend on the **raw material availability**.
- Furthermore, **energy and labor costs** affect the price.
- The **location** of the production affects logistics and energy availability.

The tool manufacturer needs to consider additional aspects:

- **Bond price** affects the manufacturer’s profit margin. **Raw material availability** is important for a consistent tool quality.
- Furthermore, **worker health and protection measures** depend on the bond type and ingredients.
- **Legislation** might demand for disclosing all bond ingredients.

The tool user is mainly interested in

- **Dressability** of the bonding because it affects tool use and process quality.

Society and local communities are worried about

- **Emissions** from bonding ingredients and tool manufacturing processes. For example, the artificial pore builder naphthalene is under strict observation.

Chapter 4

Abrasive Tool Types

It is difficult to say when abrasive technology had a beginning. Abrasives were used by man many thousands of years before he learned to write. Primitive man used abrasives for the sharpening of tools of wood, bone or flint. [...] The beginning of the science of abrasives, however, may be taken as that time when man began to select certain rocks for their peculiar properties, and to fashion these into tools for grinding. [COES71].

Grits and bonding systems have been introduced in the previous two chapters and their impact on technological, environmental, economic and social sustainability has been discussed. Yet not only the ingredients, but also the design and type of tools define sustainable grinding process performance. Therefore, this chapter discusses abrasive tools distinguished by the cutting edge engagement (Fig. 1.1). In grinding with bonded or coated tools, the grit penetrates the workpiece bound to a path. Room-bound interaction takes place in lapping and polishing, where the grits roll between workpiece and a counterbody, often within slurry. In energy-bound abrasive processes, the grits are accelerated towards the workpiece material and dash particles out of the surface. The fourth active mechanism occurs when the tool is pressed with higher force but constant pressure onto the workpiece. Vibratory grinding and honing are considered to be mostly force-bound processes.

4.1 Grinding Wheels

Grinding wheels are also known as bonded tools. The German Norm DIN 8589 specifies grinding processes by the machined workpiece area, wheel contact area, and feed direction [DIN03]. Most conventional grinding wheels consist of the conventional abrasives Al_2O_3 or SiC in a monolithic wheel body (Fig. 4.1 left). Superabrasive grits are more wear-resistant and expensive, so it is established that they are used in a thin abrasive layer on a wheel body. Depending on the bonding system, the abrasive layer is multi-layered and can be dressed (Fig. 4.1 middle) or mono-layered (Fig. 4.1 right).

For high-speed machining, vitrified bonds have higher safety requirements on grinding tool toughness. High efficiency deep grinding requires tools with appropriate porosity and high toughness. Conventional grinding tools have gained competitiveness through low-temperature sintering bonds and enhanced abrasive grits. [KLOM86, p. 9]

4.1.1 Shapes

Tools are characterized by tool shape and abrasive layer composition. The tool shape specification follows DIN ISO 525 and DIN ISO 603, FEPA standards, ANSI B74.2 (conventional tools), or ANSI B74.3 (superabrasive tools) [DIN00a, DIN00b]. In addition, the wheel specification often includes company specific terms as well as the used standard. Table 4.1 shows typical categories in tool specifications.

Table 4.1 Typical denomination of grinding wheel shapes [DIN00a, DIN00b]

Type/form number	Layer profile shape	Position of layer	Special forms (holes, etc.)	Max. wheel speed (m/s)
1 (Cylinder)	A (Straight)	1	C	20
2 (Ring)	B (Inclined)	(Circumference)	...	63
3 (Tapered one side)	E (Cone)	2 (One face side)		...
...	F (Round)	3 (Both face side)		
6 (Straight cup)	V (Face)	...		
...	...			

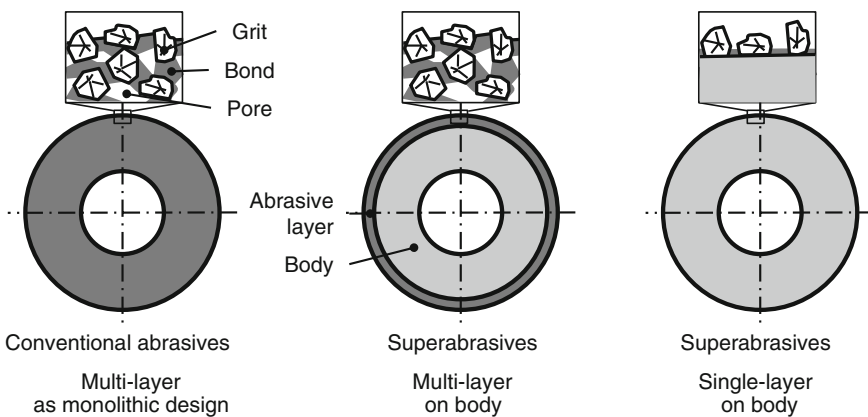


Fig. 4.1 Bonded abrasive tools

The wheel dimensions are expressed in the form of “(outer diameter) × (thickness) × (inner diameter)”; for superabrasive wheels the layer thickness is added [MARI07, p. 46]. Many examples of tool shapes are shown by Marinescu et al. [MARI07, p. 46–48].

Layer width is important for grinding forces and achievable surface roughness. Cup wheels with a higher layer width can achieve significantly lower workpiece roughness than cup wheels with a small layer width due to the higher number of passes [JUCH78].

The abrasive layer is composed of abrasive grits, bonding, and pores (see Sect. 6.1 “Abrasive Layer Composition”). The volumetric composition of grits, bonding, and pores tailors the grinding tool application. The grits have to perform the cutting action. The bonding holds the grits together and releases blunt grits. Furthermore, the bond transfers the forces from the tool rotation and conducts process heat. The pores bring cooling lubricant to the cutting zone and transport chips away from it. The pores act as chip and cooling lubricant space and can be varied in number, size and total volume in a wide range via artificial pore builders.

Table 4.2 describes typical information contained in the tool designation. Marinescu et al. summarize examples of conventional wheel specifications [MARI07, p. 109] and of vitrified CBN wheel specifications [MARI07, p. 117].

“Structure” can be defined as a characteristic proportional to the distance between grits, but this definition just works for constant grit sizes [RAMM74]. These structure grades do not necessarily provide information about the porosity of the abrasive layer [RAMM74]. Abrasive layer structure is discussed in Sect. 6.1 “Abrasive Layer Composition”.

Table 4.2 Typical specifications of grinding tool layers [KLOC09, MARI07, p. 109, 117, BORK92, p. 33, 40, DIN00a]

Abrasive grit type	Grit size	Hardness grade	Structure	Bonding type	Grit concentration	Body
A (Al ₂ O ₃) C (SiC) Maybe special grit type, e.g. 99A, 95A	Given in [mesh] 4 (coarse)–1200 (very fine)	A (softest)–Z (hardest)	0 (dense)–14 (open, high porosity)	V (vitrified) B (resin) E (shellac) Mg (magnesite)	Not applicable	Not applicable
B (CBN) D (diamond)	Mostly given in [μm] 46–1181 μm			V or VSS (vitrified) K or KSS (resin) M (sintermetallic) G (galvanic) Bz (bronze)	Given in V (Vol.%) for CBN, in C (ct/cm ³) for diamond	A (aluminum) B (phenolic resin) ...

4.1.2 *Special Grinding Wheel Types*

4.1.2.1 Centerless Grinding Wheels

Centerless grinding is commonly applied for large batch and mass production. In this circumferential grinding variant, the workpiece is not fixed along its axis between centers, but is supported on its circumference. Centerless grinding can be external or internal. In external grinding, the workpiece lies between grinding wheel, workrest plate and control wheel. In internal centerless grinding, the workpiece lies between rolls or shoes and is driven by a control wheel or a face-plate. [LINK14b]

In centerless grinding wheels, the structural density along the wheel width has to be monitored carefully. During manufacturing and pressing of large width wheels, the pressure needs to be higher and applied longer than for thinner wheels [TYRO03]. For centerless grinding wheels, wear is highest in the transition zone from grinding to spark-out zone. This is however not connected to the wheel density, but to the profile wear in transverse grinding operations as explained in Sect. 6.3.1 “Macro Effect—Tool Profile Loss”.

The contact properties between workpiece, grinding wheel, control wheel, and workrest plate define process stability [SCHR71]. The grinding wheel elasticity affects the grinding forces and depth of cut [SCHR71, p. 28 f.].

The control wheel, also known as regulating wheel, regulates the speed of the workpiece. It is a conventional grinding wheel, often rubber bonded corundum, or a steel body with a cemented carbide coating. The control wheel regulates the workpiece speed by accelerating or decelerating through friction. Control wheels have complex shapes to realize a linear support of the workpiece. Control wheel profile is influenced by control wheel inclination angle, workpiece center height, and workpiece diameter [MEIS81]. New calculation models for control wheel profile enable shorter dressing times and lower wheel wear [MEYR12].

4.1.2.2 Gear Grinding Wheels

Gear grinding is distinguished into generating grinding and profile grinding as well as continuous and discontinuous grinding [KARP08]. Generating gear grinding generates the gear shape mainly by the complex process kinematics, profile gear grinding mainly through the grinding wheel profile (Fig. 4.2).

The grinding tools have to withstand long contact lengths. The contact length in tooth flank profile grinding can be as long as in creep feed grinding [SCHL04]. Karpuschewski et al. [KARP08] describe recent developments in gear grinding applications.

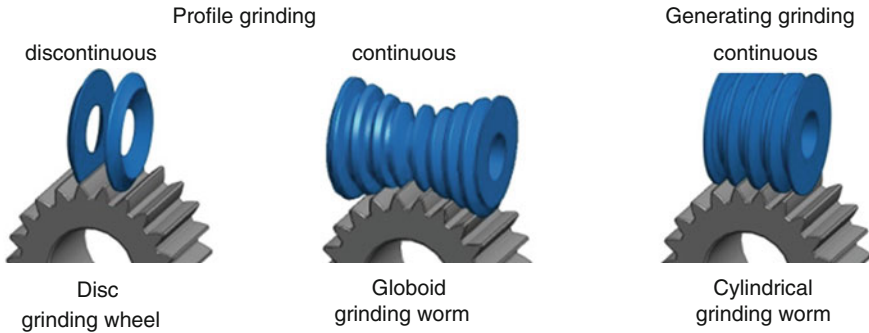


Fig. 4.2 Gear grinding tools, with permission from the Gear department, WZL of RWTH Aachen University

4.1.2.3 Cylindrical Peel Grinding Wheels

External cylindrical form grinding processes or so called peel grinding procedures are defined by a transverse feed and an inclined wheel. As consequence, the machining zone is small and approaches a punctiform contact in theory. This procedure is very flexible regarding workpiece shape and the grinding forces are comparatively small. Due to the punctiform contact zone, however, the grinding forces result in high pressure and high load on the single abrasive grit. Often superabrasive grits are used and they have to be fixed well within the binding matrix. In general, the abrasive layer exhibits a high hardness [BLAN07]. Today, mostly vitrified bonded CBN grinding wheels are used with wheel circumferential speeds of up to 160 m/s for peel grinding applications [BLAN07]. Specific material removal rates of several hundred mm^3/mms are possible [BLAN07].

The variant Quick-Point grinding was patented by Sir Erwin Junker in 1994 and integrates high wheel speeds, CBN grits, and CNC controlled paths [WANG12]. Consequently, tool layout has to be adapted [BLAN07]. Wang et al. [WANG12] suggest that future research focusses on new matrix materials with low density, thermal expansion coefficient, and high specific strength.

4.1.2.4 Tool Grinding Wheels

Tool steels and high-speed steels are machined with corundum or CBN wheels [LINK09, KÖNI80]. Carbides and ceramic tools are ground mainly with silicon carbide or diamond wheels. Diamond grit sizes for carbide tool grinding wheels lie commonly between D46 and D181 [FRIE02, p. 46]. Diamond grits with low toughness enable self-sharpening during the grinding process, whereas an irregular shape facilitates good grit retention in the bond [TOML78a]. For the machining of tough carbides and cermets, tendency goes to applying high diamond grit concentrations to have small single grit forces [FRIE02, p. 46]. As consequence, the

grinding wheel wear is low and dimensional tolerances as well as form tolerances of the machined workpieces can be kept constant. Tool grinding operations demand for grinding wheels of complex shapes. Resin bonds have advantages in easy dressability and good damping capabilities because of their soft bonding [FRIE02, p. 53].

4.1.2.5 Surface Grinding Wheels for Turbine Materials

Turbine materials such as Ni- or Al-alloys are highly ductile and produce long chips. The danger of wheel clogging is given and chip formation is characterized by smearing and burr generation. The low heat conductivity of turbine materials leads to heat induced damage of the surface layer in the grinding process. As consequence, grinding wheels for turbine materials stand out by their high porosity. In industry, continuous dressing is applied to sharpen and clean the grinding tool simultaneously to the grinding process.

The so-called Viper grinding method uses high pressure coolant flow to continuously clean and dress the grinding wheel [HILL00, HYAT10]. Highly porous wheels are used. In addition, the carbides and intermetallic phases in turbine materials object the grinding tool to abrasive wear, so that self-sharpening occurs.

4.1.2.6 Grinding Pins

Grinding pins, also called mounted wheels or mounted points, are small wheels to which a mandrel is cemented, molded or die casted into one end [LEWI76, p. 44]. These tools are often used in hand-held operations for deburring, finishing of welds, chamfering, or dental operating procedures. A large variety of shapes exists (see DIN ISO 525) [BORK92, p. 32, DIN00a]. The long shafts of grinding pins act as cantilever and grinding forces lead to deformation of the tool. An open wheel structure with soft bonding enables favorable self-sharpening.

4.1.2.7 Long Needle Diamond Grinding Wheels

In the late 1970s, long needle diamonds were offered on the market [METZ86, p. 43, DYER79]. These long needle diamonds have a proportion of length to thickness of between 2:1 and 5:1 [TOML78a]. They are synthesized with growth direction in diamond main axis direction, i.e. crystallographic [100]-direction [TOML78a]. The growth mechanism of constant buildup on (111)-areas leads to a stepwise surface structure. Diamond cleaves parallel to the octahedric planes, so that long needle diamonds are weak in rectangular direction to their main axis. In grinding, the grits can easily break along the stepwise growth planes and a controlled grit wear is likely [JUCH78, TOML78a].

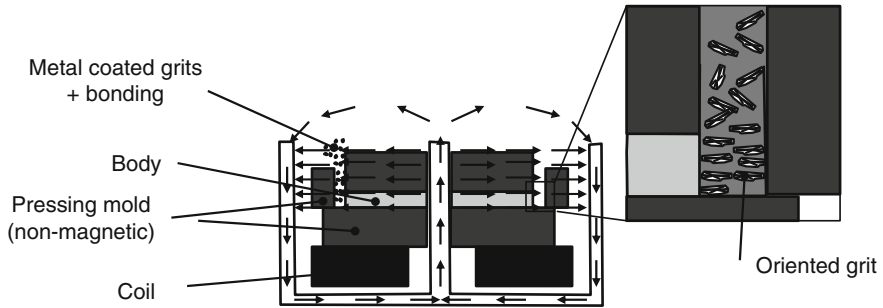


Fig. 4.3 Electromagnetic system to orientate long needle diamonds in cylindrical 1A1-wheels after [TOML78a]

The grit size classification of long needle diamonds cannot be done via conventional sieve procedures, therefore grit manufacturers have to do physical measurements with projectory microscopes [TOML78a].

To attain the theoretical breakage behavior as well as optimum grit adherence in the bond, needle grits with ferromagnetic coating can be arranged with electromagnetic systems. The example in Fig. 4.3 works with radial magnetic field lines in cylindrical 1A1 grinding wheel die forms. The grits orientate themselves parallel to the magnetic field lines when they are filled into the die form with the resin bond mixture. Pressing and curing processes are similar to other resin bonded wheels. [TOML78a]

In grinding applications, grinding wheels with needle diamonds have a higher number of active abrasive particles on the surface than similar abrasives of the same grit size. Therefore, resin bonded long needle diamond tools showed a better performance for brittle workpiece materials [TOML78b]. However, the long needle diamond grinding wheels was not popular in the market [METZ86, p. 43 f.]. In contrast to grinding, needle type diamonds find wide application in dressing of vitrified bonded grinding wheels.

4.2 Coated Abrasive Tools

Coated abrasive tools are composed of abrasive grits that are held by a bond on backing material (Fig. 4.4). Coated abrasive tools are belts, pads, or discs. Abrasive discs are used for preparing car bodies before painting [BORK92, p. 42 ff.]. Deburring, roughing, and finishing are important operations with coated tools in the metal grinding field [KÖNI86]. Coated abrasive tools cover a bigger market volume than grinding wheels [ASAM10, p. 312].

Figure 4.4 shows the abrasive layer structure and common designs of coated abrasive tools. Grinding engagement between grinding belt and workpiece is

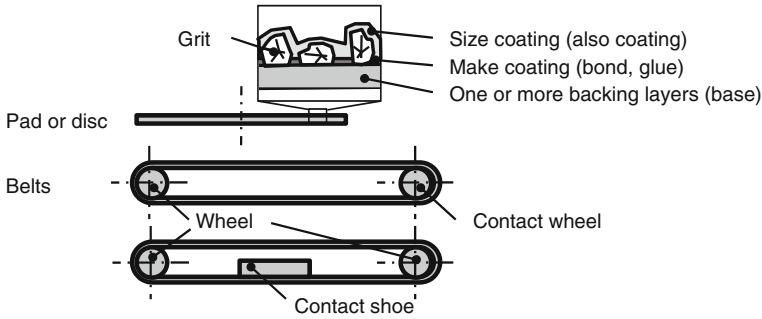


Fig. 4.4 Coated abrasive tools

established by contact shoes or wheels or the engagement can take place on the free part of the grinding belt without a contact element [KÖNI86].

Coated abrasive tools consist of the components in Table 4.3, namely grits, backing material, make coating, size coating, and splice. In addition, abrasive grit size, shape and size of the abrasive tool are important characteristics [BORK92, p. 42 ff.].

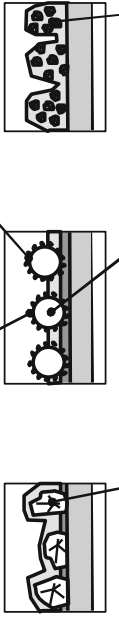
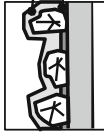
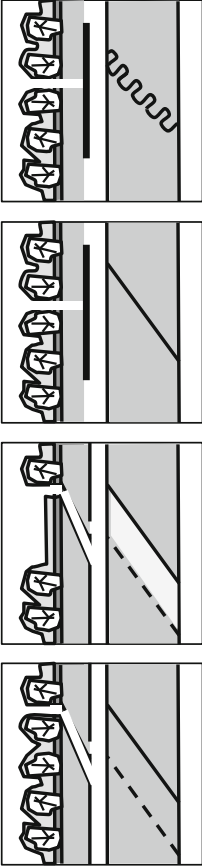
4.2.1 Manufacturing

Grinding belts are manufactured as displayed in Fig. 4.5. The manufacturing route starts with the backing material, which can be paper, cloth of natural or synthetic fiber, or metal (in the case of diamond coated abrasive tools) [BORK92, p. 47]. In addition, the backing can be wet-proofed or reinforced with wire. Strength and flexibility are main characteristics of the backing material.

The bond material to hold the abrasive grits can be applied in one or more layers, with the make coat as base bond and size coatings as upper bonds [BORK92, p. 47, KÖNI86]. Additional coatings can have dust-repellent effects [KLOC09, p. 66]. First, the make coating is applied and will form a gel after cooling or drying [KÖNI86]. This gel fixes the abrasive grits, which are applied in the so called mineral coating step either by gravitational force (gravity scattering) or by electrostatic scattering. [KLOC09, p. 69 f.]. In the gravity scattering method, a distribution device applies the grits on the coated backing material. In the electrostatic scattering method, the coated backing material is moved upside down over a transport belt, on which the abrasive grits are oriented by an electrostatic field [KLOC09, p. 69]. The advantages of the electrostatic scattering method are an even grit distribution, a higher reproducibility, and higher grit protrusion (Fig. 4.6).

After positioning the grits, the size coating is applied. It supports the retention of the grits amongst each other. After drying and hardening, the belt is rolled, cut, and possibly joined. The type of belt splice is crucial for the process stability and can be reinforced with foil [BORK92, p. 45]. Overlapping splices can be used for all

Table 4.3 Components of coated abrasive tools [BORK92, p. 47, KÖNI86, KLOC09, p. 67 ff., CHRI96, COLL88, p. 911, UAMA09]

<p>Abrasive grit</p>	<p>Single abrasive grits: Al_2O_3 (especially hollow corundum), SiC, CBN, diamond, also garnet and cerium oxide for polishing operations Compacts of multiple grits</p>  <p>Single crystal grit Grit Sphere bond Compact bound</p>
<p>Backing material, also called base</p>	<p>Paper (from light to heavy), polymeric material such as polyester, cloth of natural or synthetic fiber (such as rayon, cotton, nylon), metal (for diamond coated abrasive tools), or combinations reinforcements are optional</p>
<p>Make coating, also called bond or glue Size coating, also called coating</p>	 <p>Hide glue (animal glue), resin Resin Hide glue (animal glue), resin Hide glue Resin</p>
<p>Splice type, also called joint</p>	<p>Overlapped, straight butt, sine wave butt reinforcement is optional</p>  <p>Lap splice Lap splice with removed grits Straight butt splice Sine wave butt splice</p>

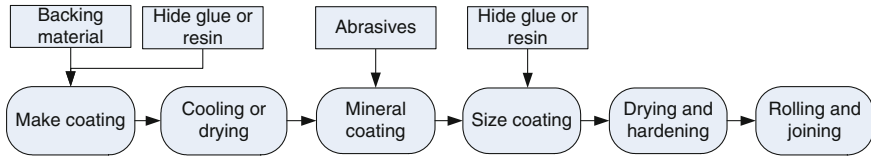


Fig. 4.5 Manufacturing of grinding belts after [KÖNI86]

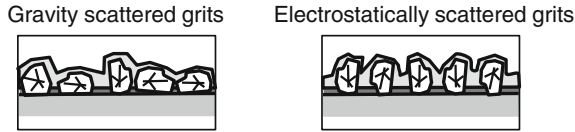


Fig. 4.6 Scattering methods for grinding belts

applications. However, the area close to the lap splice might differ in thickness, which can lead to marks on the finished surface. Therefore, lap splices with removed grits are recommended if the ground surface needs an unmarked surface finish [KÖNI86]. Straight or sine wave butt splices can withstand extremely high stresses, e.g. for high performance applications [KÖNI86]. However, every splice can set up vibrations in the machine/tool/part system, resulting in chatter and surface marks on the parts [KÖNI86]. New endless, spliceless belts overcome these troubles [CHRI96].

4.2.2 Abrasive Grits

The single crystal grits used in coated abrasives are similar to the ones used in grinding wheels. Grit sizes are usually graded in larger intervals than for grinding wheels [BORK92, p. 46]. The grits are fully embedded in the bond material, which leads to high resistance against grit-breakout [KÖNI86, KLOC09, p. 217]. Therefore, the wear mechanisms grit splintering and attritious wear are more common than grit-breakout in belt grinding [KÖNI86, KLOC09, p. 217].

Besides single crystal abrasives, polycrystalline abrasives are standard for coated abrasive tools. Hollow corundum is a sintered abrasive in the form of a hollow sphere and has proven to be a long-lasting abrasive material for belts [BORK92, p. 46]. Even if the spheres wear, they expose abrasives on their hull and perform uniform cutting action.

Compact bonds are aggregated abrasives in a bond, which can form special shapes. Recently developed examples are pyramid-shaped conglomerates of diamonds in vitrified bond, which are advantageous in lapping [ZHEN10]. The diamond particles are held in a vitreous bond and are shaped like truncated pyramids, which allows a stationary wear [ZHEN10]. The pyramids are fixed with a resin matrix to the backing material [ZHEN10].

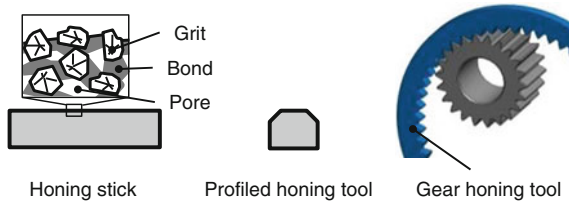


Fig. 4.7 Honing tools, with permission from the Gear department, WZL of RWTH Aachen University

4.3 Honing Tools

Honing tools are similar in bonding and grit material to grinding wheels. Prominent tools are honing sticks, profiled tools, and gear honing tools (Fig. 4.7). The shape is defined by DIN 69186.

In particular, vitrified, resin, sintered, and electro-deposited bonds are used [KOPP81]. Grit sizes and grit concentration are similar to grinding tools with relatively high concentrations. Fine grit honing sticks are used for sizing and surface finishing, not for form correction [KOPP81]. Unlike grinding operations, diamond and CBN can have similar honing results for the same material machined.

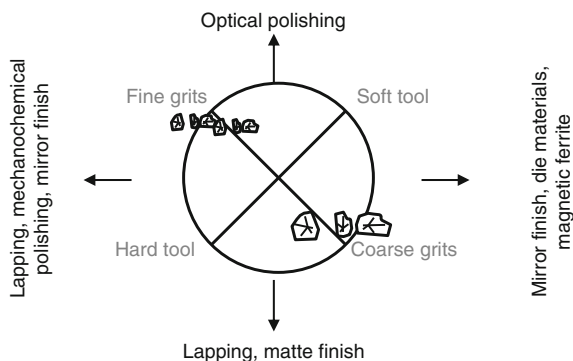
In honing tools, the bond hardness is selected in relation to abrasive grit size. Harder bonds are generally taken for coarse diamond and CBN. For honing sticks, ferrous bonds are frequently used for coarser grits (bigger than D151 or B151), softer bronze bonds are the norm for middle size grits (D64–D126 or B64–B126) and resin bond is used for finer grits to micron size. [KOPP81]

According to the German standard DIN 8589 honing is defined by the continuous contact between tool and workpiece. This does not apply to gear honing. Per definition and in consequence, gear honing processes belong to the category of grinding processes. In gear honing, the honing tool is profiled with an internal gear toothing. The honing tool is dressed with a gear dressing roller and a cylindrical dressing roller for setting back the honing wheel teeth [VUCE08]. Vucetic compared vitrified and resin bonded gear honing tools in single grit scratch tests and honing tests and found consistently that the vitrified bond can hold the grits better than resin bonds [VUCE08].

4.4 Polishing Tools

In the polishing process, the abrasive particles are finely dispersed in a liquid medium or binder and are directed over the workpiece surface by a counterbody [KLOC05a, p. 404]. Therefore, the polishing tool is rather a paste or suspension of abrasive grits in a medium or binder [MARI04, p. 442].

Fig. 4.8 Lapping and polishing after [KASA90]



In plate polishing processes, a binder retains the abrasive particles on the plate surface. The binder needs to fuse on light contact with the polishing plate and adhere well to the surface. The quality of the paste depends on fusion temperature and vaporization temperature of the binder. The greater the difference between these temperatures, the better the quality of the compound will be. [MARI04, p. 442]

Polishing processes can be classified according to abrasive grit size (fine or coarse) and counterpart (hard or soft) (Fig. 4.8) [KASA90]. Optical polishing of glass works with fine grit and a soft counterpart. This classification, however, does not give an indication of the active mechanisms for material removal [HAMB01, p. 6]. In general, an interaction of chemical and mechanical mechanisms achieves the material removal [KLOC05a, p. 404].

Polishing of steel with diamond grits in a water-alcohol suspension can be explained by the local loads between polishing grits and workpiece which can lead to plastic deformation of the steel [DAMB05, p. 125]. Due to the high thermal conductivity of the diamond grits, heat effects and chemical reactions are unlikely [DAMB05, p. 126]. Material removal takes place because of micro plowing and micro chipping [DAMB05, p. 126].

4.4.1 Abrasives for Polishing

Abrasives for polishing processes tend to be chosen according to the desired material removal rates. Common grit sizes are around $1\ \mu\text{m}$ [MARI04, p. 442]. In rough abrasive pastes, the following abrasives with higher hardness are used [MARI04, p. 381, BORK92, p. 11, 13, 20, DAMB05, p. 33]:

- Diamond (C),
- Magnesia (MgO),
- Pumice (vitreous spongy compound formed after drying of volcanic lava),
- Beryllium oxide (BeO),
- Chrome oxide (Cr_2O_3),
- Iron oxide (Fe_2O_3),

- Garnet (class of minerals with the formula $(\text{Me}_3\text{Me}_2''\text{SiO}_4)_3$, with Me'' being Fe, Mg, Co, or Mn, and Me''' being Fe, Al, or Cr),
- Corundum (60–90 % Al_2O_3),
- Emery (60 % Al_2O_3 and Fe_3O_4 , Fe_2O_3 , SiO_2),
- Quartz (SiO_2 with CO_2 , H_2O , NaCl and CaCO_3 inclusions),
- Silica carbide (SiC), and
- Glass (Processed recycled glass has been sold as an abrasive blasting medium under several brand names in the United States).

Soft abrasives as the following are employed for fine polishing paste compositions [MARI04, p. 381 f., BORK92, p. 20]:

- Kaolin,
- Chalk (obtained from crushed, rinsed and washed limestone),
- Barite (barium sulfate),
- Talc (hydrous silicate of magnesium),
- Tripoli (white sedimentary mineral obtained after coagulation of silica gels in laminae compacted into soft rock mass), and
- Vienna lime (white powdery composite of fine-crystalline calcium and magnesium oxides, obtained after burning dolomite).

4.4.2 *Binding Materials for Pastes*

Binders for pastes include the following [MARI04, p. 442 f., BORK92, p. 24]:

- Stearin—stearic acid, $\text{CH}_3(\text{CH}_2)_{16}\text{COOH}$, white, solid, crystalline substance, melting point of 140 °C; Stearin is a good binder and brings cohesion and hardness to the paste.
- Oleic acid—olein, unsaturated fatty acid, melting point of 15 °C; Oleic acid accelerates the polishing process by dissolving metal oxides.
- Paraffin—waxy, crystalline mixture of fatty hydrocarbons, melting point of 44 °C; Paraffin does not likely convert into a resin or carbonize. It brings cohesion, elasticity, hardness, and adhesion to polishing pastes.
- Fats—Organic, fusible glycerides of saturated fats and unsaturated oils; Fats are often used instead of stearin.
- Wax—Solid, unctuous or liquid fatty acid esters with higher fatty alcohols; Examples are carnauba plant wax (melting point 353–359 K), beeswax (melting point 333–340 K), and montan wax (melting point 351–353 K). Waxes provide hardness and cohesion to a paste.
- Petroleum jelly—petrolatum, obtained from asphalt less paraffin-base crude oils; This substance reduces the hardness of a paste.

Surface-active substances and emulsifiers are sometimes added to polishing pastes. Their tasks are to intensify the machining operation and to increase

durability of the abrasive compound. Thixotropic substances (including aluminum soaps, aluminum alcoholates, complex bentonite, and fine talc powder below 1 μm) are added to fluid pastes to increase viscosity [MARI04, p. 443]. For example, in glass polishing the fluid has a large effect on the tribological effects and material removal process [HAMB01, p. 127].

Polishing with pitch is used to finish high value optical components. Pitch is a viscoelastic material and primarily derived from either pine tree resins or petroleum-based resins [MULL08].

4.4.3 Counterparts

A large variety of counterparts or polishing pads is available with a lack of application based models [DAMB05, p. 30]. Three main types for counterbodies can be distinguished [KHAL79, DAMB05, p. 30]:

- Deformable polishing pads, such as pitch or cast polyurethane,
- Soft polishing pads, such as cloths and synthetic felt with porous structure,
- Hard polishing pads, such as hard felt, filled or not filled polyurethane foam, impregnated cloths, fine laminates.

The choice of the pad affects the material removal rate. Hambuecker [HAMB01, p. 126], for example, showed that polyurethane foam is superior to pitch pads in automated glass polishing.

4.5 Lapping

Lapping is a mainly room-bound process with geometrically undefined cutting edges. It is defined as a cutting process with loose grits distributed in a fluid or paste, so called lapping slurry, guided by a counterpart, which is usually shape-transferring (also called lapping tool). The cutting paths of the individual grits are ideally undirected [KLOC09, p. 338]. Effective mechanisms are complex and assumed to be a superposition of chip formation, micro-grooving, and brittle machining by micro-cracks and particle break-out [KLOC05a, p. 384 f.].

Known process variants are planar lapping with fixed or freely moving workpieces, external or internal cylindrical lapping, profile lapping and ultrasonic lapping amongst others. Karpuschewski [KARP01, p. 173 ff.] summarizes sensors for lapping operations.

4.5.1 Abrasives for Lapping

Common abrasives for lapping processes include silicon carbide, corundum, boron carbide (B_4C), and diamond [KLOC05a, p. 394, STAD62, p. 24]. Boron nitride (B_4N) is used for lapping of carbides [MARI04, p. 394]. Regular grit dimensions are as follows [MARI04, p. 442]:

- Silicon carbide and corundum: 5–1 μm
- Boron carbide: 60–5 μm
- Diamond: 5–0.5 μm
- Chromium oxide: 2–1 μm

Diamond slurries are designed so that even coarse grits remain homogeneously dispersed in the fluid. The abrasives will not settle out, even if the slurry binder has a low viscosity [KLOC05a, p. 393]. Conventional abrasives are continually fed onto the lapping plate to restore broken down particles. Recharge of diamond grits occurs less frequently [DAVI74].

In abrasive processes with loose abrasives, shape, grit size, size distribution, and grit breakdown characteristics are important variables for process control [DAVI74]. As for grit shape, blocky isometric grits are considered the best, because they lie between the extremes, sphere and needle [DAVI74]. Spherical grits tend to roll between lapping plate and workpiece instead of performing machining action; Needle particles, in contrary, can cause deep scratches. The presence of a few oversized abrasive grits can result in serious workpiece damage [DAVI74].

4.6 Tools for Abrasive Sawing

The biggest volume of diamond saws is used in cutting stone and refractory materials. Abrasive wires and saws are also used in the electronics and solar industry to cut silicon and quartz crystals into wafers. In Multi-Wire-Slicing, a wire is led by several coils to form several wire lines, which cut simultaneously [KLOC09, p. 386]. The wire can either contain grits or work within a grit containing slurry (Fig. 4.9 left).

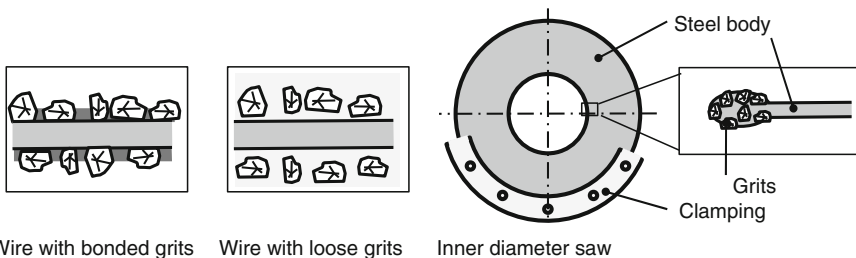


Fig. 4.9 Abrasive wires and hole saw

4.6.1 Wires with Bonded Grits

Wires with bonded grits consist of a core coated with abrasive grits, mostly diamond. The diamonds can be bonded through resin bonds or by electroplating [CHIB03, KLOC09, p. 385]. Chiba et al. [CHIB03] presented a new high-speed electroplating process to manufacture the wire saws faster and cheaper.

4.6.2 Wires with Loose Abrasives

In the wire lapping procedure, a lapping medium of grits (commonly SiC) and medium (commonly oil or glycol) is sprayed on a non-coated wire [KLOC09, p. 386]. Because of the high costs and expensive disposal of the slurry, researchers have developed strategies for slurry refreshment and recycling [KLOC09, p. 387].

4.6.3 Inner Diameter Saw

The inner diameter saw, also called inside hole saw or ID-saw, consists of a rotating steel blade, whose inner diameter is electroplated with diamond grits (Fig. 4.9 right) [KLOC09, p. 387]. The steel blade is clamped at its outer diameter and either the saw blade or the workpiece are moved radially.

4.7 Other Methods with Free Abrasives

4.7.1 Crushing

In the materials processing terminology, particle size reduction by mechanical means is called grinding [HOGG01, LYNC05]. Other terms are crushing, milling, or attrition milling. The term crushing is used for bigger end size particles (e.g. about 13–19 mm in diameter); the term milling refers to low micron sizes or below.

Machines used for these processes are often called grinding mills [SCHI10]. The grinding machines can be media mills (tumbling mill, centrifugal mill, stirred-media mill, vibratory mill), impact mills (hammer mill), or fluid energy mills [HOGG01, LYNC05]. Size reduction in crushing processes results from particle fracture under stress [HOGG01].

For size reduction processes, a huge variety of abrasive materials is used such as steel, corundum, glass, nylon, SiC, SiN, tungsten carbide, zirconium oxide, zirconium silicate, etc. [NN12]. Several factors such as abrasive grit size, hardness, specific gravity, shapes, and chemical reactions have to be considered when selecting the grinding media [NN12, SCHI10].



Fig. 4.10 Example shapes of the abrasive particles for vibratory grinding after [ROES12, WALT12]

4.7.2 Free Abrasive Machining

In barrel finishing or tumbling, workpieces, abrasive particles, and a fluid are tumbled in a slowly rotating container. In vibratory grinding, also known by the trade name “trowalizing”, the container vibrates. The fluid can be water, acid, or alkaline compound [MENA00]. Barrel finishing and vibratory grinding are applied in die and mold manufacturing, medical and aerospace engineering for deburring, degreasing, polishing, or derusting [BROC11].

The abrasive particles, also called “chips”, can be ceramic, plastic or metallic materials and have various shapes (Fig. 4.10). Sizes range from edge lengths of 3–25 mm or more. Vitrified bond is the dominant bond type for chips with abrasive action [KLOC09, p. 57]. Steel particles are used for ball burnishing, i.e. inducing compressive stresses. Coarse chips are sized through sieving according to ANSI B74.11 [ANSI03].

The liquid carrier compound ranges from acidic to basic pH values and has additional tasks such as removing contaminants from the process, keeping the machined parts clean, etc. The compound type is chosen under environmental and economic considerations.

4.7.3 Abrasive Blasting

In abrasive blasting, the abrasive grits are energized with compressed air, centrifugal force, or pressurized water and aimed at the workpiece material. Corundum, silicon carbide and quartz are typical abrasive grits for blasting [KLOC09, p. 371]. Emitted particles [particulate matter (PM)] and particulate hazardous air pollutants (HAP) are the major concerns relative to abrasive blasting [EPA97]. Several methods exist to control the air emissions, such as blast enclosures, vacuum blasters, drapes, water curtains, wet blasting, and reclaim systems [EPA97].

4.8 Tool End of Life

Product life is defined by several causes, such as physical life (break-down beyond repair), functional life (need for the product ceases), economic life (new products offer the same functionality at lower operating costs), legal life (regulations make

the product illegal) [ASHB09, p. 66]. The most important causes for end of grinding tool life are tool wear to the minimum abrasive layer dimensions or tool degradation at the end of shelf life. Options for end of life are landfill, combustion, recycling, reengineering, or re-use [ASHB09, p. 67]. Reengineering and re-use are not feasible for most used abrasive tools and are not considered here.

4.8.1 Shelf Life and Transport

Grinding tools should be stored in dry, evenly tempered, frost-free rooms [BGI10]. Direct sunlight, uneven heating, bending, and vibrations during transport might lead to dangerous cracks [BGI10]. Large grinding wheels need to be moved by a crane with specific fixtures [BGI10].

Coated abrasive tools may contain organic material and may degrade with time [UAMA09]. One recommendation is to use grinding belts and discs within 10 years from the date of manufactured if stored under ideal conditions [UAMA09]. Before use, coated abrasives should be inspected and must not be used, if they appear brittle, curled, damaged, discolored, or of the joint can be pulled apart [UAMA09]. Tools with magnesite bonding age faster in humid environments [BGI10]. Vitrified grinding wheels have an almost infinite shelf life, but the chance of tool damage during storage still applies [UAMA09].

4.8.2 Disposal

The European Waste Catalogue (EWC) [or Verordnung ueber das Europaeische Abfallverzeichnis (AVV)] classifies used honing and grinding tools with the code 12 01 21 or 12 01 20, if they contain hazardous materials [BGBI01]. The main category 12 includes waste of material removal processes and physical and chemical surface alteration. The waste generator has to determine toxicity and physical characteristics to identify the waste correctly and dispose in compliance with the applicable federal, state, and local regulations [UNIT12a]. For example, metal bonds for diamonds are often considered hazardous waste and have to be disposed accordingly [MCCL10b]. Coated abrasives can produce a huge amount of waste.

In 2010, Germany disposed 7400 t of honing and grinding tools with hazardous materials and 13,600 t of other honing and grinding tools [DEST10]. 200 t of the honing and grinding tools with hazardous materials were combusted and 5700 t got chemical-physical treatment; 1000 t of the honing and grinding tools without hazardous materials went to landfill, 200 t to combustion and 7100 to chemical-physical treatment [DEST10].

The intrinsic energy of materials can be turned into heat through combustion. Heat recovery efficiency is at best 50 % and the efficiency to generate electricity

Table 4.4 Material data on combustion (*estimated values) [GRAN10]

	Heat of combustion (net) (MJ/kg)	Combustion CO ₂ (kg/kg)
Epoxies	*30–31.5	*2.42–2.54
Phenolics	*31.5–33.1	*2.86–3.01

from recovered heat at best 35 % [ASHB09, p. 68]. Material for combustion has to be separated from non-combustible material, and the combustion process needs careful control so that the emissions are not toxic [ASHB09, p. 67 f.]. Table 4.4 shows heat and CO₂ of combusting epoxy and phenol, which are resin bond ingredients.

4.8.3 Recycling of Abrasive Tools

There is little information available about the re-use of abrasive grits. Especially for the expensive superabrasives, recycling is important under the growing awareness of material and energy efficiency. McClarence [MCCL10b] estimated in 2010 that only between 8–10 % of new diamond is reclaimed.

4.8.3.1 Conventional Tools

Conventional grinding wheels can be crushed and backfilled in roadworks. Re-use of the abrasive layer is difficult, because inhomogeneous density and heterogenous particles with variable diameter decrease tool toughness and increase the danger of cracks and tool breakage in vitrified bonded tools [BEHR11b]. Because of high safety and liability requirements for rotating abrasive tools, grinding wheel manufacturers have refrained from using recycled raw materials [BEHR11b]. There are also some attempts to regain abrasives from conventional grinding wheels for refractories, but this is a down-cycling of abrasives.

Recently, a new manufacturing procedure for vitrified bonded tools from partly recycled tool material was invented [BEHR11b]. The tools consist of an abrasive layer made from new materials and a body material made with recycled materials in the form of particles with a minimum diameter of two times the grit diameter.

4.8.3.2 Single Layer Plated Tools

Electroplated diamond grinding tools exhibit potential for recycling. In particular, the body can be reused. Electroplated grinding wheels are generally returned to the manufacturer, who will strip off the abrasive layer and re-plate the body.

Usually chemical and electrochemical stripping methods are used [BULJ99]. Chemical methods such as acid baths corrode the bonding [BULJ99, YU11].

Electrical voltage might induce reverse electroplating in addition [BULJ99]. Electrochemical approaches have lower recovery efficiency and bear the danger of corroding the tool body [YU11]. To fulfill stricter requirements on environmental friendly production, new chemical baths are cyanide-free [GEBH99]. Yu et al. [YU11] investigated a thermal shock procedure to induce stress between the abrasive layer and the tool body. The electrobonded tools are heated and then quickly cooled down in water, so that the abrasive layer peels off from the body. Other approaches aim at inventing metallic bonds that are easier to remove, such as bronze alloys with Sn, Cu, and Ti [BULJ99].

In 2010, the cost to recover diamond from metal bonds was roughly 0.25–0.40 USD/ct and the cost of new diamond grits has fallen dramatically in the last years [MCCL10b]. Recovery costs often offset the value of the reclaimed material [SAIT11].

4.8.3.3 Multi Layer Bonded Tools

Grinding wheel bodies of steel are manufactured with high dimensional quality and can easily be re-plated or re-layered. In multi-layer tools, the old abrasive layer is removed by etching of the adhesives that connect abrasive layer and body with chemical baths. A steel body can be reused up to six times [MARIO7, p. 107]. Wheel bodies of resin, however, are more often disposed than re-layered. Effenberger [EFFE01] invented a grinding disc with a releasable abrasive layer, which can be disposed separately.

4.8.3.4 Other Abrasive Processes

In abrasive blasting operations, magnetic separation, rotary brooms, or mechanical conveyors can recover grits [DREN97]. Several methods are able to recover grits from coated abrasive tools depending on the bond type [ANSI84]. The recovery is, however, mostly applied for grading and quality control. The abrasive sludge from glass processing is composed of SiO_2 and Al_2O_3 from the abrasive grits and can be reutilized as cement mixture [KWON03].

4.8.4 Conclusion and Sustainability Model for Tool End of Life

In general, the recycling or re-use of grinding tool components takes place in very few instances, although it is technically feasible in many cases. The reason lies in cost considerations. Today, the costs of recycling and re-use are higher than the benefits. This might change in the future because the decision is volatile and

depends on the constraints and limiting factors. This chapter cannot quantify the potentials for re-using grinding wheel components, but show options qualitatively.

Tool manufactures offer

- collecting and recycling of abrasive tools as **take-back service**.
- **Re-layering** of steel bodies reduces the costs and material needed for superabrasive tools.

Tool users are concerned with tool life and disposal of tools.

- Abrasive tools with organic and resin bonds have a limited **shelf life**.
- The life of all other tools is mainly limited by **tool wear**.
- Tool disposal has to follow **waste regulations** and can have high **disposal costs**. Special care has to be taken for tools with hazardous bond ingredients, such as metal bonds.
- Tool users are interested in the lower costs and shorter processing times when **re-layering** steel bodies.

The whole society takes care about

- the **reduction of waste** and **recycling** in general, because a lot of waste in form of grinding wheels and bonded tools appears each year.

Chapter 5

Grinding Wheel Macro-design—Shape, Body, and Qualification

Tools are graded by the manufacturer according to the coarseness or fineness of the particles of the abrasive material they contain, but the working qualities of the tools depend not only on the size of the particles, but also upon the quality of the binder. It thus results that tools which have the same commercial grade number, vary greatly, in cutting or abrasive qualities. Harey La Vercombe, Patent on Grinding-wheel-test-device, 1923 [LAVE23].

After having introduced the basic components and types of abrasive tools, the following chapters will focus on grinding wheel design. This chapter focuses on wheel macro-design, which includes body shapes and material. Depending on shape and application, clamping and balancing need special attention and will be described here. Furthermore, grinding wheels have to be tested for hardness, elasticity and tool breakage. The chapter closes with discussions on sustainability dimensions for all these macro-design subjects.

5.1 Body Concepts

Grinding wheels with superabrasives or tools for high-speed operations consist of an abrasive layer fixed on a body. The body is also called core, base, carrier or hub material. The body has to withstand several static and dynamic stresses such as centrifugal forces, acceleration forces, cooling lubricant friction forces, air friction forces and grinding process forces. Furthermore, the body needs to provide sufficient heat conductivity, high mechanical strength, and good vibration dampening.

Common body materials are aluminum, steel, bronze, synthetic resin with metallic or non-metallic fillers, fiber-reinforced synthetic resin, or ceramics [KLOC09]. The design of carriers has to regard expansion at rotation speed, damping behavior, thermal expansion, etc.

5.1.1 Body Shapes—Stresses and Special Design for High-Speed Applications

Grinding wheel rotation leads to centrifugal forces and stresses within the tool body. For a generic homogeneous cylinder, the tangential stresses, σ_{t_x} , at the diameter D_x follow (Eq. 5.1); the radial stresses, σ_{r_x} , follow (Eq. 5.2) [HELL05b, FRAN67].

The tangential stress has its maximum at the inner hole diameter, $H = D_x$; the radial stress reaches the maximum at $\sqrt{(DH)} = D_x$ [HELL05b]. Equations 5.1 and 5.2 show that the stresses increase with the square of the wheel speed, v_s^2 , and with the ratio of hole diameter to outer diameter, $(H/D)^2$. Hellelsberger [HELL05b] discusses several body designs and composite bodies in detail.

$$\sigma_{t_x} = \frac{\rho \cdot v_s^2}{8} (3 + \nu) \left[1 + \left(\frac{H}{D} \right)^2 + \left(\frac{H}{D_x} \right)^2 - \frac{1 + 3\nu}{3 + \nu} \left(\frac{D_x}{D} \right)^2 \right] \quad (5.1)$$

$$\sigma_{r_x} = \frac{\rho \cdot v_s^2}{8} (3 + \nu) \left[1 + \left(\frac{H}{D} \right)^2 - \left(\frac{H}{D_x} \right)^2 - \left(\frac{D_x}{D} \right)^2 \right] \quad (5.2)$$

σ_{t_x} tangential stress at diameter D_x

σ_{r_x} radial stress at diameter D_x

ρ density

v_s wheel speed

ν Poisson ratio

H hole diameter

D outer wheel diameter

Because the wheel speed has such a big influence on the internal stresses, high-speed applications have particular requirements for the grinding tool body [FERL92, p. 66]:

- High strength of body material,
- Quasi isotropic material behavior,
- Small radial elongation,
- Small weight,
- Good damping ability.

High wheel circumferential speeds, v_s , are favored for low cutting forces and wheel wear. High wheel speed can be achieved with a large wheel diameter, d_s , or a high number of revolutions, n_s (Eq. 5.3).

$$\text{Grinding wheel speed } v_s = \pi \cdot d_s \cdot n_s \quad (5.3)$$

High numbers of revolutions require special tool spindles. Not only do these spindles have to provide a high number of revolutions (such as 10,000–30,000 min^{-1}), but they should have high maximum power, convenient compliance behavior, high radial and axial runout accuracy, smallest axial deviation, and small space for installation [FERL92, p. 59 f.].

Large wheel diameters go along with large wheel perimeters and high volumes of abrasive grits. Tool life increases with diameter, however, not always in the same proportion as tool costs rise with the grit costs [FERL92, p. 53]. Whereas the grinding wheel perimeter, P , and the number of grits increase linearly to the tool diameter, d_s , (Eq. 5.4), the mass rises with the square of the diameter (Eq. 5.5). Heavier tools are harder to handle for the machinist during clamping and machine set-up. Moreover, additional disadvantages lie in the higher rotational energy and higher loss drive power [FERL92, p. 53].

The rotational energy depends on the wheel diameter to the power of 4 (Eq. 5.6) [FERL92, p. 53]. The higher the rotational energy of the tool, the more worker protection and machine encapsulation needs to be in place.

Air friction and grinding wheel mass increase the loss power of the tool drive. Ferleman [FERL92, p. 55] gives an equation for the loss drive power by air friction for turbulent flux. Here, the loss drive power depends on the wheel diameter to the power of 4.6 and the number of wheel revolutions to the power of 2.8. This emphasizes that the diameter should be as small as possible for high-speed grinding operations.

$$\text{Tool perimeter } P = \pi \cdot d_s \quad (5.4)$$

$$\text{Tool mass } m = \frac{\pi}{4} \cdot \rho \cdot b_s \cdot d_s^2 \quad (5.5)$$

$$\text{Rotational energy } E_{\text{rot}} = K_1 \cdot \rho \cdot b_s \cdot d_s^4 \cdot n_s^2 \quad (5.6)$$

- ρ wheel density
- b_s wheel width
- d_s wheel diameter
- K_1 constant factor
- n_s number of wheel revolutions

An increase in grinding wheel circumferential speed induces a decrease in the single grit chip thickness. This can be used for two different principles, enhancing quality or performance. With smaller chip thickness, the grinding process achieves similar or higher material removal rates, but with higher surface quality and extended tool life compared to lower speed applications [GÜHR67]. In addition, high efficiency grinding with much higher material removal rates is possible and often substitutes turning, milling or reaming applications [FERL92, p. 1].

Resonance vibrations can be calculated via Finite Element Analysis and measured through laser holography [FERL92, p. 66]. The number of spindle

revolutions as excitation frequency should have a security distance of 20 % to the first resonance frequency of the tool body [FERL92, p. 66]. However, the centrifugal forces are much higher than the grinding forces and need to be the focus of design optimizations for high-speed grinding operations [KIEN63].

Strain builds around the inner hole, so wheels without inner holes or special reinforcement around the hole are in use. Already in the 1930s, Krug suggested to counter the strain around the inner hole by strengthening the material by resin [KRUG35]. In 1963, Kienzle et al. suggested a two material grinding wheel with an internal ring of a material with higher Young's modulus than the abrasive layer [FERL92, p. 5, KIEN63]. Thus, the rupture circumferential speed of the grinding wheel increases in comparison to a conventional wheel with the ratio between the adhesive layer strength to the abrasive layer strength [KIEN63]. A larger inner ring increases the rupture speed further [KIEN63].

In 1967, Gühring increased the cutting speed up to $v_c = 90$ m/s with the usage of conventional vitrified grinding wheels with an optimized shape [GÜHR67, FERL92, p. 6]. The tools taper off from the inner boring to the rim to reduce the centrifugal forces. König and Ferlemann [KÖNI90] examined grinding wheel bodies for cutting speeds up to $v_c = 500$ m/s and define design features for high-speed grinding wheel bodies (Fig. 5.1).

The cutting speed has increased from 1935 to 1990 from 25 to 200 m/s; simultaneously, the specific material removal rate increased from 8 to 110 mm³/mms or even 800 mm³/mms in special cases [FERL92, p. 5]. The success of high-speed grinding applications between 1980 and 1990 was combined with the use of superabrasives, especially CBN [FERL92, p. 1].

The use of high grinding wheel speeds is tied to the development of appropriate bondings. Table 5.1 gives a range of possible wheel speeds and material removal rates for different bonding systems.

Oliveira et al. [OLIV09] found in 2009 that still a comparably low proportion of grinding machine tool manufacturers use high grinding wheel speeds with CBN.

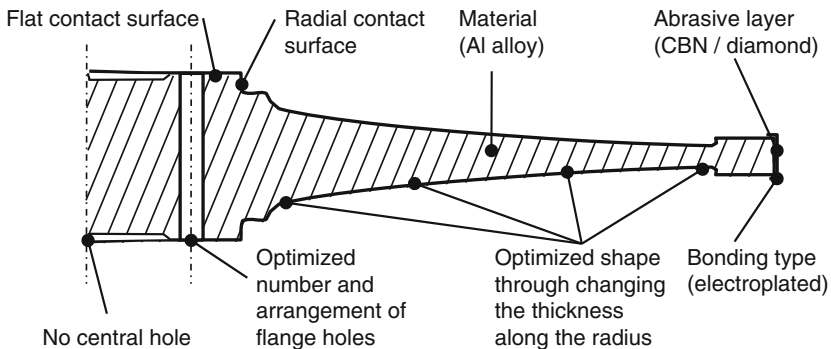


Fig. 5.1 Design features of high-speed grinding wheels [FERL92, p. 79], with copyright permission by VDI Verlag/Springer Verlag

Table 5.1 Wheel and bonding types, wheel speeds, and specific removal rates in 1997 [KLOC97]

Wheel type	Max. wheel speed, v_s (m/s)	Specific material removal rate, Q'_w (mm ³ /mms)
Vitrified bonded conventional grinding wheel	≈120	10–100
Resin bonded CBN grinding wheel	≈140	50–150
Vitrified bonded CBN grinding wheel	≈140 (to 200)	50–150
Metallic bonded CBN grinding wheel	≈180 (to 250)	50–250
Electroplated CBN grinding wheel	>300	1000–10,000

Around 39 % of the 23 interviewed manufacturers use cutting speeds of mainly $v_s = 40\text{--}80$ m/s, only 13 % of up to $v_s = 200$ m/s [OLIV09]. The major reasons given for the comparably low proportion of high wheel speeds were the complex machine tools needing additional systems and economic reasons.

5.1.2 Body Materials

The body material has to withstand the grinding forces, the centrifugal forces from wheel rotation, and the resulting internal stresses. In the grinding process, the body material should dampen vibrations and transfer heat. Furthermore, the body material needs to be shaped easily into the wanted geometry and should have low weight. These requirements translate into physical material properties:

- Young's modulus,
- Compressive strength,
- Coefficient of expansion,
- Isotropy,
- Heat conductivity.

For galvanic bonding systems, there are additional requirements for the body [FERL92, p. 66], like being electrically conductive and having a good corrosion resistance. For superabrasive grinding wheels, a couple of different body materials are used. Table 5.2 gives an overview on damping, heat conductivity, and mechanical strength. The expansion coefficient correlates with density and Young's modulus, so metal bodies have higher expansion than carbon fiber-reinforced polymers.

Table 5.2 Body materials after [WINT88, p. 9, UAMA09, KRAF08]

	Density [kg/dm ³]	Expansion coefficient (10 ⁻⁶ /K at 20 °C)	Vibration damping	Heat conductivity	Mechanical strength
Steel	7.84	12.2	–	+	++
Aluminum	2.80	23.5	–	++	++
Titanium	4.51	8.8			++
Powdered aluminum			o	o	+
Copper			o	++	+
Resin with metallic fillers (phenol aluminum)			o	o	+
Resin with non-metallic fillers			+	–	o (– for thin bodies)
Fiber reinforced resin	1.54	4.4	++		++

++ very high, very good

+ high, good

o medium, satisfactory

– low, poor

5.1.2.1 Metal Body

Metallic bodies made of steel, aluminum, aluminum resin composite, bronze, and copper are applied. For example, the aluminum and bronze blanks are turned to the proper dimensions on a lathe as bodies for resin bonded wheels [METZ86, p. 62]. The turning operation is a big portion of the manufacturing costs, because dimensional accuracy ranges from 0.01 to 0.1 mm [METZ86, p. 62].

The body for electroplated wheels is precision machined. After use, electroplated wheels are generally returned to the tool manufacturer, stripped and re-plated. Commonly, low alloy carbon steels are used or tempering steels or ball bearing steels for higher wheel speeds [KLOC07, p. 195]. Soft steels are easier to machine, but hardened and annealed steels are more wear resistant during clamping operations [KLOC07, p. 195 f.].

Grinding wheels with large diameter or large width are made from aluminum alloys to reduce weight [KLOC07, p. 196]. Breaking point and expansion are similar because the ratio of Young's modulus to density are similar for steel and aluminum [KLOC07, p. 196].

5.1.2.2 Resin Bodies with Metallic Fillers and Non-metallic Fillers

Bakelite/aluminum or Bakelite/graphite bodies are elastic and tend to dampen vibrations from the grinding system [METZ86, p. 63, SEXT82]. This body type is

connected to the abrasive layer by direct pressing without glueing [METZ86, p. 63]. Bakelite graphite or glass fiber reinforced resins can be pre-pressed to blanks and have the advantages of being light [METZ86, p. 62].

A common body material is a phenolic resin with a large amount of aluminum powder [SIOU80, VANP39]. The proportion is 25 V% or less of resin and 75 V% or more of metallic powder. The mixture is hot pressed in a mold at temperatures of around 160 °C [VANP39]. Sioui and Carver [SIOU80] introduced enhancements of powder metallic bodies, such as incorporating iron powder together with aluminum and a bonding aid (resin, tin, or zinc) into the hot pressed body. In addition to enhancing bond strength, thermal expansion, thermal conductivity, and turning characteristics, the retention on magnetic chucks is optimized for this material [SIOU80].

Thermal conductivity of phenol aluminum is more than 100 times better than bakelite [NOTT79]. In fact, the temperatures of the abrasive layer on phenol aluminium bodies is always lower than on bakelite bodies. As consequence, grinding wheels with bakelite bodies showed lower G-ratios for dry grinding of carbides [NOTT79].

5.1.2.3 Fiber Reinforced Resin

Asen [ASEN08] has patented a wheel body made from a fiber composite, specifically with carbon fibers, glass fibers, or synthetic fibers. Different fiber structures are undergoing investigation, in particular uni-directional, orthotroph (fibers in different orthogonal directions) or transversal-isotrop [KRAF08]. The fiber structure affects body strength and isotropy.

Vitrified and resin bonded abrasive layers are glued to the fiber composite body, whereas electroplated layers need an additional thin, metallic ring on the fiber composite body [ASEN08]. The mass of a fiber composite body can be as low as 1/10 of the mass of conventional metal bodies and has therefore lower energy consumption, needs shorter time to revert rotation, and is easier to change [ASEN08]. In grinding tests, tools with carbon fiber-reinforced polymer (CFRP) bodies proved to have a significantly lower contact stiffness than tools with steel bodies, which is advantageous for vibration damping [TAWA12].

Disadvantages of carbon fiber reinforced polymer bodies are the possibility of softening, unclear recyclability, and low performance in detecting the initial cut by acoustic emission. Machining of glass fiber body materials can emit hazardous particles. Furthermore, fiber reinforced resin bodies do not resonate well enough for today`s Acoustic Emission systems for process monitoring [KRAF08].

5.1.2.4 Connection Between Abrasive Layer and Body

Four major processes connect the abrasive layer with the tool body: adhesive sealing, sintering, shrinking, and electroplating [KRAF08]. With electroplating, the

Table 5.3 Mechanisms in connecting abrasive layer and body [MARI04, p. 212]

	Resin bonded layer	Vitrified bonded layer	Electroplated layer	Sintered metal bonded layer
Metal body	Adhesion	Adhesion	Cohesion	Cohesion
Ceramic body	(rare:adhesion)	Cohesion	–	(not usual: adhesion)
Resin/metal body	Adhesion/cohesion	Adhesion	–	(rare:adhesion)
Resin/non-metallic filler body	Adhesion/cohesion	(rare: adhesion)	–	(not usual: adhesion)

abrasive layer is directly deposited on the metallic body or on a metal ring. Abrasive layers of other bond types are either shrunk or sintered directly on the body or glued with adhesives.

For resin bonded tools, shrinking takes place during the resin hardening process. The inner surface of the mold is coated with a release agent to prevent adhesion of the resin and to ensure safe demolding. Oil based liquids might be used as release agents and can easily be sprayed onto the mold surface. The interface between the resin bond and the body is equipped with a first primer coat to ensure excellent bonding.

Glues connecting the abrasive rim layer and the body are often two component epoxy glues, but the exact composition of the glue is confidential information. Any thermal dilatation will disable the grinding tool [METZ86, p. 63]. Table 5.3 shows the basic mechanisms that connect the abrasive layer to wheel bodies of different materials. After combining abrasive layer and wheel body, the abrasive layer is post-processed by profiling, sharpening, and balancing for wheels of a diameter larger than 150 mm [METZ86, p. 63]. The centrifugal forces lead to radial and tangential stresses in the connection zone [HELL05b]. The Young's modulus can be changed at a constant density through different bonding systems (resin or vitrified bond) [HELL05b].

5.1.3 Layout and Reinforcements of Cut-off Wheels

Cut-off wheels need to be thin to reduce the removed material in the cut-off operation and to reduce power consumption. Reinforcement is necessary, because the resin bond of cut-off wheels is too brittle and unsafe for side forces. Therefore, cut-off wheels are reinforced with glass fibers, nylon discs, carbon, cotton cloth, linen, wood, silk, materials on aramide basis, or other materials [COLL88, p. 908 f., FRAC10]. In particular, fiberglass reinforcements unleashed great potential of manual and automated cut-off grinding with their introduction in 1952 [TYRO03b].

Fibers can be woven into different weave or interlace types. For example, glass fibers with a thickness of about 5 μm are combined into threads of rovings and then weaved like textile fabrics [TYRO03b]. The type of fiber yarn and of weave affect

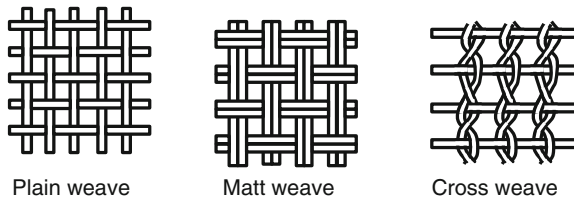


Fig. 5.2 Example weave types for reinforcements after [COLL88, p. 909]

the extension behavior of the reinforcement body [TYRO03b]. The different interlace types have different performance profiles (Fig. 5.2) [COLL88, p. 908]. For example, the plain weave is isotropic and feasible for thin wheels; the matt weave is applied as inner layer of roughing tools and large cut-off wheels; the cross weave does not experience displacements and is applied for roughing wheels and the outer layer of cut-off wheels [COLL88, p. 908 f.].

Reinforcement material is impregnated with resins that have to be similarly adhesive and wetting for both the textile and the grinding layer mixture [COLL88, p. 909]. Then the reinforcement body is put into the mold with the mixture for the abrasive layer and pressed.

During grinding, glass fiber particles can be released and inhaled by the worker. Fiber glass can induce alterations of the cellular and enzymatic components of the deep lung [ABBA06]. Natural fiber cloth such as hemp is an alternative and does not release mineralic particles during wheel use [ESCH05]. Challenges, however, are the lower strength of the natural material, inhomogeneous composition, susceptibility to micro organisms and strong water assimilation. With cleaned and preprocessed hemp fibers, Eschner et al. [ESCH05] successfully produced cut-off wheels.

Joshi et al. [JOSH04] state that the production of natural fiber reinforced resins (NFR) is more environmentally friendly than the production of glass fiber reinforced resins (GFR). Furthermore, natural fibers can be incinerated and might even give energy credit (e.g. the incineration of china reed gives an energy credit of 14 MJ/kg) [JOSH04].

5.2 Clamping and Balancing

5.2.1 Flanges

Cylindrical grinding wheels are often mounted on a hub and clamped between flanges [ROWE09, p. 49]. The adapter flange consists of a fixed flange, a lose flange, and head screws [DIN06]. Standards define the flange design, e.g. BS 4581:1970, and DIN ISO 666 [DIN06]. Some flanges have special features such as a centering section with three lobes in an angle of 120° to ensure a centricity of 2 μm and below [HIME08].

The flanges need to provide friction to accelerate and decelerate the grinding wheel and overcome grinding forces [ROWE09, p. 50]. Four forces act during wheel usage: force of gravity, centrifugal force due to speed and imbalances, contact force between workpiece and tool, and lateral force at the median clamping diameter resulting from the tangential cutting force [DIN06]. The minimum clamping force needs to counter slipping of the grinding wheel; the maximum clamping force is defined by the strength of the grinding wheel material and the stiffness of the clamping device [VOLK72]. Volkman [VOLK72] calculated appropriate clamping forces and justified the theoretical analysis with a friction test. The clamping force for industrial applications can be calculated from guidance values in [DIN06].

An interim layer between the flanges and the conventional wheel prevents local stresses on the abrasive structure [ROWE09, p. 49]. The interim layer can be a ring and has to be made of a flexible material that has to match the application requirements, e.g. paper [DIN07]. As example, the material has to be water resistant if the grinding operation is conducted with an emulsion [DIN07].

5.2.2 *Balancing Methods*

Imbalances in rotating grinding tools can be static or dynamic and are caused by excentricity, form errors, or structure errors (Fig. 5.3). Imbalance, U , is defined as the product of the mass, m , that is out of symmetry and the excentricity, e , towards the rotational axis (Eq. 5.7) [KLOC09, p. 284, DIN05]. Standards, such as DIN EN ISO 6103 define the tolerable imbalance for conventional grinding wheels depending on their application [DIN05]. Large masses can lead to spindle bearing damages [MPM12].

$$\text{Imbalance } U = m \cdot e \quad (5.7)$$

The form induced imbalances such as excentricity or tool shape errors can be eliminated by the conditioning process [KLOC09, p. 282]. Non-dressable tools such as electroplated, superabrasive grinding wheels are manufactured with a high precision, so that the abrasive layer generally is aligned to the core hole to 1 μm cylinder running [KLOC09, p. 282 f.]. Imbalances due to structural inhomogeneities or form induced errors are minimized by additional tool balancing [KLOC09, p. 283].

Most balancing systems work as static systems, i.e. in only one plane. Dynamic balancing happens in two planes and is mostly important for wide grinding wheels such as centerless grinding wheels [KLOC09, p. 283, WECK05, p. 245]. Imbalances result in vibrations, which are commonly detected by piezo sensors and oscillators.

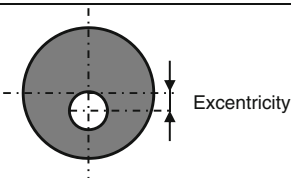
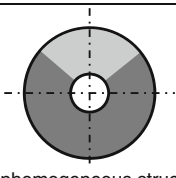
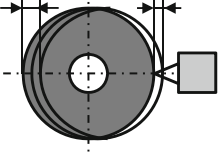


	Form induced		Structure induced
Static			 Inhomogeneous structure
Dynamic	Dressed error plus vibration  Dressing opposite to the grinding point might double run-out due to vibration	 Form error	 Inhomogeneous structure

Fig. 5.3 Example causes of imbalances after [KLOC09, p. 283, MARI04, p. 347]

5.2.2.1 Balancing of Stationary Wheels

Stationary wheels can be balanced with one or more counter-weights, whose positions are determined when the grinding tool hangs freely on a cylinder rod through its inner hole [DIN05, KLOC09, p. 284]. Wheels with flanges have a notch on the circumference to hold two or three sliding blocks [WECK05, p. 245 f.].

5.2.2.2 Balancing of Rotating Wheels Outside of the Machine Tool

Tool grinding wheels are often balanced on their exchangeable spindle outside of the machine tool. Higher process stability, higher workpiece surface quality, and longer grinding wheel life are advantages of grinding tool balancing [MPM12]. A balancing device can detect imbalance mass and angular position.

5.2.2.3 Balancing of Rotating Wheels in the Tool Spindle by Hydro Compensators

Hydro compensators use the cooling lubricant present in the machine tool. These balancing devices have several compensation chambers around the grinding wheel axis either inside the tool spindle or as balancing container on the front face of the spindle [KLOC09, p. 285]. The chambers are filled with the cooling lubricant in

opposing direction to compensate the detected imbalance [KLOC09, p. 285]. One disadvantage is that the system has to be reset when one chamber has been filled completely.

5.2.2.4 Balancing of Rotating Wheels in the Tool Spindle by Automatic Balancing Systems

Weights are moved electromechanically inside the balancing system to compensate for the original imbalance. The balancing systems can be mounted on the tool flange or inside the tool spindle [MPM12]. The position of the two masses inside the balancing system results in one angle between the masses and another angle between resulting force and tool spindle [WECK05, p. 247].

5.3 Tool Qualification

Wheel specification includes abrasive grit type, mean grit size or mesh size, bond type, structure, and effective hardness (see Sect. 6.1 “Abrasive Layer Composition”). However, the wheel specification does not give information about the topography of the abrasive tool [MARI04, p. 349]. Furthermore, the tool specification is only a rough guideline for the tool users [KLOM86, p. 14]. Unfortunately, often grinding tool specification and process results correlate only poorly. Grinding tools of different manufacturers perform differently despite similar specification, or even tools from one manufacturer from different charges [KLOM86, p. 11]. Several attempts to correlate the mechanical tool characteristics with technological performance characteristics rarely found significant correlations [KUEN98].

The properties of grinding tools show fluctuations, which may have unpredictable impacts on the grinding process. Therefore, quality control for grinding wheels is important [KLOM86, p. 11]. Fluctuations in the characteristics of grinding wheels can result in process instability and varying results. Testing the characteristics and quality of abrasive tools helps to predict process deviations [KLOC05c]. Companies apply abrasive tool testings to evaluate constant quality of self-produced products or to release newly or further developed products to market [STRA75].

Methods for tool qualification should be user-independent. Testing can be time and material intensive, in particular for testing of diamond tools [STRA75]. Consequently, tool testings have to be rigorously supported by statistical methods, not only to reduce costs but also to ensure reliability of the results [STRA75]. However, many methods are not user-independent or applicable to superabrasives because of destructive testing. Detailed material analysis of the grinding layer gives reliable information about tool performance, but is destructive and time intensive [KLOM86, LINE92].

5.3.1 Tool Hardness and Tool Elasticity

Important mechanical characteristics are tool hardness, density, and elasticity [KUEN98]. The mechanical properties of grinding tools result from their inhomogeneous structure [QUIR80, p. 6].

Grinding tool hardness is defined as resistance of abrasives to be pulled out, so hardness is a property of the whole tool not single components [DECN70]. Tool hardness is proportional to the pull-out force [TYRO03]. Tool hardness results from the relative bond volume, the breakage strength of the bond bridges, and the retention strength of the grits within the bond [TYRO03].

A grade letter represents the hardness of an abrasive tool in the tool specification (Table 4.2). Hardness is defined in terms of bond resistance against grit pull-out due to grinding forces. Ideally, the abrasive grits are pulled out as soon as they reach a certain degree of dullness, but not sooner.

5.3.1.1 Hardness Testing with Penetration Methods

Opitz and Rumbach [OPIT42] give an overview on a multitude of hardness test methods. An easy, but subjective method is to break out grits with a hand chisel. The user will relate the breakout resistance to the wheel hardness based on his or her experience [OPIT42]. This method can be improved by measuring the applied force with a spring. During the so called “Winterling” method, a rotating blade under load gives a penetration depth that relates to wheel hardness [RAMM74].

The first sand blasting test worked with blasting of sand during a defined time (e.g. 2 min) to the grinding wheel. The weight loss of the wheel indicates the wheel hardness, but the test cannot be performed more than one time per tool [KLOC05a]. The sand blasting test method invented by Mackensen is applied on a Zeiss apparatus and known as Zeiss-Mackensen method. Here a defined volume of sand (e.g. 20 cm³) is blasted by compressed air onto the grinding wheel [OPIT42]. The depth of the generated crater relates to wheel hardness and grit breakage behavior [OPIT42]. Disadvantages of this method are potential damage to the abrasive layer, deviating results for soft and coarse-grained grinding wheels, and the necessity to assume a homogeneous body [KLOC05a].

5.3.1.2 Hardness Testing by Grit Breakout Test or Scratch Test

Merbecks developed the grit breakout test and scratch test following ideas from Opitz and Peklenik [MERB03, PEKL60]. These tests are well applicable to superabrasive grinding tools as they do not damage the abrasive layer, leave holes, or measure the whole body elasticity [KLOC05c, MERB03]. In the single grit breakout test, a cemented carbide tip is fed in a defined angle towards a single grit on the wheel surface. In the grinding wheel scratch test, the carbide tip is fed along

the grinding wheel surface at a certain depth and with a defined scratch rate. Its depth should be one third of the smallest grit size tested, e.g. depth of 30 μm for a B91 CBN grit. The breakage phenomena are monitored by video, force measurement, and/or acoustic emission measurement. Grit breakage, grit pullout, and bond breakage are the three breakage phenomena. The grinding wheel hardness is characterized by the proportion of these wear mechanisms.

As example, higher bond hardness results in an increased portion of grit breakage as consequence of the stronger bond bridges and stronger grit embedding [KLOC05c]. Larger grit sizes at a constant scratch depth results in higher proportion of grit pull-out due the larger lever arm and resulting momentum on the grits [KLOC05c]. Linke used the test method to understand the wear behavior of vitrified bonded grinding tools after dressing [LINK07].

5.3.1.3 Elasticity Testing by Bending Tests

The static properties of a grinding wheel can be tested by compression, tensile or bending tests, in which the deformation of tool samples in the form of cylinders or rods is measured [QUIR80, p. 6]. Industrial practice is the three-point bending test, for example after DIN EN 993-7 [MERB03, p. 25, BOTS05, p. 88]. The bending strength is appropriate to assess the quality of brittle materials. Decneut et al. [DECN70] found a direct correlation between the Young's modulus measured by bending tests and by grindo-sonic tests.

5.3.1.4 Elasticity Testing with the Grindo-Sonic Method

There is a direct correlation between Young's modulus and hardness of the grinding wheel [DECN70, KLOC05a, RAMM74]. However, the Young's modulus of the abrasive layer cannot be calculated from a given volumetric proportion and Young's moduli of each component [RAMM74]. Therefore, the Grindo-Sonic method is used to determine the Young's modulus of grinding wheels from the tool's natural frequency (Eq. 5.8) [KLOC05a]. The Grindo-Sonic equipment measures the natural frequency of a wheel body that is positioned on three tips. The support defines the natural vibration mode. The Grindo-Sonic method can be also used for mounted points [KLOC05a].

$$\text{Natural frequency } f = F(a, \mu) \cdot C_1 = F(a, \mu) \cdot \sqrt{\frac{E}{\rho}} \quad (5.8)$$

$F(a, \mu)$ form coefficient depending on body dimensions, body form and μ
 μ Poisson's ratio

- C_1 velocity of propagation of the longitudinal elasticity oscillation
- ρ density
- E Young's modulus

Cracks change the natural frequency of grinding tools and can therefore be detected via Grindo-Sonic methods [RAMM74].

5.3.1.5 Further Analyses

Ceramographic material analysis helps to understand and qualify the grinding wheel structure by picture analysis [KLOM86, LINE92]. However, samples from the abrasive layer have to be cut and prepared by embedding and polishing. Additional element analyses unveil material composition and chemical reactions during the tool production process [LINE92, p. 39 f.]. Back pressure is a pneumatic measurement method which allows to define the smallest cross-section of a flow channel [LINE92, p. 74]. In the case of an abrasive layer, the back pressure difference indicates porosity and grit distance [LINE92, p. 74 f.].

5.3.1.6 Conclusion on Hardness and Elasticity Tests

Today, the Zeiss-Mackensen and Grindo-Sonic test methods are industrial practice for qualifying conventional grinding tools [KLOC05c]. However, they are not applicable for superabrasive tools (Table 5.4).

Rammerstorfer and Hastik [RAMM74] state that the hardness definition via E-Modulus is more reliable than via penetration methods. Künanz et al. [KUEN98] criticize that Young's modulus and sand blasting depth show no technological useful relation to the grinding ratio, i.e. the ratio between removed workpiece volume and worn grinding tool volume.

Table 5.4 Comparison of different tool qualification methods after [MERB03]

Method	Non-destroying method?	User-independent?	Reproducible results?	Applicable for superabrasive tools	Applicable for conventional tools
Zeiss-Mackensen (Sand blasting)	-	o	+	-	++
Grindo-Sonic	++	o	+	-	++
Bending strength	-	++	-	-	++
Single grit breakout test [PEKL60]	+	o		++	++
Material analysis [KLOM86, LINE92]	-	o	+	++	++

5.3.2 Tool Breakage

A robust, untroubled grinding process needs safety parameters for tool production [KLOM86, p. 11]. Tool breakage might be caused by wrong tool design, manufacturing defects, inappropriate choice, faulty handling or storage, improper use, and clamping, etc. [DIN11].

Several organizations define safety measures for grinding wheel use, such as Berufsgenossenschaft or OSHA (Occupational Safety and Health Administration). Different standards exist on tool safety (DIN EN 12413 for conventional grinding wheels, DIN EN 13236 for superabrasive grinding wheels, DIN EN 13743 for coated grinding tools, BVG D12, BGI 543, ANSI B7.1) [DIN07, DIN11].

The bursting speed of grinding tools needs to be larger than the maximum wheel speed. The standard DIN EN 13236 defines safety factors against breakage due to centrifugal forces (Eq. 5.9) [DIN11]. For example, in open grinding machines the grinding wheel speeds need to be 80 m/s or lower and the safety factor is 3.0; in housed grinding machines with safety guards wheel speeds can be up to 320 m/s and the safety factor is 1.75 [DIN11]. For manual grinding tools, safety factors of 3.5 at 80 m/s and 3.0 at 63 m/s and below apply [DIN11].

$$\text{Safety factor } S = \left(\frac{v_{\text{br}}}{v_s} \right)^2 \quad (5.9)$$

v_{br} bursting speed

v_s maximum grinding wheel speed

Vitrified bonded grinding tools with a diameter larger than 80 mm have to be tested with a ring test [DIN07]. Here the grinding tool is tapped with a non-metallic item and the tone has to be well-defined, not hollow or rattling like at a broken grinding tool [DIN07]. Spin burst tests and tests with bombardment of a retard plate give the burst energy of grinding wheels [KÖNI70] Langbein made burst tests with high-speed cameras [EVER06, p. 391, LANG76]. External cylindrical grinding has the highest safety danger [EVER06, p. 391, LANG76].

Malkin and Guo [MALK08, p. 38 f.] show how the bursting speed increases with wheel hardness and decreases with grit size. Münnich estimated the bursting speed of grinding wheels [MÜNN56, BEHR07]. However, measured bursting speeds and speeds calculated with Münnich's approach deviate up to 20 % [MÜNN56, BEHR07]. Behrens and Kammler derived a new equation based on FEA analysis, which can be used for one-sided recessed grinding wheels [BEHR07].

The guard material has to absorb the energy of broken tool pieces. Safety guards designed with pipes, pipes with intermediate metal sheets or foamed plastic covers with metal sheets provided good results [KÖNI70].

5.4 Sustainability Dimensions to the Grinding Wheel Macro Design

5.4.1 Technological Dimension

For bonded superabrasive tools, bodies of steel, aluminium, resin and resin-aluminium are common. New body designs with carbon fiber reinforced resin enable even higher circumferential speeds over 200 m/s. The productivity seems to be improved and consumed spindle power decreased.

Abrasive layers can be fixed with adhesives as segments. Glue type and tool preparation steps, e.g. degreasing, are crucial for adhesive quality.

Tool macro-design depends on process kinematics and the desired workpiece shape. Furthermore, the effective wheel width defines overall grinding power or surface quality in the case of traverse grinding processes. For example, cup wheels with a higher layer width can achieve significantly lower workpiece roughness than cup wheels with a small layer width due to the higher number of passes [JUCH78].

5.4.2 Economic Dimension

The scale of abrasive tool production and the scale of the individual tool components both are interesting for the product price, possible automation, and near-net-shape manufacturing. Superabrasive grinding tools, for example, are near-net-shape products whereas conventional tools have to be machined after the hardening/sintering process to achieve appropriate concentricity, evenness of the faces and desired profile. This leads to additional waste during shaping, auxiliary time, energy, etc.

5.4.3 Environmental Dimension

The different body materials affect the tool manufacturing chain and energy demands in tool use. Grinding tool bodies can be re-used or recycled. In particular, the following options for recycling exist:

- Bodies from steel, aluminum, or bronze can be easily recycled as metal scrap.
- Aluminum resin bodies, however, are disposed as landfill today. Since these bodies are built-into mass produced cup wheels for tool grinding, a considerable amount of material is produced.
- Bakelite bodies might be incinerated to produce heat energy or they are landfilled.

- Bodies with glass fiber reinforcements are not recyclable and have to be landfilled.
- Carbon fiber reinforced resin bodies, in contrast, can be incinerated.
- In the future, renewable fibers (e.g. hemp) in cut-off wheels might give advantages in production, emissions, and disposal.

Re-use of tool bodies accounts for only a very small percentage of the total number of these tools. Exceptions are special tools, e.g. saw blades for stone cutting. These saw blades consist of soldered or welded segments with diamond grits. The single segments can be removed mechanically and the tool body might be re-used if wear and residual stress condition allows. Re-use of these tool bodies is therefore realistically limited.

5.4.4 Social Dimension

Grinding machines need to be equipped with safety features. In particular, wheel bursting and flying wheel parts are dangerous to workers. The safety guards around the grinding wheel are designed according to the maximum allowed wheel speed and the specific bursting energies.

Above a circumferential speed of 20 m/s, bursting grinding tools are potentially harmful to machinist and machine tool [MARI07, ROWE09]. Therefore, appropriate machine encapsulation is necessary. Tool clamping needs to follow safety rules so that the tools do not get loose during use. Housing is also necessary if the coolant mist and emissions should be exhausted. In particular, the dangers of manual grinding are often underestimated and accidents with manual tools account for 2/3 of accidents with grinding machines [BGI10]. In addition, vibrations from manual tools can lead to long-term damage [DIN07]. In manual grinding operations vibrations can move from the tool to the operator's hand and arm. Vibrations from hand-held grinding tools can cause permanent health effects, such as hand-arm vibration syndrome, carpal tunnel syndrome, neurological problems, and musculoskeletal disease [WILL11].

5.4.5 Sustainability Model for Grinding Wheel Macro-design

Grinding wheel design follows technological, economic, environmental and social considerations. The tool manufacturer is mainly concerned about

- **Safety** during tool use. Tools must not burst at the high rotational speeds during grinding.

Tool users care about this and additional aspects:

- **Safety** during grinding wheel use has to be ensured through wheel design, but the **grinding machine tool** has to be equipped with appropriate safety guards against tool breakage.
- The **maximum cutting speed** of the tool results from tool and body design and affects the tool performance significantly. The cutting speed defines the maximum material removal rate and therefore productivity.

Grinding tool components, also components of superabrasive tools, are rarely re-used today. This is due to economic and technological reasons as explained above. Nevertheless, it will become important to review current practices in the future. This chapter described and analyzed qualitatively capabilities and environmental impacts of grinding tool components at the end of life.

Chapter 6

Grinding Wheel Micro-design—Abrasive Layer and Wear

The performance of a grinding wheel, however, is not only a complicated function of all grinding wheel parameters such as grain nature and grain dimensions, nature of bond material, volumetric composition of the wheel etc., but, as said before, depends on the grinding conditions also [DECN70].

Micro-design of grinding wheels, i.e. structure and composition of the abrasive layer, follows from the tool components and manufacturing processes as described in the preceding chapters and affects tool performance significantly. The tool topography in the form of the cutting edge density results from the abrasive layer composition and will be characterized in Sect. 6.2 “Cutting Edge Density”. Since grinding wheels wear constantly, tool wear effects (what?, Sect. 6.3) and mechanisms (why?, Sect. 6.4) need to be considered comprehensively when evaluating tool performance. Tool conditioning is a means to secure defined tool profile and sharpness and will also be introduced in Sect. 6.5. This knowledge will allow first discussions of sustainability about tool micro-design and wear at the end of the chapter.

Grinding tool performance is evaluated by several characteristics:

- Grinding ratio G ,
- Specific grinding energy,
- Workpiece surface roughness,
- Heat flow into workpiece surface layer,
- Grinding forces in tangential and normal direction F_t and F_n ,
- Grinding force ratio μ between tangential and normal grinding force, etc.

These characteristics are not only affected by the process design, but significantly by the tool design as described in the following.

6.1 Abrasive Layer Composition

6.1.1 Volumetric Composition

The percentages of grit volume, V_G , bond volume, V_B , and pore volume, V_P , add up to 100 % (Eq. 6.1). The mass, m , of the abrasive layer is composed of the grit mass and bonding mass, defined by their respective densities, ρ_G and ρ_B (Eq. 6.2).

$$V_G + V_B + V_P = 100 \% \quad (6.1)$$

$$m = m_G + m_B = \rho_G V_G + \rho_B V_B \quad (6.2)$$

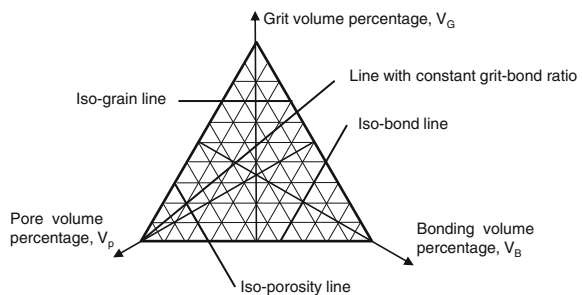
The volumetric composition of grits, bond and pores can be displayed in ternary diagrams (Fig. 6.1). The phase diagram in Fig. 6.1 displays the lines with iso-properties, such as iso-grit volume, iso-bond volume, iso-porosity, and iso-grit-bond ratio [DECN70, MALK08, p. 31 ff]. The iso-grit lines are often considered as “iso-structure lines” [DECN70]. Moreover, the iso-grit lines commonly define the packing number in conventional wheel designations or in the concentration number for superabrasive wheels [MALK08, p. 32].

Maximum packing density is obtained by shaking and pressing the grinding wheel mixture before hardening or sintering; a tool with lower packing density still needs to have enough grit contact, so that the tool does not loose its shape during hardening or sintering [DECN70].

Lines with iso-grit-bond ratio in Fig. 6.1 all pass through one tip of the ternary phase diagram, V_p , where the abrasive layer theoretically has 100 % porosity [DECN70]. The maximum grit-bond ratio with the minimum bond equivalent is defined by strength requirements of the abrasive tool body; minimum grit-bond ratio is imposed by practical manufacturing experience [DECN70].

Several researchers have displayed the most common ranges of grinding tool compositions in ternary diagrams (Fig. 6.2) [KLOC09, p. 45, MENA00, MARI07, p. 111, MALK08, p. 31]. The boundaries for these ranges can be overcome by adding artificial pore builders or using hot pressing methods [KLOC09, p. 45]. In

Fig. 6.1 Phase diagram of abrasive layers with iso lines [MALK08, p. 31 ff, DECN70]



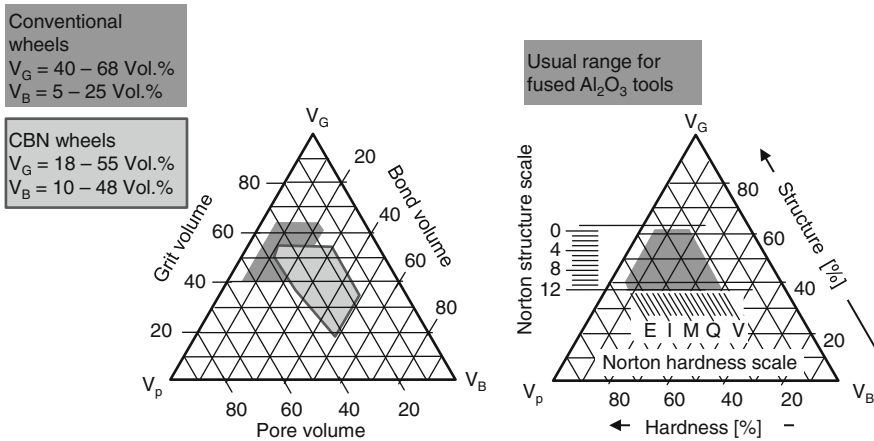


Fig. 6.2 Phase diagram of abrasive layers, *left* typical compositions of conventional and CBN wheels, after [KLOC09, p. 45]; *right* simplified mapping of hardness and structure scale to corundum wheels, after [MENA00]

general, superabrasive grinding wheels have a lower volumetric percentage of abrasive grits [METZ86, p. 52].

The simplified diagram in Fig. 6.2 right suggests that the hardness coincides with the iso-porosity lines for the shown grinding wheel brand [MENA00]. For most grinding wheels, however, hardness grade does not usually coincide with the iso-porosity lines and wheel manufacturers have more complex hardness lines in the ternary diagram [MALK08, p. 33, DECN70]. Grit concentrations for CBN tools tend to be higher than for diamond wheels (up to 50 % by volume), especially for internal and many cylindrical grinding applications [MARI04, p. 419]. Therefore, the structure number of CBN wheels is limited to a smaller range [MARI04, p. 419].

Higher bonding proportion with a constant grit proportion leads to thicker bonding bridges holding the abrasive grits tighter (Fig. 6.3 (a) and (b)). This results in increasing wheel strength, Young’s modulus, hardness, and density [KLOM86].

The amounts of grit and bond content can be calculated either by keeping the bonding specification constant and varying the grit concentration or by varying both bonding specification and grit concentration. A common approach is to calculate the grit volume, V_g , from Eq. 6.3 corresponding to the structure number, N_s [BORK92, p. 35, MALK08, p. 16].

$$V_G = (62 - 2N_s)\% \tag{6.3}$$

N_s structure number in the ranges of 0–4 (close structure), 5–8 (medium), 9–14 (wide structure)

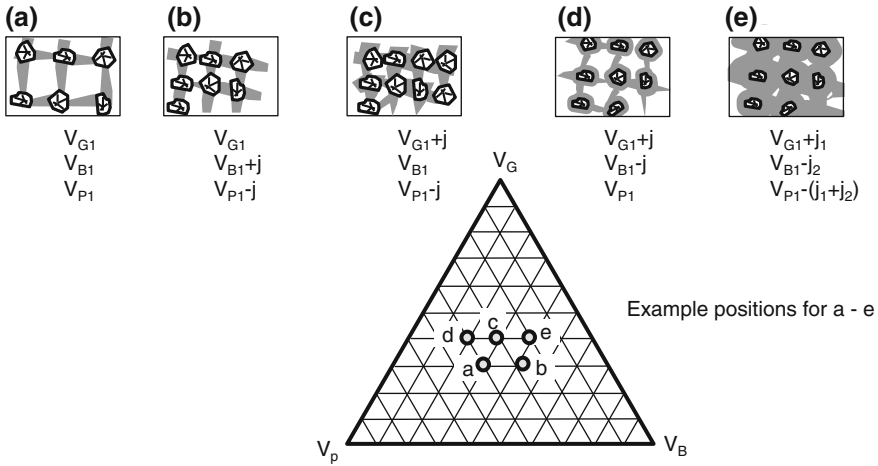


Fig. 6.3 Examples for different wheel compositions after [KLOC09]

Achieving balanced composition is a complex task (Fig. 6.3). Increased bond volume at constant grit volume leads to stronger bond bridges and raises the overall bending resistance and elasticity [BOTS05, p. 92]. A high bond volume might lead to a high proportion of grit splintering resulting from the strong retention force [BOTS05, p. 93]. A bigger grit volume implies more active cutting edges and decreases the load for the single grit resulting in less wear but increased friction.

Homogeneous distribution of abrasive grits, bonding material, and pores in the abrasive layer is crucial for a constant process performance. A non-uniform distribution of abrasive material leads to an uneven material removal process and respectively to a change in the chip thickness. This results in varying loads on the grits, affecting generated workpiece surface as well as wear behavior of the grinding wheel [KLOC05c].

Bot-Schulz published micro-computer-tomography (CT) pictures of a vitrified grinding tool sample for the first time [BOTS05, p. 108 f.]. Challenges lie within the resolution of the computer tomography microscope and the small differences between the densities of the vitrified bonding, the sol-gel corundum grits, and the white corundum grits as secondary grit material. Micro-CT pictures enable the realistic modeling of the bonding bridges between grits [BOTS05, p. 108].

6.1.2 Porosity

Pores are necessary for the transport of cooling lubricant to and chips away from the cutting point. They become more critical for high material removal rates and high-speed grinding processes to get enough cooling lubricant into the grinding

gap. Grinding wheels with discontinuous cutting faces have similar effects as highly porous wheels [BORK92, p. 36].

Porosity can be influenced by the volumetric composition of abrasives and bond material via Eq. 6.1. In principle, there are two ways to actively create porosity [YARN69], by either substances burning up during tool manufacturing, or hollow substances breaking up during the abrasive machining process.

The proportion of pores varies by grinding wheel bond type. Resin bonded wheels have nearly no porosity, whereas vitrified tools can have porosity up to 70 % of volume [MARI07, p. 113]. The pores in metallic bonded grinding wheels cannot hold the cooling lubricant as well as pores in vitrified bonded tools. The active generation of pores is explained in the manufacture of vitrified bonded tools (Sect. 3.2.2 “Manufacturing of Vitrified Bonds”) and sintered metallic bonded tools (Sect. 3.3.3 “Manufacturing of Metallic Bonds by Sintering”). Super-porous grinding wheels can have pores exceeding the grit size by several times [BORK92, p. 35].

Porosity of abrasive tools affects their mechanical strength. Yarnitsky [YARN69] states that an increase in porosity by 20 % can reduce the modulus of elasticity to about 60 % of its original value. The tool becomes softer and the effective dynamic hardness is affected. Pores can be seen as a discontinuity in the abrasive tool material bringing about a stress concentration. The latter can lead to cracks and fatigue fracture as consequence. The effect of the discontinuity, however, depends on the bonding system, geometric pore structure, pore size, uniformity and distribution. In brittle (vitrified) bonds, the effect of material discontinuity is worse than in soft bonds like plastic or bronze. Moreover, spherical pores are preferable to elongated or sharp-edged pores. A varying pore concentration in the abrasive layer leads to changing properties such as non-uniform density. Softer zones will wear quicker and can even cause tool destruction. In addition, heat conductivity is lower in zones with higher porosity. [YARN69]

The volumetric percentage of porosity in a grinding tool can be determined by several methods:

- The porosity can be calculated from the weight of the grinding wheel compared to the theoretical weight of the pore-free tool [YARN69].
- The archimedic principle can be applied if it is assumed that all pores are hollow and connected to the surface [DAUD60]. The ascending force relates to the weight of grits and bonding. The amount of remaining air in the grinding tool can be reduced by heating of the water, slowly submerging of the tool, and adding agents that reduce surface tension [DAUD60]. This method is only useful for conventional tools.
- The surface of the pore cross-sections can be measured on photographs of the wheel [YARN69]. The quotient of pore surface area to total cross-sectional area gives the porosity. This method can be applied to superabrasive tools.

Remarkable trends in changing porosity are “ultrahigh porosity vitrified wheels” [MARI07, p. 113] resulting from long needle-shaped grits (see Sect. 4.1.2 “Special Grinding Wheel Types”) and lubricated vitrified wheels (see Sect. 9.2.2 “Developments in Tool Design”).

6.1.3 Secondary Grits

It is common practice to use a second type of abrasive grits, which might or might not be displayed in the tool specification. In resin bonds, secondary grits decrease bond wear. In vitrified bonds, secondary grits are fillers in the bond or take part in chip formation. Combining primary grits with secondary grits can have a synergistic effect [HAY90]. During manufacturing, secondary grits increase mold packing density [WEBS04]. Mixing different sizes of abrasive grits and bond material has the same effect.

Adding a secondary abrasive can reduce the cost of the grinding wheel, for example in the case of pricier sintered corundum [HAY90]. Secondary grits for sintered corundum can be fused alumina, co-fused alumina zirconia, SiC, BC, garnet, emery, flint, CBN, diamond, or mixtures thereof [HAY90, WEBS04]. Secondary grits for vitrified bonded CBN can be Al_2O_3 and/or SiC and work mainly as filler and support grits [LINE92, p. 39]. Corundum grits are likely to be etched by the vitrified bond [LINE92, p. 39].

6.2 Cutting Edge Density

Cutting edge density is important to understand tool performance during the grinding process. Many researchers analyzed the statistical nature of the cutting edges [KASS69, BÜTT68, SALJ88, HOU03, LORT75, etc.].

6.2.1 Definitions

6.2.1.1 Static Cutting Edge Density

Researchers differentiate between grit number and cutting edge number because each grit can have several cutting edges. However, both values are often denoted with the same letter, N . Grit or cutting edge distances are nominated with L and are approximately inversely proportional to the grit or cutting edge number, N (Eq. 6.4, Fig. 6.5) [SALJ88]. Important metrics are also the number of grits or cutting edges per area or per volume, often denoted with the letter C .

$$\text{Grit / cutting edge density } N \sim \frac{1}{L} \quad (6.4)$$

N grit/cutting edge density in [$1/\text{mm}^2$]

L grit/cutting edge distance in [mm]

Shaw estimated the number of active grits per unit area, or so-called approximate grain spacing, from the grit size (Eq. 6.5) [SHAW96, ROWE09]. However, Rowe stressed that wheel structure, depth of cut, and wheel deflection affect the number of active grits [ROWE09, p. 81].

$$N = \frac{1}{2.25 d_g^2} \tag{6.5}$$

N grit density
 d_g mean grit diameter

ISO 3002-5:1989 defines the static grit number at a certain depth, N_{st} , as the counted grit number at a certain band depth measured by a quasistationary method such as stylus, thermocouple, or microscope [ISO89]. Figure 6.4 visualizes the cutting edges emanating from the cutting area. The cutting area depth extends in normal direction to the outer tool envelope [SALJ88]. The measurement directions can be in the feed direction or perpendicular for circumferential grinding wheels and honing stones and towards the wheel center or in circumferential direction for face grinding operations [SALJ88].

The apparent contact area is the area between wheel and workpiece after Eq. 6.6 [ROWE09, p. 315]. The real contact area, however, is the sum of all contact areas on the grit tips in the respective depth of cut and much smaller than the apparent contact area (see Fig. 6.4).

$$\text{Apparent contact area } A_c = b_{\text{seff}} \cdot l_g \tag{6.6}$$

b_{seff} effective grinding wheel width
 l_g geometric contact length (Eq. 6.7)

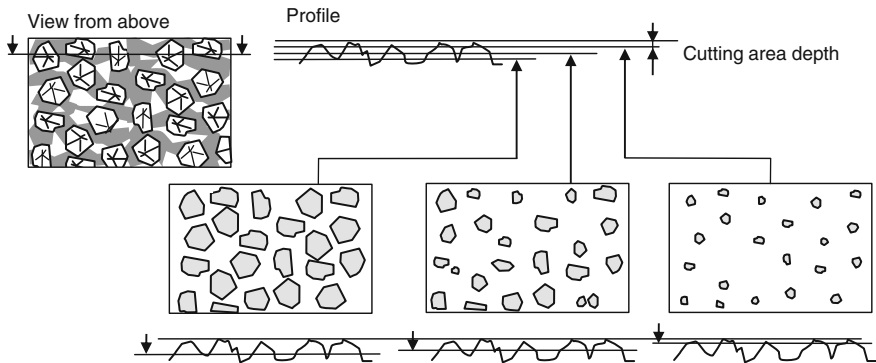


Fig. 6.4 Static grit number in different cutting area depths after [PEKL57, p. 61, SALJ88]

$$l_g = \sqrt{a_e \cdot d_{seq}} \tag{6.7}$$

- l_g contact length
- a_e depth of cut
- d_{eq} equivalent grinding wheel diameter (Eqs. 6.15, 6.16 and 6.17)

Linke calculates the grit distance, K_{ab} , for CBN grits under the assumption of spheric grits and face centered cubic model [LINE92, p. 51 f.]. The face centered cubic model has the highest packing density of a cubic structure (74 %) [LINE92, p. 52].

$$\text{Grit distance } K_{ab} = d_g \cdot \left(\frac{\pi}{3 \cdot 2^{0.5} \cdot V_{CBN}} \right)^{\frac{1}{3}} \tag{6.8}$$

- d_g grit size
- V_{CBN} volumetric grit concentration in [%]

6.2.1.2 Kinematic Cutting Edge Density

Kinematic cutting edges or grits are only those of the static edges or grits engaging into the workpiece material (Fig. 6.5). The kinematic grit number, N_{kin} , can be counted at small contact forces so that the tool contact deformation is negligible [ISO89].

Equation 6.9 offers an empirical approach to calculate the number of kinematic grains per unit area, N_{kin} [WERN71]. Grit density, c_{gw} , arises from grit size, grit

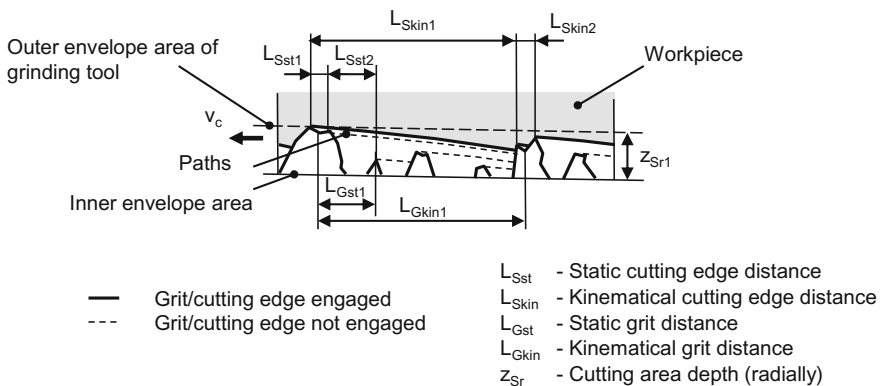


Fig. 6.5 Static and kinematic distances of grits and cutting edges at a circumferential grinding wheel [SALJ88]

shape and grit concentration. A single grit can have one or more cutting edges depending on grit shape. Yegenoglu found a formula to describe the kinematic cutting edge number in CBN grinding wheels quite accurately (Eq. 6.10) [LINE92, YEGE86].

$$N_{kin} = c_{gw} \left(\frac{v_w}{v_s} \right)^{e_1} \left(\frac{a_e}{d_{eq}} \right)^{\frac{e_1}{2}} \quad (6.9)$$

$$N_{kin} = C_1 \left(\frac{V_g}{d_g^3} \right)^{C_2} \left(\frac{Q'_w}{q \cdot d_{eq} \cdot v_c} \right)^{C_3} \times 10^6 \quad (6.10)$$

N_{kin}	kinematic cutting edge number in [1/mm ²]
C_1, C_2, C_3	empirical constants
V_g	volumetric grit concentration
d_g	grit size
Q'_w	specific material removal rate]
q	speed ratio
d_{eq}	equivalent grinding wheel diameter
v_c	cutting speed

6.2.1.3 Active Cutting Edge Density

Furthermore, ISO 3002-5:1989 defines the active grit count, N_{act} , as grit that are actually engaged [ISO89]. Werner expressed this as number of momentary grains per unit area, N_{mom} (Eq. 6.11) [WERN71].

$$N_{mom} = \frac{1}{1 + \alpha} b_s \cdot l_k \cdot N_{kin} \quad (6.11)$$

N_{mom}	number of momentary grains per unit area
α	empirical factor
b_s	wheel width
l_k	kinematic contact length
N_{kin}	kinematic cutting edges

Resin or vitrified bonded grinding wheels flatten due to wheel flexibility [ROWE09, p. 82]. Tool deflection increases contact length and number of grits (Fig. 6.6) [BORK92, ROWE09, SAIN80]. Figure 6.6 shows deformations at flat grinding; similar deformations happen during cylindrical grinding operations, with the difference that the contact zone deforms as well [PEKL57].

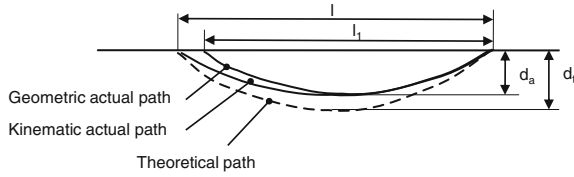


Fig. 6.6 Actual and theoretical grit engagement paths after [SAIN80], with permission from Elsevier

Grits in bonding can be viewed as a spring-damper system (Eq. 6.12) [PEKL57, p. 113]. Saini and Brown derived Eq. 6.13, where grit workpiece deflection, δ , results from actual depth of cut, d_a , and theoretical depth of cut, d_t (Fig. 6.6) [SAIN80]. Measured groove length, l , deviates from the groove length, l_t , that occurs when the workpiece stands still (workpiece speed $v_w = 0$).

$$\delta = \frac{F_{n,\text{grit}}}{c} \quad (6.12)$$

$$\delta = d_t - d_a = \frac{l^2}{4d_s} \left(\frac{v_s}{v_s + v_w} \right)^2 - d_a \quad (6.13)$$

- δ elastic grit deflection rectangular to cutting direction
- $F_{n,\text{grit}}$ normal force at grit
- c spring constant of bonding
- d_t theoretical depth of cut
- d_a actual depth of cut
- l measured groove length
- d_s grinding wheel diameter
- v_w workpiece speed
- v_s wheel speed

Furthermore, workpiece speed affects the spring/damper system of grits and bond. Chip thickness per grit increases with higher workpiece speed v_w (Fig. 6.7) [PEKL57, p. 113]. Higher chip thicknesses lead to higher single grit forces and larger elastic grit deviation, δ (Eq. 6.12). Therefore, the grits engage less deeply and more grits have to remove the material. In addition, the distance between cutting edges gets shorter at higher workpiece speeds [PEKL57, p. 113].

6.2.1.4 Wheel Deformation Effects

The grinding system consists of several elastic elements in series, such as motors, bearings, feed axis, spindle, grinding wheel, etc. [KING86, p. 171]. The overall stiffness, k , adds up reciprocally from the stiffness of each element (Eq. 6.14)

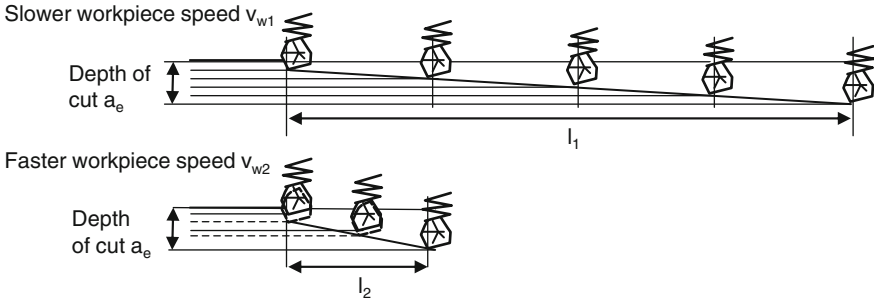


Fig. 6.7 Decrease in cutting edge distance at higher workpiece speed, v_{w2} , after [PEKL57, p. 114]

[KING86, p. 171]. The element with the lowest rigidity will dominate system rigidity.

$$\text{Inverse of total stiffness } \frac{1}{k_t} = \frac{1}{k_1} + \frac{1}{k_2} + \dots + \frac{1}{k_i} \quad (6.14)$$

k_t total stiffness

k_i stiffness of each element in the grinding system

Geometry of the contact zone between grinding wheel and workpiece depends on the tool and workpiece diameter. To compare kinematics and engagement conditions of different grinding processes, the equivalent grinding wheel diameter is calculated from Eqs. 6.15, 6.16 and 6.17 [KLOC05a, p. 190, STEF83, p. 21].

Hahn calculates the curvature between tool and workpiece for these different cases depending on the speed ratio, q [HAHN55]. Depending on the load conditions, either the tool reproduces its own circumference (low workpiece speeds) or the curvature difference approaches the inverse of the equivalent radius [HAHN55].

$$\text{External cylindrical grinding: } d_{eq} = \frac{d_w \cdot d_s}{d_w + d_s} \quad (6.15)$$

$$\text{Internal cylindrical grinding: } d_{eq} = \frac{d_w \cdot d_s}{d_w - d_s} \quad (6.16)$$

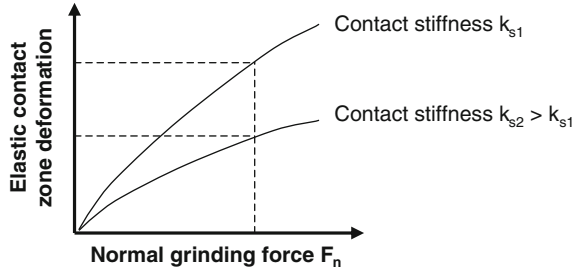
$$\text{Surface grinding: } d_{eq} = d_s \quad (6.17)$$

d_{eq} equivalent grinding wheel diameter

d_w workpiece diameter

d_s grinding wheel diameter

Fig. 6.8 Wheel deflection after [SCHR71]



The contact zone deformation of two touching cylinders increases with the normal forces [SCHR71, p. 40]. Higher contact stiffness leads to smaller elastic deformation (Fig. 6.8).

Gerhardt relates the grinding wheel contact stiffness to the individual grit spring constant and the preload force (Eq. 6.18) [GERH70]. The wheel stiffness can be measured by applying both a static and a dynamic force and measuring the local deformation [GERH70]. King and Hahn give Eq. 6.19 as example for a specific grinding wheel stiffness of a vitrified grinding wheel (2A60K6VLE, $d_{eq} = 4.93$ in. = 125.2 mm) [KING86].

$$k^* = A \cdot k^{1-b} \cdot (F'_n)^b \quad (6.18)$$

$$k^* = k_0 \cdot d_{eq}^{0.25} \cdot (F'_n)^{0.75} \quad (6.19)$$

- k^* grinding wheel stiffness per unit width of contact zone in [lb/in.²]
- A constant in [1/in.]
- k spring constant of individual grit in [lb/in.]
- b constant depending on cutting edge distribution
- F'_n normal force per unit width in [lb/in.]
- k_0 constant (0.58×10^5 lb/in.²)
- d_{eq} equivalent grinding wheel diameter (Eqs. 6.15, 6.16 and 6.17) in [in.]

6.2.2 Measuring, Replicating and Modeling of the Tool Topography

Already in 1936, Goedecke emphasized that the process performance of a grinding tool depends strongly on the spacial distribution of the cutting edges [GOED36, EVER06, p. 383]. Several methods to measure, replicate and model the tool topography exist. Karpuschewski summarizes sensors and methods for measuring the grinding tool microtopography [KARP01, p. 131 ff].

6.2.2.1 Tactile Measurement

The static cutting edge number can easily be obtained by tactile measurement of the grinding wheel topography [DAUD60, p. 47 ff, PAHL68, LORT75]. However, the tactile measurement does not differentiate between grits, bonding, or chips [DAUD60, p. 48]. Stylus tip geometry affects resolution. Furthermore, the tip will be abraded by the abrasive grits. Compared to optical measurements, tactile methods are rather time consuming.

6.2.2.2 Optical and Electron Measurement Methods

Several optical measurement methods exist to analyze the actual wheel topography or topography replica. Goedecke charted replicated cutting edges with a light microscope [GOED36, EVER06, p. 383]. Stereoscopy enables obtaining three dimensional surfaces and grit shapes [DEPE05]. White stripe projection can also be used for 3D measurements. Although light scattering methods work best on a small measuring range and homogeneous surfaces, they can be used for abrasive tools when self-shadowing phenomena are analyzed [LUKI05].

Scanning Electron Microscopy has a better resolution than light microscopical methods. Stereoscopic SEM pictures even give detailed information about abrasive layer profile and potential cutting edges [MATS75]. The disadvantage is, however, that the abrasive layer has to fit into the SEM chamber, be cleaned for the chamber vacuum, and potentially be coated with conductive gold or graphite coatings.

6.2.2.3 Other Methods

The dynamical cutting edge number results from the process kinematics and can be obtained with a thermo-element inside the machined workpiece. Each impulse during grinding should indicate a grit-workpiece contact [PEKL57, DAUD60]. The smaller the contact area of the thermo-element is, the more reliably the temperature peaks can be related to grits.

Luminescence offers another approach. Known luminescence of diamonds for X-rays allows to measure number and size of free-standing diamond grits in a resin bonded diamond wheel after it has been irradiated with focussed X-rays [TOML78a].

6.2.2.4 Replica Methods

The grinding wheel topography itself exhibits some challenges to most measurement methods, such as reflectivity, transparency of grits, or abrasiveness. Therefore, the abrasive layer topography is replicated, but the reproduction quality has to be considered. A simple method is to press a plain paper and a carbon paper onto the

wheel surface [GOED36, LORT75]. Every blackened area can be interpreted as cutting edge.

Another method by Nakayama and Shaw works with grinding in an inclined polished plate [NAKA66, KÖNI70]. Through plate inclination, the grit density in different depths can be obtained. Grinding wheel topography can also be copied onto a workpiece, if workpiece rotations and grinding wheel rotations are coupled with an integer value [PAHL68].

6.2.2.5 Modeling

Several researchers have been working on describing the cutting edge shape because this knowledge is crucial for modeling of wheel and workpiece topography [DOMA06]. Cubes, spheres, ellipses, or octahedrons are common approximations for grit shapes.

Much research has been done on kinematical-geometrical models, where the grinding wheel topography engages with the workpiece. Heinzel, Brinksmeier et al. [HEIN09b, BRIN06] give a broad overview on the state-of-the-art. Kassen [KASS69] did 2D computer simulation. Today 3D simulations help to understand generated surfaces [KOSH03]. New research uses randomly shaped and distributed polyhedrons as grits, which is particularly suited for porous wheels [ZHAG11].

6.3 Tool Wear Effects

Tool wear is an important factor of grinding tool performance. Already in 1914, Alden proved that a larger depth of cut causes greater tool wear [MALK68, ALDE14]. Tool wear can be split into macro effects (tool profile loss) and micro effects (sharpness loss). Marinescu et al. [MARI07] add roundness deviation as performance characteristic to profile and sharpness loss.

6.3.1 Macro Effect—Tool Profile Loss

Dimensional wear at the grinding tool leads to a loss in workpiece dimension and profile. Cylindrical abrasive layers wear at the radius and at the edges, so that both wear volumes define the dressing allowance to retrieve the original tool profile (Fig. 6.9). Corner wear [MALK08] is also known as edge wear [KLOC09]; radius wear [WERN73] is called radial wear [KLOC09] or uniform wear [MALK08].

Werner explains that both wear effects are induced by similar process characteristics, which are average single grit cutting force, friction speed, contact time, and contact frequency [WERN73, p. 69]. At tool corners, grit support within the abrasive layer is weaker, so wear rate is faster [WERN73, p. 69]. During each wheel

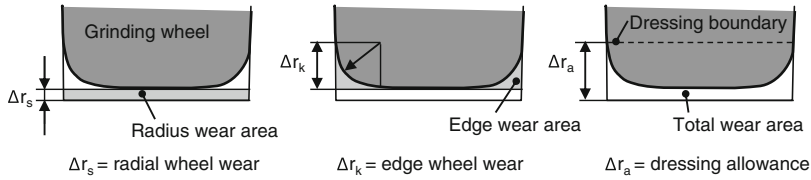


Fig. 6.9 Radius wear and edge wear at a plunge grinding wheel [WERN73, p. 70]

rotation, the grinding forces are more likely to overload the weaker bond bridges at the wheel edges until an equilibrium between grit retention forces and grinding forces is achieved [BIER76, p. 77 ff]. In external cylindrical plunge grinding, the edge wear appears with an elliptical contour [WEIN76, BIER76, p. 77 ff]. Circular edge profiles occur only for small material removal rates or short process times [BIER76].

König and Henn [KÖNI84] explained the wear behavior of grinding wheels in centerless throughfeed grinding or other traverse grinding operations (Fig. 6.10). The grinding wheel can be divided in parts being as wide as the workpiece feed per wheel revolution. Every part has to remove a certain amount of workpiece volume. Due to inevitable wear, each part cannot remove as much material as originally intended, causing higher work load for the following part. This results in even more wear at the next parts until the spark-out zone of the grinding wheel is reached, where originally no material removal took place. The spark-out zone works as buffer and takes over some part of grinding of the workpiece allowance. Decreasing spark-out zone width leads to decreasing overlap ratio and increasing workpiece roughness. If the whole spark-out zone is worn, the workpiece dimension will deviate [KÖNI84].

Load direction, e.g. defined by feed direction, affects the wear profile (Fig. 6.11). Furthermore, similar profile wear behavior exists at other tool types. Büttner

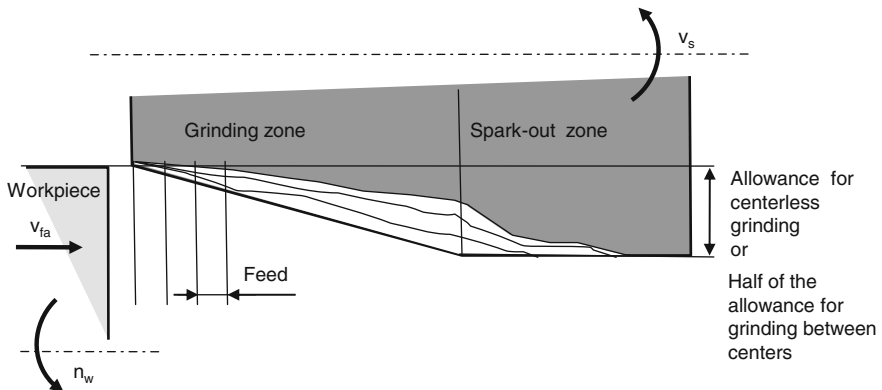


Fig. 6.10 Profile wear in longitudinal grinding [KÖNI84]

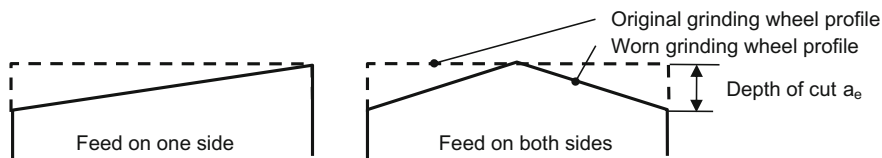


Fig. 6.11 Wear in different profiles or paths [METZ86, p. 68]

[BÜTT68, p. 64 f.] for example examined the formation of main wear area and side wear area at cup grinding wheels.

6.3.1.1 Wear Measurement

In most industrial applications, wheel wear is assumed from workpiece profile deviations. In research settings, wheel wear is commonly determined by reproducing the rotating grinding wheel into a steel plate. The grinding wheel needs an unworn reference part such as a part of the abrasive layer that did not interact with the workpiece. Karpuschewski [KARP01, p. 126 ff] gives an overview about sensors for measuring the macroscopic profile of grinding tools.

6.3.2 *Micro Effect—Sharpness Loss*

High initial tool wear is observed after dressing or for a new tool; then a steady-state tool wear follows [JACK11, p. 50, 92, BUTT79]. Wheel collapse occurs as third wear phenomena presumably because of wheel dulling and high grinding forces [BADG09b]. The dressing process affects the initial wear dominantly, whereas the steady-state wear is dominated by the grinding process conditions. The reasons for sharpness loss are explained in Sect. 6.4 “Tool Wear Mechanisms”.

Loss of wheel sharpness, or dulling, leads to a change in surface roughness and higher process energy, which bears the risk of thermal workpiece damage. Excessive wear with large volume grit breakout reduces grinding forces and enlarges surface roughness, but dimensions are hard to keep and the shorter wheel life increases tool costs. A balance between self-sharpening and wheel costs is favored. For example, high performance processes need a grinding tool with high grit retention over a longer period [BAIL02]. Precision parts need high surface quality and high process stability, which is commonly accomplished through shorter dressing intervals.

Dressing restores tool sharpness and profile (see Sect. 6.5 “Tool Conditioning”). Multi-layered superabrasive tools enable longer intervals between dressing operations than conventional tools (Fig. 6.12). Single-layered tools show an initial wear

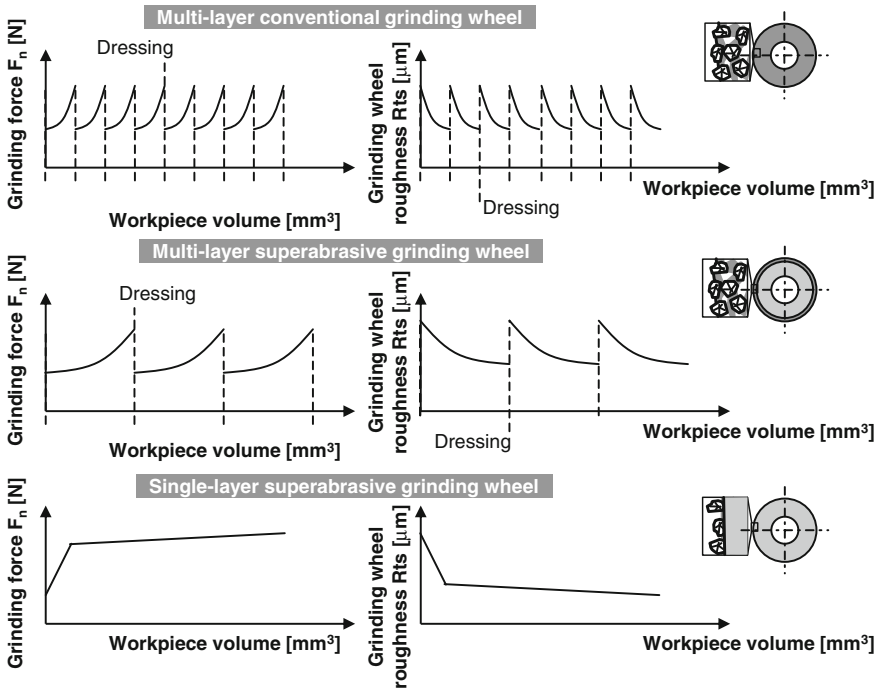


Fig. 6.12 Example wear behavior of different grinding wheel types

phase followed by quasi-stationary behavior until the tool's end of life defined by thermal damage to the workpiece [KLOC09]. Single-layered tools are not profiled or sharpened in the common sense, although sometimes so-called touch-dressing is applied to level protruding edges.

6.3.3 *G-Ratio*

Tool life between conditioning is measured in time, per number of machined workpieces or workpiece volume removal [PAUC08, p. 343]. The *G-ratio* is a common parameter for describing the tool lifespan as ratio of machined workpiece volume, V_w , and worn grinding tool volume, V_s (Eq. 6.20) [MALK08]. The *G-ratio* depends on the machined material, tool design, grinding operation and parameters, cooling lubricant, machine tool, etc. Therefore, no certain value can be given for a generic application, but literature provides ranges of *G-ratios* (e.g. Table 6.1 or [PAUC08, p. 350]). In addition, tool suppliers have databases on case studies (Fig. 6.13).

In precision grinding of steel, maximum values for the *G-ratio* of about $50 \text{ mm}^3/\text{mm}^3$ can be reached with alumina wheels and *G-ratios* of more than $10,000 \text{ mm}^3/\text{mm}^3$ with CBN wheels [HELL05a]. In contrast, a *G-ratio* of

Table 6.1 Typical G-ratios or relative wear resistance values for grain types [JACK11, p. 9 f.]

	Grinding alumina	Grinding steel	Grinding nickel	Grinding titanium
Diamond (9000 HV)	100,000	1000	100	500
CBN (4500 HV)	1000	10,000	5000	100
Alox (1800 HV)	<1	5–10	10	1
SiC (2800 HV)	10	1–5	1	10

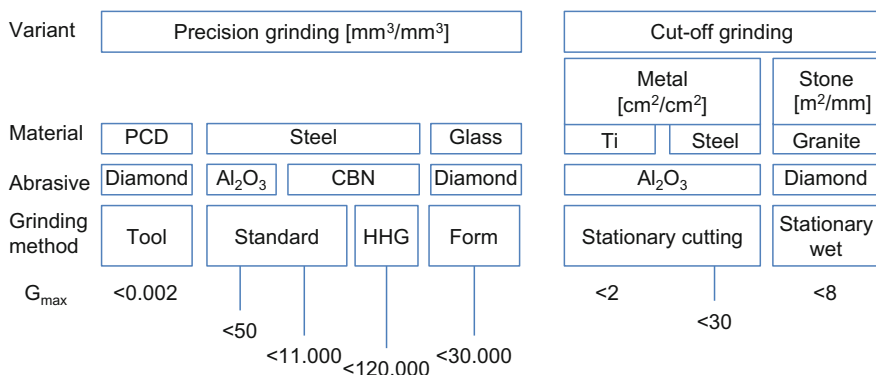


Fig. 6.13 Maximum values for G-ratios [HELL05a]

0.02 mm³/mm³ represents an excellent value for precision grinding of polycrystalline diamond with diamond wheels [HELL05a].

$$G\text{-ratio } G = \frac{V_w}{V_s} \tag{6.20}$$

V_w workpiece volume
 V_s grinding wheel volume

The highly complex and multivariant grinding setup complicates modeling of the wear rate, although Werner claims that the high number of simultaneous grit engagements decouple the process results from the failure of a single cutting edge [WERN73, p. 67]. A wear rate model is necessary for calculating waste streams and tool costs.

Decneut et al. [DECN74] relate the G-ratio to the equivalent chip thickness, h_{eq} (Eq. 7.9), with charts. Werner [WERN73, p. 80 ff] built a wear model by multiplicative superposition. He included the four wear criteria of contact pressure,

friction velocity, engagement time, and engagement frequency and derived Eq. 6.21 [WERN73, p. 90]. Factor P includes the grinding wheel diameter, cutting edge density and edge shape factor and was derived through experimental tests [WERN73].

$$W = P \cdot (v_w)^{2m-h} \cdot (v_s)^{h+i-e-2m} \cdot (a_e)^{\frac{e}{2}+m-h} \cdot \left(\frac{d_w}{d_w \pm d_s}\right)^{\frac{e}{2}-m} \cdot (d_s)^{\frac{e}{2}-m-h} \cdot (V'_w)^h \quad (6.21)$$

W wear cross-sectional area
 P linear factor from grinding wheel specifications in [mm²/mm*kp]
 e, h, i, m system constants (0.5 < m < 1.5; 0.5 < i < 1.0)
 V'_w specific workpiece volume [mm³/mm]

Bierlich [BIER76, p. 83] derived the tool life volume, V'_{stand}, between two dressing operations in Eq. 6.22. This criterium can be integrated easily as cost function. Osterhaus [OSTE94] combined regression models of wheel wear in cylindrical and surface grinding processes.

$$V'_{stand} = C_4(Q'_w)^{\alpha_4}(v_s)^{\beta_4} \quad (6.22)$$

V'_{stand} tool life volume per mm wheel width
 C₄, α₄, β₄ constants
 Q'_w specific material removal rate
 v_s wheel speed

G-Ratio and maximum material removal rate are often contradictory, so Helletsberger proposes to regard the performance factor, L, as factor from G-ratio and specific material removal rate, Q'_w, (Eq. 6.23) [HELL05a]

$$\text{Performance factor } L = G \cdot Q'_w \quad (6.23)$$

G G-ratio
 Q'_w specific material removal rate

Interrupted cuts increase the number of entry and exit impacts on the grinding tool leading to higher tool wear, so that uninterrupted cuts are preferable [METZ86, p. 78 ff].

Literature mostly disregards that tools can have the same G-ratio but with different machined workpiece volume, such as $G = V_w/V_s = 10/0.1 = 500/5 = 2000/20 = 100$. If the same G-ratio is achieved in the same time, the tool performance varies greatly. Figure 6.14 shows an example where the grinding forces propagate differently and the dressing intervals vary, although the G-ratio is similar. Although high G-ratio is

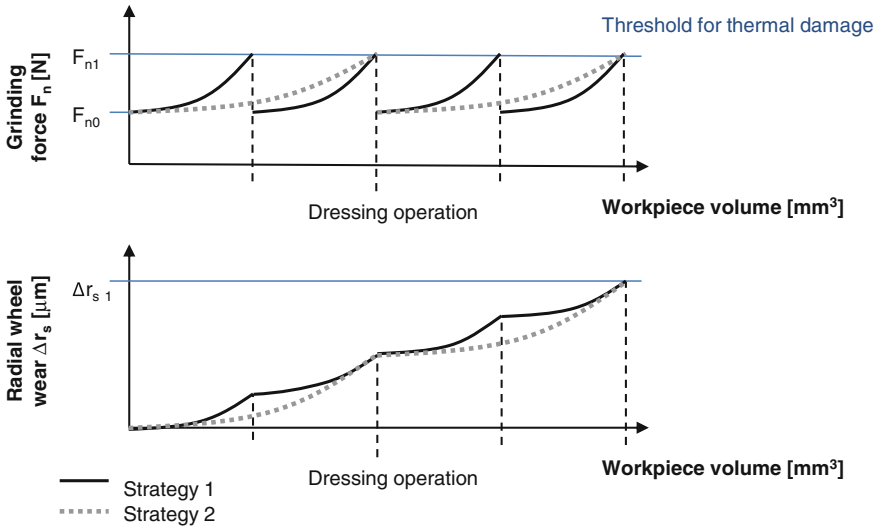


Fig. 6.14 Different grinding forces for dressing strategies with similar G-ratio

desirable, a highly wear-resistant tool may generate higher forces and grinding energies, thus increasing the potential of thermal workpiece damage.

6.4 Tool Wear Mechanisms

Abrasive machining processes themselves can be regarded as tribological systems where workpiece material and abrasive tool interact under the influence of cooling lubricant and atmosphere [MARI04]. Abrasive tools are subjected to high temperatures and high pressures in the active cutting zone. Consequently, tool wear occurs. Tool wear happens because of mechanical effects (vibrations and grinding forces), chemical effects (reactions with cooling lubricant and workpiece material), and thermal effects (grinding pressure and friction) [BOLD02, KLOC09, p. 15].

6.4.1 Wear Types

Like in all tribological systems, the wear mechanisms do not appear in single but occur as superposition or sequence [HABI80]. The tribological definition of wear is that particles are removed from the surface of one friction partner under the conditions of the surrounding environment, such as lubricant and atmosphere, and friction parameters, such as pressure, friction speed, temperatures.

Table 6.2 Taxonomy and types of wear mechanisms in the literature

	Grit surface layer wear	Grit splintering	Grit-bond-interface wear	Bond wear
[KLOC09]	Compressive softening, chemical wear, abrasion	Micro-breakage, grit breakage		Bonding breakage, chemical and thermal wear of bonding
[KÖNI81]	Abrasion, micro-cracks, corrosion, diffusion	Micro-fracture, grain fracture		Bond fracture, chemical bond wear
[MALK08, MALK68]	Attritious wear	Grain fracture		Bond fracture
[JACK11]	Abrasive wear (surface flats)	Fracture of abrasive grains	Fracture at interface grit/bond	Fracture of bond bridges
[BORK92]	Attrition, surface microchipping	Grain chipping and cracking	Grit pull-out	Bonding bridge failure
[ROWE09]	Rubbing	Grain micro- and macro fracture	Grain pull-out	Bond fracture
[PEKL58]	Compressive softening	Splintering of crystal clusters, partial grit break-out	Total grit break-out	

Different researchers use various terms for tool wear (Table 6.2), but the main categories are wear of the grit surface, wear of the grit by splintering, wear of the grit-bond-interface, and wear of the bond. The wear mechanisms of grinding tools leading to profile and sharpness loss as explained in Sect. 6.3 are complex.

Peklenik [PEKL57] highlights the alternating temperature load on the grits, because every grit contact heats up the workpiece surface on a small contact area and the grits are cooled down by the cooling lubricant (Fig. 6.15).

The wheel hardness is an important impact factor on the wear phenomena [STET74]. Softer wheels show higher wear rate, but can also be longer in a sharp

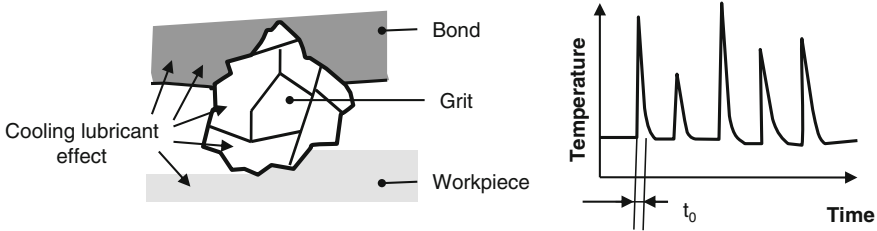


Fig. 6.15 Load at a single grit, *left*: Cooling effect by the cooling lubricant, *right*: Peak temperatures during grit engagements of intervals, t_0 [PEKL57, p. 88]

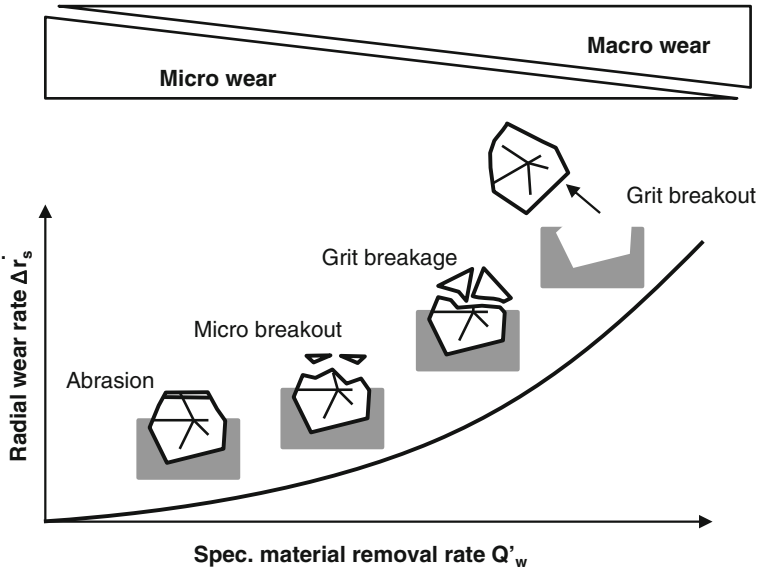


Fig. 6.16 Influence of material removal rate on wear phenomena [KLOC09, p. 254, BIER76], with kind permission from Springer Science + Business Media

cutting state [STET74]. In addition, the process parameters affect also the wear phenomena. For example, higher specific material removal rates result in higher single grit loads, which change the wear mechanism from abrasion to particle break-out and total grit break-out (Fig. 6.16). The different wear phenomena then result in different amounts of wheel profile loss [STET74].

The grit type affects how the grits get dull. For example, green silicon carbide and white aluminum oxide are friable and offer new cutting edges easily [PAUC08, p. 346]. Regular aluminum oxide acts comparatively tough and gets blunt [PAUC08, p. 346].

One way to analyze the wear phenomena is to collect the grinding debris from the grinding zone, wash the debris in benzene and separate the metallic chips magnetically [STET74]. The chips can be weighted and compared to the sieved and weighted wheel wear particles.

6.4.2 Grit Surface Wear

Malkin defines attritious wear referring to the development and growth of wear flats on the tips of active grains. Attritious wear is measured by the percentage of the wheel surface covered with wear flats [MALK68, p. 36]. Jackson defines attritious wear as wear that occurs “atom by atom” by physical and chemical interaction

between grain and workpiece [JACK11, p. 8]. Several wear mechanisms are responsible. Surface shattering, fatigue, and softening result from the basic wear mechanisms explained in the following.

6.4.2.1 Abrasion

Abrasion occurs when roughness peaks of a counter-body or particles in a medium penetrate the body's surface and perform a movement parallel to the surface simultaneously. This leads to formation of grooves and micro chips [HABI80, RABI95]. The extreme grinding pressures and temperatures initiate oxidation and diffusion processes in the grit surface layers, which decrease the abrasion resistance of the grit material [KLOC05a].

Abrasion occurs differently at ductile and brittle materials. Brittle materials wear by particle breakouts [HABI80]. Anisotropic materials such as diamond have different resistances against abrasion in their different crystallographic planes. Abrasion at diamonds is a micro fracture process. Micro cracks spread in the loaded zone and atom bonds break due to stress accumulation [SEN91, WILK91]. Micro fracture processes occur mostly along octaheder planes because there are less atom bonds to break than along the other planes [WILK62]. The border between abrasion and breakage as failure mechanisms is hard to define.

Minke [MINK88] found groove marks on dressing diamonds which gave the impression that the diamonds were scratched by softer corundum grits. This effect is explained by temperature related hardness decrease of the counter parts. The thermal stability limit of diamond (about 700 °C) is attained earlier than the one of corundum (about 1160 °C).

Ludewig [LUDE94, p. 61 ff] derives that plastic deformation of corundum grits is possible. The grinding temperatures of 1400 °C lead to a decrease in toughness (about 40 % of toughness left compared to 25 °C). In this region, the bearable compressive stresses of corundum are met during the grinding of hardened steels.

6.4.2.2 Adhesion

The direct contact of body and counter body can lead to atomic bonds ("micro weldings"), which are defined as adhesion [GAHR87, RABI95]. A relative movement of the contact partners does not necessarily involve that the bonds break within the original contact areas, so that material transfer can happen [HABI80].

Adhesive layers change the friction conditions. When steel components are ground with diamond wheels, built-up edges are formed on the diamond grits. They are mainly caused by the adhesion of steel particles on the diamond and not by welding processes of chips with the bonding [LINB70].

Focussed Ion Beam (FIB) separation allows damage free cutting of material samples out of the surface layer with electron transparency. Engelhorn [ENGE02, p. 90] found adhesive layers on sol-gel corundum grits after single grit scratch tests.

Supposedly, the nanocrystalline layer was molten and in a highly viscous state during grit engagement, so that friction and wear were reduced. Zeppenfeld [ZEPP05] found adhesive layers on diamond grits after scratch tests at γ -titanium aluminide and identified the layers as workpiece material via Electron Beam Microanalysis (EBMA). Werner also discussed the wear minimizing effect of tribo-layers with cooling lubricant, but pointed out that the adhesive layers will wear also at some point [WERN73, p. 79].

6.4.2.3 Tribochemical Reaction

Tribochemical wear is the most complex wear mechanism [MARI04, RABI95]. It includes a reaction between body, counter body and environment [DIN79, HABI80]. A large reactive surface or friction heat accelerate these reactions.

Beads of molten workpiece material give evidence of the high temperatures during the cutting action. For example, Müller [MÜLL01, p. 57] found beads of molten workpiece material (bearing steel) on SiC grits after single grit scratch tests. Reactions of the workpiece surface, the grit or bond material are promoted by grinding process heat. Possible reactions of the abrasive grits were explained in Chap. 2 “Abrasives”.

6.4.3 Grit Splintering or Breakage

In brittle materials, such as grit materials, it is hard to differentiate between microscopic breakage processes, or wear by abrasion [WILK91]. This is because the grooves and small chips, which generally help to detect abrasion, are missing in brittle materials due to their low tensile yield point [WILK91].

In monocrystalline diamonds, breakage occurs along the cleavage planes. Polycrystalline diamonds break along the crystal boundaries. Wear by micro-chipping occurs at friable diamond [BAIL99]. When machining hard, brittle, short chipping workpiece materials with the more friable diamonds, the grinding forces tend to be lower and surface roughness smaller [BAIL99].

Alternating thermal or mechanical load lead to elastic and plastic deformation, change of material hardness (softening or hardening), crack formation and crack propagation [GAHR87, RABI95, PEKL57, p. 86 ff]. Surface shattering is a fatigue mechanism occurring at impact load [DIN79, HABI80]. Grain boundaries or cleavage planes open and the cracks start at or near the surface [GAHR87].

6.4.4 Grit-Bond-Interface Wear

For **resin bonded grinding tools** grit break-out is the main wear mechanism and, therefore, the grit holding forces within the bond are essential for tool wear [TOML76]. Abrasive particles worn more than 50 % of their diameter are not likely to retain in the bond any more. Moreover, there are details in the literature that not even 35 % of blocky grits can be used in the machining process before break-out [TOML76].

However, abrasives to be used in resin bonds should have high surface roughness and irregular shapes to have high bond adherence. Often metallic coatings optimise the retention of superabrasives by providing even rougher surfaces and possible chemical reactions to the bond additional the mechanical clamping.

Büttner found that diamond grits in resin bonding showed more grit break-outs than grits in bronze bonding, which were held more strongly and showed attritious wear [BÜTT68, p. 72].

6.4.5 Bond Wear

Several chemical reactions can happen at the wheel bonding [BRIN04]. There Brinksmeier and Walter found chemical reactions of the fillers in a resin bonded corundum wheel with the cooling lubricant additive [BRIN00].

In many cases, grit wear leads indirectly to mechanical bond wear. Worn and flattened cutting edges expose an enlarged friction surface, which leads to an increase in cutting forces on the individual grit. Consequently, the bond can be mechanically overloaded and entire grits or grit sections can break out of the bond [KLOC05a].

6.4.6 Clogging of the Abrasive Layer

Clogging or loading of the abrasive layer describes the adhesion of chips to the abrasive grits or interlocking of chips in the pore space. With more wheel clogging, the danger of thermally induced damage of the workpiece surface layer, the workpiece roughness and the grinding wheel wear rise [LAUE79]. Lauer-Schmaltz [LAUE79] pointed out that the effect of grinding wheel loading depends not only on the particle spacial size, but furthermore on the particle positioning within the abrasive surface layer.

Lauer-Schmaltz [LAUE80] and Koenig defined three loading types: Chip nests, welded chips, and grit adhesions:

- Chip nests or clustered chips are long, solitary chips in front of active cutting edges [LAUE79]. This type of loading results from mechanical clustering of

chips in the neighbored pores of active grains and does not necessarily disturb the grinding process.

- Welded chips consist of pressure welded chips and adhere, in contrary, on the active cutting edge and, thus, increase the effective cutting edge radius. As consequence, the single grit chip thickness increases. Lauer-Schmaltz [LAUE79] found areas up to 2 mm² of the grinding wheels covered.
- Grit adhesions cover groups of grits thinly and do not impair the cutting edge shape, but only the friction properties at the flanks [LAUE79]. This type of loading was examined during the machining of chromium and nickel containing materials as well as titanium and aluminium alloys. There can be chemical reactions in the boundary layer between chips and active grains [LAUE80].

Wheel loading depends on the machined material. Pai et al. [PAI89] compared chips from grinding ductile and brittle materials and found that the chips tend to be longer in ductile machining. These longer chips can cause clogging problems of the grinding tool. In comparison, brittle materials tend to exhibit a smaller chip storage problem than ductile materials and hence allow a greater removal rate for the same available chip storage volume [PAI89].

Nagaraj and Chattopadhyay [NAGA89] concluded that chemical reactions have an effect on loading, for example, iron oxide layers are formed on machined C45 steel and prevent adhesion to the abrasive grits. Titanium alloys in contrast might form strong bonds to the corundum grits and form adhesions [NAGA89]. Pure iron led to a relatively high wear rate because of its high ductility and, consequently, chip layers [LUDE94, p. 89 ff]. Furthermore, steels with abrasive Zementit particles in a soft Ferrite matrix like C135 W induced wear due to loading [LUDE94, p. 92]. On the one hand, the Zementit crystals were pushed into the softer matrix and caused minor abrasion. On the other hand, adhesions of workpiece material on the grits resulted in high tangential forces and grit particle break-out.

Normalized steels with higher carbon content lead to less overall wear, because the increasing Perlite content decreases clogging [LUDE94, p. 93]. Nevertheless, the Zementit lamellas of the Perlite cause wear by abrasion, but to a minor proportion compared to the wear by adhesions.

To grind highly ductile material like pure iron, a grinding tool with open pores and low bond strength is advantageous, so that loaded abrasive cutting edges can break out off the abrasive layer [LUDE94, p. 102]. With higher possible material removal rate, higher grinding wheel wear goes along.

There are approaches to monitor grinding wheel wear and loading via CCD camera images [ARUN07, HEIN12]. Various texture analysis methods such as variance, energy, ASM, diagonal moment, IDM, and Ga parameter can be used to characterize texture changes, which are related to the grinding wheel surface condition. However, it is difficult to assure constant measurement conditions, such as illumination. The analysis for each grinding wheel and workpiece material has to be calibrated [ARUN07].

6.5 Tool Conditioning

6.5.1 Overview on Conditioning Principles

Grinding wheel topography is influenced by grinding wheel structure, profiling and sharpening process as well as by the wear during the use of the grinding wheel [MARI04]. The dressing process changes the working behavior of the grinding tool, the Young's modulus and the effective hardness of the grinding layer [MARI04]. In addition, the abrasive layer will change during the grinding process [STUF96]. The dressing process should enable a grinding process as consistent as possible considering grinding wheel wear.

Abrasive tools are prepared for use to be set up for a new grinding application according to profile and micro topography, to true their roundness deviation and to compensate their wear. The term "dressing" envelopes the processes of "profiling" or "truing", i.e. the generation of the demanded grinding tool profile, and "sharpening", i.e. the generation of cutting ability [KLOC05a, SPUR89, TÖNS04]. Sometimes "dressing" refers only to sharpening. Depending on abrasive tool specification and machine set-up, profiling and sharpening have to be conducted as separate processes. In general, dressing consumes a lot of grinding wheel volume [STET74], sometimes up to 90 % of the grinding wheel volume.

The various dressing methods can be organized by different criteria, such as active medium, active principle, or process kinematics [HESS03, KLOC05a, SPUR89, LINK07]. Active dressing media can be with or without diamond. Active principles are cutting of grits and bond, setting back the bond, or removing the bond. To set back the bond, diamond free tools like steel rollers, silicon carbide wheels, or sharpening tools of bonded abrasives are used. Material removal processes are restricted to metallic bonds and work with electro-chemical or electro discharge processes [SPUR89]. In laser conditioning, bonding is vaporized before the abrasive grits are harmed [SHAW96]. Laser assisted dressing is a hybrid procedure. The laser beam softens vitrified bonding to support dressing with diamond tools [ZHAN03]. Sand blasting is used for bond sharpening at honing sticks. The applied dressing strategy always depends on quality and cost requirements and the available machine concept. Wegener et al. [WEGE11] give a detailed overview on profiling and sharpening strategies.

6.5.2 Dressing with Diamond Tools

Today, dressing tools with diamond material are commonly used for grinding wheels [KLOC05a], using either stationary or rotating dressing tools. Stationary tools move parallel along to the grinding wheel axis on a path defined via NC

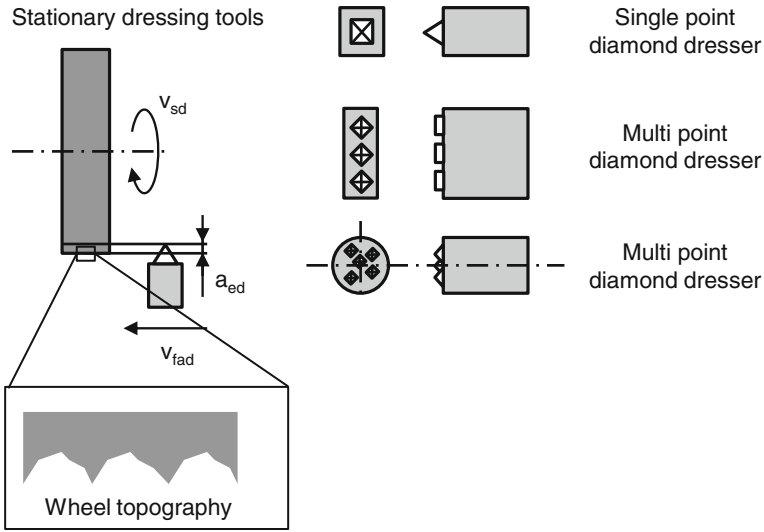


Fig. 6.17 Stationary dressing tools

programming or guide ruler (Fig. 6.17). The grinding wheel topography is generated like in a turning process [KLOC05a]. The stationary dressing tools consist of one or more diamond grits or synthetic diamond logs in metallic bond. Single grit dressers often are made of profiled natural diamonds of high purity, which can be re-positioned when worn. Diamond splinters or synthetic logs are often utilised in multi-grain dressers or dresser tiles.

Rotating dressing tools have an additional movement in circumferential direction of the grinding tool and provide a layer of diamonds along their perimeter (Fig. 6.18). The larger diamond volume of rotating tools improves wear resistance and profile retainability and, therefore, leads to higher dressing process stability [FALK98, WARN88].

Rotating tools are form rollers, profile rollers, or cup disc dressers. Form rollers and cup dressers have an axial feed rate along the grinding wheel axis, whereas profile rollers display the grinding wheel negative profile and are fed radially towards the grinding tool. Form rollers can be used flexibly for different profiles, while profile rollers are limited to one application [HARB97, KLOC87, SALJ84]. Wear formation at a form roller effects not only contour accuracy but also abrasive layer topography because of the changing effective dressing width [SALJ84]. With appropriate wear monitoring these effects can be compensated. However, profile wear at profile rollers leads inevitably to tool life end.

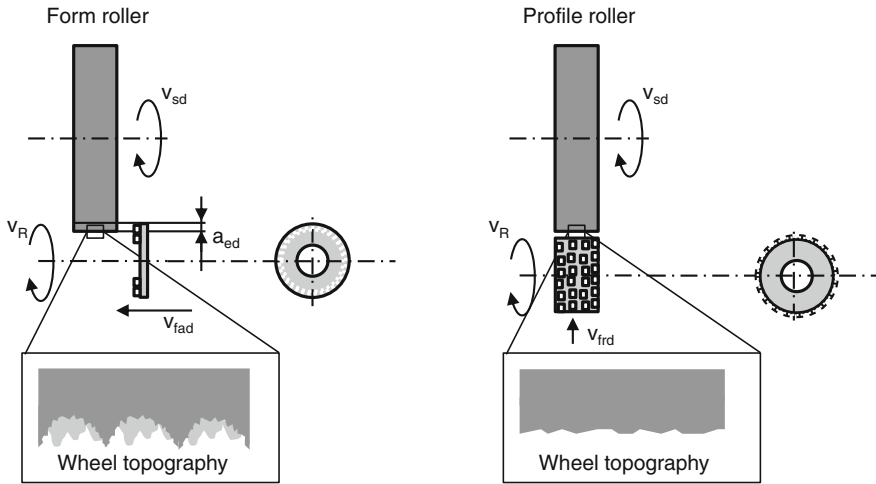


Fig. 6.18 Rotating dressing tools

6.5.3 Dressing Parameters

6.5.3.1 Overlap Ratio

Overlap ratio, U_d , is an important metric for dressing processes with axial feed rate [SALJ84]. It indicates how frequently the dressing tool overtravels a point on the grinding wheel. Overlap ratio is calculated from engagement width of the dressing tool, a_{pd} , and axial feed per grinding wheel revolution, f_{ad} (Eq. 6.24).

$$U_d = \frac{a_{pd}}{f_{ad}} \tag{6.24}$$

$$\text{with } a_{pd} = \frac{b_d + f_{ad}}{2} \tag{6.25}$$

- a_{pd} engagement width
- f_{ad} axial feed
- b_d active dressing tool width

For inclined contour elements of the grinding wheel profile, the overlap ratio can be calculated for the direction of the contour, axial, or radial direction [HARB97]. For cylindrical dressing tools and in most industrial applications the simplified Eq. 6.26 is used [KLOC05a, VDI04]. Active dressing tool width, b_d , depends on the depth of dressing cut, a_{ed} .

$$U_d = \frac{b_d}{f_{ad}} \quad (6.26)$$

b_d active dressing tool width

f_{ad} axial feed

Small dressing feed or high overlap ratio results in grinding wheel topography with small active surface roughness, low grit protrusion, and a high number of kinematic cutting edges [KLOC05a, MARI04, SCHU96, STUF96]. The favorable small part surface roughness is accompanied by the danger of higher grinding forces and stronger grinding wheel loading. Therefore, grinding wheels for roughing operations are dressed with small overlap ratios.

Workpiece surface roughness decreases with increasing overlap ratio, so that a maximum overlap ratio exists above which the part surface roughness cannot be improved significantly. Messer [MESS83] found a maximum value, U_{dmax} , in empirical tests, which depends on grinding grit size (Eq. 6.27).

$$U_{dmax} = \frac{\text{grit size in US Mesh}}{15} \quad (6.27)$$

6.5.3.2 Depth of Dressing Cut

For stationary dressers and form rollers, depth of dressing cut, a_{ed} , defines engagement depth of the dressing diamonds with the grinding tool in normal direction. For profile rollers radial dressing feed, f_{rd} , has the same implication.

Grinding wheel wear and grit size define the depth of dressing cut [AVER82]. The depth of dressing cut should be smaller than grit size to ensure that the grinding tool structure stays connected [MARI04]. One strategy is to conduct final dressing strokes with no depth of cut, so that the elastic deformations between grinding wheel and dressing tool are leveled out and the wheel topography is smoothed [MALK08, MARI04, SHAW96]. The same effect takes place if profile rollers are kept rotating at the end of the dressing process without further radial infeed.

The influence of depth of dressing cut is not homogeneous in the literature. Messer, Marinescu et al. found an increase of the theoretical effective grinding wheel roughness increases slightly with the depth of dressing cut [MARI04, MESS83]. Inasaki [INAS77] obtained that the workpiece roughness increases degressively. Larger depth of dressing cut leads to more splintering of abrasive grits [STUF96] and to shorter instationary wear phase of the grinding tool [SCHU96].

6.5.3.3 Dressing Speed Ratio

Dressing speed ratio, q_d , gives the ratio between dressing roller speed and wheel speed (Eq. 6.28). In up-dressing, the speed vectors are counter-directional in the contact point and the speed ratio is denoted with a negative value; in down-dressing everything is inverted.

$$q_d = \pm \frac{v_R}{v_s} \quad (6.28)$$

v_R dressing roller speed

v_s wheel speed

Dressing speed defines the engagement curves of dressing diamonds into the grinding wheel [SCHU96]. The rotations of dressing roller and grinding wheel superpose, so that the dressing diamonds move along cycloidal paths viewed from the grinding wheel [SCHE73]. Dressing diamond paths for down-dressing have steeper flanks for the same value of the speed ratio in up-dressing, $|q_d|$ [SCHM68]. Therefore, rougher grinding wheel topography results. Contact length between dressing diamond and grinding wheel decreases with increasing value of the speed ratio, $|q_d|$, and the engagement angle gets steeper [STUF96]. This affects the wear mechanisms of the abrasive grits. Grits dressed in down-dressing mode splinter and break more, whereas grits dressed in up-dressing are rather flattened [STUF96]. At the dressing speed ratio of $q_d = +1$ grinding and dressing tool move with the same speed and high normal forces occur. The grinding layer is shattered by high normal forces and the dressing principle is called “Crushing” [HESS03]. Special brittle bond systems work best for crushing, for example brittle bronze bonding.

Experiments have shown that not only the dressing speed ratio, but also the relative speed between dressing roller and grinding wheel are important.

6.5.3.4 Dressing Mechanisms

During dressing with diamond tools, the active mechanisms are grit breakage and splintering, bonding breakage, grit break-out of the bonding, and grit deformation [MARI04, WIMM95, MINK88, MESS83, KLOC08b]. For vitrified bonded wheels, dressing forces seem to have a crucial effect on the disruption of the abrasive layer and therefore on the wear behavior after dressing [LINK07].

Çinar [CINA95] developed a grit collision model to describe mechanisms in cup dressing and predict workpiece surface roughness. Linke [LINK07] extended the model to other dressing tool types and combined it with a dressing force model.

The initial grinding wheel wear after dressing can be high, before the wheel wear gets into a steady state that is defined by the grinding process conditions only (see Sect. 6.3.2 “Micro Effect—Sharpness Loss”). In industrial practice, the grinding wheel wear often is compensated with a few dressing strokes with a high depth of

dressing cut followed by a last stroke with a smaller depth of dressing cut to reduce the grinding wheel surface roughness. However, grinding wheel scratch tests verified that a higher depth of dressing cut and a smaller dressing overlap ratio disrupt the abrasive layer [LINK07, KLOC08b]. In a dressing process with several dressing strokes, the grinding wheel surface roughness is determined by the last dressing stroke. However, the grinding wheel structure is damaged also by the previous strokes. This will result in an instationary grinding process after dressing depending on all previous dressing conditions.

6.5.4 Dressing of Superabrasive Tools

The high wear resistance of superabrasive grits provides challenges to dressing procedures. CBN grinding wheels are commonly dressed with rotating diamond tools because of the lower toughness and hardness of CBN compared to diamond [MARI07]. However, the dressing forces for CBN are higher than for conventional wheels, which needs to be considered for the dressing system design [JACK11, LINK14a]. Superabrasive wheels are dressed with much smaller depth of cut than conventional wheels [WEGE11].

Diamond grinding wheels are dressed with diamond dressing tools only in limited cases. More commonly, they vitrified bonded silicon carbide rollers are used on brake-controlled truing devices or on driven truing spindles [WEGE11, LINK14a]. The expendable and much cheaper silicon carbide wheel grinds away the diamond tool [MALK08].

Resin or metal bonded superabrasive tools sometimes require a subsequent sharpening process after the profiling process to generate sufficient grain protrusion [WEGE11]. The bonding can be set back for example with a block sharpening process [LINK14a]. Electrolytic in-process dressing (ELID) is an established method for metal bonded diamond wheels [ROWE09]. More dressing procedures using electro chemical and electro physical mechanisms exist for metal bonds [WEGE11].

6.6 Sustainability Dimensions to Grinding Wheel Micro-Design and Wear

6.6.1 Technological Dimension

Tool wear and conditioning are important factors for the tool user as they define product quality, grinding forces, maximum material removal rate and auxiliary times. Grinding tool performance impacts workpiece dimensions and surface integrity. Tool manufacturers are able to generate desired tool capabilities within a

certain range, but the tool use also decides on tool performance. Several researchers conducted detailed grinding experiments on how tool specification (structure grade, grit concentration, grit size, wheel hardness) affects grinding forces, and surface roughness and quality [LINE92, KLOM86].

6.6.2 Economic Dimension

Tool wear affects wheel life time and tool costs. However, the direct costs of different grinding wheel designs need to be compared with the total costs for process stability, auxiliary times, scrap rate, etc. (see Sect. 7.1.3 Life Cycle Costing (LCC)). Dressing is non-productive auxiliary time and the dressed wheel volume is lost for processing. The tool micro-design, i.e. abrasive layer design, defines process productivity decisively.

6.6.3 Environmental Dimension

Tool wear is waste that should be reduced to enhance material efficiency. However, as tool performance decides on product quality and scrap rate, there might be a trade-off between tool wear and scrap parts. Furthermore, trade-offs between grinding process and product performance in its use phase, defined by the surface integrity, are possible [HELU11].

Additional material output comes from wheel wear. In grinding or dressing, such high peak temperatures occur that grit and bond material melt [LINK07, ZEPP05]. Grinding tool manufacturers proved in unpublished tests that no harmful gaseous emissions derive from the grinding wheels during the machining process. Furthermore, aerosols from machinery or workpiece material are produced during grinding [RIVE07, p. 158]. Aerosols from the cooling lubricant are in particular prominent for high grinding wheel speeds.

In tool grinding of cemented carbides, cobalt leaching into the cooling lubricant can occur [REHB03]. Inhibitors and the correct choice of cooling lubricant suppress leaching [REHB03]. However, there are opposite and unproven opinions if leaching effects from metal bonds exist. The literature indicates that reactions of cooling lubricants with heavy metals or non-ferrous metals exist, but without further detailing. Inhibitors in the cooling lubricant are therefore important. Metals from the ground material can dissolve into the cooling lubricant [LIED99]. After using ester based grinding oil with vitrified bonded wheels small amounts of boron and aluminum accumulated in the oil [LIED99].

6.6.4 *Social Dimension*

The grinding tool user might be affected directly by grinding dust through inhalation, eye or skin contact [UNIT09b]. Respiratory problems with the grinding process emissions were already addressed in the 19th century [KNIG22]. Here, the so-called Grinder's asthma from inhaled particles was recognized and led to the development of exhaust air systems [KNIG22]. The small size of the grinding swarf or chips makes them more hazardous for the worker because they can be inhaled.

Sparks and hot chips can be dangerous, in particular when using manual grinding tools [BGI10]. Manual grinding tools are portable and therefore extra care has to be taken to remove explosive and flammable materials from the machining environment.

6.6.5 *Sustainability Model for Tool Use Phase*

Tool performance in the use phase is most important to the tool user, but also for the tool manufacturer and the society. The tool manufacturer is concerned with

- the **tool price**, which is a balance between the raw material and production costs and the price a tool user is willing to pay.
- **Tool wear** is an important quality factor during tool use and needs to be adjusted to the customer satisfaction.
- **Safety** for the tool user needs to be ensured.

The tool user focuses on the technological and economic tool performance.

- **Tool wear** decides on process quality and stability as well as on process costs.
- **Dressability** is important for process setup and process stability.
- The **tool price** a tool user is willing to pay arises from the subjective tool usefulness for a certain application.
- Tool performance affects the tool user's **competitiveness**.
- The tool user needs to be sure of **safety**.
- **Hazards** from tool use and tool wear are to be avoided.

The society is interested in tool user **safety** and in **product life and performance** at a larger scale.

Chapter 7

Sustainability of Grinding Tools

*In 1822, grinders did not become old:
About thirty years ago, the steam engine was first adapted to the purposes of grinding; and then a very important era arrived in the annals of the grinder. He now worked in a small low room, where there were ten or twelve stones; the doors and windows were kept almost constantly shut; a great quantity of dust was necessarily evolved from so many stones, and there was scarcely any circulation of air to carry it away. [...] If, then, the grinders' asthma were a disease of not unfrequent occurrence before, it is probable that its frequency would have been much increased now. Such, indeed, was the fact; and it is at the present time become so general, that out of twenty-five hundred grinders, there are not thirty-five who have arrived at the age of fifty years. [KNIG22].*

Sustainability of grinding tools can only be discussed with a deep understanding of all relevant system components. This chapter summarizes the analyses and conclusions from the preceding chapters into a holistic description model. The study on abrasive tooling systems began with explaining the abrasive grits, followed by the bonding systems (Chaps. 2 and 3). Then it eluded on the different tooling types and grinding wheel body shapes and materials (Chaps. 4 and 5). The composition and structure of the abrasive layer has complex implications on tool manufacturing and use (Chap. 6). Understanding of wear and tool conditioning is crucial to the grinding process. Based on this technological base a comprehensive evaluation of sustainability of tooling systems becomes possible. Therefore, existing methods of life cycle engineering, namely Life Cycle Assessment, Life Cycle Costing, Social Life Cycle Assessment, and Sustainability Indicators are introduced in the following chapter. The Input-Output streams of grinding will be derived to provide the life cycle inventory. As a new method axiomatic design principles will be applied to analyze all functions and design parameters of grinding. The generated matrix will allow a new, detailed evaluation of grinding process sustainability.

7.1 Life Cycle Engineering

Companies have to find ways to capture and measure their sustainability performance. The overall goal of sustainability encompasses the three dimensions of economic, environmental and social sustainability [HAUS05]. Life Cycle Costing (LCC), Life Cycle Assessment (LCA), and Social Life Cycle Assessment (SLCA) are methods to assess each dimension. Sustainability indicators evaluate the overall performance in all dimensions. In this study, technology is added as fourth dimension to sustainability.

Life cycle engineering (LCE) incorporates concepts, approaches, and methodologies to address environmental challenges, such as generation of waste, releasing hazardous substances, resource depletion, and green house gas emissions [UMED12]. Considering life cycles enlarges the narrow view on product, production, and use onto viewing the whole product life from raw material extraction to disposal [HERR10, p. 83]. Umeda et al. [UMED12] propose that product design and life cycle flow design should be integrated to reduce the resource consumption and environmental loads of the entire product life cycle.

7.1.1 Environmental Aspects—Life Cycle Assessment (LCA)

Many different standards and methodologies exist to evaluate the environmental impacts of products, processes and manufacturing systems. The most commonly used method is Life Cycle Assessment (LCA), including its variants process LCA, Economic Input-Output LCA and hybrid LCA [REIC10]. Reich-Weiser et al. [REIC10] discussed the differences between frameworks and sorted them into different spatial and temporal levels of complexity. Hybrid LCA methodologies were found to be effective at capturing full supply chain and enterprise level emissions; however, trade-offs at the factory or machine tool level are best analyzed by process LCA approaches [REIC10]. LCA focuses on environmental aspects.

ISO14040 gives a framework to conduct a process LCA. Figure 7.1 transfers the framework to grinding tool production. First, goal and scope of the study are defined as well as functional unit, i.e. the basis for the quantification of resource and energy streams. In the next step, life cycle inventory (LCI) analysis, all resource and energy streams are collected. Table 7.1 summarizes common environmental attributes, but are not grinding process specific. For grinding analysis, water, air, sound, resources, and human aspects are most important.

The third step consists of the life cycle impact assessment (LCIA). The inventory data is converted into impact indicators, which will form the environmental fingerprint of the process. Impact is defined as the consequences caused by the input and output streams on the Areas of Protection (AoP). Four AoP are defined: human health, man-made environment, natural environment, and natural resources [DEHA99]. Typical impact categories enclose global warming, stratospheric ozone

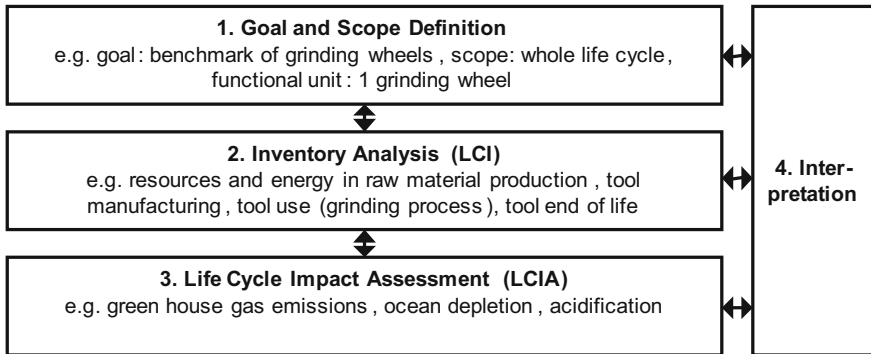


Fig. 7.1 Life cycle assessment of abrasive tooling systems (after ISO14044)

Table 7.1 Environmental attributes [JAIN12, p. 459 ff]

<p>Water—physical</p> <ul style="list-style-type: none"> • Aquifer safe yield • Flow variations • Oil • Radioactivity • Suspended solids • Thermal discharge 	<p>Water—chemical</p> <ul style="list-style-type: none"> • Acid and alkali • Biochemical oxygen demand • Dissolved oxygen • Dissolved solids • Nutrients • Toxic compounds 	<p>Water—biological</p> <ul style="list-style-type: none"> • Aquatic life • Fecal coliforms
<p>Air</p> <ul style="list-style-type: none"> • Diffusion factor • Particulate matter • Sulfur oxides • Hydrocarbons • Nitrogen oxides • Carbon monoxide • Photochemical oxidants • Hazardous toxicants • Odors 	<p>Sound</p> <ul style="list-style-type: none"> • Physiological effects • Psychological effects • Communication effects • Performance effects • Social behavior effects 	<p>Ecology</p> <ul style="list-style-type: none"> • Large animals (wild and domestic) • Predatory birds • Small game • Fish, shellfish, and waterfowl • Field crops • Listed species • Natural land vegetation • Aquatic plants
<p>Land</p> <ul style="list-style-type: none"> • Erosion • Natural hazards • Land-use patterns 	<p>Human aspects</p> <ul style="list-style-type: none"> • Lifestyles • Psychological needs • Physiological systems • Community needs 	<p>Resources</p> <ul style="list-style-type: none"> • Fuel resources • Nonfuel resources • Aesthetics

depletion, acidification, eutrophication, photochemical smog, terrestrial toxicity, aquatic toxicity, human health, resource depletion, land use, and water use [CURR06, p. 49].

LCIA methods are either midpoint or endpoint oriented. The midpoint methods model impacts at some midpoint in the environmental mechanism [HAUS05]. The endpoint methods are also called damage oriented methods and calculate an overall

impact score for the AoP at the end [HAUS05]. Normalization and weighting is conducted on the impact indicators. The environmental attributes in Table 7.1 have been of interest to life cycle assessment over time [JAIN12, p. 459 ff].

7.1.2 Social Life Cycle Assessment (SLCA)

Companies start to include Corporate Social Responsibility into their corporate culture [MCCL10]. Traditionally, lower need levels of people were regarded, such as food, health and safety, but in the future the social aspects will likely be extended to higher levels such as worker satisfaction, self-esteem, etc. [HUTC10]. Societal aspects of product or process assessment include furthermore customer requirements, legislation, cooperative strategies, market trends, technological development, and consumers' behavior [UMED12].

Social Life Cycle Assessments are still in development [HAUS08]. Hauschild et al. suggests to add “human dignity and well-being” as fifth Area of Protection (AoP), including having a good and decent life enjoying respect and social membership and with fulfilment of the basic needs for food, water, medical care [HAUS08, WEID06, DREY06]. The Committee on Sustainable Development of the United Nations has a large set of indicators with a strong focus on social sustainability and countries [UN07]. Social indicators include poverty, governance, health, education [UN07]. Hutchins et al. [HUTC10] propose a social sustainability indicator framework, which maps the needs to the different entities involved into the manufacturing system (Fig. 7.2).

		Need				
		Basic needs	Safety/ Security needs	Affiliation needs	Esteem needs	Actualization needs
		- requirements to maintain the primary functions of the entity	- freedom from real or perceived external threats to the entity	- an understood role within a group and meaningful relationships with other entities	- having both self-respect and the respect of other entities	- realizing the full potential of the entity
Entity	Employees					
	Customers					
	Stockholders/ Owners					
	Suppliers					
	Community					
	Public					

Fig. 7.2 Social sustainability indicator framework after [HUTC10]

7.1.3 Life Cycle Costing (LCC)

The method of Life Cycle Costing has been developed in the USA for calculation of the economic feasibility and design for projects in industrial plant construction [VDI05]. Life Cycle costs include not only the product’s manufacturing costs, but also usage and disposal costs.

The grinding costs per part enclose the machine costs, labor costs, tool costs, coolant costs, and nonconformity costs as shown in Fig. 7.3 [HENN84]. The time per part needs to incorporate nonproductive time per part besides the primary processing time, which is defined by the material removal rate and the process set-up (Fig. 7.4).

Increasing material removal rate reduces processing time and time dependent costs (Fig. 7.5). Higher material removal rate also leads to higher load on the grinding system components, higher tool wear, potentially higher scrap rate, etc. Therefore, the load dependent costs rise. The total costs as the sum of the load and time dependent costs has a minimum.

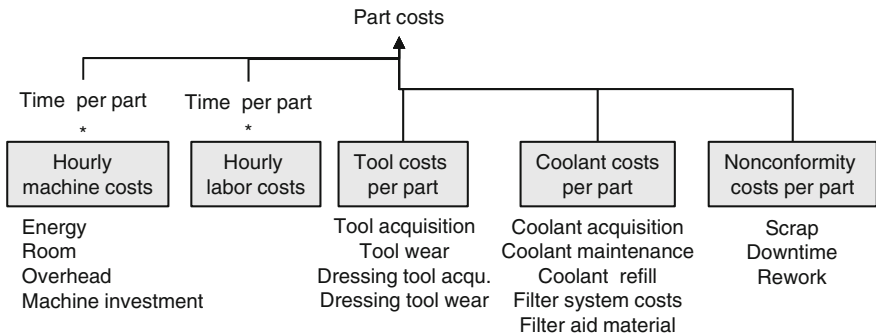


Fig. 7.3 Grinding costs per part

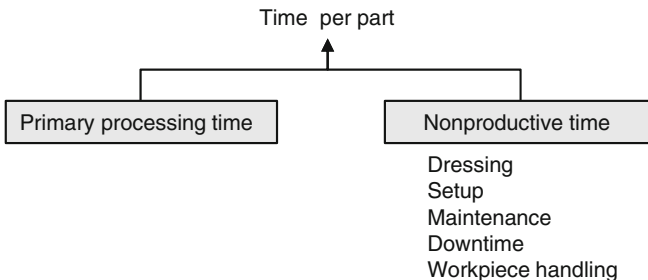


Fig. 7.4 Grinding time per part

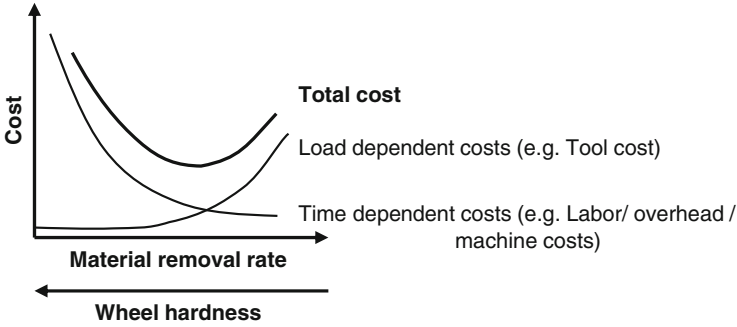


Fig. 7.5 Part costs after [METZ86, p. 11, COES71, p. 13]

A comparison of superabrasive and conventional tools highlights how important it is to account for all costs. The superabrasive tool costs more and, despite the higher tool life, the tool costs per part might be higher (Fig. 7.6). However, the time dependent costs such as labor and machine costs are likely much smaller per part, because the superabrasive tool needs fewer tool changes, cycle times are likely higher, process stability is better and less rejects happen, less down-time occurs by dressing, etc. [KING86, p. 105]. The total costs per machined part are then lower for the superabrasive tool than for the conventional wheel (Fig. 7.6).

Costs for cooling lubricant need to be split between costs per batch or part and costs per disposal interval. Coolant treatment costs appear per liter of coolant, disposal costs for old coolant, and purchase costs for new coolant. Coolant treatment includes maintenance and control, adding of additives such as biozides, emulgators, foam inhibitors, and filtering. In emulsions, water needs to be refilled due to evaporation. Filtering systems can be belt filters with filter material, separators, magnetic filters, hydrocyclones, or others [KLOC09, p. 131].

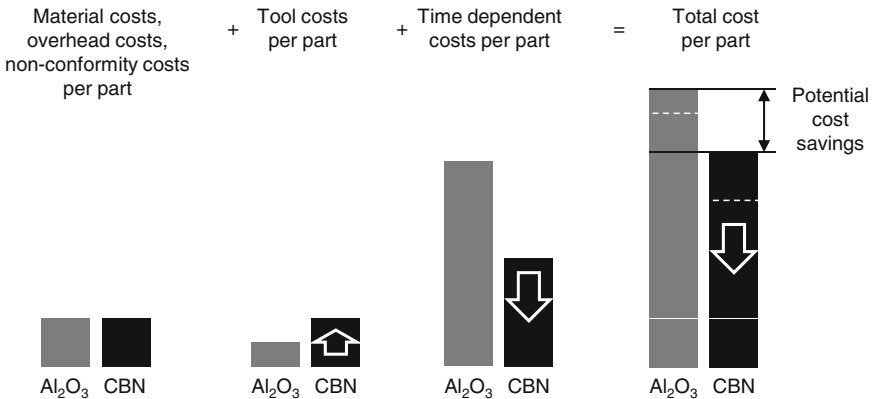


Fig. 7.6 Part costs for conventional and superabrasive grinding tools after [KING86, p. 105]

7.1.4 Sustainability Indicators

Sustainability indicators are less formalized assessment indicators than the ones in LCA, SLCA or LCC and can capture more than one dimension of sustainability. An indicator is “a measure or an aggregation of measures from which conclusions on the phenomenon of interest can be inferred” [JOUN12]. Sustainability indicators are good for users with limited databases and resources. Companies can assess their actual situation with the indicators, raise their awareness and set their goals [KRAJ03].

In the last years, different approaches to measure sustainability performance have arisen [JOUN12, SING12, JAYA10]. For example, the Process Sustainability Index (ProcSI) regards the six clusters: manufacturing costs, energy consumption, waste management, environmental impact, operator safety, and personnel health [LU127]. The methods should be simple and affordable to apply, have low assessment time, and should not rely on user experience. The indicators have to be specified in the period of tracking and calculating (e.g. fiscal year, calendar year, month, etc.), boundaries (e.g. process level, factory level, etc.), and units of measurement [KRAJ03].

It is advisable not to choose too many indicators to keep the analysis manageable [LINK13]. In addition, sustainability indicators should be independent. Indicators should be normalized, which means they do not present their value as absolute amount but show relative terms as a ratio of performance per specific unit of output [OECD12]. A wide variety of factors can be used to normalize performance, such as number, weight or units of products produced in the facility, value added, person-hours worked in the facility, or lifetime of the products produced [SING12, OECD12]. Example sustainability indicators are energy intensity, residuals intensity, non-renewable materials intensity, safety, blood lead level, product costs, etc. For grinding, a smaller set of indicators seems to be useful (Fig. 7.39) [LINK13].

7.2 Life Cycle Inventory of Grinding Processes

7.2.1 Evaluating Sustainability of Unit Processes

In addition to economic, environmental and social sustainability, the technological dimension needs to be considered as a fourth dimension. Yuan et al. [YUAN12] suggest three strategies to increase sustainability in manufacturing processes: (1) Optimizing of the manufacturing technology by detecting and changing the parameters that affect material and energy streams, (2) Using clean energy, (3) Using lower impact materials.

The production of a part can be broken down from all involved production chains into discrete manufacturing processes. The unit process consists of inputs, process, and outputs of an operation. Each unit process is converting material or chemical inputs into a transformed material or chemical output. Cradle to grave views a product from raw material extraction to end of life, cradle to cradle

considers re-use and recycling, cradle to gate or gate to gate evaluates only parts of the life cycle.

The CO₂PE! UPLCI-Initiative provides a framework to acquire data for unit manufacturing processes [KELL11]. The in-depth approach in the CO₂PE! UPLCI-Initiative studies energy through power consumption measurements and time studies, as well as consumables and manufacturing emissions [KELL12a, KELL12b, KELL11]. The basic screening approach in the CO₂PE! UPLCI-Initiative quantifies energy consumption as well as other environmental impact information of manufacturing processes, and is largely based on data from publications, catalogs, and handbooks [KELL11]. It focuses on manufacturing energy and chemicals/materials required at the machine level and can be refined by measured data.

Energy and resource efficiency of manufacturing processes can be enhanced by reducing the machine basic and idle energy through machine setup or shorter production times or by minimizing the processing energy [DORN10].

7.2.2 Input-Output Streams of Grinding

The complex tool design with multiple cutting edges and the complex chip formation mechanisms complicate the analysis of the grinding process [KLOM86]. Figure 7.7 shows all input and output streams that can be considered in grinding and provides a basis for a life cycle inventory. The items have different relevance for different applications.

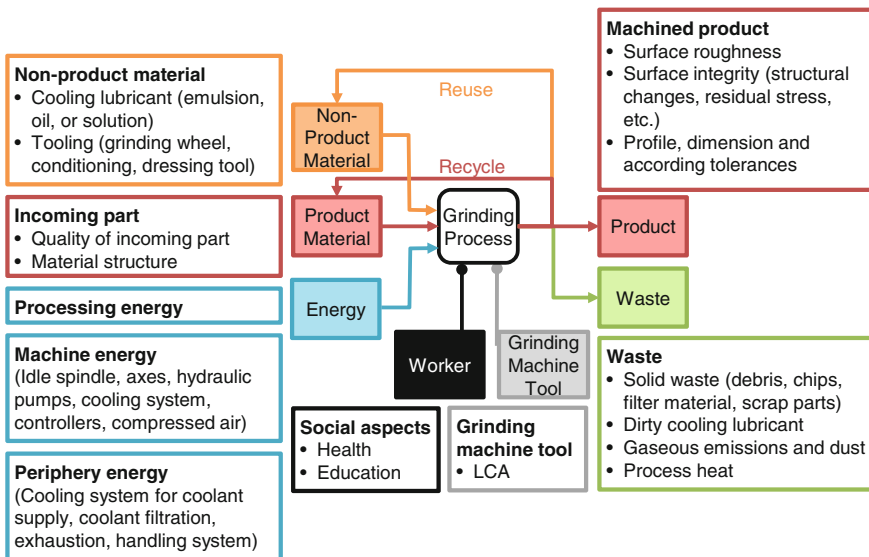


Fig. 7.7 Comprehensive input-output diagram of a grinding process [LINK12], with kind permission from Springer Science and Business Media

The tooling is part of non-product material. Grinding wheel design, tool conditioning, and dressing tools are described in Sects. 6.3.3 “G-Ratio” and 6.5 “Tool Conditioning”. Cooling lubricant is important to cool and lubricate the grinding process, clean, transport chips, cool the machine tool, and protect against corrosion [BRIN99, KLOC09, MARI07].

Grinding oil, water-based emulsions or watery solutions are common cooling lubricants. These coolants have a different amount of non-renewable material content and affect the environmental attributes of water differently, such as contents of oil, acids, alkalis, toxic compounds, etc. [JAIN12, p. 497 ff]. Furthermore, the grinding fluid can attract bacteria and fungi or be irritating to the worker’s skin.

Water scarcity is a local measure, which predicts the long-term sustainability of a manufacturing location [REIC09]. The importance of water use is perceived differently in different geographical regions. The German industry, for example, does not perceive water scarcity in the same way as the Californian industry does. Research on new coolant media is ongoing to address the growing concerns on recyclability, toxicity and water consumption [KALI11, ZEIN11b].

Cooling lubricant type, flow volume, flow rate and supply systems affect the grinding process performance [BADG09a, BRIN99, KLOC09, WITT07, MORG08]. However, there is no easy estimation for the necessary flow volume and the flow rate of cooling lubricant, and it is often adjusted by the rule of thumb of 1 l / (min mm) [liter per minute and millimeter of grinding wheel width] [LINK12]. The high process heat limits dry grinding or Minimum Quantum Lubrication (MQL) to few applications [BECK02, MARI07].

The total energy consumed to generate part shape and surface by grinding consists of the processing energy and the energy consumed by machine tool and periphery (Fig. 7.7) [CRAT10, LINK12]. The processing energy or specific grinding energy, e_c , is defined as energy to remove one volumetric unit of material and is used for forming grinding chips, plowing material, and mastering friction between grinding grits, tool bond and the workpiece [MALK08, OLIV09].

Commonly, the specific grinding energy, e_c , is calculated from the grinding power, P_c , and the material removal rate, Q_w , after Eq. 7.1 [KLOC09]. Grinding power consists of the forces and speeds in tangential, normal and axial direction (Eq. 7.2) [ROWE09, p. 25]. However, normal and axial feed rates are much smaller than cutting speed in tangential direction and workpiece speed is smaller than the wheel speed, so that the simplified Eq. 7.3 is commonly used.

$$\text{Specific grinding energy } e_c = \frac{P_c}{Q_w} \quad (7.1)$$

$$\text{Grinding power } P_c = F_t \cdot (v_s \pm v_w) + F_n \cdot v_{fr} + F_a \cdot v_{fa} \quad (7.2)$$

$$\text{Simplified grinding power } P_c = F_t \cdot v_s \quad (7.3)$$

Q_w	material removal rate
F_t	tangential grinding force
v_s	grinding wheel speed
v_w	workpiece speed
F_n	normal grinding force
v_{fr}	radial feed rate
F_a	axial grinding force
v_{fa}	axial feed rate

Researchers have developed several grinding force models in close relationship to the undeformed chip thickness, but these grinding force models are empirical and hardly applicable for generic applications [TÖNS92]. Grinding energy cannot be predicted accurately and variations in wheel sharpness lead to large variations in grinding energy [ROWE09]. Table 7.2 gives example processing energies.

Machine tool energy and peripheral energy can add much to the total energy [DAHMO4]. This includes energy to run machine control, hydraulics, lighting, coolant system, compressed air, etc. Some machine power profiles have been published and databases provide basic information on machine power demands [ZEIN11, DENK05, KLOC10, BANI05]. Coolant pumps can account for a big portion of grinding energy as well as heating, ventilation and air conditioning (HVAC) and lighting [LINK12, DIAZ10].

The total grinding energy per part, E_{total} , can be calculated from processing, handling, setup and dressing time per single part (Eq. 7.4, Fig. 7.8) [LINK12]. Here, the power consumed by the dressing spindle and axes is neglected.

Table 7.2 Examples for specific grinding energies [LINK12]

Application	Specific energy in [J/mm ³]	Reference
Grinding of brittle materials like glass or ceramics	1–7	[HELL05a]
Surface grinding of aluminum	2.5–10	[KALP97]
Grinding of the metal matrix composite Al-2009/SiC-15 W with alumina wheel	10–25	[ILIO09]
Speed stroke grinding of γ -titanium aluminum alloy with vitrified diamond wheel	10–30	[ZEPP05]
Surface grinding of cast iron	12–60	[KALP97]
Surface grinding of tool steels	18–82	[KALP97]
Grinding of steels with conventional aluminum-oxide wheels	30–50	[OLIV09]
Grinding of cemented carbide	80–200	[HELL05a]

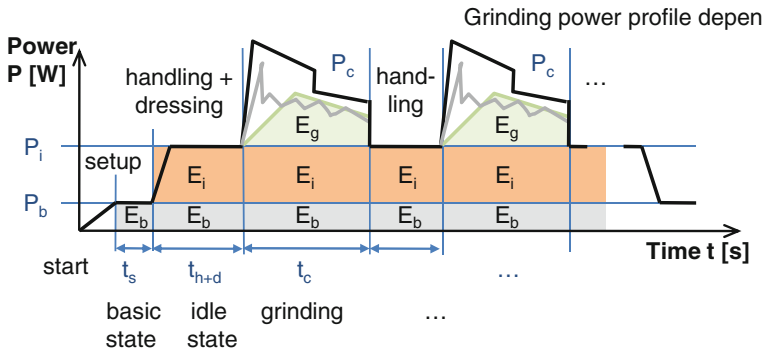


Fig. 7.8 Simplified power profile for grinding processes [LINK12], with kind permission from Springer Science and Business Media

$$E_{total} = \underbrace{t_s \cdot (P_b)}_{\text{setup energy}} + \underbrace{t_{h+d} \cdot (P_b + P_i)}_{\text{handling and dressing energy}} + \underbrace{t_c \cdot (P_b + P_i) + e_c \cdot V_w}_{\text{grinding energy}} \quad (7.4)$$

- t_s setup time
- t_{h+d} handling and dressing time
- t_c grinding time
- P_b base power
- P_i idle power
- e_c specific grinding energy
- V_w machined material volume

The specific grinding energy, e_c , can be calculated through Eq. 7.1 if forces are measured or through Eq. 7.5 if the spindle power profile is measured [LINK12].

$$e_c = \frac{\int (P_c(t) - P_b(t) - P_i(t))dt}{V_w} \quad (7.5)$$

- P_c spindle power
- P_b base power
- P_i idle power
- t time
- V_w machined material volume

Higher material removal rate decreases process energy for the same volume of material removed [MARI07, LINK11, ZEIN11, KLOC10]. This results from the decreasing processing time, which dominates over the increasing processing power demand. Nevertheless, higher material removal rates lead to higher process forces, larger tool wear, and higher surface roughness.

Waste streams from the grinding process include heat waste. The common assumption is that nearly the total energy in the contact zone is converted to the total heat flux, q_t (Eq. 7.6) [MARI07]. Abrasive grits with higher thermal conductivity can reduce temperatures drastically, e.g. CBN instead of Al_2O_3 , [ROWE09].

Grinding debris and filter material are another waste stream from the grinding process [ECKE00]. Grinding debris can be composed of 10–80 % of chips, 2–75 % of grinding tool swarf and up to 50 % of filter aid [SCHÖ03]. The oil or emulsion content defines the recyclability of the grinding debris. Recycling options for abrasive tools are addressed in Sect. 4.8 “Tool End of Life”.

Machine tools have a life cycle of their own [DIAZ10]. Enparantza et al. [ENPA06] calculated life cycle costs for a centerless grinding machine tool. In this case study, 80 % of the life cycle costs happen during the use phase due to the grinding operation itself and maintenance. Direct labor accounted for 51 % of the total costs, the grinding wheel for 13 %, the machine tool purchase for 8 % and energy consumption for 6 % [ENPA06].

$$q_t = \frac{F'_t \cdot v_c}{l_c} = q_{\text{ch}} + q_{\text{cool}} + q_w + q_s \quad (7.6)$$

q_t	total heat flux
F'_t	specific tangential force
v_c	cutting speed
l_c	contact length (Eq. 6.7)
q_{ch}	heat flux to the chip
q_{cool}	heat flux to the cooling lubricant
q_s	heat flux to the wheel
q_w	heat flux to the workpiece

7.3 Axiomatic Grinding Process Model

Section 7.1 described different methods for evaluating sustainability and Sect. 7.2 derived the life cycle inventory for grinding to implement these methods. Data for the analysis is either measured empirically, estimated or obtained from databases. Ideally, fundamental process knowledge would allow calculating all input and output streams from physical and analytical models. The following study uses axiomatic design principles to display how sustainability characteristics are connected with physical process principles. This new approach is still in development but creates a holistic model and points out where further research and quantitative equations are needed.

7.3.1 Methodology

Axiomatic design is a way to describe systems and products systematically and was laid out by Suh [SUH01, COCH01]. The idea of axiomatic design is to generalize the principles of the investigated system by axioms. This design method has been used for environmental considerations of manufacturing systems and product services [STIA07]. However, grinding processes have too many interdependencies between their process components and, therefore, some axiomatic design rules cannot be fulfilled completely, such as the interdependence axiom [LINK12c].

The axiomatic design process works within four domains, which are shown in Fig. 7.9 for the abrasive process including process setup, tool, and cooling lubricant. The customer domain is characterized by the customer attributes {CAs} of the grinding application at a defined workpiece. For example, we are aim at a certain surface integrity, roughness or dimensional tolerance. In the functional domain, the functional requirements {FRs}, such as “take away heat from the workpiece”, “control chemical reactions on the work surface”, etc., and constraints {Cs}, such as maximum dimensions of the components, are defined.

The design parameters {DPs} in the physical domain satisfy the FRs. Here, DPs are cooling lubricant properties (heat capacity, supply system, etc.), process setup (thermal conductivity, kinematics, etc.) and tool characteristics (grit type, wheel hardness, etc.).

Finally, in the process domain the procedure to generate the specific DP is characterized by process variables {PVs} [SUH01]. Here, PVs describe machine tool components or the production procedures of grinding tool and cooling lubricant. In concurrent engineering the last three design phases interact constantly with each other.

The relation between FR and DP can be expressed by vectors, see example in Eq. 7.7. This way of describing an abrasive tool system offers the possibility to implement qualitative connections or quantitative equations, which then can be used for energy and resource calculations. Additionally, we are able to separate the objectives (here FR) from the means (DP), evaluate necessity of all items and get a holistic overview [COCH01].

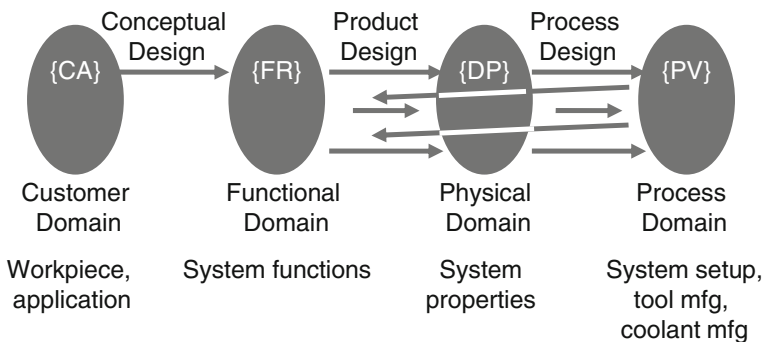


Fig. 7.9 Axiomatic description of a grinding process after [SUH01], reprinted from [LINK12c] with permission from Elsevier

$$\begin{Bmatrix} FR_1 \\ FR_2 \\ FR_3 \end{Bmatrix} = \begin{bmatrix} X & 0 & 0 \\ X & X & 0 \\ X & 0 & X \end{bmatrix} \begin{Bmatrix} DP_1 \\ DP_2 \\ DP_3 \end{Bmatrix} \tag{7.7}$$

Axiomatic design demands that the functional requirements should be independent from each other (Independence Axiom) [SUH01]. This is not fulfilled in grinding processes because many components serve multiple functions, e.g. cooling lubricant or grits [LINK12c]. Additionally, in axiomatic design the information content should be minimal, i.e. the design with highest probability for success should be chosen (Information Axiom) [SUH01]. This axiom is not satisfied within most common discrete processes because the high process complexity does not allow for optimizing all variables simultaneously. For example, if oil is chosen as cooling lubricant instead of water-based emulsion, the heat from friction will be reduced, but chip formation will be less effective and less heat will be removed from the grinding zone [LINK12c].

In conclusion, representing grinding by axioms is one way to visualize the process mechanisms and aims at understanding the technology. Figure 7.10 explains how the axiomatic grinding process model is visualized in the following. Every functional requirement is met by a design parameter and the according boxes are connected by a line (Fig. 7.10). In axiomatic design, the model has to be decomposed until only one DP appears for one FR [BROW11]. DPs can be prioritized and additional DP create an alternative tree. In this study, this decomposition was not completely possible because the real grinding process has overlaying DPs. In addition, each DP should have more than one FRs [BROW11]. Final design

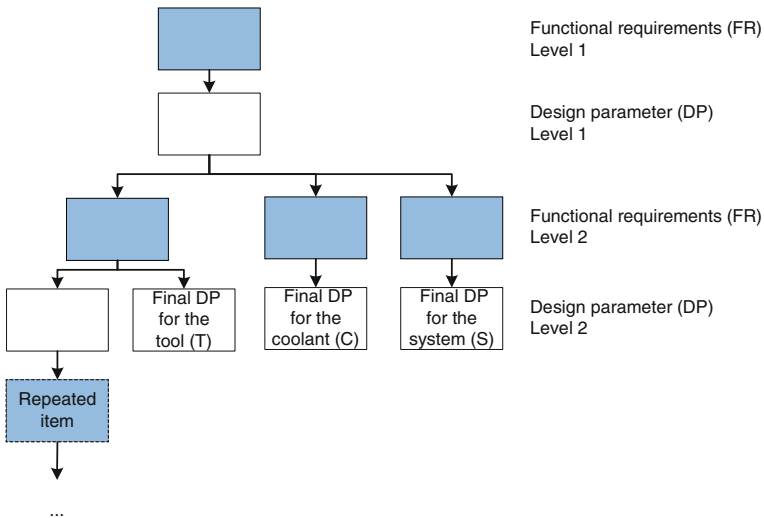


Fig. 7.10 Legend for visualizing the axiomatic grinding model

parameters, which cannot be broken down to smaller variables, are indicated by the letters (S), (T), or (C) (Fig. 7.10). A dashed line indicates a functional requirement or design parameter that is repeated elsewhere in the axiomatic model on the same or earlier level.

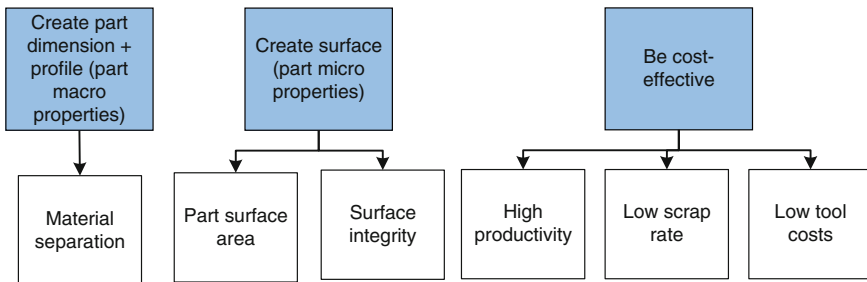
7.3.2 Grinding Process Model

7.3.2.1 Traditional Fundamental Requirements in Grinding

Manufacturing processes have to accomplish certain tasks depending on workpiece material, stock removal (finishing or roughing operation), availability of machines, batch size, form and dimension tolerances, achieved surface roughness and integrity, and more [LINK12c]. The following discussions focus on ductile material in finishing operations and the choice of the grinding tool, but the model can be easily adapted to other applications.

Dominant traditional functional requirements are creating part dimension and profile, i.e. the part’s macro properties, creating the part surface, i.e. the part’s micro properties, and being cost-effective (Fig. 7.11 top row). The first requirement for a given raw part can be achieved by several physical or chemical principles, such as material separation, evaporation, dissolution, additive processes, etc. These principles underlie in fact all manufacturing processes as described by Todd, Allen and Alting [TODD94] or in the DIN8580 standard. In here, material separation is chosen (Fig. 7.11 left).

For the second requirement to create the part surface, the design parameters of part surface area and the surface integrity have to be considered (Fig. 7.11 middle). The third requirement for cost-effectiveness calls for high productivity, low scrap rate, and low tool costs (Fig. 7.11 right). Having more than one design parameter



Alternatives:
 Material evaporation,
 Material dissolution,
 etc.

Fig. 7.11 Main fundamental requirements

for one functional requirement does not follow the axiomatic design rules for a good design [SUH01, BROW11]. The system is overdetermined, but these conflicts highlight problems and could give hint at improvements for future grinding process designs.

The main mechanism of material separation depends on the workpiece material and is dominated by material shearing and chip formation for ductile material or fracture and crack propagation for brittle material. Either way, shear stresses have to be induced by forces applied to the material through cutting edges (Fig. 7.12 top). In grinding, abrasive particles and a track-bound principle are selected over of the alternatives shown in Fig. 7.12.

The abrasive grits have to be held together, which is done by a bonded tool in the shown axiomatic model. Alternatives are coated tools or polishing pads. The abrasive material separation generates chips, which have to be carried out of the contact zone. The grinding tool is chosen as transport mechanism to achieve this.

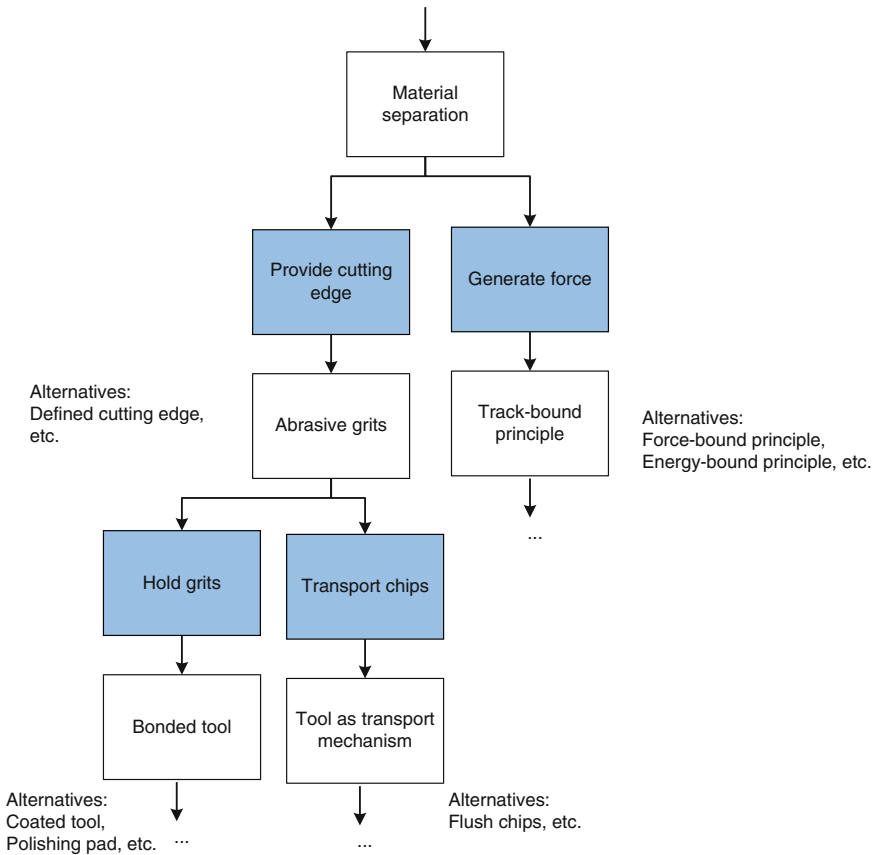


Fig. 7.12 Material separation (diagram follows Fig. 7.11)

7.3.2.2 Implications of a Bonded Tool

The design parameter of a bonded tool implies that an initial tool profile needs to be defined and then maintained as well as an initial tool sharpness needs to be defined and maintained (Fig. 7.13). Design parameters to define profile and sharpness are profiling and sharpening respectively. Profiling and sharpening can be combined to one dressing process, but then the design parameters are coupled (Fig. 7.15).

Loosing the tool profile can be overcome by a sufficient bond strength, low grit friability, and high grit hardness (Fig. 7.13). Loosing the tool sharpness is partially conquered by low grit wear and partially by tool self-sharpening (Fig. 7.14). In the case of a single-layered grinding tool, only low grit wear counts, whereas the multi-layered tools need self-sharpening largely.

Low grit wear is achieved by avoiding abrasive, thermal, and chemical grit wear. The according design parameters are high grit hardness, grit heat resistance, and chemical resistance of the grit material respectively (Fig. 7.14). Tool self-sharpening leads to the functional requirements of having grit splintering and providing new grits. The design parameters high grit friability and adjusted bond strength or a continuous dressing process respectively serve these requirements.

If only one dressing process is conducted instead of separate profiling and sharpening, the initial tool profile and initial sharpness are coupled (Fig. 7.15). The functional requirements of a dressing process are defining the dressing tool, the engagement of the dressing grits into the tool and the dressing intervals. Here, a diamond form roller is chosen as dressing tool, so the axial dressing feed rate v_{fad} , dressing speed ratio q_d , and depth of dressing cut a_{ed} are the parameters defining the

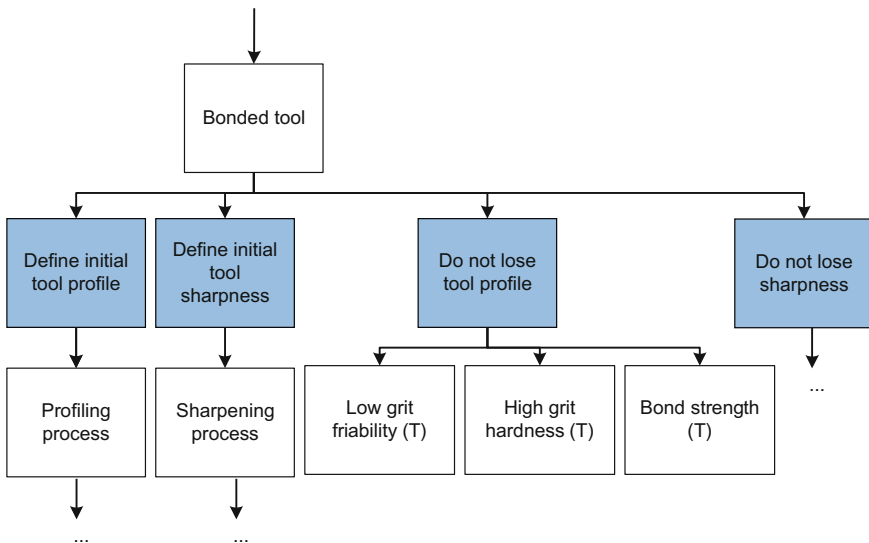


Fig. 7.13 Bonded tool (diagram follows Fig. 7.12)

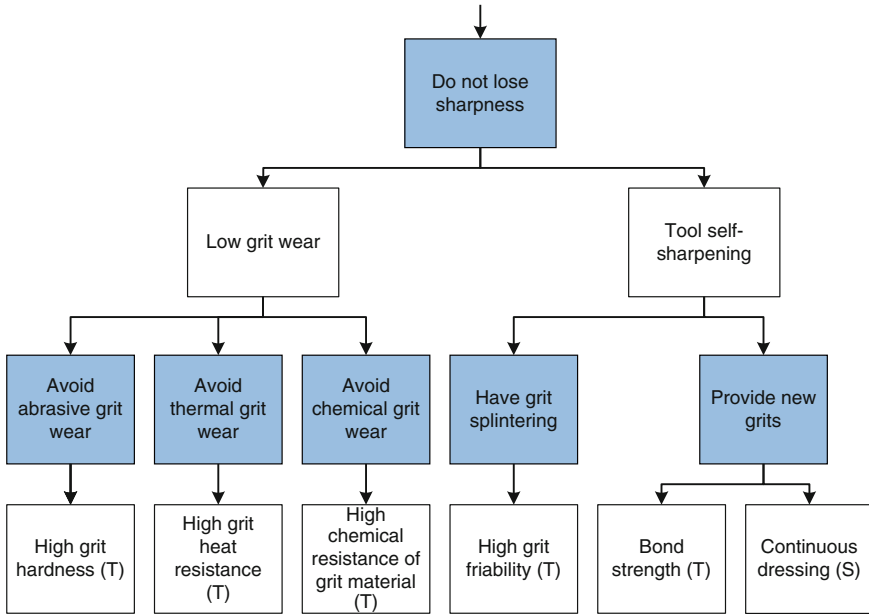


Fig. 7.14 Sharpness (diagram follows Fig. 7.13)

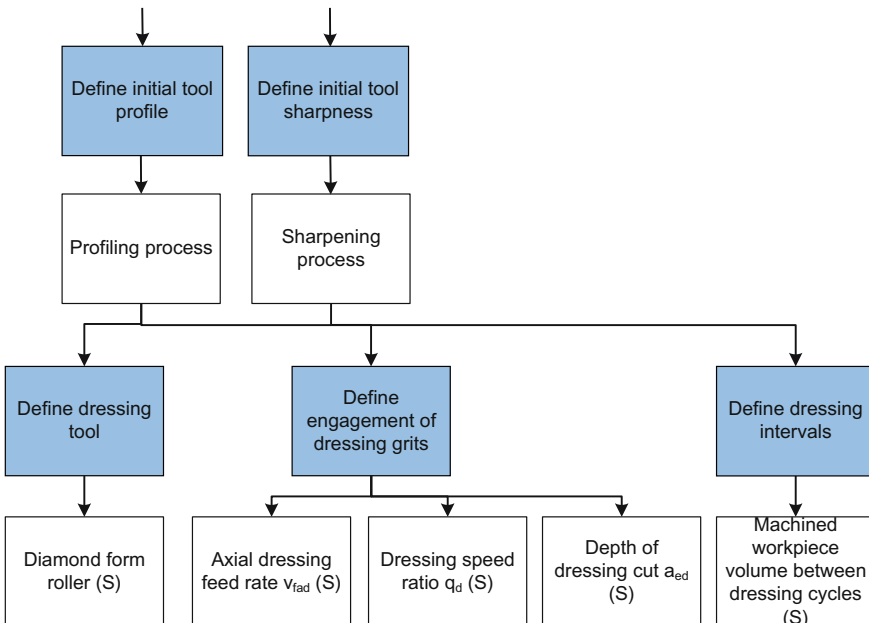


Fig. 7.15 Profiling and sharpening (diagram follows Fig. 7.13)

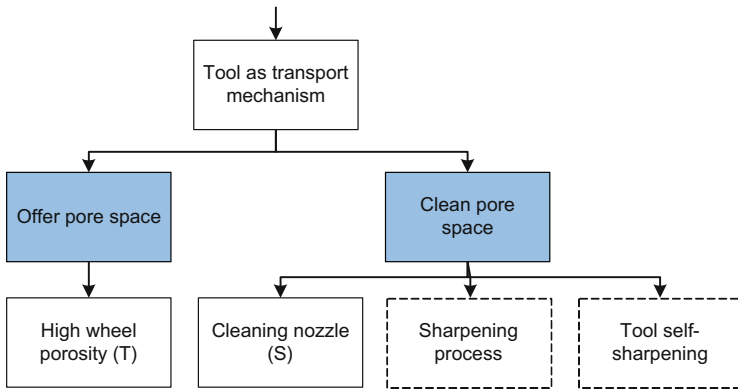


Fig. 7.16 Chip removal (diagram follows Fig. 7.12)

interaction between dressing tool and grinding tool. The machined workpiece volume between the dressing cycles defines the dressing intervals.

The grinding tool transports the generated chips (Fig. 7.16). On the one hand, pore space needs to be available, i.e. the design parameter is high wheel porosity. On the other hand, the pore space needs to be cleaned, which is done by a cleaning nozzle, the sharpening process, and/or self-sharpening of the tool.

7.3.2.3 Implications of the Track-Bound Principle

Having chosen the track-bound principle for force generation, the functional requirements arise to hold the workpiece, provide the cutting speed and feed of the grits, and reduce the mechanical impact that is not crucial for the cutting action (Fig. 7.17). The workpiece can be held by mechanical or magnetic clamping, or the centerless principle can be applied for cylindrical parts that are machined on their external circumference or the inner diameter (Fig. 7.17 left). In addition, deflections, bending of cylindrical workpieces, etc. have to be considered as sources of errors, so that additional counter-measures have to be taken [ROWE09].

The cutting speed results from the wheel spindle rotation and the grinding wheel diameter (Fig. 7.17 middle). The grit feed is generated by the tool axis movement and the process kinematics, such as face or circumference grinding, transverse or plunge cut grinding, external diameter, internal diameter, etc. (Fig. 7.17 right). Mechanical impact on the workpiece is a side effect of the chip formation and has to be minimized (Fig. 7.18). A low normal force per single grit and a small number of grit contacts both reduce the mechanical impact on the workpiece (Fig. 7.18). The normal single grit force is decreased by having a small load per grit and by changing the chip formation process to be more effective.

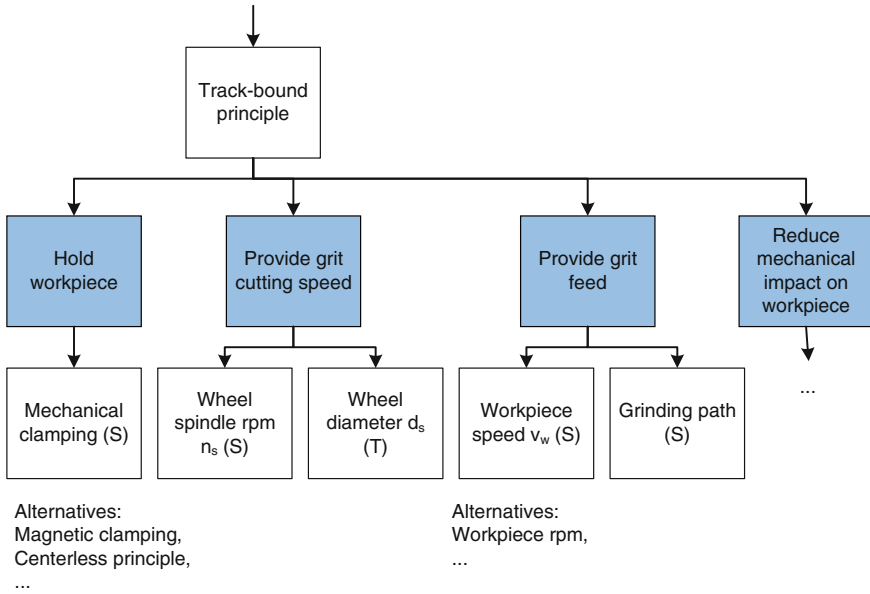


Fig. 7.17 Track-bound principle (diagram follows Fig. 7.12)

The maximum undeformed chip thickness, $h_{cu,max}$, is directly tied to the single grit load (Fig. 7.19). Chip thickness is related to statistical cutting edge density, C_{stat} , workpiece speed, v_w , grinding wheel speed, v_s , depth of cut, a_e , and equivalent grinding wheel diameter, d_{eq} (Eq. 7.8) [WERN71, TÖNS92]. Factors, k , α , β , γ , have to be found empirically, and Eq. 7.8 does not account for elastic and plastic material deformation. A common assumption is $\alpha = \beta = 1/3$, $\gamma = 1/6$, showing that the factor (a_e/d_{eq}) is of smaller significance than the other factors [WERN71]. A simplified approximation for the chip thickness is the equivalent chip thickness, h_{eq} (Eq. 7.9).

In reality, the real chip thickness is smaller than the maximum undeformed chip thickness [KLOC09, ROWE09]. This results from the elastic and plastic deformation effects overlaying the chip formation process (Fig. 7.20). The grit cutting depth, T_μ , is the grit engagement depth, at which chip formation starts. A high chip thickness increases the effectivity of the chip formation process, because the grit cutting depth T_μ is reached sooner. The same applies for the down-grinding mode in comparison to up-grinding and the use of a cooling lubricant with low lubrication properties to increase friction.

$$\text{Maximum undeformed chip thickness } h_{cu,max} \approx k \left(\frac{1}{C_{stat}} \right)^\alpha \left(\frac{v_w}{v_s} \right)^\beta \left(\frac{a_e}{d_{eq}} \right)^\gamma \quad (7.8)$$

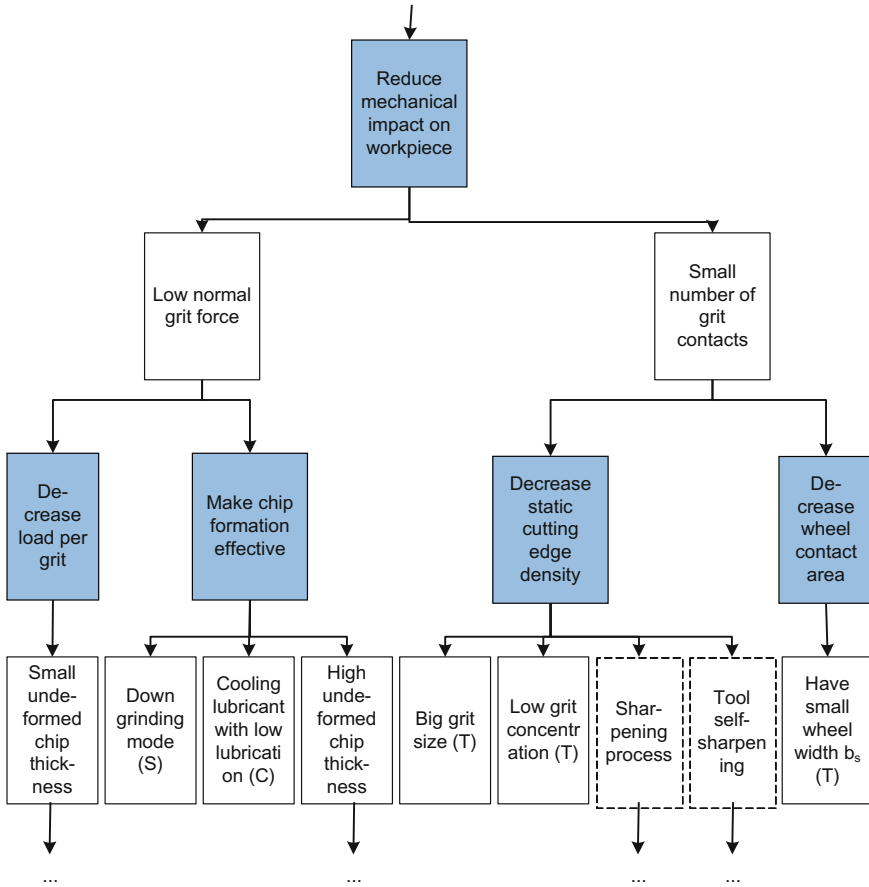


Fig. 7.18 Mechanical impact (diagram follows Fig. 7.17)

$$\text{Equivalent chip thickness } h_{cq} = \frac{Q'_w}{v_s} \tag{7.9}$$

- k constant depending on grinding wheel; e.g. $k = 0.695$ [WERN71]
- C_{Stat} static cutting edge density; e.g. $C_{stat} = 4420 \text{ mm}^{-3}$ for A46 [WERN71]
- κ half of the cutting edge angle; e.g. $\kappa = 82.4^\circ$ [WERN71]
- v_w workpiece speed
- v_s wheel speed
- a_e depth of cut
- d_{cq} equivalent grinding wheel diameter (Eqs. 6.15, 6.16 and 6.17)
- α, β, γ empirical coefficients

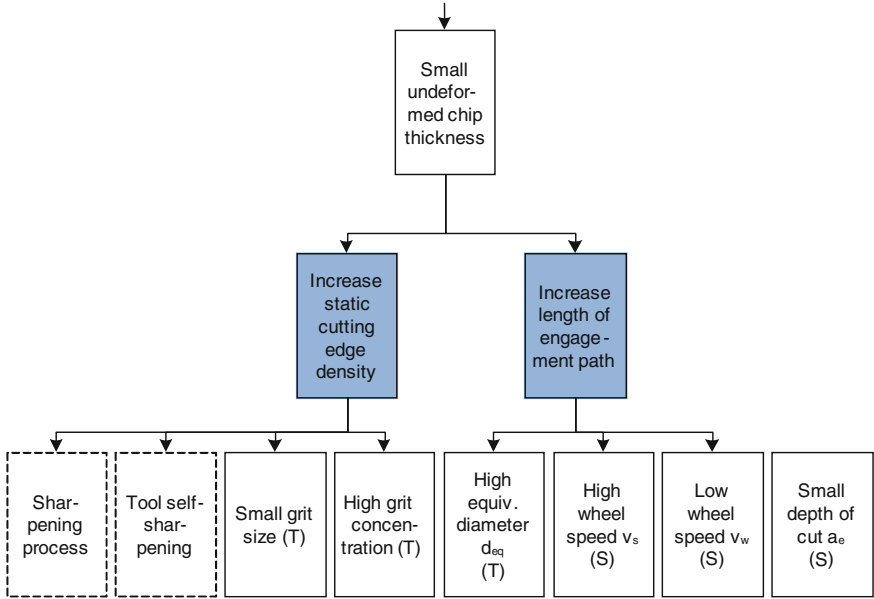


Fig. 7.19 Undeformed chip thickness

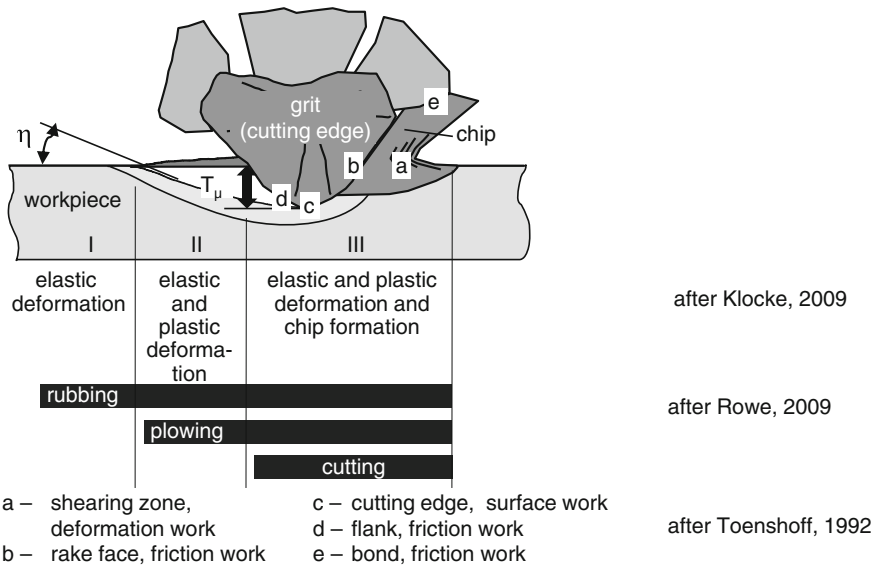


Fig. 7.20 Three phases of ductile chip formation [KLOC09] including the different contact types rubbing, plowing and cutting [ROWE09, TÖNS92], reprinted from [LINK12c] with permission from Elsevier

7.3.2.4 Functional Requirements of Controlling Workpiece Surface Pattern

The track-bound principle and use of abrasive grits in combination generate grooves and a pattern on the workpiece surface (Fig. 7.21). The pattern can be important for component function, e.g. in sealing systems where directionality of grinding grooves have to be avoided, or in engine cylinders where oil reservoirs are built. To get a random surface pattern, neither the grit engagement paths nor the grit pattern on the grinding tool should be regular. A statistic grit pattern on the tool serves the latter requirement. Engineered grit patterns [AURI03] or slotted wheels [UHLM10] have regular grit patterns, yet need higher care in process control to generate a random surface pattern (see Sect. 9.2 “Innovative and More Sustainable Tools”).

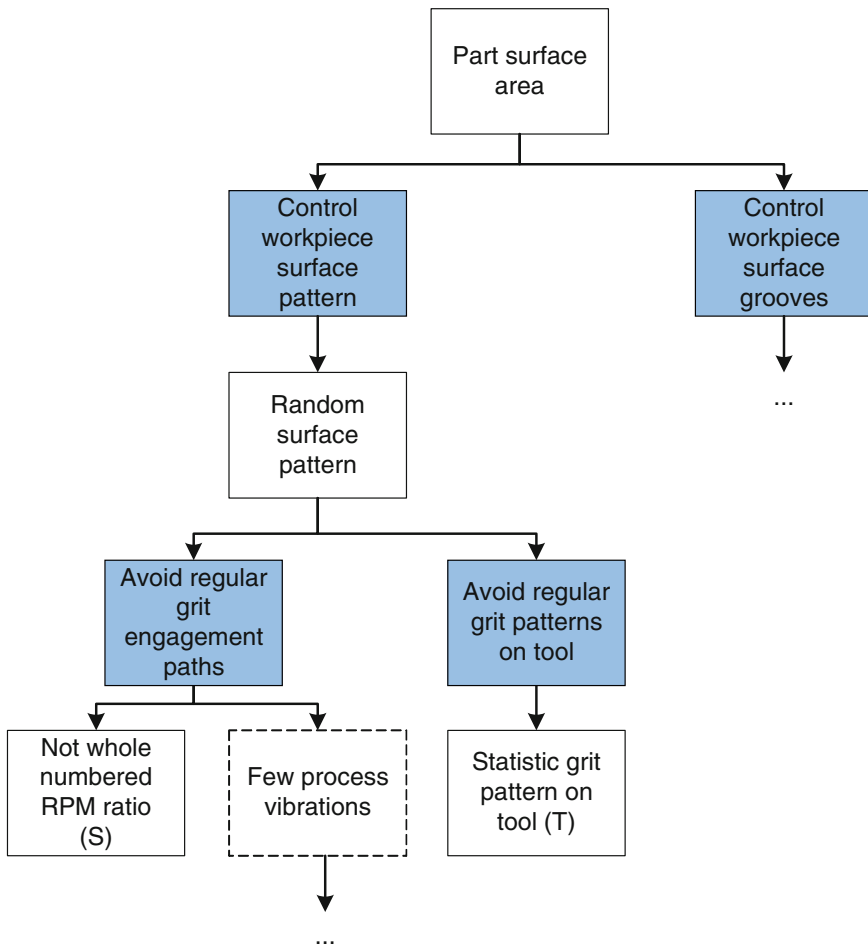


Fig. 7.21 Workpiece surface pattern (diagram follows Fig. 7.11)

The process kinematics defines how the abrasive grits engage the workpiece. Whole numbered RPM ratios and process vibrations lead to repeated surface pattern and should be avoided (Fig. 7.21). The 3D appearance of the surface pattern and its influence on components function offers a lot of potential for studies.

7.3.2.5 Functional Requirement of Controlling Workpiece Surface Grooves

The workpiece surface profile is defined by the generated surface grooves. A small roughness band needs shallow grooves and small chip thicknesses (Figs. 7.22 and 7.19). Shallow grooves can only be generated when both groove bottom shape and wheel deflection are controlled. The groove bottom is shallow for grits with large cutting edge radius and small depth of cut. Bond elasticity defines wheel deflection and groove generation [BORK92].

7.3.2.6 Functional Requirement of Reducing Heat Generation

Process heat is a dominant challenge in grinding technology and affects the part’s surface integrity. It is favorable that little heat is generated, existing heat is removed, and chemical reactions are suppressed to reduce the impact on surface integrity (Fig. 7.23).

Control of heat generation includes low heat per single grit interaction, few grit interactions per time, and short interaction time between workpiece and grinding tool. Heat generation per grit is very complex and includes heat generated by rubbing, plowing and cutting during all three phases of grit engagement (Fig. 7.20).

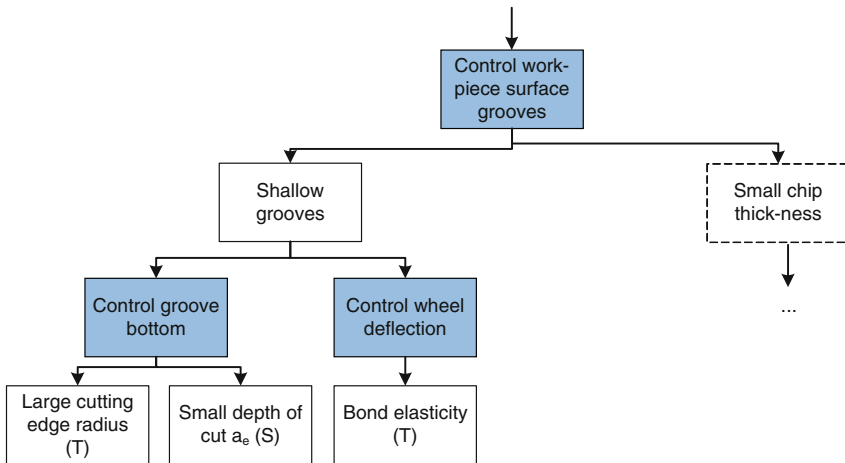


Fig. 7.22 Workpiece surface grooves (diagram follows Fig. 7.21)

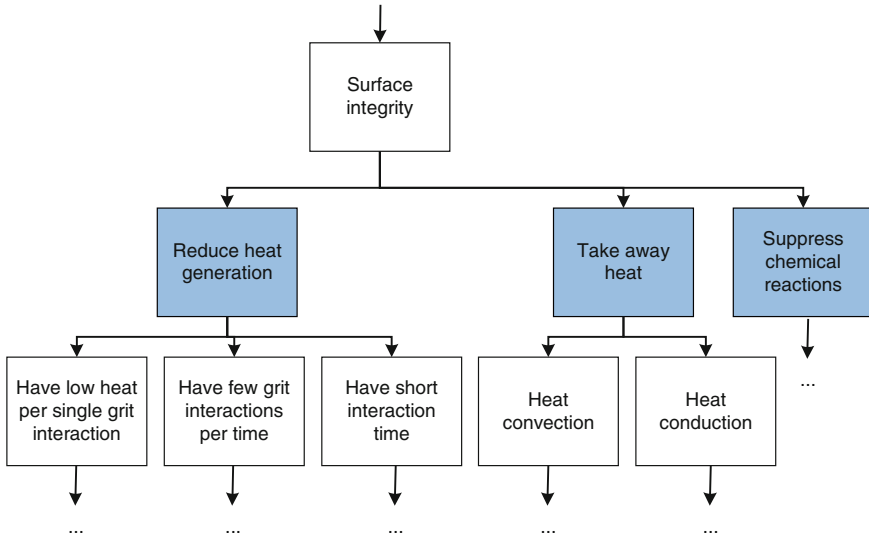


Fig. 7.23 Surface integrity (diagram follows Fig. 7.11)

Although Fig. 7.20 applies for ductile material, brittle material experiences similar chip formation phases, but cracks are induced and expanded in phases II and III and particles will break out rather than chips formed.

Sliding heat can be reduced by lubricants with high lubrication ability, a small contact area in normal direction, and short kinematic contact length, l_k (Fig. 7.24). The kinematic contact length, l_k , evolves from the contact arc and the grit engagement angle (Eq. 7.10). Malkin and Guo propose to obtain the sliding energy by measurements of the grit wear flat area [MALK08].

$$l_k = l_g \cdot \left| 1 - \frac{1}{q} \right| \tag{7.10}$$

- l_k kinematical contact length
- l_g geometrical contact length (Eq. 6.7)
- q speed ratio between v_s and v_w , positive for down-grinding, negative for up-grinding

There are only few examinations and models for the heat from plowing [ROWE09]. Contact conditions and shape of grit contact area seem to be most important.

Heat from cutting is produced at different shear zones within the single grit engagement (Fig. 7.20) [TÖNS92]. Shear zones are beneath the grit (c, d), at the grit rake face (b) as well as in the chip formation zone (a). The friction work between chip and tool bond (e) can be reduced by a higher grit protrusion (Fig. 7.25).

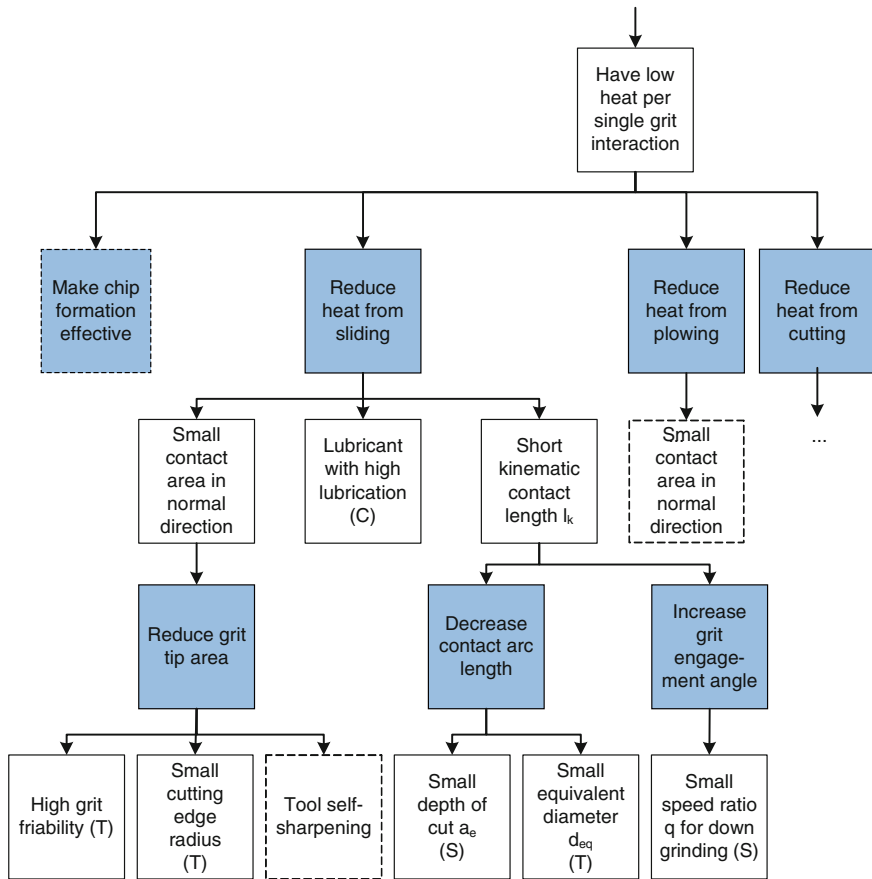


Fig. 7.24 Low heat per single grit interaction—sliding heat (diagram follows Fig. 7.23)

Rowe argues that shear energy at the shear plane (zone a) and at the rake face (zone b) add up to the total energy depending on the shear plane angle [ROWE09, p. 343 f., ROWE79]. A favorable shear plane angle near 45° exists with minimum shear energy. The mechanisms are not modeled. Qualitatively, the favorable shear plane angle has to regard grit shape and friction conditions. Furthermore, shear energy is reduced by a small shear strain rate, i.e. small grinding wheel speed, v_s , and by a small chip cross-sectional area, which can be achieved by a small undeformed chip thickness (Fig. 7.19).

The heat sources at zones b and d can be minimized by changing rake angle respectively clearance angle (Fig. 7.25). These strategies are derived from machining with defined cutting edges and can therefore only be applied if grit shape and orientation on the grinding tool are taken into account [KLOC11]. The heat at zones b, c, and d seem to have minor influence and a sensitivity analysis can indicate their relevance for process heat.

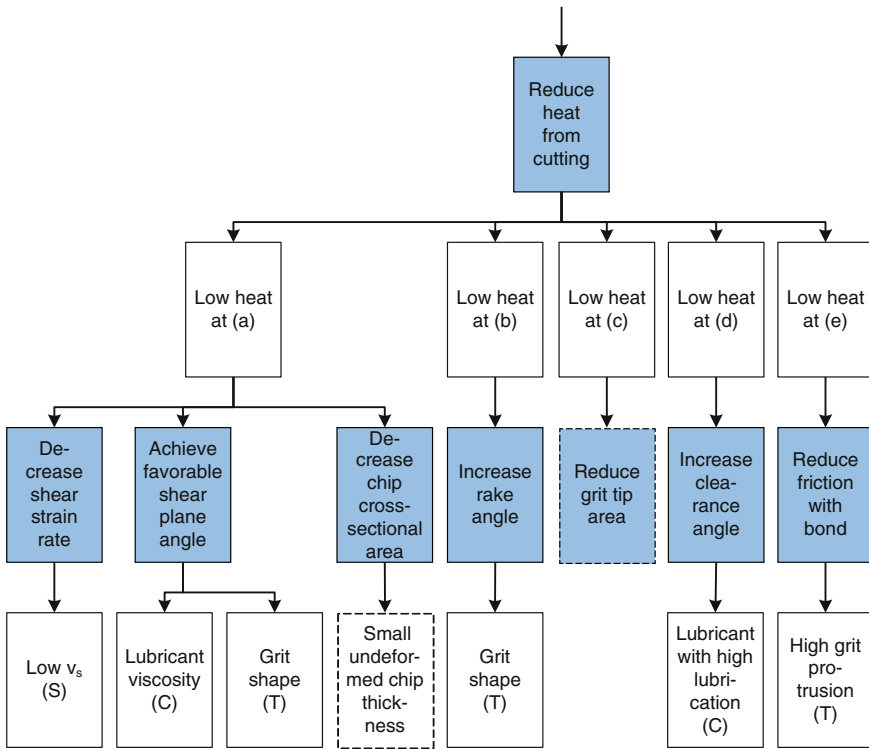


Fig. 7.25 Low heat per single grit interaction—cutting heat (diagram follows Fig. 7.24)

Few grit interactions per time express the second design parameter to serve the requirement of reduced heat generation during grinding (Figs. 7.23 and 7.26). On the one hand, the contact area between workpiece and tool has to be decreased, for example by a small wheel width, b_s (Fig. 7.26) [METZ86, 78]. One example for a small wheel width is the traverse grinding variant “Quick Point Grinding”.

On the other hand, the active cutting edge density should be minimal, for example by a low number of kinematic cutting edges. The kinematic cutting edges, N_{kin} , are the only ones from the overall static number of cutting edges, N_{stat} , that are exposed to the workpiece (see Sect. 6.2). Therefore, N_{kin} is influenced by N_{stat} , by process parameters, tool wear and grinding tool deflection (Fig. 7.26).

A short interaction time of workpiece and grinding wheel comes from increased heat source speed, which is the workpiece speed, v_w (Fig. 7.26).

7.3.2.7 Reducing Heat by Convection and Conduction

Heat removal includes all aspects of cooling and lubrication and has been researched a lot [HEIN09b]. The basic principles for heat removal are heat convection

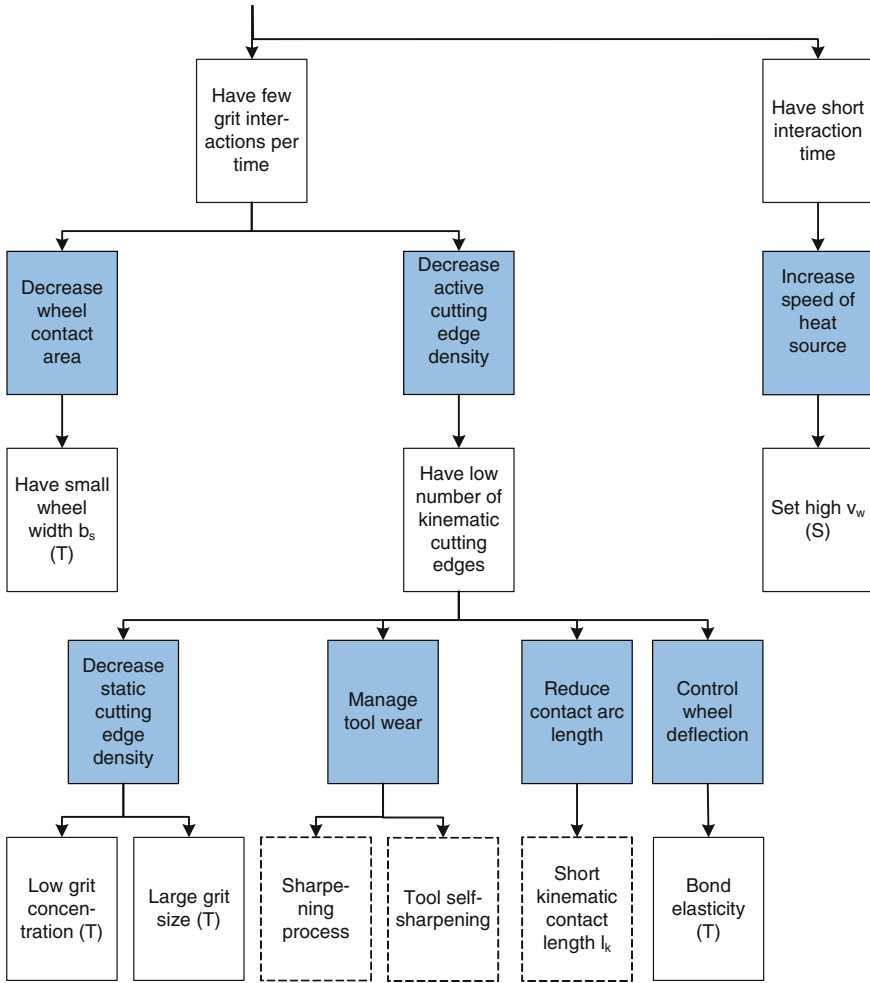


Fig. 7.26 Few interactions per time and short interaction time (diagram follows Fig. 7.23)

and heat conduction (Figs. 7.23, 7.27 and 7.28). It is commonly assumed, that all process energy is converted into the heat flux, q_f , during grinding (Eq. 7.6) [ROWE09, MALK08]. Heat convection takes place into fluids or air, even though convection into air is neglected in many considerations and cooling lubricant is most important for heat convection in grinding. The cooling lubricant must be present in the grinding zone and have a high heat transfer coefficient and high heat capacity (Fig. 7.27).

Equation 7.11 offers one approach to calculate the heat flux into the cooling lubricant, q_{cool} [ROWE09, p. 376]. The temperature before boiling, T_{max} , estimates the maximum energy flow into the fluid. The heat transfer coefficient, h_f , depends

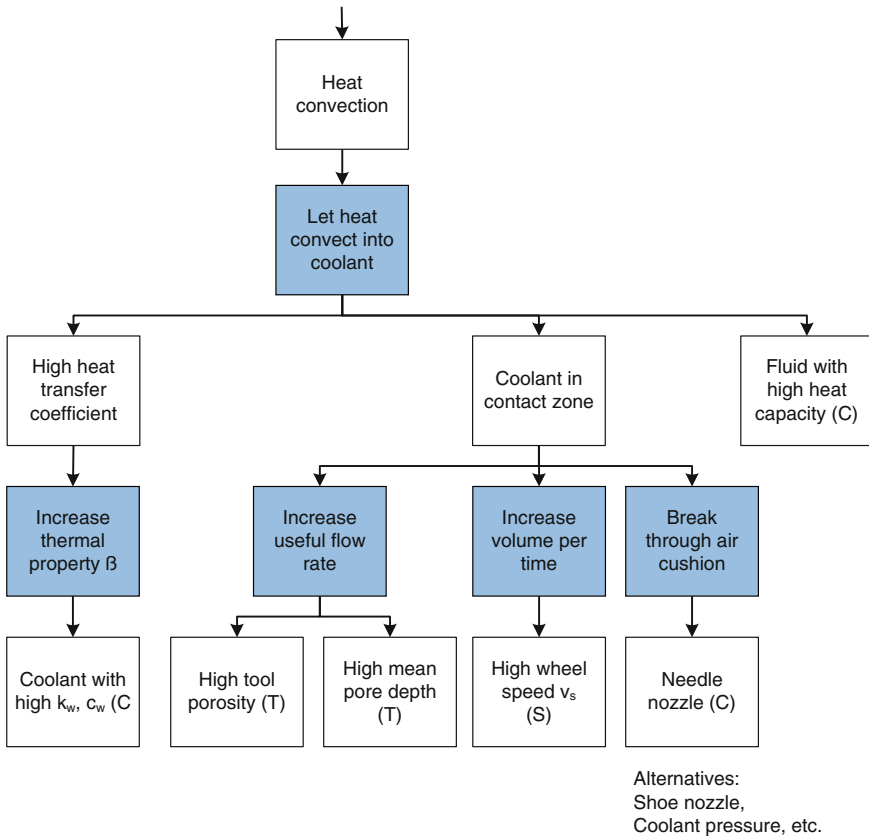


Fig. 7.27 Heat convection (diagram follows Fig. 7.23)

on the thermal properties of the fluid as well as on the contact arc length, l_c (Eqs. 7.12 and 7.13).

$$q_{cool} = \frac{2}{3} \cdot h_f \cdot T_{max} \tag{7.11}$$

$$h_f = \frac{3}{2} \cdot \beta_f \cdot \sqrt{\frac{v_s}{l_c}} \tag{7.12}$$

$$\beta_f = \sqrt{k_f \cdot \rho_f \cdot c_f} \tag{7.13}$$

- q_{cool} heat flux into the cooling lubricant
- h_f fluid convection coefficient
- T_{max} temperature before boiling

β_f	fluid thermal property
k_f	thermal conductivity
c_f	specific heat

Cooling lubricant can be brought into the contact zone by a high useful flow rate and high volume per time (Fig. 7.27). The air cushion around the rotating grinding wheel is particularly important for high grinding wheel speeds and can be broken by several supply systems, such as needle nozzles (Fig. 7.27).

The useful cooling lubricant flow, Q_u , is defined as flow volume through the contact zone of grinding tool and workpiece [MALK08]. Morgan et al. [MORG08] estimated the achievable useful flow rate based on wheel porosity, wheel speed and empirical factors.

$$Q_u = f \cdot h_{\text{pores}} \cdot b \cdot v_s \cdot \Phi \quad (7.14)$$

Q_u	useful cooling lubricant flow
f	factor based on measurement (approximately equal to 0.5)
h_{pores}	mean pore depth (roughly equal to mean grit size)
b	wheel width
v_s	wheel speed
Φ	porosity (typically 0.5 for a medium porous wheel)

Heat conduction happens into the grits, grinding wheel, and workpiece material (Eq. 7.6) (Fig. 7.28). Malkin and Guo [MALK08] defined the limit to the shear zone energy which can be carried away by the chips, q_{ch} , as the melting energy. Heat to the grinding wheel, q_{gw} , depends on the grinding wheel properties including grit, bond and structure characteristics. Wheel contact analysis and grain contact analysis are two approaches to estimate the partition ratio for q_{gw} [ROWE09]. Grit and bond conductivity should be high as well as grit coating conductivity (Fig. 7.28). In addition, grit and bond need high heat resistance to avoid damage.

Heat flux into the workpiece material, q_{wp} , is a main challenge for surface integrity, but forms an important transfer process especially for materials with high heat conductivity.

7.3.2.8 Functional Requirement to Suppress Chemical Reactions

Chemical reactions arise from the reactivity between the system components. Therefore, low chemical reactivity between all system components including grits, tool bonding, workpiece material, cooling lubricants and their additives is favored (Fig. 7.29). In addition, low mechanical pressure slows down chemical reactions as does low heat, which has been tackled earlier.

Brinksmeier and Wilke [BRIN04] gave case studies about chemical reactions within grinding technology. There is still big demand for research. The effect of

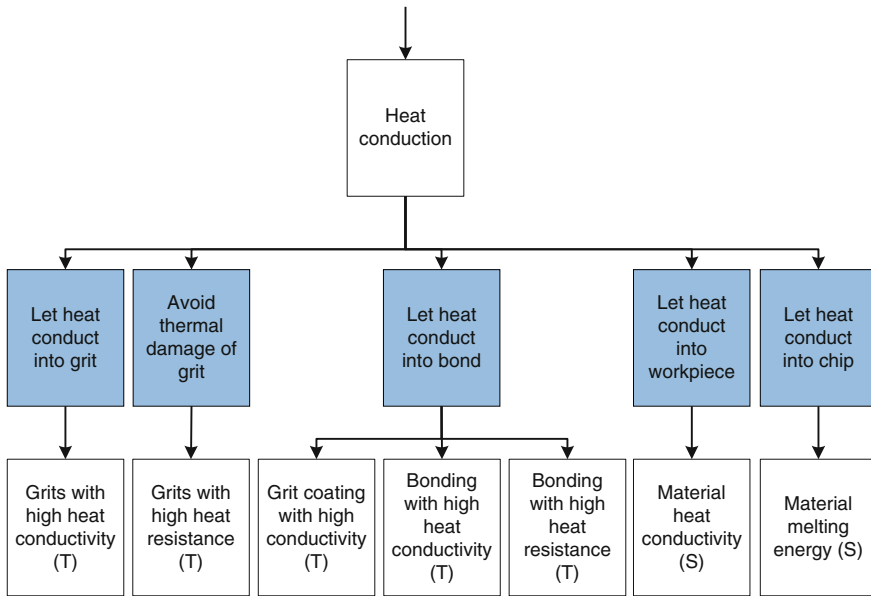


Fig. 7.28 Heat conduction (diagram follows Fig. 7.23)

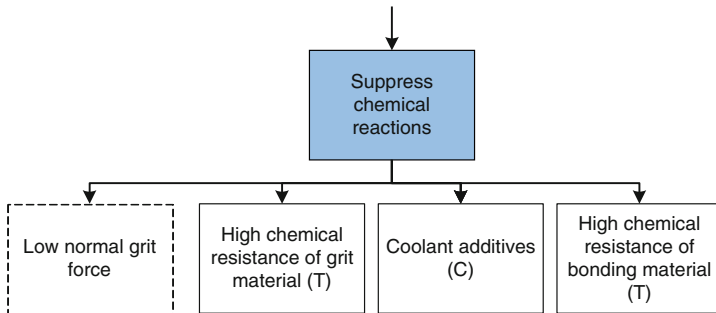


Fig. 7.29 Chemical reactions (diagram follows Fig. 7.23)

contact time between grits and workpiece needs to be discussed in further grinding models.

Depending on the process temperature, the mechanisms of cooling lubricant/part surface interaction change. At low temperatures, physisorption and chemisorption occur resulting in weakly linked sorption layers [BRIN00]. At higher processing temperatures, reactions between additives in the cooling lubricant and the part surface can take place and result in reaction layers on the workpiece [BRIN00].

In chip formation, many side effects overlay, such as heat generation, heat reduction, chemical reactions, mechanical load, and disturbances. Often these side

effects are tackled separately, although grinding is a complex superposition of all these physical effects. Mahdi and Zhang [MAHD00] examined, for example, how the temperature gradients, mechanical stresses and phase transformations affect residual stresses in grinding. Duscha et al. [DUSC11] used an FEM-approach to simulate phase transformation during grinding, adding residual stresses resulting from phase transformations. Brinksmeier et al. [BRIN03] investigated the phase transformation of steel during grind-hardening which involves multiple effects on surface integrity. Yet, very few models take the coupled interaction of the effects during chip formation into account [HEIN09b].

7.3.2.9 Functional Requirement of Being Cost-Effective

An important requirement is being cost-effective. For this, the time-dependent costs, scrap rate, tool costs and auxiliary costs need to be low (Fig. 7.30). Time-dependent costs come from the processing time and dressing time (Figs. 7.3, 7.4 and 7.31). Processing time can be reduced by a high material removal rate either by more effective chip formation at given process parameters or increased material removal rate.

Low scrap rate is achieved by monitored and increased process stability and regarding outer disturbances from the environment, in particular heating (Fig. 7.32). HVAC, sunlight, friction in machine tool elements, hydraulics, pumps systems, etc. heat the process from outside. Process vibrations can be reduced by smaller tool vibrations, lower system stiffness, less mechanical impact on the workpiece, and a sharp tool (Fig. 7.32).

Tool costs summarize grinding tool costs and dressing tool costs (Fig. 7.33). Tool wear during the grinding process needs to be minimized as well as the dressing frequency.

Dressing tool wear is induced by thermal and mechanical load (Fig. 7.34). Thermal load can be explained by friction processes and the dressing grit collision

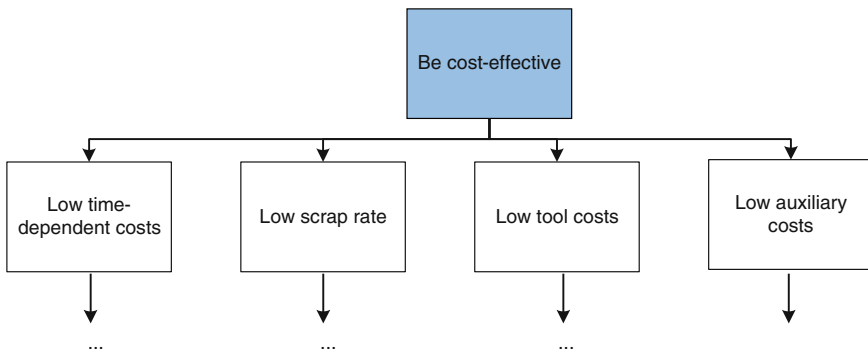


Fig. 7.30 Being cost-effective (diagram follows Fig. 7.11)

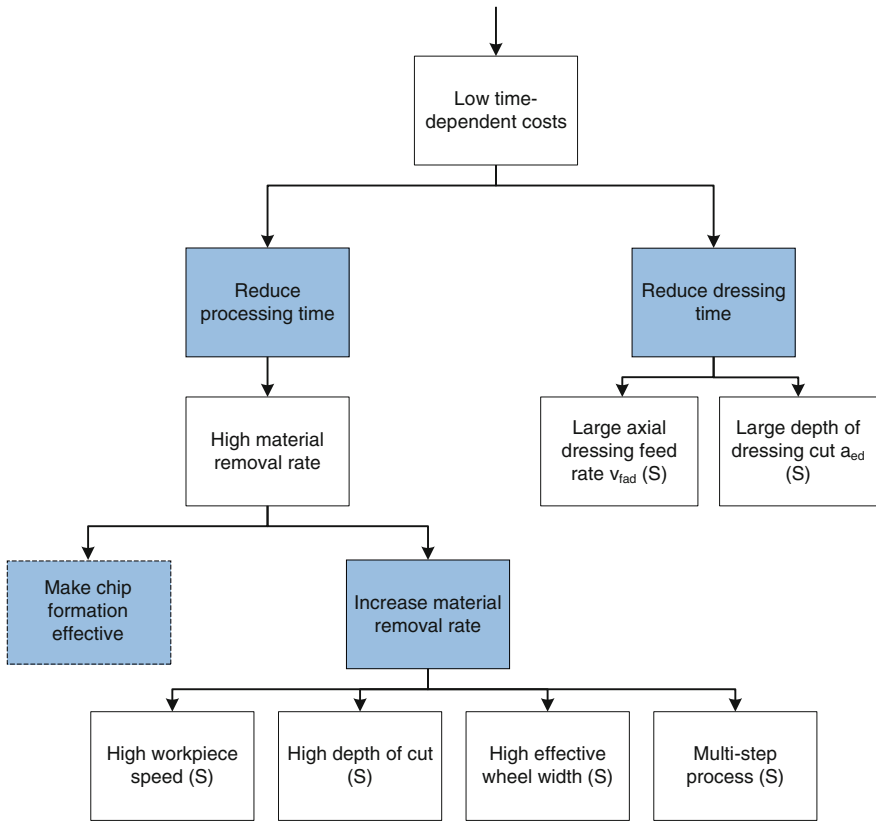


Fig. 7.31 Low time-dependent costs (diagram follows Fig. 7.30)

model [CINA95, LINK07]. Mechanical load arises from the single dressing grit forces, which is modeled through the dressing chip cross section [LINK07]. A dressing tool with higher wear resistance, e.g. by high quality diamond grits or a large diamond volume, withstands wear better (Fig. 7.34).

The most relevant auxiliary costs are the cooling lubricant costs (Fig. 7.35). They are impacted by the filtering system, exchange intervals, additives, maintenance, and cooling lubricant loss when fluid stays on the workpieces and chips.

7.3.3 Matrixes from Axiomatic Model

All discussed effects produce a complex grinding process model. This axiomatic model, however, is simplified and based on existing models. The main application is fine grinding of ductile material, leaving exemptions, special process variants and

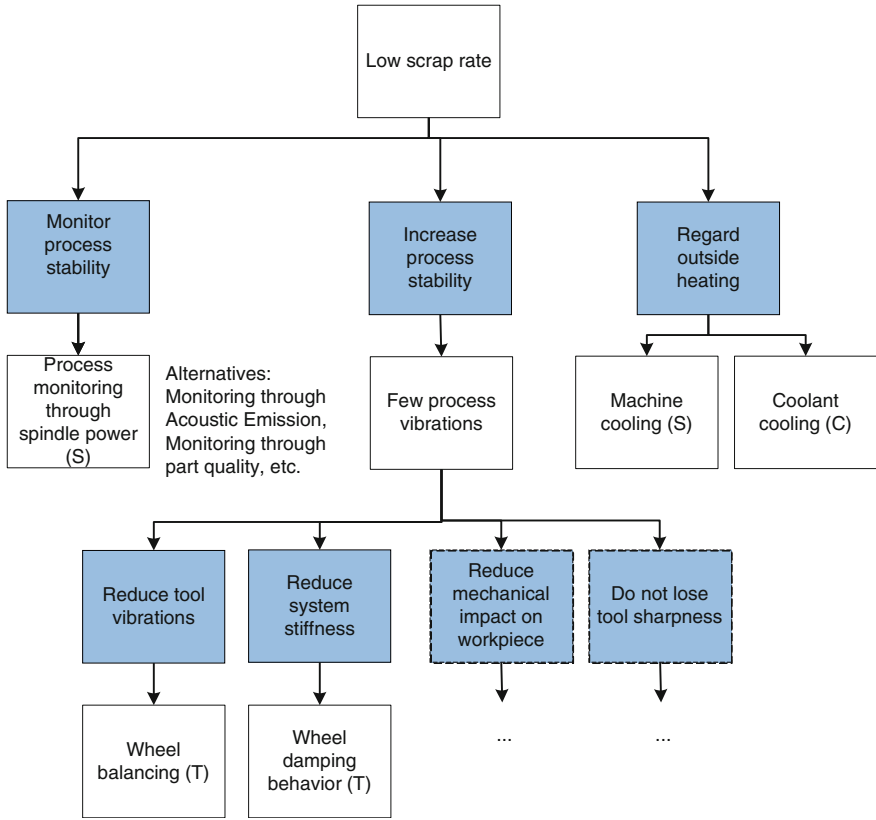


Fig. 7.32 Low scrap rate (diagram follows Fig. 7.30)

other applications open. Experimental data, sensitivity analyses and empirical data could enhance the axiomatic grinding process model a lot.

Relations between the functional requirements and design parameters can now be expressed through matrixes according to Eq. 7.7. Figure 7.36 shows the matrix for tool properties, Fig. 7.37 for the grinding system, and Fig. 7.38 for the cooling lubricant properties. A known interdependence is marked with “x”, an enlarging or positive effect of the parameter on the functional requirement on the left by “+”, a minimizing or negative effect by “-”, and a known bilateral effect by “±”. Equations are given where known and important. The contradictory dependencies would need sensibility analyses to determine the dominant trend.

The matrixes Figs. 7.36, 7.37 and 7.38 are not exhaustive. They do not display linear relationships, but rather general dependencies that have to be put into equations. For example, the functional requirement “Reduce mechanical impact on workpiece” is a function, but not a sum, of grit size, grit concentration, equivalent wheel diameter, wheel speed, workpiece speed, depth of cut (Eq. 7.15), and also grit friability, wheel width, grinding mode, and lubrication ability of the cooling

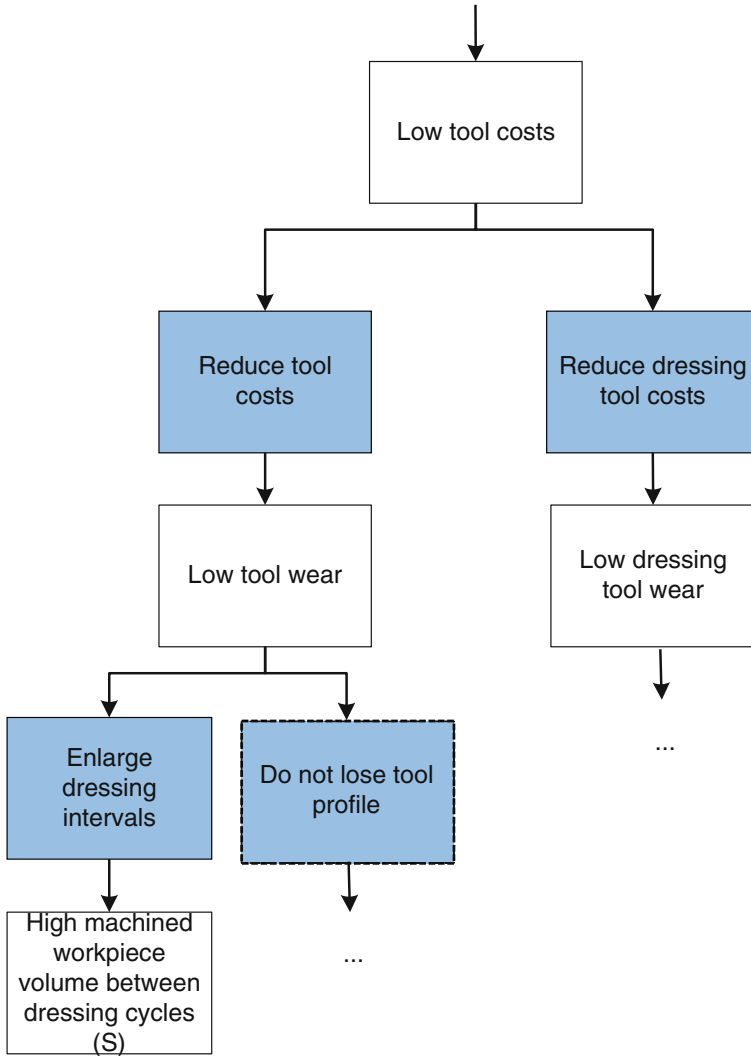


Fig. 7.33 Low tool costs (diagram follows Fig. 7.30)

lubricant. The impact of each of the parameters can be found by sensitivity analyses.

Reduce mechanical impact on workpiece

$$= f(\text{max. undeformed chip thickness (7.10), grit friability, wheel width, grinding mode, lubrication ability of the coolant})$$

(7.15)

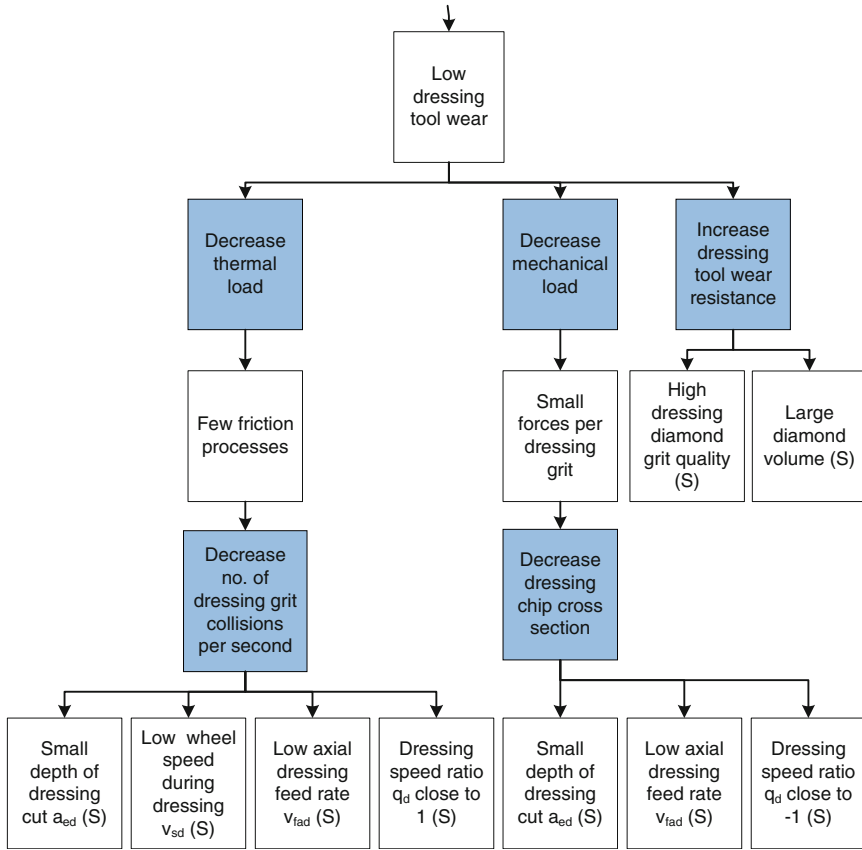


Fig. 7.34 Low dressing tool wear (diagram follows Fig. 7.33)

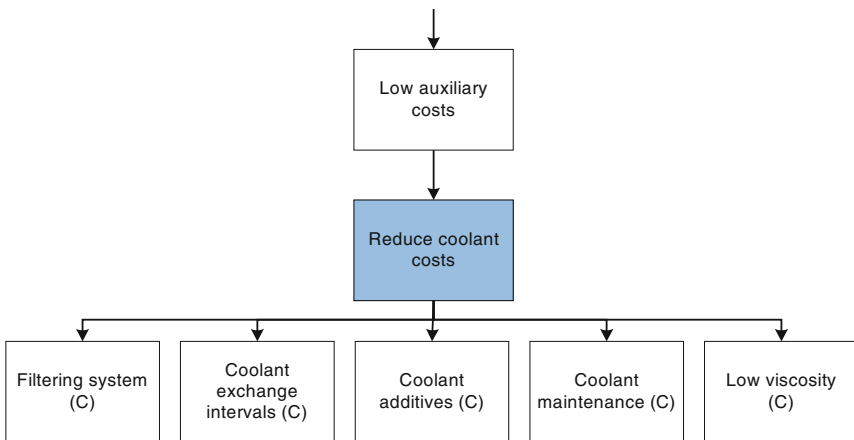


Fig. 7.35 Low auxiliary costs (diagram follows Fig. 7.30)

	Grit properties												Tool properties												Bond properties							
	Grit shape (T)	Grit cutting edge radius (T)	Grit size (T)	Grit heat conductivity (T)	Grit heat resistance (T)	Grit coating heat conductivity (T)	Grit hardness (T)	Grit friability (T)	Chemical resistance of grit materials (T)	Grit concentration (T)	Bond strength (T)	Grit pattern on tool (T)	Wheel porosity (T)	Mean pore depth (T)	Grit protrusion (T)	Eq. wheel diameter (T)	Wheel diameter (T)	Wheel width b _s (T)	Wheel damping behavior (T)	Wheel balancing (T)	Chemical resistance of bonding material (T)	Bond heat resistance (T)	Bond heat conductivity (T)	Bond elasticity (T)								
Make chip formation effective			+					+	-	x						-																
Do not lose tool sharpness					+		+	+		x	x	x																				
Transport chips										x		+																				
Reduce mechanical impact on workpiece			±				x		±	x						± (7-8)		.							x							
Control workpiece surface grooves		+	-						+	x	x					± (7-8)		.	x	x												
Control workpiece surface pattern			±		+		+	+	±	x	x					± (7-8)			x				+									
Take away heat				+	+							+	+										+									
Reduce heat generation	x		±				x		±	x	x			+		± (7-8), + (6-7)		.						x								
Suppress chemical reactions			±				x	x	±	x	x					± (7-8)					x											
Be cost-effective			±		+		x	+	±	x	x					±			x													

Fig. 7.36 Axiomatic matrix for the grinding tool (“+”: enlarging or positive effect, “-”: minimizing or negative effect, “±”: enlarging and minimizing effects are known, “x”: effect with unclear tendency)

	Cooling lubricant properties							Cooling lubricant supply				
	Lubrication ability (C)	Lubricant viscosity (C)	Degeneration stability (C)	Coolant properties k_w, c_w (C)	Heat capacity (C)	Cooling lubricant and additives (C)	Maintenance (C)	Needle nozzle (C)	Cleaning nozzle (C)	Coolant cooling (C)	Filtering system (C)	Coolant exchange intervals (C)
Make chip formation effective	-											
Do not lose tool sharpness												
Transport chips								+				
Reduce mechanical impact on workpiece	-											
Control workpiece surface grooves												
Control workpiece surface pattern	-											
Take away heat				+					x			
Reduce heat generation	±											
Suppress chemical reactions	-					x						
Be cost-effective	-	-				x	x				x	-

Fig. 7.38 Axiomatic matrix for the cooling lubricant (“+”: enlarging or positive effect, “-”: minimizing or negative effect, “±”: enlarging and minimizing effects are known, “x”: effect with unclear tendency)

The matrix can be helpful in clarifying how the system components and parameters in grinding are intertwined [LINK12c]. The functional requirements that are related most to process sustainability can be discussed with the matrix.

Sustainability needs to consider the four dimensions of technology, economics, environment, and society. Specific sustainability indicators cover these dimensions, depending on the framework and user. Figure 7.39 lists the most useful indicators for common grinding processes [LINK13]. These indicators are connected to functional requirements of the axiomatic grinding process model from Figs. 7.36, 7.37 and 7.38.

The matrixes Figs. 7.36, 7.37 and 7.38 highlight where research is needed on better process understanding and quantitative equations for grinding.

7.3.4 Case Study on Grit Size Choice

Grit size and grit size distribution affects tool manufacturing and tool use (see Sect. 2.8.1 “Grit Size”). Therefore, these grit characteristics provide a good case study on sustainability [LINK12c]. Grit size can be controlled by different standardized methods, such as sieving and sedimentation (Sect. 2.9.1 “Grit Size Selection”). The user might want to consider the three conventional pillars of sustainability plus the technological pillar. The costs of tool making is not included.

Figure 7.39 suggests looking into productivity and process stability for economic sustainability, which is affected by the functional requirements “Make chip formation effective” and “Be cost-effective”. Figure 7.36 shows that grit size has a positive effect on the effective chip removal and on high material removal rate, but grit size has a bipolar effect on cost-efficiency. The undeformed chip thickness increases with grit size (Eq. 7.8), leading to a more effective chip formation with an earlier cutting phase and shorter phases of rubbing and plowing (Fig. 7.20). The grit forces however increase with chip thickness leading to higher mechanical load, a less stable process, and higher scrap rate and costs (Fig. 7.32). These mechanisms are contrasting, but the more effective chip formation is mostly dominating so that economic sustainability is basically improved with bigger grits.

Environmental sustainability can be evaluated through energy intensity for example (Fig. 7.39). Bigger grits at constant grit concentration make chip formation more effective, i.e. less plowing and rubbing happens and chip formation consumes less processing energy per material volume removed.

Social sustainability is connected to labor intensity and therefore processing time (Fig. 7.39). A high material removal and effective chip formation coming from bigger grits as discussed both reduce processing time, hence improving social sustainability.

Technological sustainability includes surface integrity and roughness, which are affected by heat, chemical reactions, and grinding grooves. Bigger grit sizes have a mainly reducing effect on heat generated, although the inner material shearing at large chip thicknesses increases heat generated. Low process heat has a positive

	Indicators	Acquainted functional requirements
Technological sustainability	<ul style="list-style-type: none"> • Product quality, e.g. surface structure, surface integrity, and • Product performance and lifetime 	Suppress chemical reactions Reduce mechanical impact on workpiece Control workpiece surface grooves Control workpiece surface pattern Take away heat Reduce heat generation Do not loose tool sharpness ...
Economic sustainability	<ul style="list-style-type: none"> • Grinding costs, • Productivity, • Process stability and capability. 	Make chip formation effective Be cost-effective ...
Environmental sustainability	<ul style="list-style-type: none"> • Energy intensity, • Residuals intensity, • Intensity of pollutant releases to air. 	Suppress chemical reactions Do not lose tool profile Reduce heat generation Make chip formation effective ...
Social sustainability	<ul style="list-style-type: none"> • Labor intensity, • Worker noise level, • Hours of training and education per operator. 	Reduce processing time ...

Fig. 7.39 Useful sustainability indicators for grinding technology and acquainted functional requirements [after LINK13]

influence on surface integrity. However, big grits lower the surface quality due to the larger undeformed chip thickness. A high distribution of grit sizes might result in a surface profile with large variation of depth and low predictability due to outlier grits [LINK12c]. The technological sustainability is therefore affected controversially by grit size. The negative effect on surface roughness is often dominating over the positive impacts on the other three pillars of sustainability, leading the user to choose small grit sizes after all.

This case study showed how the axiomatic matrixes on grinding tool user highlight qualitative knowledge on grinding process functions and help to compare sustainability of different scenarios [LINK12c]. Quantitative equations would allow to calculate the benefits and impacts of the grinding system components.

Chapter 8

Sustainability Case Studies

8.1 Case Study on Conventional Abrasives Versus Superabrasives for Vitrified Bonded Tools

The user can decide between conventional tools with corundum or silicon carbide or superabrasive tools with diamond or cubic boron nitride. Not only do the tools have different performance profiles, but also different embodied energies, which is important for accounting manufacturing energy to products. Embodied energy is usually understood as the energy that must be used to create 1 kg of usable material measured in MJ/kg [ASHB09]. It is more than the theoretical energy and includes inefficiencies and losses in the processing systems and transport.

Comparing sustainability of conventional and superabrasive grinding tools is of high interest to the research community. However, there is no comprehensive information available on tool manufacturing. To foster understanding of energy use in grinding tool manufacturing, the following case study evaluates the energy for the manufacturing of two different types of vitrified bonded grinding wheel, with CBN and with corundum grits.

8.1.1 *Scope and Method*

This study focuses on vitrified grinding wheels with corundum and cubic boron nitride as abrasive grit material. The raw material production is not analyzed itself, but the available data on embodied energy is reviewed and included in the analysis. The boundaries are from the cradle (i.e. raw material mining and processing) to the tool manufacturer's outer gate (i.e. the finished grinding tool ready to be shipped to the customer) (Fig. 8.1). Tool manufacturing includes the steps of measuring, mixing, molding, pressing, drying, sintering, and finishing. Transport of material and tools is neglected, even though it might add substantially to the energy used for tool manufacturing. Furthermore, the subsequent use and disposal of the grinding

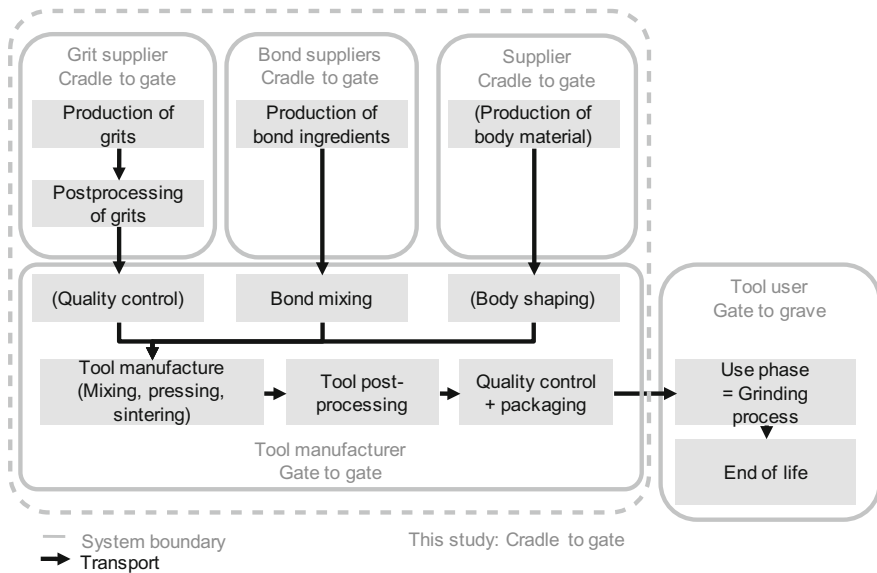


Fig. 8.1 Wheel life cycle and system boundaries for analysis

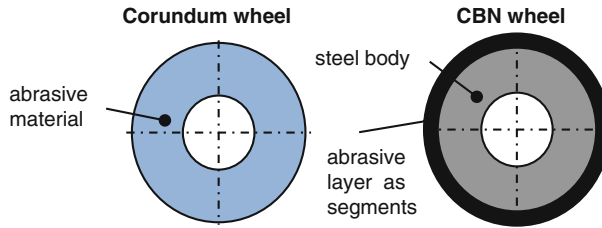
tools is not analyzed in detail, but the discussion highlights how the tools will be applied and disposed differently.

The functional unit of this study is a single grinding wheel. Figure 8.2 shows the respective grinding wheel designs. The conventional wheel is a monolithic cylinder; the superabrasive wheel consists of a steel body of low carbon tool steel and segments of the abrasive layer. The outer and inner diameters of both wheels are similar.

The results have to be evaluated carefully, because the grinding wheel specification includes various parameters such as abrasive grit type, mean grit size or mesh size, bond type, structure, and effective hardness. Abrasive tools are often adapted to a special application, e.g. high porosity for high material removal processes, CBN for precision grinding of hardened steel, soft bond for internal grinding, etc. Therefore, the comparison of different tools without regarding the application is difficult and not always reasonable. However, this study regards a use case where conventional or superabrasive wheels are interchangeable. For example, in a gear shaft grinding process, vitrified bonded corundum wheels or vitrified bonded CBN wheels can be used. The necessary change of process parameters such as wheel speed, machine periphery or coolant have to be considered.

8.1.2 Energy of Raw Materials

Manufacturing of the abrasives corundum and CBN is described in Chap. 2 “Abrasives”. The energy consumed in their primary production can be estimated



Grinding wheel width	20 mm	20 mm
Outer diameter	400 mm	400 mm
Inner diameter	200 mm	200 mm
Segment length	-	31.4 mm
Segment height	-	5 mm
Number of segments	-	40

Fig. 8.2 Examined grinding wheels

with a maximum value of 54.7 MJ/kg for alumina (99.95 % purity) and a maximum of 133 MJ/kg for HBN (Table 2.9) [GRAN12]. HBN is the basic raw material to produce CBN. Expert interviews indicate that the synthesis of CBN from HBN consumes presumably much less energy than the initial HBN production, so the energy values for HBN are taken as estimation for CBN in this study.

Table 8.1 shows the composition of a representative vitrified bond including the proportion of ingredients within the bond, densities, and embodied energies from raw material processing. Here the bond ingredients are not added as frits, which would lead to additional embodied energy, because frits have additional pre-processing steps (see Sect. 3.2.2 “Manufacturing of Vitrified Bonds”). In industry, the bond composition can be adjusted precisely to the abrasive type, desired wheel properties, expertise of the particular manufacturer, etc. Table 8.1 leads to an assumed embodied energy of 43.3–54 MJ/kg for the bonding mixture. Table 3.5 gives more information on environmental and health properties of critical bond ingredients.

8.1.3 Manufacturing Energy of a Vitrified Bond

Vitrified bonded tools are manufactured through mixing of the components, molding, pressing, sintering, pre-processing, and quality control (see Sect. 3.2 “Vitrified Bonds”). This study leaves out the embodied energy in the tooling equipment and assumes that a sufficiently large number of grinding wheels are

Table 8.1 Bond ingredients for a representative bond

Bond ingredient [BOTS05]	Formula	Proportion in bond (w%) [BOTS05]	Density (g/cm ³) [GRAN12, GEST12]	Embodied energy (MJ/kg) [GRAN12]
Silicon oxide	SiO ₂	56.88	2.65	37.4–41.4
Boron oxide	B ₂ O ₃	16.61	2.46	Estimated 50–75
Aluminum oxide	Al ₂ O ₃	10.01	3.94	49.5–54.7
Calcium oxide	CaO	8.14	3.37	Estimated 50–75
Sodium oxide	Na ₂ O	4.62	2.27	Estimated 50–75
Potassium oxide	K ₂ O	3.52	2.32	Estimated 50–75
Magnesium oxide	MgO	0.22	3.58	120–133

Table 8.2 Volumetric structural composition of the grinding wheels

	Corundum wheel (V%)	CBN wheel (V%)
Bond volume	15	30
Grit volume	55	45
Pore volume	30	25

produced, so that the equipment accounts for a negligible amount of embodied energy per grinding wheel. The proportion of grit, bond and pore volume defines the structure and hardness of a grinding tool. Close to industrial practice, this study assumes the structural compositions as in Table 8.2.

The raw materials need to be mixed and pressed before the actual sintering process can take place. For the analysis of the mixing energy two representative mixing machines were chosen. The total amount of raw material for the production of a conventional grinding wheel greatly differs from the amount used for superabrasives. Table 8.3 provides basic information for each mixer and possible production rates. The larger mixer has a maximum capacity of material for 26 conventional grinding wheels whereas the small mixer can contain material for the abrasive layer of 15 superabrasive wheels.

Table 8.3 Mixer characteristics and energy consumption [WAB09]

	Corundum wheel	CBN wheel
Volume	50 l	2 l
Material capacity	5–26 wheels	2–15 wheels
Power	1.1 kW	0.18 kW
Mixing time	1 h	1 h
Total mixing energy (power over time)	3.96 MJ	0.648 MJ
Mixing energy per grinding wheel (at max. capacity)	0.152 MJ	0.0432 MJ

Table 8.4 Molding press characteristics and energy consumption, adapted from [SCHT11]

	Corundum wheel	CBN wheel
Table size	710 × 800 mm	400 × 400 mm
Plunger size	500 × 630 mm	320 × 320 mm
Max. press capacity	2500 kN	125 kN
Power	22 kW	4 kW
Molding time	5 min	5 min
Molding and pressing energy per grinding wheel	6.60 MJ	1.20 MJ

The total mixing time can be up to one hour in which the material is mixed by a three-dimensional movement in a sealed chamber. An advantage of this method is that no potentially hazardous dust can exhaust during the mixing process. Table 8.3 gives the consumed energy for the mixing time of 1 h in total and per grinding wheel. The overall energy consumption for the mixing of one grinding wheel is 0.152 MJ for the conventional type and 0.0432 MJ for the superabrasive. In the case that the wheels are produced in smaller batches, the mixing energy per wheel will be higher.

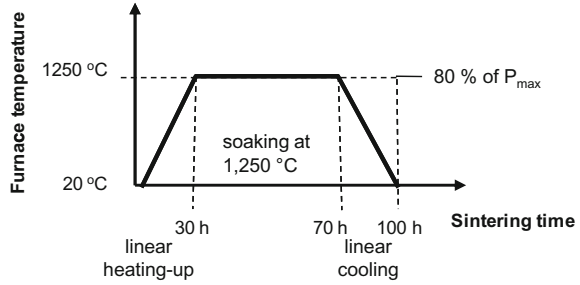
In the next step, the homogenous tool mixture needs to be molded into the appropriate form. To achieve a certain porosity, a preselected pressure is applied to the mixture in the mold until the mixture reaches a predefined volume. The pressure depends on the mixture itself, its volume, and the desired porosity of the final abrasive layer. The segments for a superabrasive grinding wheel require a comparably lower pressure and are sometimes even molded manually. In contrast, the compressive force for a complete vitrified bonded grinding wheel can range from 500 up to 45,000 kN. For this study, two hydraulic single column presses were selected according to Table 8.4. Selecting a molding time of 5 min for both grinding wheels results in total molding energy of 6.60 MJ for a conventional grinding wheel and 1.20 MJ for the segments on a superabrasive wheel.

For the sintering process, two example industrial furnaces are chosen with the same maximum temperature of 1600 °C, but different chamber sizes (Table 8.5).

Table 8.5 Furnace data and consumed energy during sintering, adapted from [NABE12]

	Corundum wheel	CBN wheel
Dimensions of working chamber	500 mm × 550 mm × 550 mm	150 mm × 150 mm × 150 mm
Segments produced per cycle	–	360
Max. number of wheels produced per cycle	22	9
Max. furnace power P_{\max}	21.0 kJ/s	5.2 kJ/s
Max. temperature	1600 °C	1600 °C
Sintering temperature	1250 °C	1250 °C
Sintering time	100 h	100 h
Consumed energy for one sintering process	4162.62 MJ	1030.77 MJ
Consumed sintering energy for one wheel (at max. capacity)	189.21 MJ	114.53 MJ

Fig. 8.3 Sintering temperature profile



The CBN segments are sintered in a smaller furnace. A total amount of 22 conventional wheels can be stacked including a 5 mm thick spacer between each layer in the larger furnace. The smaller furnace holds 15 layers of superabrasive material segments. Each layer consists of 24 individual segments. In total, an amount of 360 segments can be stacked in the small furnace. This is enough material for nine superabrasive grinding wheels.

Both furnaces feature a maximum temperature of 1600 °C at the maximum heating power, P_{max} . As the sintering process requires a lower sintering temperature of 1250 °C, the maximum sintering power is only 80 % of P_{max} . The sintering temperature profile in Fig. 8.3 left is representative and allows for calculating the sintering energy for both grinding tools. In the first 30 h of the heating cycle the furnaces, containing the abrasive material are heated-up linearly from room temperature to the sintering temperature of 1250 °C. The wheels are then soaked at this sintering temperature for 40 about hours. After the soaking period, the grinding wheels and segments are cooled down linearly to room temperature in about 30 h. The same heating cycle applies to both wheel type and segments, because sintering temperature and time does not depend on the volume of the sintered material, but on the material and chemical reactions.

For simplification, it is assumed that the power consumption runs linearly to the temperature. The total consumed energy during the sintering process is the power over time. For the large furnace with conventional grinding wheels, energy accounts to 4162.62 MJ, leading to an energy consumption of 189.21 MJ for one conventional grinding wheel. The smaller furnace uses 1030.77 MJ, which results in 114.53 MJ for the segments needed for one superabrasive grinding wheel.

8.1.4 Manufacturing Energy of the Steel Body for Superabrasive Wheels

This case study assumes that the body of the superabrasive wheel is made of tempered low alloy steel 42CrMo4 (oil quenched). This steel offers a high strength along with good durability and advantageous thermal characteristics.

First, the steel is cast into a round steel bar of a diameter of 394 mm. Then the bar is forged and rough rolled. A sawing process follows in which blanks of 25 mm

Table 8.6 Material and machining properties for tempered 42CrMo4 [GRAN12]

Density	7.8 g/cm ³
Embodied energy of cast material per mass	0.0288–0.0319 MJ/g
Rough rolling and forging energy per mass	0.0056–0.0061 MJ/g
Max. casting energy for blank with a width of 30 mm	910.10 MJ
Max. rolling energy	174.89 MJ

Table 8.7 Sawing process on a representative band saw [MASC12]

Power	110 kW
Sawing blade width	5 mm
Machining time for blank with a diameter of 394 mm	160 s
Sawing energy	17.60 MJ

thickness are produced. Because the sawing blade (5 mm width) produces waste, the casting energy and rolling energy has to be calculated for blanks with 30 mm thickness. Table 8.6 shows the respective energies for casting and rolling. The sawing process can be estimated with the values in Table 8.7 to account for a maximum energy of 17.6 MJ per steel body. This is an upper boundary for a not optimized sawing process.

The steel cylinders are then machined to the desired final shape through different turning processes. With coarse machining the outer diameter of 394 mm is reduced to 390.2 mm, the body width is reduced from 25 to 20.2 mm, and an inner hole is produced with a diameter of 199.8 mm. With the specific machining energies from Table 8.8 the coarse machining energy accounts to 6.10 MJ. The final fine machining operations reduce the outer diameter to 390 mm, the body width to 20 mm, and opens the inner diameter to 200 mm, resulting in fine machining energy of 1.54 MJ. The CBN segments are then glued to the steel body, but the gluing energy is neglected. Material data and energy data for rough rolling, coarse machining, and fine machining are taken from a database [GRAN12].

8.1.5 Embodied Energy in Grinding Tools

Mixing, pressing and finishing energy are negligible in comparison to the raw processing and sintering energies. All relevant energies for both grinding wheels are summed up in Fig. 8.4. The corundum wheel has only around 36 % of the embodied energy of a CBN grinding wheel of similar dimensions (Fig. 8.4). Then main energy proportion, however, lies in the steel body of CBN wheels.

Nevertheless, CBN grits have much higher wear resistance and the tool body can be re-used. The maximum useful abrasive volume in Table 8.9 depends on stability

Table 8.8 Machining properties for tempered 42CrMo4 [GRAN12]

Coarse machining energy per mass	0.0013–0.0014 MJ/g
Fine machining energy per mass	0.0084–0.0093 MJ/g
Coarse machining energy	6.10 MJ
Fine machining energy	1.54 MJ

aspects, clamping setup, and number of spindle revolutions. Here it is assumed that a diameter of 250 mm is the limit for the conventional grinding wheel. For the superabrasive wheel, it is assumed that the segments can be used down to 1 mm in thickness before they start to lose their stability and begin to crumble away. This leads to a minimum diameter of 392 mm.

With the G-ratios in Table 8.9, the CBN wheel in this case study can produce 13 times more workpieces than the conventional wheel, so that the energy per workpiece volume is only 1.3 J/mm³ for the CBN tool compared to 5.9 J/mm³ for the corundum wheel (Table 8.9). With a tool body re-use of five times, the embodied energy even decreases to only 0.4 J/mm³ for the CBN tool, which is about 7 % of the embodied energy per workpiece volume of the corundum wheel.

Yet there is more to consider. Abrasive tools are often adapted to a special application, e.g. high porosity for high material removal processes, CBN for

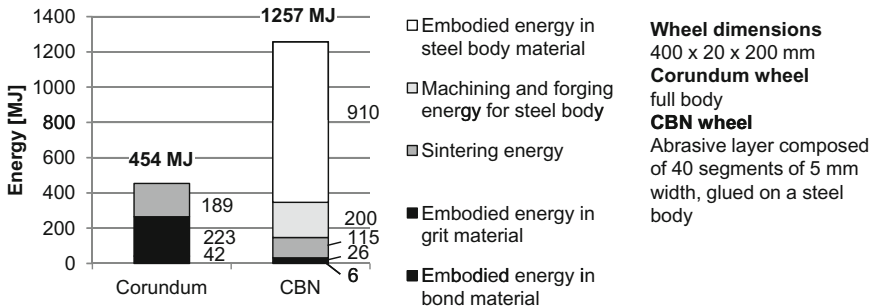


Fig. 8.4 Results for grinding tool manufacturing energy (upper boundary)

Table 8.9 Embodied tool energy per workpiece volume

	Corundum wheel	CBN wheel
Max. useful volume (mm ³)	1,531,526.40	99,525.70
Max. G-ratio when grinding steel [JACK11, HELLO5a]	50	10,000
Max. workpiece volume per wheel (mm ³)	76,576,320	995,257,000
Embodied energy per wheel (MJ)	454	1257
Embodied energy per workpiece volume in (J/mm³)	ca. 5.9	ca. 1.3
Embodied energy per workpiece volume in (J/mm³) when steel body is re-used five times		ca. 0.4

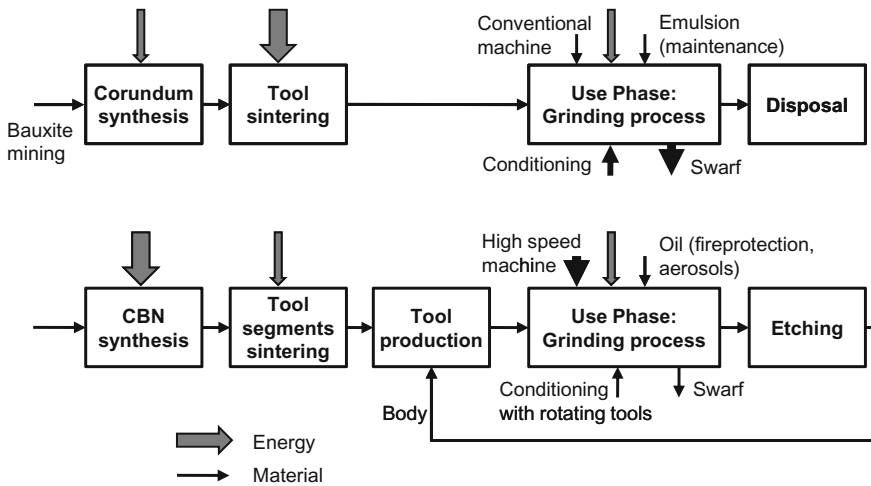


Fig. 8.5 Wheel life cycle with qualitative resource streams

precision grinding of hardened steel, soft bond for internal grinding, etc. Therefore, the comparison of different tools without regarding the application is difficult and not always reasonable. Moreover, the applications of superabrasive and conventional wheels differ in terms of machine tool, coolant supply, dressing, machine periphery, etc. (Fig. 8.5).

Superabrasives are in particular highly wear resistant in combination with high grinding wheel speeds. However, choosing superabrasives as grinding tool material should follow a thorough evaluation of the higher tool costs and the requirements on machine tool and cooling lubricant supply [LINK12b]. Further discussions touch the following aspects:

- **Flexibility**—In small or single batch production it is often required to use an abrasive tool with several effective surface roughnesses or even different profiles. For this, conventional tools are superior against superabrasives because of their better dressability and lower costs. New conventional tool systems with sol-gel corundum even allow to be used at high cutting speeds with the according advantages [KLOC03].
- **Machine park**—Often the high efficiency of superabrasives is only emerging from high cutting speeds. High-speed applications hold the advantage of small chip thicknesses resulting in tight workpiece form tolerances and high surface quality or high productivity. However, the complex machine setup needed (spindle power, encapsulation, more complex cooling lubricant system, etc.) might dissolve the technological advantages.
- **Tool costs**—Superabrasive tools are commonly more expensive than conventional tools, so that their economic efficiency is focussed on larger scale production [KLOC03].

The embodied energy of a product can vary along its life time depending on the intensity of usage and end of life stages [KARA10]. A manufacturer can manage the embodied energy from cradle-to-factory gate better than the users because the usage behavior and maintenance may vary [KARA10].

Kara and Manmek [KARA10] reviewed the embodied energy of composite materials in a cradle-to-gate analysis and found location of the suppliers was a significant factor for embodied energy. The embodied energy could be reduced considerably by carefully selecting local suppliers and by using rail or water transportation in the case of high quantities of raw materials and long distances.

8.2 Case Study on Comparing Hard Turning and Grinding

Araujo and Oliveira [ARAU12] compared the sustainability of hard turning and grinding based on 29 sustainability indicators in a case study. They chose five social indicators for the comparison:

- labor relations: hourly wages,
- health and safety: number of occupational accidents, noise level, operator risk level,
- training and education: average number of hours of training per operator.

From their data, Araujo and Oliveira [ARAU12] found that the grinder earns higher salary and gets more hours of training and education, but health and safety indicators were worse (higher noise level, more accidents and higher operator risk per accident). In particular, grinding has a potential for more severe accidents if the rotating grinding tools get damaged [ARAU12].

The overall sustainability assessment of hard turning versus grinding can be done considering different scenarios, weighting the criteria differently. When the environmental and social dimensions grow in relevance, hard turning has an advantage because of lower specific energy per unit of material processed. The economic performance of grinding appears to be superior to turning. [ARAU12]

8.3 Leveraging Abrasive Machining

Leveraging is a term known in financial discussions and describes employing resources in such a way as to insure a larger return on the effort than might otherwise be realized [DORN11]. One example is using higher efforts to improve the machining tolerances of an aircraft airframe and gaining high savings in fuel during the life time of the produced airplane [DORN11]. Dornfeld [DORN11] points out that manufacturing-driven improvements are indeed responsible for substantial environmental impact reductions. Leveraging is critical for abrasive machining since it is often decisive for product function [AURI13].

8.3.1 Case Study on Speed-Stroke Grinding with High Grinding Wheel Speeds

Speed-stroke grinding is surface pendulum grinding with increased table speeds up to $v_w = 200$ m/min. Advantages arise from the changing active chip formation mechanisms [INAS88, ZEPP05]. Chips get shorter and thicker, which accounts for a more effective chip formation. The specific material removal rate, Q'_w , results from depth of cut, a_e , and workpiece speed, v_w (Eq. 8.1). Increasing the material removal rate by the workpiece speed v_w affects the maximum undeformed chip thickness stronger than the depth of cut a_e [DUSC12].

$$Q'_w = a_e \cdot v_w \quad (8.1)$$

a_e depth of cut

v_w workpiece speed

The total power consumed by a machine tool sums up from idle power of spindles, axes, and periphery, and the processing power to accomplish the chip formation. As the specific grinding energy accounts for a minor part of the total energy consumed by the machine tool, the grinding time reduction by a higher table speed facilitates higher energy efficiency [DUSC12].

CBN grinding tools have higher wear resistance than conventional grinding tools resulting in reduced waste. However, due to the higher thermal conductivity, positive compressive stresses can be added to the workpiece surface. Because of the higher price and the needed high spindle power finding the proper process window is crucial for a sustainable usage of CBN tools [LINK11, DUSC12].

Speed stroke grinding of bearing steel with CBN grinding wheels can produce lower tensile stresses than other grinding variants [DUSC12]. These surface conditions are favorable for low crack propagation in rolling contacts. The product life for rolling contact or cyclic load applications can be prolonged through speed-stroke grinding, which would result in products with lower overall environmental impact [DUSC12].

8.3.2 Leveraging Example for Gear Grinding

The use phase rather than the manufacturing phase of most consumer products dominates the environmental impacts [ASHB09]. The case study of an automotive manual transmission drivetrain exemplifies how higher manufacturing efforts can reduce the overall environmental impact [HELU11].

The automotive powertrain consists of the engine, transmission, and drivetrain (drive shaft, differentials and drive wheels). Gears are functional elements in the transmission. Several abrasive processes exist for gear finishing [KARP08]. In this

study, general grinding processes are applied [HELU11]. The empirical equation (8.2) relates the average surface roughness, R_a , to the specific material removal rate and wheel speed [MALK08, HELU11].

$$R_a = R_1 \cdot \left(\frac{Q'_w}{v_s} \right)^x \quad (8.2)$$

- R_a average surface roughness
- R_1 experimentally determined constant
- Q'_w specific material removal rate
- v_s wheel speed
- x experimentally determined constant ($0.15 < x < 0.6$)

The specific energy requirement is assumed as $200,000 \text{ J/cm}^3$ for a process rate of about $10^{-3} \text{ cm}^2/\text{s}$ [GUTO06]. With this specific energy, a constant wheel speed, and a Michigan energy mix, the specific energy to decrease the surface roughness of the gears in the final drive reduction is calculated [HELU11]. The roughness, R_a , can be decreased to 20–60 % for less than 0.5 MMBtu of primary energy [HELU11].

In the gear use phase, the powertrain delivers power to accelerate the vehicle, overcome losses in the drivetrain and engine and to power accessories [HELU11]. With the frictional losses and all accessories constant, fuel power changes with drivetrain efficiency. For a helical gear pair modeled after a final drive reduction the gear mesh efficiency depends on the root mean square surface roughness, R_q , of the gear [XU07]. During vehicle usage, the power to overcome tractive losses and accelerate the vehicle depends on the vehicle velocity, climbing resistance, rolling resistance, and aerodynamic drag [HELU11]. Assuming a standard driving cycle from the U.S. EPA Federal Test Procedure 75 and a regular gasoline, the primary energy demand of the transmission can be calculated in dependence of a range of the root mean square surface roughness, R_q [HELU11]. Decreasing R_q lowers primary energy demand relative to a standard finished final drive reduction in a range of 2–5 MMBtu depending on the lubricant temperature in the final drive reduction [HELU11].

Comparing the manufacturing energy for decreasing surface roughness and gained reduction of use phase energy demand shows that manufacturing precision has a big impact. Since there are several gears in a vehicle in addition to the final drive reduction there is an even much bigger opportunity for manufacturers to improve efficiency [HELU11].

Chapter 9

Future Prospectives

From the time we enter the world with the help of medical instruments, until our final tombstone, polished to a glittering hardness, we live in the shadow of the grinding wheel. Name the product. Somewhere there lurks an abrasive operation; this has been so since the cave man, millions of years ago sharpened his tools and weapons by rubbing them together.
[LEWI76, p. 3]

The preceding Chaps. 2–6 mapped out how abrasive tooling systems are designed, composed and manufactured. It then was explained how sustainability can be assessed with existing and new methods in Chap. 7, followed by case studies in Chap. 8. To gain an outlook on abrasive tooling systems, the general market trends for abrasive tools and grit material need to be examined. It will then be shown how recent research and innovations lead to more sustainable tools. Service options for tool manufacturers will be discussed followed by a comprehensive, concluding summary of sustainability of abrasive tooling systems for all main stakeholders.

9.1 Market Trends for Abrasive Tools and Grit Material

The global market for abrasive products is tied to the overall economic activity. The production of abrasives by industrial nations is moving to the developing countries such as China and India [ASAM10, p. 313]. In 2010, China consumed about 20 % of the world's abrasives [MCCL10]. The main markets for abrasives in 2008 were metallic abrasives and fused corundum; the application of superabrasives was almost negligible [MCCL10]. Common types of metallic abrasives are steel shots and grits to be mostly used for blast cleaning. The Taiwanese company FACT predicts a worldwide trend that the consumption and manufacturing of diamond tools will shift massively from Europe and the USA to Asia and China [FACT12].

The Asian market for abrasives will grow with increasing grit quality. Already in 2011, China was the world's leading producer of fused corundum and silicon carbide, challenging the abrasive grit producers in other countries (Figs. 9.1 and 9.2)

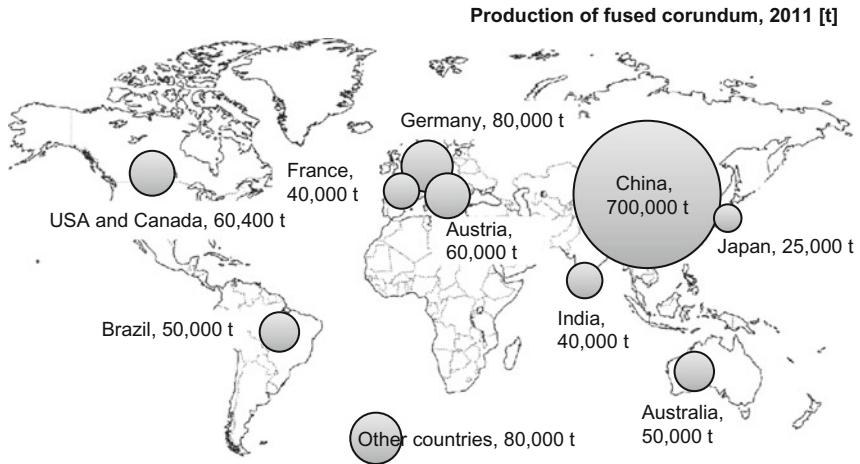


Fig. 9.1 World wide production capacity of fused corundum in 2011, total of 1.19 Mio t [USGS12A]

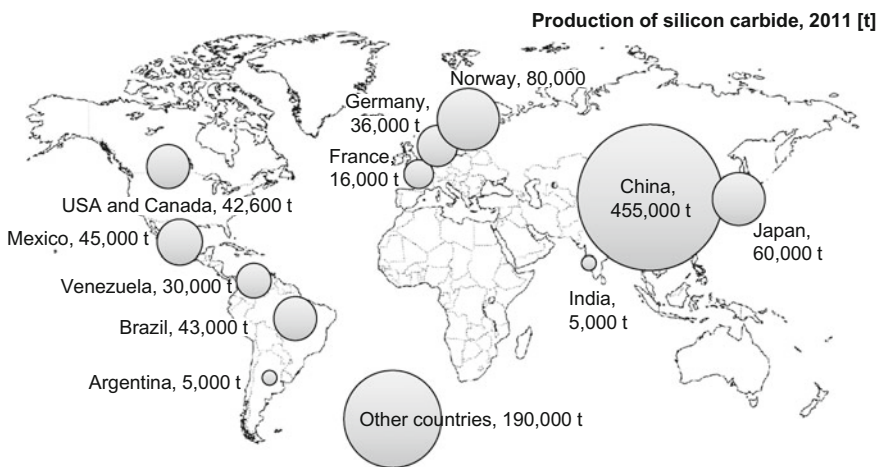


Fig. 9.2 World wide production capacity of silicon carbide in 2011, total of more than 1 Mio t [USGS12a]

[USGS12A]. In addition, China has become the biggest producing country of synthetic diamond (Fig. 9.3) [LIZH11]. One reason is the close or equal quality of Chinese diamonds compared to the Western products; another reason is the low price (Table 9.1) [LIZH11].

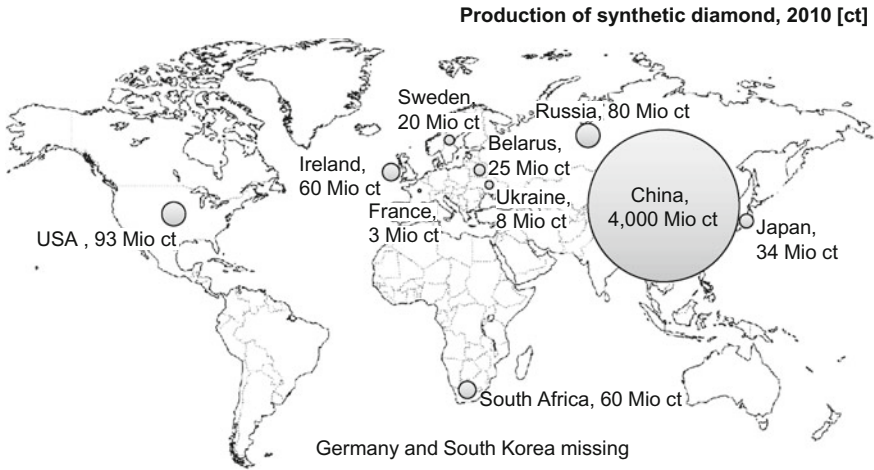


Fig. 9.3 World wide production of industrial diamond in 2010, values of Germany and South Korea are missing, total of 4383 Mio ct = 876 t [USGS12B]

Table 9.1 Approximated costs of abrasive grit material in US\$

	Appr. costs per kg in 1976 [LEWI76, p. 36]	Appr. costs per kg in 2007–2012
Corundum	\$0.55	\$1.3 (high-purity) in 2011 \$0.60 (regular) in 2011 [USGS12A]
SiC	\$0.77	\$0.55 in 2007 to \$1.25 in 2011 [USGS12A]
Zirconium corundum	\$1.32	\$1.00–5.80 in 2012
Diamond	\$5512.00	\$250.00 in 2011 [LIZH11]
CBN	\$5512.00	\$450.00 in 2012

The amount of synthetic diamond shown in Fig. 9.3 include more uses than abrasive grits, such as wear-resistant coatings, electronic applications, etc. [USGS12B]. Li et al. [LIZH11] anticipate that producers of superhard materials will rather focus on more technical and knowledge intensive areas such as the production of PCD and PCBN than try to compete with the Chinese diamond grit manufacturers. Not discussed here is the mining and production of natural diamonds. Dressing operations will likely still use natural industrial diamond [USGS12B]. Figure 9.4 shows that the CBN market is still dominated by Europe and North America.



Fig. 9.4 World wide production of CBN in 2008, total of 125.5 Mio ct = 25.1 t, error tolerance for the data is $\pm 15\%$ [MCCL10c]

9.2 Innovative and More Sustainable Tools

9.2.1 Future Requirements

Common trends in grinding technology are tighter form and size tolerances, smaller surface roughness, engineered surface textures, higher productivity, and smaller process costs [KRAF08]. There is a natural trend towards higher grinding wheel speeds and higher grinding performance [KREB06].

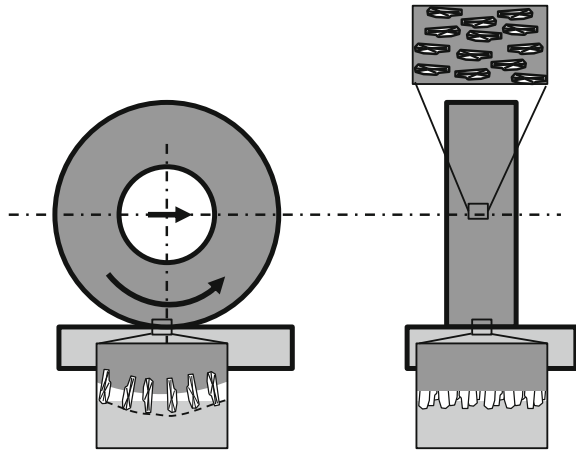
New products and new applications demand for adjusted tools designs. The tool user demands for higher bonding strength of vitrified bonding bridges, as well as harder and more porous vitrified bonds [KRAF08, KREB06]. This can happen through recrystallization or embedding of disperse particles, leading to new production steps for vitrified bonding in the areas of bonding preprocessing or sintering technology [KREB06].

9.2.2 Developments in Tool Design

9.2.2.1 Engineered Tools

The grinding tool can be designed to be similar to a milling tool with defined distances between the grits (Fig. 9.5) [OKAM78]. Grinding wheels with defined grit distribution and defined grit orientation reduce the randomness in grinding [WEBS04]. Hand set superabrasive grits allow for a defined grit pattern on grinding wheels [AURI03]. In the case of grinding belts, oriented grits have been used for decades.

Fig. 9.5 Model of surface generation with an engineered grinding wheel after [BORK92, p. 119]



Burkhard and Rehsteiner [BURK02] developed a brazing technology to produce single-layer tools with arranged grits. Honing tools with a single layer of CBN grits in a defined pattern were applied successfully in single-stroke operations on case-hardened steels, and showed a 10 fold increase in tool life [BURK02].

For glass grinding, Brinksmeier et al. [BRIN12] successfully applied coarse-grained, single-layered, metal-bonded diamond grinding wheels. Both stochastically distributed and placed diamond grits were used. After dressing, the favorable ductile removal mode and optical surface quality were achieved [BRIN12].

The workpiece surface finish is a strong function of the axial offset between adjacent rows of grits in an engineered tool [KOSH03]. Aurich and Kirsch [AURI12] give a recent overview on simulation for engineering tools.

9.2.2.2 Slotted Tools

Slotted tools or so-called segmented tools consist of a discontinuous abrasive layer either with geometrically defined or undefined cavities [KIRC10, p. 9]. Grooves can be perpendicular to the wheel perimeter or inclined.

The so-called T-Tool wheel consists of a metal bonded, segmented superabrasive layer and can significantly reduce forces and temperatures in SiC grinding compared to the process with a non-segmented wheel [TAWA11]. Kirchgatter [KIRC10] examined several different designs for slotted grinding tool in outer diameter grinding applications. He highlighted that improper slot design can lead to dynamical problems in the grinding process, but proved a lower thermal damage of the workpiece. Slotted wheels allow for reduced cooling lubricant flow [UHLM10].

9.2.2.3 Controlled Abrasive Clusters

Yuan et al. [YUAH10] invented an electroplated tool with controlled abrasive clusters (CAC) and used it successfully to grind carbon/epoxy composites with reduced wheel loading. The use of covers during the electroplating process allows the control of shape and pattern of superabrasive grit clusters.

9.2.2.4 Internally Cooled or Lubricated Wheels

The pores of vitrified grinding wheels may be filled with lubricants such as sulfur, wax, or resin after sintering [MARI07, p. 113, KING86, p. 79]. Sulphur is in use as high-temperature extreme pressure lubricant in internal grinding operations in the bearing industry; yet, the use is declining because of environmental considerations [MARI07, p. 113].

Other concepts for internal tool cooling involve coolant supply through the tool body. Aurich et al. [AURI11] present a channel design similar to centrifugal pump impellers in a steel body. Nguyen and Zhang [NGUY08] invented a tool body with a coolant chamber for grinding operations on aerospace alloys.

9.2.2.5 Sensor Integrated Grinding Wheels

Many grinding machinists still rely on their sense of hearing for monitoring, for example, to define the contact position between dressing tool and grinding wheel or find out if the dressing tool is in continuous contact with the grinding wheel. In the case of superabrasives and small depths of dressing cut, it is very hard to hear the contact between dressing and grinding tool, so automatic sensors become necessary [STUC88, p. 107 f.].

Besides acoustic emission, grinding wheel spindle power is the main control parameter in grinding [BRIN07]. The spindle power relates to the tangential grinding forces (Eq. 7.2). Direct force measurement gives higher resolution, but sensors might be hard to apply to the workpiece, e.g. in external grinding. Brinksmeier et al. [BRIN07] successfully integrated force sensors and temperature sensors into a grinding wheel.

Miniaturized sensors can be integrated in grinding tools to form an “intelligent grinding tool”. Superabrasive tools with a reusable body are a special case, and can hold temperature, acoustic emission or force sensors. Challenges lie in the wireless data and energy transfer to the rotating tool [KARP01, p. 190 ff.].

9.2.2.6 New Wheel Bodies

Yan et al. [YAN12] invented a bamboo charcoal composite that has vascular bundles as pores and is coated with abrasive particles in a metal bond layer around

the vascular bundles. The advantage is claimed to be an easy fabricating process with low cost and high quality; the abrasive tool can be used for polishing operations [YAN12].

9.2.2.7 Deposition of Diamond Layers

Directly deposited diamond can act as abrasive layer [WEBS04]. Brinksmeier et al. [BRIN12] produced chemical vapor deposited (CVD) diamond coated wheels. The CVD process achieved equal sized grits with a uniform distribution in a grit size between 0.5 and 30 μm [BRIN12]. Good results with small chip thicknesses were obtained in ultra-precision glass grinding [BRIN12].

Gäbler et al. produced abrasive pencils (burs) with a rough CVD diamond layer [WEBS04, GÄBL03]. They varied substrate diameters down to 60 μm , coating time between 10 and 90 h, and coating temperatures and achieved different crystal sizes.

9.2.2.8 Micro Tools

Aurich et al. [AURI09] produced micro grinding tools with a diameter down to 20 μm for tool grinding. They developed a desktop sized precision machine to electroplate the diamond tool and produce a defined cutting tool.

9.2.2.9 Ice Bonded Tools

Mohan and Ramesh Babu [MOHA11] developed an ice bonded abrasive polishing process for flat surfaces. The process kinematics are close to those of chemical mechanical polishing (CMP). The tool itself consists of a frozen slurry and is cooled by liquid nitrogen. The slurry composition and freezing methods play a significant role on how the abrasives are distributed in the ice matrix [MOHA11].

9.2.2.10 Magnetic Abrasive Particles

Magnetic abrasive finishing was first mentioned by Coats in a patent filed in 1938 [COAT40, SINL10]. It is a finishing method for flat, cylindrical, and ball grinding and especially suited for hard to machine materials [SINL10]. The magnetic abrasive particles can be produced by sintering, adhesive based processes, plasma based process (powder melting or plasma spraying), mixing (loose bonding), or other methods [SINL10]. Sing et al. [SINL10] summarize existing production methods.

Magnetorheological abrasive flow finishing is one variant that works with magnetorheological effects exhibited by carbonyl iron particles along with abrasive

particles in a non-magnetic base viscoplastic medium [JHA06]. Magneto-abrasive machining is used to prepare defined cutting edges at HSS drills so that the run-in phase of the drill can be avoided and tool life is increased [KARP09].

9.2.2.11 Vortex Machining

Vortex machining is a new abrasive process for nano applications and works with vortices that are caused by an oscillating fiber in colloidal abrasive slurry [HOWA12]. The fiber is close to the workpiece surface (about 20 μm), but does not touch it. The resulting material removal footprints have micrometer sized lateral dimensions and nanometer depths [HOWA12].

9.2.3 Options for Tool Manufacturers

In the long run, the manufacturing paradigm has to shift from non-sustainable mass production, mass consumption, and mass disposal to sustainable environmentally conscious ones [UMED12]. The eco-efficient layout of manufacturing processes and products will be a core competency for engineers in the future.

It is important to integrate all the life cycle phases from the product development phase to the end-of-life phase, including closed-loop supply chain management [UMED12]. A holistic life cycle management aims to minimize costs, optimize revenues and reduce risks and impacts on environment in all product life cycle phases and beyond individual enterprises [HERR10, p. 96]. The tool manufacturer can act as a life cycle partner for the tool user. The manufacturer can support process ramp-up, monitor tool condition and process performance, and support production output [SCHH10].

9.2.3.1 Service Options, End of Life and Incentives

Grinding tool manufacturers could offer a “greener” tool option, which might cost more than the comparatively not so green version, but have a certified smaller impact on environment and society. Green in this context would be a tool with less hazardous ingredients or less sintering energy needed.

Several studies have investigated the environmental behavior of consumers. For example, in hotels, it was found that in-room signs and messages could create awareness and induce environmentally friendly behavior such as reusing towels [BACA13]. Even more, letting the consumers choose to sign a commitment statement or receiving a pin as symbol for environmental commitment increased the positive behavior, here reusing towels [BACA13]. Abrasive tool manufacturers could offer to display the name of companies, which buy the “greener” tools. The tool users could also pride themselves with using greener abrasive tools.

Rickli and Camelio [RICK10] investigated how incentives affect the consumer’s decisions on the product’s end of life. Buy-back incentives, such as a monetary amount, encourage consumers to voluntarily return a product [RICK10]. This is an easy means to be implemented for abrasive tools and take-back options.

9.2.3.2 Labelling and Customer Information

Labelling is important for the consumer to decide if a product is green. Customers are more likely to buy environmentally friendly products if they know about those attributes in the use phase which are both environmentally friendly and of high quality [ABEL05, p. 173].

Table 9.2 Global model of grinding tool sustainability

		Grit manufacturer and other raw materials manufacturers	Tool manufacturer	Tool user (Machine tool manufacturer)	Society and local community
Raw material processing and tool manufacturing	Techn.	Material availability and quality		Dressability	
	Econ.	Production location			
		Energy costs, labor costs			
		Material price		Tool price	
	Env.	Mining hazards (env., soc.)			Mining hazards, emissions (env., soc.)
Soc.	Worker health, protection measures, legislation				
Tool use	Techn.	Grit wear	Tool wear		
				Machine tool, max. cutting speed, dressability	Product life, product performance
	Econ.		Tool price		
			Competitiveness		
	Soc.		Safety		
Tool end of life	Techn.			Tool wear, shelf life (techn., econ.)	
	Econ.		Re-layering, recycling, take-back service (techn., env., econ.)		
	Env.			Disposal costs, waste reduction, waste regulations (env., econ.)	
	Soc.				

9.3 Conclusion on Abrasive Tool Sustainability

Global trends on raw material pricing and availability drive tool manufacturers and raw material suppliers to strive for new materials and tool designs. Research alliances with universities and research institutions boost these efforts.

Sustainability can be regarded in four dimensions: economics, environment, society, and technology. Different stakeholders are interested in the grinding tool life cycle. Most important stakeholders are the grit manufacturers, other raw material suppliers, tool manufacturers, tool user, society and local communities. Machine tool manufacturers have similar concerns as the tool user. Table 9.2 summarizes the most important aspects for these stakeholders along the four life stages of abrasive tools.

Today, environmental sustainability in tool use or social sustainability in tool end of life are rarely regarded (Table 9.2). Tool manufacturers who incorporate these aspects can therefore gain a competitive edge.

Furthermore, raw material manufacturers are rarely concerned with tool use and tool end of life. The tool manufacturer is also only involved in few tool use and end of life aspects (Table 9.2). A close cooperation between material suppliers, tool manufacturers, tool users and machine tool manufacturers help to enhance overall tool sustainability. In particular, the functionality of the machined part is very important to consider for resource efficiency and offers a new perspective to global sustainability in production engineering.

Literature

- [ABBA06] Abbate, C., Giorgianni, C., Brecciaroli, R., Giacobbe, G., Costa, C., Cavallari, V., Albiero, F., Catania, S., Tringali, M.A., Martino, L.B., Abbate, S.: Changes induced by exposure of the human lung to glass fiber-reinforced plastic. *Environ. Health Perspect.* **114**(11), 725–1729 (2006)
- [ABEL05] Abele, E., Anderl, R., Birkhofer, H. (eds.): *Environmentally-Friendly Product Development-Methods and Tools*. Springer, Berlin (2005)
- [ALDE14] Alden, G.I.: Operation of grinding wheels in machine grinding. *Trans. ASME* 451–460 (1914)
- [ANSI01] ANSI B74.12-2001: Specifications for the Size of Abrasive Grain-Grinding Wheels, Polishing and General Industrial Uses. Norm American National Standards Institute, 20 Feb 2001
- [ANSI03] ANSI B74.11-1993(R2003): Specifications for Tumbling Chip Abrasives. Norm American National Standards Institute (R2003)
- [ANSI64] ANSI B74.5-1964: American standard test for Capillarity of Abrasive Grains. Norm American National Standards Institute (1964)
- [ANSI77] ANSI B74.10-1977: Specifications for Grading of Abrasive Microgrits. Norm American National Standards Institute, 12 Oct 1977
- [ANSI81] ANSI B74.20-1981: Standard Specifications for Grading of Diamond Powder in Sub-Sieve Sizes. Norm American National Standards Institute, 14 Aug 1981
- [ANSI84] ANSI B74.18-1984: Specifications for Grading of Certain Abrasive Grain on Coated Abrasive Products. Norm American National Standards Institute, 27 Jan 1984
- [ANSI86] ANSI B74.14-1986: Methods of Chemical Analysis of Aluminum Oxide Abrasive Grain and Abrasive Crude. Norm American National Standards Institute, 9 Jan 1986
- [ANSI90] ANSI B74.19-1990: Test for Determining Magnetic Content of Abrasive Grains. Norm American National Standards Institute, 4 Jan 1990
- [ANSI92] ANSI B74.4-1992: Procedure for Bulk Density of Abrasive Grain. Norm American National Standards Institute, 12 Nov 1992
- [ARAU12] de Araujo, J.B., de Oliveira, J.F.G.: Evaluation of two competing machining processes based on sustainability indicators. In: *Proceedings of the 19th CIRP Conference on Life Cycle Engineering*. University of California at Berkeley, Berkeley, USA, 23–25 May 2012
- [ARUN07] Arunachalam, N.; Ramamoorthy, B.: Texture analysis for grinding wheel wear assessment using machine vision. *Proc. ImechE Part B J. Eng. Manuf.* **221**(3), 419–430 (2007)

- [ASAM10] Asami, M., Santorelli, M.: Abrasives (Chap. 13). In: Pilato, L. (ed.) *Phenolic Resins: A Century of Progress*. Springer, Berlin. ISBN 978-3-642-04714-5, pp. 307–343 (2010)
- [ASEN08] Asen, N.: Trägerkörper für ein rotierendes Schleif- bzw. Schneidwerkzeug sowie daraus hergestelltes Schleif-bzw. Schneidwerkzeug (2008). Patent EP1928633A1, 11 Jun 2008
- [ASHB09] Ashby, M.F.: *Materials and the Environment: Eco-Informed Material Choice*. BH (2009)
- [ASHL96] Ashley, P.J.: Saint-Gobain/Norton Industrial Ceramics Corporation: Process for production of alumina/zirconia materials (1996). Patent US 5,567,214, 22 Oct 1996
- [AURI03] Aurich, J.C., Braun, O., Warnecke, G., Cronjäger L.: Development of a superabrasive grinding wheel with defined grain structure using kinematic simulation. *Ann. CIRP* **52**(1), 275 (2003)
- [AURI08] Aurich, J.C.: Infobrief FBK Ausgabe 28/08. ISSN 1615-2492. http://www.paulmak.de/fbk-kl/pdfdocs/Infobrief_Ausgabe_28-08.pdf
- [AURI09] Aurich, J.C., Engmann, J., Schueler, G.M., Haberland, R.: Micro grinding tool for manufacture of complex structures in brittle materials. *Ann. CIRP* **58**(1), 311–314 (2009)
- [AURI11] Aurich, J.C., Kirsch, B., Herzenstiel, P., Kugel, P.: Hydraulic design of a grinding wheel with an internal cooling lubricant supply. *Prod. Eng. Res. Dev.* **5**, 119–126 (2011)
- [AURI12] Aurich, J.C., Kirsch, B.: Kinematic simulation of high-performance grinding for analysis of chip parameters of single grains. *CIRP J. Manuf. Sci. Technol.* **5**, 164–174 (2012)
- [AURI13] Aurich, J.C., Linke, B., Hauschild, M., Carrella, M., Kirsch, B.: Sustainability of abrasive processes, *Annals of the CIRP* 62/2/2013, p. 653–672, <http://dx.doi.org/10.1016/j.cirp.2013.05.010>
- [AVER82] Averkamp, T.: Überwachung und Regelung des Abricht- und Schleifprozesses beim Außenrund-Einstechschleifen. Dissertation RWTH Aachen (1982)
- [BACA13] Baca-Motes, K., Brown, A., Gneezy, A., Keenan, E.A., Nelson, L.D.: Commitment and behavior change: evidence from the field. *J. Consum. Res.* **39** (2013). doi:[10.1086/667226](https://doi.org/10.1086/667226)
- [BADG09a] Badger, J.: Cooling in grinding - environmental considerations of quantity, disposal and energy consumption. In: *The 7th CIRP Conference on Sustainable Manufacturing, India* (2009)
- [BADG09b] Badger, J.: Factors affecting wheel collapse in grinding. *Ann. CIRP* **58**(1), 307–310 (2009)
- [BAIL02] Bailey, M.W., Juchem, H.O., Cook, M.W., Collins, J.L., Butler-Smith, P.: The importance of PCD/diamond/CVD diamond and PCBN/CBN tooling in the automotive industry. *Ind. Diam. Rev.* **1**, 53–60 (2002)
- [BAIL98] Bailey, M.W., Juchem, H.O.: The advantages of CBN grinding: low cutting forces and improved workpiece integrity. *IDR* **3**(98), 83–89 (1998)
- [BAIL99] Bailey, M.W., Garrard, R., Juchem, H.O.: Characteristics of diamond and their effect on grinding behaviour. *Ind. Diam. Rev.* **1**(99), 10–19 (1999)
- [BANI05] Baniszewski, B.: An environmental impact analysis of grinding. B.Sc. Thesis at the Massachusetts Institute of Technology (2005)
- [BECK02] Beck, T.: Kühlschmierstoffeinsatz beim Schleifen mit CBN. Doctoral Thesis at RWTH Aachen University (2002)
- [BEHR07] Behrens, B.-A., Kammler, M.: Calculation of the bursting speed of one side recessed grinding wheels. *Prod. Eng. Res. Devel.* **1**, 213–218 (2007)

- [BEHR11] Behrens, B.-A., Seidel, H.-J., Kammler, M.: Vergleichende experimentelle und numerische Untersuchungen zum schwingungsüberlagerten Pressen zweier Pulvermaterialien. *Mat.-wiss. u. Werkstofftech.* **42**, 705–711 (2011). doi:[10.1002/mawe.201100757](https://doi.org/10.1002/mawe.201100757)
- [BEHR11b] Behrens, B.-A., Kammler, M., Lange, F.: Universitaet Hannover: Schleifkörper mit Zusatzpartikeln aus recycelten Schleifkörpern und Verfahren zur Herstellung hiervon (2011). Patent WO2011/092021A1, 4 Aug 2011
- [BENE03] Benea, I.C., Griffin, S.: Mechanical strength and fracture characteristics of micron diamond. *Ind. Diam. Rev.* **3**, 53–60 (2003)
- [BENE03b] Benea, I.C., Griffin, S.: Micron diamond types/products. In: Proceedings of the Intertech 2003, Vancouver B.C., 28 July–1 Aug 2003
- [BENE10] Benea, I.C.: Particle size and size distribution of superabrasive powders. Part 1: *Diam. Tooling J.* **3**(10), 39–46; Part 2: *Diam. Tooling J.* **4**(10), 41–46
- [BENZ91] Benz, E.: Vakuumlöten von Diamantwerkzeugen. *Industrie Diamanten Rundschau* **4**(91), 233–235 (1991)
- [BEYE04] Beyer, P.: Hochproduktives Schleifen mit keramisch gebundenen Superabrasives Teil 1: Die HPB-Technologie für Vit-CBN-Schleifwerkzeuge. *Industrie Diamanten Rundschau*, Ausgabe 4/2004, p. 344 ff
- [BGBI01] BGBl: Verordnung über das Europäische Abfallverzeichnis (Abfallverzeichnis-Verordnung-AVV), 10 Dec 2001. URL:<http://www.gesetze-im-internet.de/avv/>. Last accessed: 29 Nov 2012
- [BGI10] Vereinigung der Metall-Berufsgenossenschaften; Maschinenbau- und Metall-Berufsgenossenschaft; Hütten- und Walzwerks-Berufsgenossenschaft; Berufsgenossenschaft Metall Nord Süd: BG-Information Schleifer BGI 543, Edition 2010, print 09.2010/3.900 (2010)
- [BIER76] Bierlich, R.: Technologische Voraussetzungen zum Aufbau eines Adaptiven Regelungssystems. Doctoral Thesis at RWTH Aachen University (1976)
- [BIFA99] Bifano, T., Krishnamoorthy, R., Fawcett, H., Welch, E.: Fixed-load electrolytic dressing with bronze bonded grinding wheels. *ASME J. Manuf. Sci. Eng.* **121**(1), 20–27 (1999)
- [BLAN07] Blankenburg, S., Stabenow, R., Göhler, V.: Nutzung des Zerspanungspotenzials mit keramisch gebundenen Schleifscheiben. *Diam. Bus.* **2**, 32–36 (2007)
- [BLUN96] Blunt, L., Ebdon, S.: The application of three-dimensional surface measurement techniques to characterizing grinding wheel topography. *Int. J. Mach. Tools Manuf.* **36**(11), 1207–1226 (1996)
- [BOGA09] Bogatyreva, G.P., Petasyuk, G.A., Bazalii, G.A., Shamraev, V.S.: On morphometric uniformity of diamond micron powders. *J. Superhard Mater.* **31**(2), 126–134 (2009)
- [BOLD02] Bold, L.: Galvanische Werkzeuge - Ein Leitfaden, company brochure. Saint-Gobain Abrasives (2002)
- [BORC07] Borchers, W.: Die elektrischen Öfen: Erzeugung von Wärme aus elektrischer Energie und Bau elektrischer Öfen. Google eBook (1907)
- [BORK92] Borkowski, J.A., Szymanski, A.M.: Uses of Abrasives and Abrasive Tools. Ellis Horwood Limited and PWN Polish Scientific Publishers (1992)

- [BOTS05] Bot-Schulz, R.: Untersuchung der Reaktionen an der Schnittstelle Korn/Bindung für Sol-Gel-Korund. Doctoral Thesis at RWTH Aachen University (2005)
- [BOUW99] Van Bouwelen, F.M., Van Enckevort, W.J.P.: A simple model to describe the anisotropy of diamond polishing. *Diam. Relat. Mater.* **8**, 840–844 (1999)
- [BRAU09] Braungart, M., McDonough, W.: *Cradle to Cradle*. Random House, UK (2009)
- [BREC73] Brecker, J.N., Komanduri, R., Shaw, M.C.: Evaluation of unbonded abrasive grains. *Ann. CIRP* **22**(2), 219–225 (1973)
- [BRIN00] Brinksmeier, E., Walter, A.: Generation of reaction layers on machined surfaces. *Ann. CIRP* **49**(1), 435–438 (2000)
- [BRIN03] Brinksmeier, E., Heinzl, C., Böhm, C., Wilke, T.: Simulation of the temperature distribution and metallurgical transformation in grinding by using the finite-element-method. *Prod. Eng. Res. Dev.* **10**(1) 9–16 (2003)
- [BRIN04] Brinksmeier, E., Lucca, D.A., Walter, A.: Chemical aspects of machining processes. *Ann. CIRP* **53**(2), 685 (2004)
- [BRIN04b] Brinksmeier, E., Wilke, T.: Erfassung und Vermeidung thermischer Randzonenbeeinflussung beim Schleifen, Moderne Schleiftechnologie und Feinstbearbeitung. In: Proceedings of the 5th Seminar “Moderne Schleiftechnologie und Feinstbearbeitung”, Stuttgart, Selbstverlag, Villingen-Schwenningen, pp. 2-1-2-22, ISBN 3-00-013657-6, 13 May 2004
- [BRIN06] Brinksmeier, E., Aurich, J.C., Govekar, E., Heinzl, C., Hoffmeister, H.-W., Peters, J., Rentsch, R., Stephenson, D.J., Uhlmann, E., Weinert, K., Wittmann, M.: Advances in modeling and simulation of grinding processes. Keynote Paper. *Ann. CIRP* **55**(2) (2006)
- [BRIN07] Brinksmeier, E., Heinzl, C., Meyer, L.: Werkzeugseitige Temperatur- und Kraftsensoren zur Charakterisierung von Schleifprozessen; Jahrbuch Schleifen, Honen, Läppen und Polieren, H.-W. Hoffmeister, B. Denkena (Hrsg.), 63. Ausgabe, Vulkan-Verlag, Essen, pp. 256–276 (2007)
- [BRIN12] Brinksmeier, E., Mutlugünes, Y., Antsupov, G., Rickens, K.: New tool concepts for ultra-precision grinding. *Key Eng. Mater.* **516**, 287–292 (2012)
- [BRIN82] Brinksmeier E.: Randzonenanalyse geschliffener Werkstücke. Doctoral Thesis at the University of Hannover (1982). ISBN 3-180145002-2
- [BRIN95] Brinksmeier E., Çinar M.: Characterisation of dressing processes by determination of the collision number of the abrasive grits. *Ann. CIRP* **44** (1), 299–303 (1995)
- [BRIN99] Brinksmeier, E., Heinzl, C., Wittmann, M.: Friction, cooling and lubrication in grinding. Keynote Paper. *Ann. CIRP* **48**(2), 1–18 (1999)
- [BROC11] Brocker, R., Klocke, F.: Das Fertigungsverfahren Gleitschleifen. *wt Werkstattstechnik online Jahrgang 101* H. 6, 385–389 (2011)
- [BROW11] Brown, C.A.: Decomposition and prioritization in engineering design. In: Proceedings of ICAD2011, The Sixth International Conference on Axiomatic Design, Daejeon, pp. 41–47, 30–31 Mar 2011
- [BRUN62] Brunton, J.H.: Fracture propagation in diamond. In: Proceedings of the First International Congress on Diamonds in Industry, Paris, pp. 329–341 (1962)
- [BULJ99] Buljan, S.-T., Eagar, W.T., Miller, J.B., Shiue, R.-K., Norton Company: Removable bond for abrasive tool. EP0921907 A1, 16 June 1999

- [BUND63] Bundy, F.P., Wentorf, R.H.: Direct transformation of hexagonal boron nitride to denser forms. *J. Chem. Phys.* **38**, 1144 (1963). doi:[10.1063/1.1733815](https://doi.org/10.1063/1.1733815)
- [BUND96] Bundy, F.P., Bassett, W.A., Weathers, M.S., Hemley, R.J., Mao, H.U., Goncharov, A.F.: The pressure-temperature phase and transformation diagram for carbon; updated through 1994. *Carbon* **34**(2), 141–153 (1996). ISSN 0008-6223, [10.1016/0008-6223\(96\)00170-4](https://doi.org/10.1016/0008-6223(96)00170-4)
- [BURK02] Burkhard, G., Rehsteiner, F.: High efficiency abrasive tool for honing. *Ann. CIRP* **51**(1), 271–274 (2002)
- [BÜTT68] Büttner, A.: Das Schleifen sprödharter Werkstoffe mit Diamant-Topfscheiben unter besonderer Berücksichtigung des Tiefschleifens. Doctoral Thesis at Technical University, Hannover (1968)
- [BUTT79] Buttery, T.C., Statham, A., Percival, J.B.: Some effects of dressing on grinding performance. *Wear* **55**, 195–219 (1979)
- [CAVE75] Caveney, R.J., De Beers Industrial Diamond Division Limited: Diamond particle having a composite coating of titanium and a metal layer (1975). Patent US 3,929,432, 30 Dec 1975
- [CERA10] Ceratizit: As precious as gold and virtually as hard as diamond-CBN manufacturer swears by CERATIZIT. url:http://www.ceratizitusa.com/9357_ENG_HTML.htm. Last accessed 09 Dec 2013
- [CHAL72] Chalkley, J.R., Thomas, D.M.: Improvements in abrasive wheels and other tools (1972). Patent GB1279413 (A), 28 June 1972
- [CHAT90] Chattopadhyay, A.K., Chollet, L., Hintermann, H.E.: On performance of chemically bonded single-layer CBN grinding wheel. *Ann. CIRP* **39**(1), 309–312 (1990)
- [CHAT94] Chattopadhyay, A.K.; Hintermann, H.E.: On performance of brazed single-layer CBN wheel. *Ann. CIRP* **43**(1), 313–317 (1994)
- [CHIB03] Chiba, Y., Tani, Y., Enomoto, T., Sato, H.: Development of a high-speed manufacturing method for electroplated diamond wire tools. *Ann. CIRP* **52**(1), 281–284 (2003)
- [CHR196] Christianson, T.J., Benedict, H.W., Minnesota Mining and Manufacturing Company: Method for making a spliceless coated abrasive belt and the product thereof. Patent US 5,578,096, 26 Nov 1996
- [CINA95] Çinar, M.: Einsatzvorbereitung und Verschleißentwicklung keramisch gebundener CBN-Schleifscheiben, Doctoral Thesis at University Bremen (1995)
- [CO2PE] CO2PE! Cooperative Effort on Process Emissions in Manufacturing website. <http://www.mech.kuleuven.be/co2pe>. Last accessed 20 June 2011
- [COAT40] Coats, H.P.: Method of and apparatus for polishing containers (1940). Patent US 2,196,058, 2 Apr 1940
- [COCH01] Cochran, D.S., Arinez, J.F., Duda, J.W., Linck, J.: A decomposition approach for manufacturing system design. *J. Manuf. Syst.* **20**(6), 371–389 (2002)
- [COEL00] Coelho, R.T., Oliveira, J.F.G., Campos, G.P.: Experimental and theoretical study of the temperature distribution in diamond dressing tools for precision grinding. *Abrasives Mag.* 7–15 (2000)
- [COES71] Coes, L., Jr.: *Abrasives*. Springer, Berlin (1971). ISBN 0-387-80968-6
- [COLL88] Colleselli, K., Schwieger, K.H.: 11.2. Schleifscheiben und Schleifkörper. In: Becker/Braun (ed.) *Kunststoff-Handbuch 10-Duroplaste*, pp. 894–908, Hanser Verlag, (1988). ISBN 3446144188
- [CORR75] Corrigan, F.R., Bundy, F.P.: Direct transitions among the allotropic forms of boron nitride at high pressures and temperatures. *J. Chem. Phys.* **63**, 3812 (1975). doi:[10.1063/1.431874](https://doi.org/10.1063/1.431874)

- [CRAT10] UPLCI: Online database and taxonomy (Screening Approach) (2010). Last accessed 20 June 2011. <http://cratel.wichita.edu/uplci>
- [CROM73] Crompton, D., Hirst, W., Howse, M.G.W.: The wear of diamond. *Proc. R. Soc. Lond. A* **333**, 435–454 (1973)
- [CURR06] Curran, M.A., Scientific Applications International Corporation (SAIC): Life Cycle Assessment: Principles and Practice. Contract No. 68-C02-067, Work Assignment 3-15, EPA/600/R-06/060, May 2006
- [DAHMO4] Dahmus, J.B., Gutowski, T.G.: An environmental analysis of machining. In: Proceedings 2004 ASME International Mechanical Engineering Congress and RD&D Expo, Anaheim, California USA, 13–19 Nov 2004
- [DAMB05] Dambon, O.: Das Polieren von Stahl für den Werkzeug- und Formenbau. Doctoral Thesis at RWTH Aachen University (2005)
- [DAUD60] Daude, O.: Untersuchung des Schleifprozesses - Zusammenhang zwischen Schleifscheibe, Bearbeitungsbedingungen und Arbeitsergebnis. Doctoral Thesis at RWTH Aachen University (1960)
- [DAVI73] Davies, C.E.: Untersuchung der Einflußgrößen beim Flachläppen mit Diamant-Mikrokörnungen. *Industrie Diamanten Rundschau* **7**(4), 185–199 (1973)
- [DAVI74] Davies, C.E.: A study of the influences on flat lapping with diamond micron abrasives - part 1. *Ind. Diam. Rev.* 54–61 (1974)
- [DAVS04] Davisa, T.D., DiCorletob, J., Sheldon, D., Vecchiarelli, J., Erkey, C.: A route to highly porous grinding wheels by selective extraction of pore inducers with dense carbon dioxide. *J. Supercrit. Fluids* **30**(3), 349–358 (2004)
- [DECN70] Decneut, A., Snoeys, R., Peters, J.: Sonic testing of grinding wheels. Centre De Recherches Scientifiques et Techniques de L'Industrie des Fabrications Metalliques, Nov 1970
- [DECN74] Decneut, A., Peters, J., Snoeys, R.: The significance of chip thickness in grinding. *Ann. CIRP* **23**(2), 227–237 (1974)
- [DEHA99] De Haes, U., Jolliet, O., Finnveden, G., Hauschild, M., Krewitt, W., Mueller-Wenk, R.: Best available practice regarding impact categories and category indicators in life cycle impact assessment. Background document for the second working group on Life Cycle Impact Assessment of SETAC-Europe (WIA-2), *Int. J. LCA* **4**(3), 167–174 (1999)
- [DENK05] Denkena, B., Reichstein, M., Kramer, N., Jacobsen, J., Jung, M.: Eco- and energy-efficient grinding processes. *Key Eng. Mater.* **291–292**, 39–44 (2005)
- [DEPE05] De Pellegrin, D.V., Torrance, A.A.: Characterisation of abrasive particles and surfaces in grinding. In: Diamond at Work Conference, Barcelona (2005)
- [DEST10] Statistisches Bundesamt: Umwelt-Abfallentsorgung, Fachserie 19 Reihe 1, Wiesbaden. url:www.destatis.de. Accessed 29 Nov 2012
- [DIAZ10] Diaz, N., Helu, M., Jayanathan, S., Chen, Y., Horvath, A., Dornfeld, D.: Environmental analysis of milling machine tool use in various manufacturing environments. In: IEEE International Symposium on Sustainable Systems and Technology (ISSST2010), Washington, D.C., USA (2010)
- [DIN00a] Norm DIN ISO 525: Schleifkoerper aus gebundenem Schleifmittel. Allgemeine Anforderungen (ISO 525:1999), Aug 2000
- [DIN00b] Norm DIN ISO 603-1 to 12: Schleifkörper aus gebundenem Schleifmittel-Maße, May 2000
- [DIN03] Norm DIN 8589-11: Fertigungsverfahren Spanen-Teil 11: Schleifen mit rotierendem Werkzeug-Einordnung, Unterteilung, Begriffe, Sept 2003

- [DIN05] Norm DIN EN ISO 6103: Bonded abrasive products - permissible unbalances of grinding wheels as delivered-static testing (ISO 6103:2005); German version EN ISO 6103:2005, July 2005
- [DIN06] Norm DIN ISO 666:2006: Machine tools - mounting of grinding wheels by means of hub flanges (ISO 666:2006). Beuth Verlag (2006)
- [DIN07] Norm DIN EN 12413: Sicherheitsanforderungen fuer Schleifkoerper aus gebundenem Schleifmittel. Beuth Verlag, Sept 2007
- [DIN11] Norm DIN EN 13236: Sicherheitsanforderungen fuer Schleifwerkzeuge mit Diamant oder Bornitrid. Beuth Verlag, Feb 2011
- [DIN79] Norm DIN 50 320: Verschleiß-Begriffe, Systemanalyse von Verschleißvorgängen, Gliederung des Verschleißgebietes. Beuth Verlag Berlin, Norm ausgeschieden (1979)
- [DIN97] Norm DIN ISO 8486-1: Schleifkörper aus gebundenem Schleifmittel-Bestimmung und Bezeichnung der Korngrößenverteilung Teil 1: Makrokörnungen F4 bis F220, Sept 1997. Norm DIN ISO 8486-2: Schleifkörper aus gebundenem Schleifmittel-Bestimmung und Bezeichnung der Korngrößenverteilung Teil 2: Mikrokörnungen F230 bis F1200, Sept 1997
- [DING05] Ding, W.F., Xu, J.H., Fu, Y.C., Xiao, B., Su, H.H., Xu, H.J.: Interfacial reaction between cubic boron nitride and Ti during active brazing. *J. Mater. Eng. Perform.* **15**(3), 365–369 (June 2006)
- [DOMA06] Doman, D.A., Warkentin, A., Bauer, B.: A survey of recent grinding wheel topography models. *Int. J. Mach. Tools Manuf.* **46**(2006), 343–352 (2006)
- [DONO04] Donoghue, A.M.: Occupational health hazards in mining: an overview. *Occup. Med.* **54**, 283–289 (2004)
- [DORN08] Dornfeld, D., Lee, D.-E.: *Precision Manufacturing*. Springer, Berlin. ISBN 978-0387324678 (2008)
- [DORN10] Dornfeld, D.: Sustainable manufacturing: greening processes, systems and products. In: *Proceedings of ICMC Sustainable Production for Resource Efficiency and Ecomobility*. Fraunhofer Institute for Machine Tools and Forming Technology, Chemnitz University of Technology, Chemnitz, Germany, Sept 2010
- [DORN11] Dornfeld, D.: Leveraging manufacturing for a sustainable future. In: *Proceedings of the 18th CIRP International Conference on Life Cycle Engineering*. Technische Universität Braunschweig, Braunschweig, Germany, 2nd–4th May 2011
- [DREN97] Dreuter, J.C.: Allebach, D.C., Konitzer, D.A.: Abrasive grit material recovery system (1997). Patent US 5,657,876, 19 Aug 1997
- [DREY06] Dreyer, L.C., Hauschild, M.Z., Schierbeck, J.: A framework for social life cycle impact assessment. *Int. J. Life Cycle Assess.* **11**(2), 88–97 (2006)
- [DRFR05] Dr. Fritsch: Hot stuff! New sintering press makes high temperatures quick and easy, *Metal-powder.net*, May 2005, pp. 14–15. url:http://www.dr-fritsch.de/tl_files/aktuelles/publikationen/06_mpr_5_2005_hochsinter.pdf. Last accessed 1 Dec 2012
- [DRFR11] Dr.Fritsch: Eisenbasislegierungen haben einen festen Platz in der Diamantwerkzeugindustrie, *dihw* 3, 3, p. 64–66 (2011)
- [DUBR05] Dubrovinskaia, N., Dubrovinsky, L., Crichton, W., Langenhorst, F., Richter, A.: Aggregated diamond nanorods, the densest and least compressible form of carbon. *Appl. Phys. Lett. USA* **87**(8), 83106-1-3 (2005)

- [DUSC11] Duscha, M., Eser, A., Klocke, F., Broeckmann, C., Wegner, H., Bezold, A.: Modeling and simulation of phase transformation in grinding. *Adv. Mater. Res.* **223**, 743–753 (2011)
- [DUSC12] Duscha, M., Linke, B., Klocke, F., Dornfeld, D.: Higher competitiveness of speed-stroke grinding by using increased wheel speeds (MSEC2012-7240). In: ASME 2012 International Manufacturing Science and Engineering Conference (MSEC 2012), Notre Dame, IN, USA, 4–8 June 2012
- [DYER79] Dyer, H.B.: Ultra-hard abrasives in resin bond application. *IDR* 15–20, Jan 1979
- [ECHA12] European Chemicals Agency: Information on chemicals. url:<http://echa.europa.eu/information-on-chemicals>. Accessed 29 Nov 2012
- [ECKE00] Eckebrecht, J.: Umweltverträgliche Gestaltung von spanenden Fertigungsprozessen-Forschungsansätze und Wissenstransfer. Doctoral Thesis at the University of Bremen (2000). ISBN 978-3-8265-7661-4
- [EFFE01] Effenberger, R.: Schleifscheibe (Grinding Disk) (2001). Patent WO 01/08850 A1, 8 Feb 2001
- [EICH97] Eichhorn, H.: Drehzahlsynchronisation der Wirkparameter beim Abrichten und Schleifen. Doctoral Thesis at TU Berlin (1997)
- [ENDO81] Endo, T., Fukunga, O., Iwata, M.: The synthesis of CBN using $\text{Ca}_3\text{B}_2\text{N}_4$. *J. Mater. Sci.* **16**, 2227–2232 (1981)
- [ENGE02] Engelhorn, R.: Verschleißmerkmale und Schleifeinsatzverhalten zweiphasig verstärkter Sol-Gel-Korunde. Doctoral Thesis at RWTH Aachen University (2002)
- [ENGL03] Engels, A.: The role of particles per carat in diamond tool behaviour. *IDR* **2** (2003)
- [ENPA06] Enparantza, R., Revilla, O., Azkarate, A., Zendoia, J.: A life cycle cost calculation and management system for machine tools. In: Proceedings of the 13th CIRP Conference on Life Cycle Engineering (LCE), pp. 717–722 (2006)
- [EPA94] US Environmental Protection Agency, by Midwest Research Institute (MRI): Emission factor documentation for AP-42, Section 11.31. Abrasives Manuf. Final Report, 18 May 1994. url:<http://www.epa.gov/ttnchie1/ap42/ch11/bgdocs/b11s31.pdf>. Accessed 22 Oct 2012
- [EPA97] US Environmental Protection Agency: Miscellaneous sources, AP 42, 5th edn., vol I (Chap. 13). 13.2.6 Abrasive Blasting, Final Section-Supplement D, Oct 1997, url:<http://www.epa.gov/ttn/chie/ap42/ch13/final/c13s02-6.pdf>. Accessed 3 July 2012
- [EPPL94] Eppler, W.F.: *Praktische Gemmologie*, 5. Auflage (1994)
- [ESCH05] Eschner, M., Fritzlär, B., Schnabel H.-D., Sedner, A.: Untersuchungen zum Einsatz von Naturfasern in Phenolharzmatrix-Kompositen. In: Proceedings of the 15th Symposium Verbundwerkstoffe und Werkstoffverbunde, April 2005, Kassel, pp. 223–228. http://www.dgm.de/download/tg/706/706_7.pdf
- [EVAN62] Evans, T.: Graphitization of Diamond. In: Proceedings of the First International Congress on Diamonds in Industry, Paris, pp. 275–282 (1962)
- [EVAS90] Evans, A.G.: Perspective on the development of high-toughness ceramics. *J. Am. Ceram. Soc.* **73**(2), 187–206 (1990)
- [EVER06] Eversheim, W., Pfeifer, T., Weck, M. (eds.): 100 Jahre Produktionstechnik - Werkzeugmaschinenlabor WZL der RWTH Aachen von 1906 bis 2006. Springer, Berlin. ISBN 978-3-540-33315-9

- [FACT12] Product information from Fine Abrasives Taiwan Co., Ltd.; url:<http://www.factdiamond.com/index.htm>. Accessed 30 Aug 2012
- [FALK98] Falkenberg, Y.: Elektroerosives Schärfen von Bornitridschleifscheiben. Doctoral Thesis at University Hannover (1998)
- [FARK72] Farkas, P.: Permattach diamond tool corporation: method of coating diamond particles with metal. Patent US 3,650,714, 21 Mar 1972
- [FEPA06] FEPA-Standard 42-1:2006: Grains of fused aluminium oxide, silicon carbide and other abrasive materials for bonded abrasives and for general industrial applications Macrogrits F 4 to F 220 (2006). FEPA-Standard 42-2:2006: Grains of fused aluminium oxide, silicon carbide and other abrasive materials for bonded abrasives and for general industrial applications Microgrits F 230 to F 2000 (2006)
- [FERL92] Ferlemann, F.: Schleifen mit höchsten Schnittgeschwindigkeiten. Doctoral Thesis at RWTH Aachen University (1992)
- [FHG08] Study of the Fraunhofer Gesellschaft FhG: Energieeffizienz in der Produktion-Untersuchung zum Handlungs- und Forschungsbedarf, funded by the German Federal Ministry of Education and Research (BMBF) (2008). url:http://www.produktionsforschung.de/ucm/groups/contribution/@pft/documents/native/ucm01_000308.pdf. Accessed 11 Aug 2012
- [FIEL79] Field, J.E.: The Properties of Diamond. Academic Press, London (1979)
- [FIEL81] Field, J.E., Freeman, C.J.: Strength and fracture of diamond. *Philos. Mag.* **43**(6), 595–618 (1981)
- [FRAC10] Francois, E.C., Zhang, G., Klett, M.W., Saint Gobain Abrasives Inc.: Reinforced bonded abrasive tools. Patent Application Publication US 2010/0190424 A1, 29 Jul 2010
- [FRAN67] Frank, H.: Schleifscheiben fuer das Hochgeschwindigkeitsschleifen. Vortragsveroeffentlichungen Haus der Technik Essen. **149**, 56 ff. (1967)
- [FRIE02] Friemuth, T.: Herstellung spanender Werkzeuge. Habilitation Thesis, University of Hanover (2002)
- [GÄBL03] Gäbler, J., Schäfer, L., Menze, B., Hoffmeister, H.-W.: Micro abrasive pencils with CVD diamond coating. *Diam. Relat. Mater.* **12**, 707–710 (2003)
- [GAHR87] Zum Gahr, K.-H.: *Microstructure and Wear of Materials*. Tribology Series 10. Elsevier, New York (1987)
- [GAHR88] Zum Gahr, K.-H.: Modelling of two-body abrasive wear. *Wear* **124**(1), 87–103 (1988). ISSN 0043-1648, [10.1016/0043-1648\(88\)90236-0](https://doi.org/10.1016/0043-1648(88)90236-0).
- [GANI77] Gani, M.S.J., McPherson, R.: Glass formation and phase transformations in plasma prepared $\text{Al}_2\text{O}_3\text{-SiO}_2$ powders. *J. Mater. Sci.* **12**, 999–1009 (1977)
- [GARD88] Gardinier, C.F.: Physical properties of superabrasives. *Ceram. Bull.* **67**(6), 1006 (1988)
- [GÄRT82] Gärtner, W.: Untersuchungen zum Abrichten von Diamant- und Bornitridschleifscheiben. Doctoral Thesis at University Hannover (1982)
- [GARZ00] Gardziella, A., Pilato, L., Knop, A.: *Phenolic Resins: Chemistry, Applications, Standardization, Safety, and Ecology*, 2nd completely revised edn. Springer, Berlin (2000). ISBN 978-3-540-65517-6
- [GEBH99] Gebhardt, H., Macht, W.: Innovatives Nickel-Ablöseverfahren für Diamantwerkzeuge. *Industrie Diamanten Rundschau* **33**(1), 78 (1999)
- [GERH70] Gerhardt, J.S.: Thermal problems and grinding wheel characteristics. SME Technical paper, MR70-805, 1970-01-10, Product ID: TP70PUB278
- [GEST12] Institut fuer Arbeitsschutz der Deutschen Gesetzlichen Unfallversicherung: GESTIS-Stoffdatenbank. url:<http://gestis.itrust.de/>. Accessed 15 Oct 2012

- [GESU00] GE Superabrasives: Diamond Characterization, company brochure (2000). www.AbrasivesNet.com
- [GOED36] Goedecke, H.: Die Vorgänge im schleifenden Gefüge von Schleifscheiben und deren zahlenmäßige Erfassung. Doctoral Thesis at RWTH Aachen University (1936)
- [GOGO99] Gogotsi, Y.G., Kailer, A., Nickel, K.G.: Transformation of diamond to graphite. *Nature* 663–664 (1999)
- [GRAN10] Granta CES Edupack 2010, Version 6.2.0, 2010, Granta Design Limited
- [GRAN12] Granta CES Edupack 2012, Version 11.9.9, 2012, Granta Design Limited
- [GREI06] Greim, J., Schwetz, K.A.: Boron carbide, boron nitride, and metal boride. In: Ullmann's Encyclopedia of Industrial Chemistry. Wiley-VCH Verlag GmbH & Co. KGaA. Published Online: 15 Dec 2006. doi:[10.1002/14356007.a04_295.pub2](https://doi.org/10.1002/14356007.a04_295.pub2)
- [GRÜN88] Grün, F.-J.: Fräsabrichten-Ein neuartiges Verfahren zur Einsatzvorbereitung konventioneller und hochharter Schleifscheiben. VDI-Z **130**, 67–68 (1988)
- [GÜHR67] Gühring, K.: Hochleistungsschleifen-Eine Methode zur Leistungssteigerung der Schleifverfahren durch hohe Schnittgeschwindigkeiten. Doctoral Thesis at RWTH Aachen University (1967)
- [GUTO06] Gutowski, T., Dahmus, J., Thiriez, A.: Electrical energy requirements for manufacturing processes. In: Proceedings of the 13th CIRP International Conference on LCE, Leuven, Belgium (2006)
- [HABI80] Habig, K.H.: Verschleiß und Härte von Werkstoffen. Carl Hanser Verlag, München, Wien (1980). ISBN 3446129650
- [HADE66] Hadert, H.: Aufbau von Schleifscheiben und Schleifpapieren. *Chemiker-Zeitung/Chemische Apparatur* **90**(23), 801 (1966)
- [HAHN55] Hahn, R.S.: The effect of wheel-work conformity in precision grinding. *Trans. ASME* **77**, 1325–1329 (1955)
- [HALL60] Hall, H.T., Strong, H.M., Wentorf, R.H.: General Electric Company: Method of Making Diamonds. Patent US 2,947,610, 2 Aug 1960
- [HAMB01] Hambuecker, S.: Technologie der Politur sphärischer Optiken mit Hilfe der Synchronspeed-Kinematik. Doctoral Thesis at the RWTH Aachen University (2001)
- [HARB97] Harbs, U.: Beitrag zur Einsatzvorbereitung hochharter Schleifscheiben. Doctoral Thesis at Technische University Braunschweig (1997)
- [HARI83] Harris, D.I.: Norton Company: microwave heating process for grinding wheels. Patent US 4,404,003, 13 Sep 1983
- [HARP03] Harper, C.A., Petrie, E.M.: *Plastics Materials and Processes: A Concise Encyclopedia*. Wiley, New York (2003). ISBN 9-780-471-456-032
- [HARR89] Harris, G.I.: Long life resin bond wheels. *IDR* **3**(89), 123–125
- [HAUB02] Haubner, R., Wilhelm, M., Weissenbacher, R., Lux, B.: Boron nitrides—properties, synthesis and applications. In: Jansen, M. (ed.) *High Performance Non-Oxide Ceramics II*, vol. 102, pp. 1–45 (2002). Springer, Berlin, ISBN 978-3-540-43132-9
- [HAUE07] Hauer, B.: Tiny bubbles, *Ceramic Industry*, October 2007, p. 20–21
- [HAUS05] Hauschild, M., Jeswiet, J., Alting, L.: From life cycle assessment to sustainable production: status and perspectives. *Ann. CIRP* **54**(2), 1–21 (2005)
- [HAUS08] Hauschild, M., Dreyer, L.C., Jørgensen, A.: Assessing social impacts in a life cycle perspective-lessons learned. *Ann. CIRP* **57**(1), 21–24 (2008)
- [HAY90] Hay, J., Markhoff-Matheny, C.J., Swanson, B.E., Norton Company: frit bonded abrasive wheel. Patent US 4,898,597, 6 Feb 1990

- [HEIN09a] Heinzl, C., Rickens, K.: Engineered wheels for grinding of optical glass. *Ann. CIRP* **58**(1), 315–318 (2009)
- [HEIN09b] Heinzl, C.: Schleifprozesse verstehen: Zum Stand der Modellbildung und Simulation sowie unterstützender experimenteller Methoden. Habilitation Thesis at the University of Bremen (2009). ISBN 978-3-8322-8614-9
- [HEIN12] Heinzl, C., Antsupov, G.: Prevention of wheel clogging in creep feed grinding by efficient tool cleaning. *Ann. CIRP* **61**(1), 323–326 (2012)
- [HELL05a] Helletsberger, H.: Grindology Papers G3 Schleifverhaeltnis/G-Faktor. Grindology College of Tyrolit Schleifmittelwerke Swarovski K.G., 2005–2010
- [HELL05b] Helletsberger, H.: Grindology Papers G1 Arbeitsgeschwindigkeit. Grindology College of Tyrolit Schleifmittelwerke Swarovski K.G., 2005–2010
- [HELL11] Helletsberger, H., Huber, W., Larch, C.: Grindology Movie GM2-Grinding Stock Removal. Grindology College, Tyrolit Schleifmittelwerke Swarovski KG, A-6130 Schwaz
- [HELL94] Helletsberger, H., Sigwart, K., Neururer, K., Noichl, H.: CBN-Schleifscheiben in Keramik; Eine neue Ära hat begonnen; Folge 1, Schleifen und Trennen, Tyrolit (120), pp. 13–20 (1994)
- [HELU11] Helu, M., Vijayaraghavan, A., Dornfeld, D.: Evaluating the relationship between use phase environmental impacts and manufacturing process precision. *Ann. CIRP* **60**(1), 49–52 (2011)
- [HENN84] Henn, K.: Qualität und Kosten beim spitzenlosen Durchlaufschleifen. Doctoral Thesis at RWTH Aachen University (1984)
- [HERB80] Herbert, S.: Norton 're-invents' the resinoid wheel. *IDR* 281–283 (1980)
- [HERB81] Herbert, S.: Micron diamond-an advancing technology. *IDR* **3**(81), 115–119 (1981)
- [HERR10] Herrmann, C.: Ganzheitliches Life Cycle Management - Nachhaltigkeit und Lebenszyklusorientierung im Unternehmen (2010). Springer, Berlin. ISBN 978-3-642-01420-8
- [HESS03] Hessel, D.: Punktcrushieren keramisch gebundener Diamantschleifscheiben. Doctoral Thesis at University Hannover (2003)
- [HICK91] Hickory, G.E., White, M.J., Norton Company: grinding wheel abrasive composition. Patent US 5,061,295, 29 Oct 1991
- [HIGG04] Higgins, A.C.: Electric furnace. Patent US 775,654, 22 Nov 1904
- [HILL00] Hill, C.P.R., Watkins, J.R., Ray, C., Rolls-Royce PLC: Method and apparatus for grinding. Patent US 6,123,606, 26 Sept 2000
- [HIME08] Himmelsbach, G., Erwin Junker Maschinenfabrik GmbH: Clamping device comprising a centring device on a grinding spindle rotor, and rotary part comprising one such centring device. Patent EP 1,827,761, 16 Apr 2008
- [HIMM90] Himmel, T., Bettles, C.J., Swain, M.V.: Crushing strength of diamond grits. *J. Hard Mater.* **1**(2), 103–121 (1990)
- [HITC05] Hitchiner, M.P., McSpadden, S.B., Webster, J.A.: Evaluation of factors controlling CBN abrasive selection for vitrified bonded wheels. *Ann. CIRP* **54**(1), 277–280 (2005)
- [HOGG01] Hogg, R., Cho, H.: Grinding. In: *Encyclopedia of Materials: Science and Technology*, pp. 3652–3658. Elsevier, New York (2001). ISBN 0-08-0431526
- [HOLL95] Hollemann, A.F., Wiberg, E.: *Lehrbuch der Anorganischen Chemie*, 101st edn. Walter der Gruyter, Berlin (1995)
- [HORI10] Horiba Instruments, Inc.: A Guidebook to Particle Size Analysis, company brochure (2010)

- [HOU03] Hou, Z.B., Komanduri, R.: On the mechanics of the grinding process - part I. Stochastic nature of the grinding process. *Int. J. Mach. Tools Manuf.* **43**, 1579–1593 (2003)
- [HOWA12] Howard, S.C., Chesna, J.W., Mullany, B., Smith, S.T.: Observations during vortex machining process development. In: Proceedings of the ASME 2012 International Manufacturing Science and Engineering Conference MSEC2012, Notre Dame, Indiana, USA, 4–8 June 2012
- [HUTC10] Hutchins, M.J., Gierke, J.S., Sutherland, J.W.: Development of a framework and indicators for societal sustainability in support of manufacturing enterprise decisions. *Trans. NAMRI/SME* **38**, 759–766 (2010)
- [HÜTT72] Hütt, R.: Untersuchung der Zerspanung von Steinen mit Diamantspitzen. Doctoral Thesis at University Hannover (1972)
- [HUZI00] Huzinec, G.M., Milacron Inc.: Vitreous bond compositions for abrasive articles. Patent US 6123744, 26 Sep 2000
- [HUZI12] Huzinec, G.M., Koval, W.F.: 3M innovative properties company: abrasive composition and article forme therefrom. Patent US 8206473, 26 June 2012
- [HYAT10] Hyatt, G., Sahasrabudhe, A., Mori Seiki USA, Inc.: Machine including grinding wheel and wheel dresser. Patent US 7,797,074 B2, 14 Sept 2010
- [ILIO09] Ilio, A.Di, Paoletti, A., D'Addona, D.: Characterization and modelling of the grinding process of metal matrix. *Ann. CIRP* **58**(1/2009), 291–294 (2009)
- [INAS77] Inasaki, I.: Monitoring of dressing and grinding processes with acoustic emission signals. *Ann. CIRP* **34**(1), 277–280 (1985)
- [INAS88] Inasaki, I.: Speed stroke grinding of advanced ceramics. *Ann. CIRP* **37**(1), 299–302 (1988)
- [ISO89] International standard ISO 3002-5:1989: Basic quantities in cutting and grinding—Part 5: Basic terminology for grinding processes using grinding wheels (1989)
- [ITOH98] Itoh, N., Ohmori, H., Moriyasu, S., Kasai, T., Karaki-Doy, T., Bandyopadhy, B.P.: Finishing characteristics of brittle materials by ELID-lap grinding using metal - resin bonded wheels. *Int. J. Mach. Tools Manuf.* **38**, 747–762 (1998)
- [JACK00a] Jackson, M.J., Mills, B.: Interfacial bonding between corundum and glass. *J. Mater. Sci. Lett.* **19**, 915–917 (2000)
- [JACK00b] Jackson, M.J., Mills, B.: Materials selection applied to vitrified alumina and CBN grinding wheels. *J. Mater. Process. Technol.* **108**, 114–124 (2000)
- [JACK07] Jackson, M.J.: Sintering and vitrification heat treatment of cBN grinding wheels. *J. Mater. Process. Technol.* **191**(1–3), 232–234 (2007)
- [JACK11] Jackson, M.J., Davim, J.P.: *Machining with Abrasives*. Springer, Berlin (2011). doi:[10.1007/978-1-4419-7302-3](https://doi.org/10.1007/978-1-4419-7302-3)
- [JACK95] Jackson, M.J.: A study of vitreous-bonded abrasive materials. PhD-Thesis at Liverpool John Moores University (1995)
- [JACO00] Jacobs, C.B.: Process of manufacturing abrasive material. Patent US 659,926, 16 Oct 1900
- [JACO00] Jaeger, H., Frohs, W., Collin, G., von Sturm, F., Vohler, O., Nutsch, G.: Carbon, 1. General. In: *Ullmann's Encyclopedia of Industrial Chemistry*. Wiley-VCH Verlag GmbH & Co. KGaA. Published Online 15 Jan 2010

- [JAIN12] Jain, R., Urban, L., Balbach, H., Webb, M.D.: Handbook of Environmental Engineering Assessment: Strategy, Planning, and Management. Butterworth-Heinemann, Oxford (2012). ISBN 978-0-12-388444-2
- [JAYA10] Jayal, A.D., Badurdeen, F., Dillon, O.W., Jawahir, I.S.: Sustainable manufacturing: modeling and optimization challenges at the product, process and system levels. *CIRP J. Manuf. Sci. Technol.* **2**(3), 144–152 (2010)
- [JHA06] Jha, S., Jain, V.K.: Modeling and simulation of surface roughness in magnetorheological abrasive flow finishing (MRAFF) process. *Wear* **261**, 856–866 (2006)
- [JOSH04] Joshi, S.V., Drzal, L.T., Mohanty, A.K., Arora, S.: Are natural fiber composites environmentally superior to glass fiber reinforced composites? *Composites Part A* **35**, 371–376 (2004)
- [JOUN12] Joung, C.B., Carrell, J., Sarkar, P., Feng, S.C.: Categorization of indicators for sustainable manufacturing. *Ecol. Ind.* **24**, 148–157 (2012)
- [JUCH78] Juchem, H.: Einsatz von Hochleistungs-Schleifmitteln für die Bearbeitung metallischer Werkstoffe. *Industrie Diamanten Rundschau* **12**(2), 88–95 (1978)
- [KAIS97] Kaiser, M.: Fortschrittliches Abrichten moderner Schleifscheiben, *Jahrbuch Schleifen, Honen, Läppen und Polieren*, 58, pp. 324–339. Ausgabe, Hsrg. Tönshoff, H.K.; Westkämper, E., Vulkan-Verlag (1997). ISBN 3-8027-2915-3
- [KALI11] Kalita, P., Malshe, A.P., Kumar, S.A., Yoganath, V.G., Gurusurthy, T.: Study of specific energy and friction coefficient in minimum quantity lubrication grinding using oil-based nanolubricants. *Proc. NAMRI/SME* **39** (2011)
- [KALL11] Kalla, D., Corcoran, S., Twomey, J., Overcash, M.: Energy consumption in discrete part production. In: *Proceedings of the ASME 2011 International Manufacturing Science and Engineering Conference MSEC2011*, Corvallis, Oregon, USA, 13–17 June 2011
- [KALP97] Kalpakjian, S.: *Manufacturing Processes for Engineering Materials*, 3rd edn. Addison-Wesley, Boston (1997). ISBN 0-201-82370-5
- [KAMM06] Kammler, M.: Untersuchungen zur Bestimmung der Biegebruchfestigkeit gebundener Schleifmittel. *Materialwissenschaft und Werkstofftechnik* **37** (5), 396–401 (2006)
- [KARA10] Kara, S., Manmek, S.: Cradle-to-gate embodied energy of products. In: *Proceedings of the 17th CIRP International Conference on Life Cycle Engineering LCE 2010*, Hefei, pp. 66–70, 19–21 May 2010
- [KARP01] Karpuschewski, B.: *Sensoren zur Prozessüberwachung beim Spanen*. University Delft, Habilitationsschrift (2001)
- [KARP08] Karpuschewski, B., Knoche, H.-J., Hipke, M.: Gear finishing by abrasive processes. *Ann. CIRP* **57**(2), 621–640 (2008)
- [KARP09] Karpuschewski, B., Byelyayev, O., Maiboroda, V.S.: Magneto-abrasive mahining for the mechanical preparation of high-speed steel twist drills. *Ann. CIRP* **58**(1), 295–298 (2009)
- [KASA90] Kasai, T., Horio, K., Karaki-Doy, T., Kobayashi, A.: Improvement of conventional polishing conditions for obtaining super smooth surfaces of glass and metal works. *Ann. CIRP* **39**(1), 321 (1990)
- [KASS69] Kassen, G.: *Beschreibung der elementaren Kinematik des Schleifvorgangs*. Doctoral Thesis at RWTH Aachen University (1969)

- [KELL11] Kellens, K., Dewulf, W.; Duflou, J.R.: Preliminary environmental assessment of electrical discharge machining. In: Proceedings of the 18th CIRP International Conference on Life Cycle Engineering. Technische Universität Braunschweig, Braunschweig, Germany, 2nd-4th May 2011
- [KELL12a] Kellens, K., Dewulf, W., Overcash, M., Hauschild, M., Duflou, J.: Methodology for systematic analysis and improvement of manufacturing unit process life cycle inventory (UPLCI) CO2PE! initiative (cooperative effort on process emissions in manufacturing). Part 1: Methodology description. *Int. J. Life Cycle Assess.* **17**(1), 69–78 (2012)
- [KELL12b] Kellens, K., Dewulf, W., Overcash, M., Hauschild, M., Duflou, J.: Methodology for systematic analysis and improvement of manufacturing unit process life cycle inventory (UPLCI) CO2PE! initiative (cooperative effort on process emissions in manufacturing). Part 2: case studies, The. *Int. J. Life Cycle Assess.* **17**(2), 242–251 (2012)
- [KHAL79] Khaladji, J.E.: Das Polieren von Mineralglas. Vortrag im Rahmen eines Seminars im Institut Tele-Iraiotecniczny, Warschau (1979)
- [KHVO08] Khvostantsev, L.G., Slesarev, V.N.: Large-volume high-pressure devices for physical investigations. *Physics ± Uspekhi* **51**(10), 1059–1063 (2008)
- [KIEN63] Kienzle, O., Crasemann, H.I., Gruening, K.: Wege zur Erhoehung der Umfangsgeschwindigkeit von Schleifscheiben. *Zeitschrift des Vereins Deutscher Ingenieure.* **105**(26) (1963)
- [KING86] King, R.I., Hahn, R.S.: Handbook of Modern Grinding Technology. Chapman and Hall, London (1986). ISBN 0-412-01081-X
- [KIRC10] Kirchgatter, M.: Einsatzverhalten genuteter CBN-Schleifscheiben mit keramischer Bindung beim Aussenrund-Einsteichschleifen. PhD Dissertation at the University of Berlin (2010)
- [KIRK74] Kirk, J.A., Syniuta, W.D.: Scanning electron microscopy and microprobe investigation of high speed sliding wear of aluminum oxide. *Wear* **27**(3), 367–381 (1974)
- [KLAU76] Klaus, J.: Der Einsatz von Grafit bei der Herstellung von Diamantwerkzeugen. *Industrie Diamanten Rundschau* **10**(4), 223–228 (1976)
- [KLEB98] Kleber, W., Bausch, H.-J., Bohm, J.: Einführung in die Kristallographie. Verlag Technik GmbH Berlin, 18. Auflage (1998)
- [KLIN09] Klink, A.: Funkenerosives und elektrochemisches Abrichten feinkoerniger Schleifwerkzeuge. Doctoral Thesis at the RWTH Aachen University (2009)
- [KLOC02] Klocke, F., Engelhorn, R., Mayer, J., Weirich, T.: Micro-analysis of the contact zone of tribologically loaded second-phase reinforced sol - gel - abrasives. *Ann. CIRP* **51**(1), 245–250 (2002)
- [KLOC03] Klocke, F.: Flexible Hochgeschwindigkeitsbearbeitung mit Schleifscheiben aus mikrokristallinem Aluminiumoxid. End report, Project S 498 Stiftung Industrieforschung (2003)
- [KLOC05a] Klocke, F., König, W.: *Fertigungsverfahren Band 2-Schleifen, Honen, Läppen*, 4. Auflage. Springer, Berlin. ISBN: 3-5402-3496-9 (2005)
- [KLOC05b] Klocke, F., Linke, B.: FWF Forschungsvorhaben Nr. AiF 13811 N/1 “Verschleißausbildung an Diamantformrollen”, Abschlussbericht, Projektlaufzeit: 1.10.2003–30.9.2005
- [KLOC05c] Klocke, F., Groening, H.: Characterization of vitrified bonded CBN grinding wheels. *Prod. Eng.* **12**, 15–18 (2005)
- [KLOC05d] Klocke, F., Brinksmeier, E., Weinert, K.: Capability profile of hard cutting and grinding processes. *Ann. CIRP* **54**(2), 557 ff. (2005)

- [KLOC06a] Klocke, F., Nachmani, Z., Telle, R., Kuhl, I.: Haftungskriterien an der Schnittstelle Korn/Bindung für Sol-Gel-Korund-Schleifwerkzeuge, Abschlussbericht, AiF-Projekt 13 972 N, Laufzeit 01.02.04–31.01.06
- [KLOC06b] Klocke, F., Zeppenfeld, C., Linke, B.: Verschleißausbildung an Diamantformrollen, wt Werkstatttechnik online. Ausgabe 6-2006
- [KLOC07] Klocke, F., König, W.: Fertigungsverfahren Band 3-Abtragen, Generieren, Lasermaterialbearbeitung, 4. Auflage. Springer, Berlin (2007). ISBN: 3-5402-3492-6
- [KLOC08b] Klocke, F., Linke, B.: Mechanisms in the generation of grinding wheel topography by dressing. In: WGP Annals of the German Academic Society for Production Engineering, vol. 2, pp. 157–163 (2008). ISSN 0944-6524 (Print) ISSN 1863-7353 (Online)
- [KLOC09] Klocke, F.: Manufacturing Processes 2-Grinding, Honing, Lapping (RWTH Edition, Trans.: Kuchle, A.). Springer, Berlin (2009). ISBN 978-3-540-92258-2
- [KLOC10] Klocke, F., Linke, B., Meyer, B., Roderburg, A.: Sustainability aspects in centerless grinding. In: Proceedings of the Conference of Sustainable Life in Manufacturing SLIM2010, Egirdir, Turkey, 24–25 May 2010
- [KLOC11] Klocke, F.: Manufacturing Processes 1-Cutting (RWTH Edition, Trans.: Kuchle, A.). Springer, Berlin (2011). ISBN 978-3-642-11978-1
- [KLOC82] Klocke, F.: Gewindeschleifen mit Bomitridschleifscheiben. Doctoral Thesis at the Technical University of Berlin (1982)
- [KLOC87] Klocke, F., Blanke, G.: Abrichten mit Diamant-Abrichtrollen. Industrie Diamanten Rundschau Ausgabe 1, 14–19 (1987)
- [KLOC97] Klocke, F., Brinksmeier, E., Evans, C., Howes, T., Inasaki, I., Minke, E., Toenschhoff, H.K., Webster, J.A., Stuff, D.: High-speed grinding—fundamentals and state of the art in Europe, Japan and the USA. Ann. CIRP 46 (2), 715–724 (1997)
- [KLOM86] Klocke, M.: Einfluss des Gefüges von Edelkorundschleifscheiben auf ihre Werkstoffkennwerte und das Schleifverhalten. Doctoral Thesis at TU Berlin (1986)
- [KNIG22] Knight, A.: Observations on the grinder's asthma. University of London Library (1822)
- [KOMA01] Komanduri, R., Iyengar, S.: Conventional and super abrasive materials. In: Encyclopedia of Materials: Science and Technology, pp. 1629–1652. Elsevier, New York (2001). ISBN 0-08-0431526
- [KOMA07] Komanduri, R., Iyengar, S.: Conventional and super abrasive material. In: Mortense, A. (ed.) Concise Encyclopedia of Composite Materials, pp. 275–298. Elsevier, New York. ISBN 9-780-080-451-268
- [KOMA76] Komanduri, R., Shaw, M.C.: On the diffusion wear of diamond in grinding pure iron. Philos. Mag 34(2) (1976)
- [KOMA76b] Komanduri, R., Shaw, M.C.: Attritious wear of silicon carbide abrasive. Trans. ASME J. Engg. Ind. 98, 1125 (1976)
- [KOMA97] Komanduri, R., Lucca, D.A., Tani, Y.: Technological advances in fine abrasive processes. Ann. CIRP 46(2), 545 (1997)
- [KOMP05] Kompella, S., Turner, D.W., Proske, K.: Coatings for superabrasive crystals. In: Proceedings of the Diamond at Work Conference, Barcelona (2005)
- [KONE94] Konetzke: 4. Seltene Pneumokoniosen. In: Konietzko, N., Wendel, H., Wiesner, B. (eds.) Erkrankungen der Lunge, de Gruyter (1994). ISBN 3-11-012130-1

- [KÖNI70] König, W., Schreitmüller, H., Sperling, F., Werner, G., Younis, M.: A survey of the present state of high speed grinding. *Ann. CIRP* **19**(2), 275–283 (1970)
- [KÖNI79] König, W., Saljé, E., Messer, J., Rohde, G.: Systematische Analyse der Zusammenhänge zwischen Schleifscheibe, Maschinenstellgrößen und Arbeitsergebnis am Beispiel des Außenrundscheifens bei ausgesuchten Werkstoffen, VDW-Forschungsbericht Nr. A 3902, Aug 1979
- [KÖNI80] König, W., Schleich, H.: Deep grinding of high speed tool steel with CBN. *IDR*, 372–377 (1980)
- [KÖNI81] König, W., Messer, J.: Influence of the composition and structure of steels on grinding process. *Ann. CIRP* **30**(2), 547–552 (1981)
- [KÖNI84] König, W., Henn, K.: Mehrstufige Prozeßführung beim spitzenlosen Schleifen im Durchlaufverfahren. *Forschungsbericht des Landes Nordrhein-Westfalen*, Westdeutscher Verlag (1984)
- [KÖNI85] König, W., Vits, R.: Optimales Kühlschmiermittel beim Abrichten. *Industrie Anzeiger* Heft **63**, 24–26 (1985)
- [KÖNI86] König, W., Tönshoff, H.K., Fromlowitz, J., Dennis, P.: Belt grinding. *Ann. CIRP* **35**(2), 487–494 (1986)
- [KÖNI90] König, W., Ferlemann, F.: CBN-Schleifscheiben fuer 500 m/s Schnittgeschwindigkeit. *Industrie Diamanten Rundschau* **24**(4), 242–251 (1990)
- [KOPP81] Kopp, O.: A new mult-spindle honing and step reaming machine. *IDR* **1**, 4–8 (1981)
- [KOSH03] Koshy, P., Iwasaki, A., Elbestawi, M.A.: Surface generation with engineered diamond grinding wheels: insights from simulation. *Ann. CIRP* **52**(1), 271 (2003)
- [KRAF08] Kraft, I., Mertens, U.: Trends in der Schleifscheibenentwicklung bei Diamant- und CBN-Werkzeugen, 3. Dortmunder Schleifseminar, 25 Sept 2008
- [KRAJ03] Krajnc, D., Glavic, P.: Indicators of sustainable production. *Clean. Technol. Environ. Policy* **5**, 279–288 (2003)
- [KREB06] Krebs & Riedel Schleifscheibenfabrik GmbH & Co. KG company brochure: Schleifwerkzeuge KAD-100/2006
- [KREL95] Krell, A., Blank, P.: Grain size dependence of hardness in dense submicrometer alumina. *J. Am. Ceram. Soc.* **78**(4), 1118–1120 (1995)
- [KRIS04] Krishnan, N., Raoux, S., Dornfeld, D.: Quantifying the environmental footprint of semiconductor equipment using the environmental value systems analysis (EnVS). *IEEE Trans. Semicond. Manuf.* **17**(4), 554–561 (2004)
- [KRUG35] Kurt, C.: Grinding Disk. Patent US 2,004,630, 11 June 1935
- [KUEN98] Künanz, K., Knösel, E., Franke, A.: Diagnose zur Bewertung des Leistungsvermögens von Schleifwerkzeugen. *Industrie Diamanten Rundschau* **32**(3), 206–217 (1998)
- [KUMA84] Kumagai, N., Kamei, K.: Grinding of titanium with jet infusion of grinding fluid, *Titanium Science and Technology*. In: *Proceedings of the Fifth International Conference on Titanium*, Munich, pp. 1015–1022, 10–14 Sept 1984
- [KUNZ91] Kunz, R., Strittmatter, R., Lonza Ltd.: Hydrophobically Coated Abrasive Grain. Patent US 5,042,991, 27 Aug 1991
- [KWON03] Kwon, W.-T., Kim, Y.-H., Kim, S.R., Lim, T.-Y.: Characterization of glass abrasive sludge and its reutilization as a cement admixture. *Mater. Sci. Forum* **439**, 176–179 (2003)

- [LANG76] Langbein, R.: Maßnahmen zur Steigerung der Sicherheit an Hochgeschwindigkeitsschleifmaschinen. Doctoral Thesis at the RWTH Aachen University (1976)
- [LAUE79] Lauer-Schmaltz, H.: Zusetzung von Schleifscheiben. Doctoral Thesis at RWTH Aachen University (1979)
- [LAUE80] Lauer-Schmaltz, H., König, W.: Phenomenon of wheel loading mechanisms in grinding. *Ann. CIRP* **29**(1), 201–206 (1980)
- [LAVE23] La Vercombe, H.H.: Grinding-Wheel-Test device. Patent US1,446,977, 27 Feb 1923
- [LENZ86] Lenzen, G., Günther, B.: Diamantenkunde mit kritischer Darstellung der Diamantengraduierung. Lenzen, Kirschweiler (1986)
- [LEWI76] Lewis, K.B., Schleicher, W.F.: The grinding wheel—a textbook of modern grinding practice, 3rd edn. The Grinding Wheel Institute, Cleveland (1976)
- [LIO2] Li, Z.C., Lin, B., Xu, Y.S., Hu, J.: Experimental studies on grinding forces and force ratio of the unsteady-state grinding technique. *J. Mater. Process. Technol.* **129**(1–3), 76–80 (2002)
- [LIEB96] Liebe, I.: Auswahl und Konditionierung von Werkzeugen für das Außenrund-Profileschleifen technischer Keramiken. Doctoral Thesis at TU Berlin (1996)
- [LIED99] Liedtke, S.: Schleifschlamm-entölung und Qualitätskontrolle der zurückgewonnenen Kühlschmierstoffe. Doctoral Thesis at the University Carolo-Wilhelmina (1999)
- [LIER01] Lierse, T., Kaiser, M.: Abrichten von Schleifwerkzeugen für die Verzahnung. *Industrie Diamanten Rundschau* Ausgabe **4**, 297–310 (2001)
- [LIER02] Lierse, T., Kaiser, M.: Dressing of grinding wheels for gearwheels. *Ind. Diam. Rev.* **4**, 273–281 (2002)
- [LIET08] Liethschmidt, K., Garbes, J.: Silicon carbide. In: *Ullmann's Encyclopedia of Industrial Chemistry*. Wiley-VCH Verlag GmbH & Co. KGaA. Published Online 15 Apr 2008. doi:[10.1002/14356007.a23_749.pub2](https://doi.org/10.1002/14356007.a23_749.pub2)
- [LINB70] Lindenbeck, D.-A.: Schleifen von Eisenwerkstoffen mit Diamantschleifscheiben, *Fortschr.-Ber. VDI-Z. Reihe 2 Nr. 22*, VDI-Verlag GmbH Düsseldorf (1970)
- [LIND69] Lindsay, R.P.: Dressing and its effect on grinding performance. *American Society of Tool Manufacturing Engineering Technology Paper MR*, pp. 69–568 (1969)
- [LINE92] Linke, K.: Kennwerte keramisch gebundener Schleifscheiben aus kubischem Bornitrid. Doctoral Thesis at the University of Berlin (1992)
- [LINK05] Linke, B., Friedrich, D., Klocke, F.: Beeinflussung des Rundheitsfehlers beim spitzenlosen Schleifen. In: Hoffmeister, H., Denkena, B. (ed.) *Jahrbuch Schleifen, Honen, Läppen und Polieren 62*. Ausgabe. Vulkan-Verlag GmbH Essen, pp. 77–90 (2005). ISBN 978-3-8027-2934-8
- [LINK07] Linke, B.: Wirkmechanismen beim Abrichten keramisch gebundener Schleifscheiben. Doctoral Thesis at RWTH Aachen University (2007)
- [LINK08a] Linke, B., Klocke, F., Wegner, H., Zeppenfeld, C.: Manufacturing of ophthalmic ceramic scalpels. In: 3rd International CIRP Conference High Performance Cutting (HPC). Proceedings, Dublin, vol. 2, pp. 841–848, 12th–13th June 2008. ISBN 978-1-905254-32-3
- [LINK08b] Linke, B., Wegner, H.: Total Life Cycle Management für Werkzeuge im “Arbeitskreis Werkzeugtechnik (AKWT)”. In: *Schleifen + Polieren* **3**, 84–85 (2008)
- [LINK08c] Linke, B., sponsored by Prof. Klocke: Dressing process model for vitrified bonded grinding wheels. In: *Ann. CIRP* **57**(1), 345–348 (2008)

- [LINK09] Linke, B., Caliskanoglu, D., Schluetter, D., Wegner, H., Klocke, F.: Influence of material structure on creep feed grinding of high-speed steels. In: Proceedings of the Tool 2009, Aachen, 2–4 June 2009
- [LINK10] Linke, B., Klocke, F.: Temperatures and wear mechanisms in dressing of vitrified bonded grinding wheels. *Int. J. Mach. Tools Manuf.* **50**(6), 552–558 (2010). doi:[10.1016/j.ijmactools.2010.03.002](https://doi.org/10.1016/j.ijmactools.2010.03.002)
- [LINK11] Linke, B., Duscha, M., Klocke, F., Dornfeld, D., Combination of speed stroke grinding and high speed grinding with regard to sustainability. In: Proceedings of the 44th CIRP International Conference on Manufacturing Systems, Madison, WI, USA, 1–3 June 2011
- [LINK12] Linke, B.; Overcash, M.: Life cycle analysis of grinding, leveraging technology for a sustainable world. In: Proceedings of the 19th CIRP Conference on Life Cycle Engineering, Berkeley, CA, USA, pp. 293–298. 23–25 May 2012. ISBN 978-3-642-29068-8
- [LINK12b] Linke, B.: Superabrasives. In: CIRP (ed.), Luc Laperrière and Gunther Reinhart (Editors-in-Chief). *Encyclopedia of Production Engineering*. Accessed on 17 Sept 2012
- [LINK12c] Linke, B., Dornfeld, D.: Application of axiomatic design principles to identify more sustainable strategies for grinding. *J. Manuf. Syst.* **31**(4), 412–419
- [LINK13] Linke, B., Corman, G.; Dornfeld, D., Tönissen, S.: Sustainability indicators for discrete manufacturing processes applied to grinding technology (NAMRC41-1531). In: Proceedings of NAMRI/SME, vol. 41, Madison, WI, USA, 10–14 June 2013
- [LINK14a] Linke, B.: Superabrasives: CIRP. In: International Academy for Production Engineering Research (ed.) *Encyclopedia of Production Engineering*. doi:[10.1007/978-3-642-20617-7](https://doi.org/10.1007/978-3-642-20617-7) (2014)
- [LINK14b] Linke, B.: Centerless grinding: CIRP. In: International Academy for Production Engineering Research (ed.) *Encyclopedia of Production Engineering* (2014). doi:[10.1007/978-3-642-20617-7](https://doi.org/10.1007/978-3-642-20617-7)
- [LINK15] Linke, B.: A review on properties of abrasive grits and grit selection. *Int. J. Abrasive Technol.* **7**(1), 46–58 (2015)
- [LIST06] List, E., Frenzel, J., Vollstädt, R.: Ein neues System zur Ermittlung der Einzelkornfestigkeit von Schleifkörnungen. *Industrie Diamanten Rundschau* **40**(II), 6–21 (2006)
- [LIST08] List, E., Vollstaedt, H., Frenzel, J.: Counting particles per carat by means of two-dimensional image analysis. In: 5th ZISC Zhengzhou International Superhard Materials and Related Products Conference in Zhengzhou, Henan, China, 5–7 Sept 2008
- [LIZH11] Li, Z.H., Zhao, B., Li, L., Wong, J.: China's diamond in the world market. *Key Eng. Mater.* **487**, 526–532 (2011)
- [LORT75] Lortz, W.: *Schleifscheibentopographie und Spanbildungsmechanismus beim Schleifen*. Doctoral Thesis at the RWTH Aachen University (1975)
- [LU127] Lu, T., Rotella, G., Badurdeen, F., Dillon, O.W., Rouch, K.E., Jawahir, I.S.: 9.12 A metrics-based sustainability assessment for different coolant applications in a turning process. In: Proceedings of the CIRP GCSM, Turkey, pp. 564–569 (2012)
- [LUC13] Lucek, J.: Sandvik Hyperion, private communication, Dec 2013
- [LUDE94] Ludewig, T.: *Auswahlkriterien für SiC- und Korundschleifkorntypen beim Schleifen von Stählen*. Doctoral Thesis at RWTH Aachen University (1994)

- [LUKI05] Łukianowicz, C., Iaquinta, J.: Assessment of surface topography of abrasive sheets by light scattering and self-shadowing methods. *Arch. Civil Mech. Eng.* **V**(2) (2005)
- [LUND68] Lundblad, E.: Die Diamantsynthese. *IDR, Jahrgang* **2**(3), 156–161 (1968)
- [LYNC05] Lynch, A.J., Rowland, C.A.: *The History of Grinding*, Society for Mining, Metallurgy, and Exploration (2005). ISBN 0-87335-244-0
- [MADL08] Madl, A.K., Donovan, E.P., Gaffney, S.H., McKinley, M.A., Moody, E.C., Henshaw, J.L., Paustenbach, D.J.: State-of-the-science review of the occupational health hazards of crystalline silica in abrasive blasting operations and related requirements for respiratory protection. *J. Toxicol. Environ. Health Part B Crit. Rev.* **11**(7), 548–608 (2008)
- [MAHD00] Mahdi, M., Zhang, L.: A numerical algorithm for the full coupling of mechanical deformation thermal deformation and phase transformation in surface grinding. *Comput. Mech.* **26**, 148 f. (2000)
- [MALK08] Malkin, S., Guo, C.: *Grinding Technology: Theory and Application of Machining with Abrasives*, 2nd edn. Industrial Press (2008). ISBN 9780831132477
- [MALK68] Malkin, S.: The attritious and fracture wear of grinding wheels. PhD-Thesis at MIT, Boston (1968)
- [MALK85] Malkin, S.: Current trends in CBN grinding technology. *Ann. CIRP* **34**(2), 557–563 (1985)
- [MALZ00] Malzahn, H.u.A.: *Extra Lapis 18 Diamant-Der extreme Edelstein, das geniale Werkzeug*. Christian Weise Verlag München (2000)
- [MARI00] Marinescu, I.D., Tönshoff, H.K., Inasaki, I.: *Handbook of Ceramic Grinding and Polishing*, William Andrew (2000). ISBN 0815514247
- [MARI04] Marinescu, I.D., Rowe, W.B., Dimitrov, B., Inasaki, I.: *Tribology of abrasive machining processes*. William Andrew, Inc. (2004). ISBN 0-8155-1490-5
- [MARI07] Marinescu, I.D., Hitchiner, M., Uhlmann, E., Rowe, W.B., Inasaki, I.: *Handbook of Machining with Grinding Wheels*. CRC Press, Boca Raton (2007). ISBN 9781574446715
- [MASC12] Maschinenfabrik Liezen: Säge- und Fraestechnik. url:http://www.mfl.at/downloads/Saage-undFraestechnik_deutsch_2012.pdf. Accessed 15 Nov 2012
- [MATS75] Matsuno, Y., Yamada, H.: The microtopography of the grinding wheel surface with SEM. *Ann. CIRP* **24**(1), 237–242 (1975)
- [MCCL10] McClarence, E.: Report: Abrasive Trends, Growth factors driving the Chinese abrasives market. The AbrasivesHub 2010-08-09
- [MCCL10b] McClarence, E.: Diamond recovery—what’s it worth? *Diam. Tooling J.* **70**(626), 32–33 (2010)
- [MCCL10c] McClarence, E.: Report: Trends for cubic boron nitride. The AbrasivesHub, 2010-09-01
- [MEIS81] Meis, F.U.: Geometrische und kinematische Grundlagen für das spitzenlose Durchlaufschleifen. Doctoral Thesis at RWTH Aachen University (1981)
- [MENA00] Menard, J.-C., Thibault, N.W.: Abrasives. In: *Ullmann’s Encyclopedia of Industrial Chemistry*. Wiley-VCH Verlag GmbH & Co. KGaA (2000). http://dx.doi.org/10.1002/14356007.a01_001
- [MERB03] Merbecks, T.: Entwicklung eines Charakterisierungsverfahrens für keramisch gebundene CBN-Schleifscheiben. Doctoral Thesis at RWTH Aachen University (2003)

- [MERZ94] Merz, R.: Konzept zur Auswahl der Abrichtbedingungen bei der Einsatzvorbereitung konventioneller Schleifscheiben mit Diamantprofilrollen. Doctoral Thesis at TU Kaiserslautern (1994)
- [MESP91] Messer, P.: Batching and mixing. In: ASM International (Hrsg.). Engineered Materials Handbook: Ceramics and Glasses, pp. 95–99 (1991)
- [MESS83] Messer, J.: Abrichten konventioneller Schleifscheiben mit stehenden Werkzeugen. Doctoral Thesis at RWTH Aachen University (1983)
- [METZ86] Metzger, J.L.: Superabrasive Grinding. Butterworth & Co (1986). ISBN 0-408-01586-1
- [MEYE91] Meyen, H.-P.: Acoustic Emission (AE)-Mikroseismik im Schleifprozess. Doctoral Thesis at RWTH Aachen University (1991)
- [MEYR12] Meyer, B.: Prozesskräfte und Werkstückgeschwindigkeiten beim Spitzenlosschleifen. Doctoral Thesis at RWTH Aachen University (2012)
- [MINK88] Minke, E.: Grundlagen der Verschleißausbildung an nicht-rotierenden Abrichtschneiden zum Einsatz an konventionellen Schleifwerkzeugen. Doctoral Thesis at University Bremen (1988)
- [MINK99] Minke, E.: Handbuch zur Abrichttechnik, Verlag Riegger Diamantwerkzeuge GmbH (1999). ISBN 3-9800-5325-3
- [MOHA11] Mohan, R., Ramesh Babu, N.: Design, development and characterisation of ice bonded abrasive polishing process. *Int. J. Abrasive Technol* **4**(1) (2011)
- [MÖHL87] Möhlen, H.: Verschleißverhalten von Diamantschleifscheiben bei der Bearbeitung hochfester Keramikwerkstoffe, Schleifen, Honen, Läppen und Polieren, 54. Ausgabe. ISBN 3-8027-2675-8 (1987)
- [MOOR85] Moore, M.: Diamond morphology. *IDR* **2**(85), 67–71 (1985)
- [MORG08] Morgan, M.N., Jackson, A.R., Wua, H., Batako, A., Rowe, W.B.: Optimisation of fluid application in grinding. *Ann. CIRP* **57**(1/2008), 363–366 (2008)
- [MORT87] Mortimer, Ch. E.: Chemie-Das Basiswissen der Chemie, 5. Auflage (1987)
- [MOSE80] Moser, M.: Microstructures of ceramics, structure and properties of grinding tools. Akadémiai Kiadó, Budapest (1980)
- [MPM12] MPM Micro Präzision Marx GmbH: Company brochures. url: <http://www.mpmgmbh.de>. Last accessed 2 Sept 2012
- [MÜLB04] Müller, B.: Thermische Analyse des Zerspanens metallischer Werkstoffe bei konventionellen und hohen Schnittgeschwindigkeiten. Doctoral Thesis at RWTH Aachen University (2004)
- [MÜLL01] Müller, N.: Ermittlung des Einsatzverhaltens von Sol-Gel-Korund-Schleifscheiben. Doctoral Thesis at RWTH Aachen University (2001)
- [MULL08] Mullany, B., Corcoran, E.: An innovative look at precision polishing tools. In: 3rd International CIRP Conference High Performance Cutting (HPC), 12th–13th June 2008, Dublin, Proceedings, vol. 2, pp. 841–848. ISBN 978-1-905254-32-3
- [MÜNN56] Münnich, H.: Beitrag zur Sicherheit von umlaufenden Schleifkörpern. Doctoral Thesis at the University of Hanover (1956)
- [NABE12] Nabertherm GmbH: High-temperature furnaces/Sintering (2012). url: http://www.nabertherm.de/produkte/details/en/labordental_hochtemperaturofen. Accessed 02 Oct 2012
- [NAGA89] Nagaraj, A.P., Chattopadhyay, A.K.: On some aspects of wheel loading. *Wear* **135**(1), 41–52 (1989). doi:10.1016/0043-1648(89)90094-X
- [NAKA66] Nakayama, K.; Shaw, M.: An analytical study of the finish produced in surface grinding. 3rd Annual Report, Oct 1966, Grinding Wheel Institute Investigations of Grinding Fundamentals

- [NETT84] Netterscheid, T.: Rechnerunterstützte externe Schnittwertoptimierung beim Außenrundscheifen. Doctoral Thesis at RWTH Aachen University (1984)
- [NGUY08] Nguyen, T., Zhang, L.: Performance of a new segmented grinding wheel system. *Int. J. Mach. Tool Manuf.* **49**(1–3), 291–296 (2008)
- [NN00] Ceramic Industry, Fused Brown Alumina Production in China, 6 Aug 2000. url:<http://www.ceramicindustry.com/articles/fused-brown-alumina-production-in-china>. Accessed 21 June 2012
- [NN10] UK Carbon Trust 2010: url:<http://www.carbontrust.co.uk/>. Accessed 21 June 2012
- [NN12] Union Process, Grinding Media, url:http://www.unionprocess.com/pdf/grinding_media.pdf. Accessed 21 June 2012
- [NN74] NN., Norton Co.: Resin bonded abrasive products. Patent GB1344681, 23 Jan 1974
- [NOTT76] Notter, A.T., Nicolls, M.O.: CDA-the new high performance diamond abrasive for grinding carbide. *Ind. Diam. Rev.* Dec 433–438 (1976)
- [NOTT79] Notter, A.T., Shafto, G.R.: Einflußgrößen für das Einsatzverhalten von CDA-Körnungen beim Schleifen von Hartmetall mit kunstharzgebundenen Scheiben. *Industrie Diamanten Rundschau* **13**(2), 76–87 (1979)
- [NOTT80] Notter, A.T.: EDC and its acceptance by industry. *IDR* 46–49 (1980)
- [NOVI08] Novikov, N.V., Bogatyreva, G.P., Petasyuk, G.A.: Computer-aided analytical control of diamond and cubic boron nitride grits. *J. Phys. Conf. Ser.* **121**, 062004 (2008)
- [NOVI10] Novikov, N.V., Petasyuk, G.A., Bogatyreva, G.P.: A study of the influence of the sieve modulus and shape of openings on the fraction-wise yield of powder and size uniformity of the fractions identified by the sieve analysis. *J. Superhard Mater.* **32**(4), 280–291 (2010)
- [NPCA02] National Paint and Coatings Association: HMIS chemical ratings guide, hazardous materials identification system. In: *Chemical Ratings Guide*, 3rd edn. J.J. Keller & Associates, Inc. ISBN 1-59042-019-5
- [ODON76] O'Donovan, K.H.: Synthetische Diamanten. *Fertigung* **2**(76), 41–48 (1976)
- [OECD12] OECD: Sustainable Manufacturing Toolkit (2012). url:www.oecd.org/innovation/green/toolkit. Accessed 15 May 2012
- [OHMO90] Ohmori H., Nakagawa, T.: Mirror surface grinding of silicon wafers with electrolytic in-process dressing. *Ann. CIRP* **39**(1), 329–332 (1990)
- [OKAM78] Okamura, K., Tsukamoto, S.: What is the ideal grinding wheel? *Ann. CIRP* **27**(1), 211–215 (1978)
- [OLIV00] Oliveira, J.F.G., Coelho, R.T., Tundisi, J.E.M., Gomes, J.J.F., Bellini, P.: A new system to get information about the grinding wheel performance. *Abrasives Mag.* 24–30 (2000)
- [OLIV01] Oliveira, J.F.G., Dornfeld, D.A.: Application of AE contact sensing in reliable grinding monitoring. *Ann. CIRP* **50**(1), 217 ff. (2001)
- [OLIV09] Oliveira, J.F.G., Silva, E.J., Guo, C., Hashimoto, F.: Industrial challenges in grinding. *Ann. CIRP* **58**(1), 663–680 (2009).
- [OLIV94] Oliveira, J.F.G., Dornfeld, D.A.: Dimensional characterization of grinding wheel surface through acoustic emission. *Ann. CIRP* **43**(1), 291 (1994)
- [ONIS97] Onishi, H., Kobayashi, M., Takata, A., Ishizaki, K., Shioura, T., Kondo, Y., Tukuda, A.: Fabrication of new porous metal-bonded grinding wheels by HIP method and machining electronic ceramics. *J. Porous Mater.* **4**(3), 187–198 (1997). doi:[10.1023/A:1009667017929](https://doi.org/10.1023/A:1009667017929)
- [OPIT42] Opitz, H., Rumbach, J.: Pruefung von Schleifscheiben, TZ fuer praktische Metallbearbeitung, 52. Jahrgang **17**(18), 177–181 (1942)

- [OPIT58] Opitz, H.; Schwartz, K.-E.: Das Abrichten von Schleifscheiben mit Diamanten, Forschungsberichte des Wirtschafts- und Verkehrsministeriums Nordrhein-Westfalen, Nr. 521. Westdeutscher Verlag Köln und Opladen (1958)
- [OSHA12] Occupational Safety & Health Administration: OSHA 1910.215—Abrasive wheel machinery. 39 FR 23502, 27 June 1974, as amended at 43 FR 49750, Oct. 24, 1978; 49 FR 5323, Feb. 10, 1984; 61 FR 9227, 7 Mar 1996. url:<http://www.osha.gov>. Accessed on 26 Nov 2012
- [OSHA12b] Occupational Safety & Health Administration: OSHA Occupational Chemical Database. url:<http://www.osha.gov/chemicaldata/>. Accessed on 29 Nov 2012
- [OSTE94] Osterhaus, G.: Verfahrensübergreifende Simulation und Auslegung von Schleifprozessen. Doctoral Thesis at RWTH Aachen University (1994)
- [PADB93] Padberg, H.-J.: Aufbau und Bindungsmatrix hochbeanspruchter keramisch gebundener Zerspanungswerkzeuge. Industrie-Forum cfi/Berichte der Deutschen Keramischen Gesellschaft **70**(11/12), 598–600 (1993)
- [PAHL68] Pahlitzsch, G., Schmitt, R.: Einfluß des Abrichtens mit diamantbestückten Rollen auf der Schleifscheiben-Schneidfläche. Werkstattstechnik **58**(1), 1–8 (1968)
- [PAI89] Pai, D.M., Ratterman, E., Shaw, M.C.: Grinding swarf. Wear **131**, 329–339 (1989)
- [PAUC08] Paucksch, E., Holsten, S., Linß, M., Tikal, F.: Zerspantechnik, Prozesse, Werkzeuge, Technologien, 12th edn (2008). ISBN 978-3-8348-0279-8
- [PEKL57] Peklenik, J.: Ermittlung von geometrischen und physikalischen Kenngrößen. Doctoral Thesis at RWTH Aachen University (1957)
- [PEKL58] Peklenik, J.: Untersuchungen über das Verschleißkriterium beim Schleifen. Industrie-Anzeiger Essen **27**, 397–401 (1958)
- [PEKL60] Peklenik, J.: Untersuchungen der Härte von Schleifkörpern. Industrie-Anzeiger, Essen **28**, 431–436 (1960)
- [PINT08] Pinto, F.W., Vargas, G.E., Wegener, K.: Simulation for optimizing grain pattern on engineered grinding tools. Ann. CIRP **57**(1), 353–356 (2008)
- [PIRA03] Pirard, E.: The cutting edge of superabrasives quality control. Ind. Diam. Rev. **3**, 49–50 (2003)
- [PRES08] Presser, V., Nickel, K.G.: Silica on silicon carbide. Crit. Rev. Solid State Mater. Sci. **33**(1), 1–99 (2008)
- [QUIR80] Quiroga, E.-S.: Spannungen und Verformungen der Schleifscheibe. Doctoral Thesis at RWTH Aachen University (1980)
- [RAAL72] Raal, F.A.: Hochleistungsfähige Wärmesenken aus Typ Iia-Diamanten. Industrie Diamanten Rundschau Ausgabe **6**, 102–107 (1972)
- [RABI95] Rabinowicz, E.: Friction and Wear of Materials, 2nd edn. Wiley, New York (1995). ISBN 0-471-83084-4
- [RAED02] Raedt, J.W.: Grundlagen für das schmiermittelreduzierte Tribosystem bei der Kaltumformung des Einsatzstahles 16MnCr5. Doctoral Thesis at RWTH Aachen University (2002)
- [RAMM74] Rammerstorfer, F.G., Hastik, F.: Der dynamische E-Modul von Schleifkörpern. Werkstatt und Betrieb **107**(9), 527–533 (1974)
- [REHB03] Rehbein, W.: Cobaltaufnahme in nichtwasseremischbaren Kühlschmierstoffen. url:http://www.oelheld.de/fileadmin/content/pages/Innovation/pdf-Wissenschaftliche_Berichte/Cobaltaufnahme.pdf. Accessed 8 July 2012
- [REIC08] Reich-Weiser, C., Dornfeld, D., Home, S.: Greenhouse gas return on investment: a new metric for energy technology. In: 15th International CIRP Conference on Life Cycle Engineering, Australia (2008). Retrieved from: <http://www.escholarship.org/uc/item/5fw407kf>

- [REIC09] Reich-Weiser, C., Dornfeld, D.: A discussion of greenhouse gas emission tradeoffs and water scarcity within the supply chain. *J. Manuf. Syst.* **28**(1), 23–27 (2009)
- [REIC10] Reich-Weiser, C., Vijayaraghavan, A., Dornfeld, D.: Appropriate use of green manufacturing frameworks. In: *Proceedings of the 17th CIRP Life Cycle Engineering Conference LCE 2010*, Hefei, pp. 196–201, 19–21 May 2010
- [RICK10] Rickli, J.L., Camelio, J.A.: Impacting consumer end-of-life product return decisions with incentives. In: *Proceedings of the 17th CIRP International Conference on Life Cycle Engineering LCE 2010*, Hefei, pp. 346–351, 19–21 May 2010
- [RIVE07] Rivera, J.L., Michalek, D.J., Sutherland, J.W.: Air quality in manufacturing (Chap. 7). In: Kutz, M. (ed.) *Environmentally Conscious Manufacturing*
- [ROES12] Roesler Oberflächentechnik GmbH: *Consumables, company brochure* (2012)
- [RÖSL91] Rösler, H.J.: *Lehrbuch der Mineralogie*. Deutscher Verlag für Grundstoffindustrie, Leipzig (1991)
- [ROTH91] Roth, P., Wobker, H.-G.: Keramische Werkstoffe in der Fertigungstechnik-Schleifbearbeitung keramischer Werkstoffe. *Fachberichte Sprechsaal* **124**(4), 254–262 (1991)
- [ROWE09] Rowe, W.B.: *Principles of modern grinding technology*, William Andrew (2009). ISBN 9780815520184
- [ROWE79] Rowe, G.W.: *Elements of metal working theory*. Edward Arnold (1979). ISBN 0713134003
- [ROWE93] Rowe, W.B., Morgan, M.N., Qi, H.S., Zheng, H.W.: The effect of deformation on the contact area in grinding. *Ann. CIRP* **42**(1/1993), 409–412 (1993)
- [SAIN80] Saini, D.P., Brown, R.H.: Elastic deflections in grinding. *Ann. CIRP* **29**(1), 189–194 (1980)
- [SAIT11] Saint-Gobain Abrasives: *Recycle used diamond dressing rolls, company brochure*, May 2011. Url: <http://www.nortonindustrial.com/uploadedFiles/SGindnortonabrasives/Documents/DressingRollRecyclingFlyer-8088.pdf>. Last accessed 1 Dec 2012
- [SALJ53] Saljé, E.: *Grundlagen des Schleifvorganges*. Werkstatt und Betrieb **86**(4), 177–182 (1953)
- [SALJ84] Saljé, E., Mackensen, H.G.: Dressing of conventional and CBN grinding wheels with diamond form rollers. *Ann. CIRP* **33**(1), 205–209 (1984)
- [SALJ88] Saljé, E., Paulmann, R.: *Definition der Korn- und Schneidenzahlen beim Schleifen und Honen*, Jahrbuch Schleifen, Honen, Läppen, 55. Auflage, pp. 193–198 (1988)
- [SALJ91] Saljé, E.: *Begriffe der Schleif- und Konditioniertechnik*. Vulkan-Verlag, Essen (1991)
- [SALM07] Salmang, H., Scholze, H., Telle, R. (Hrsg.): *Keramik*, 7. Auflage, Springer, Berlin (1982). ISBN: 3-540-63273-5
- [SALM82] Salmang, H., Scholze, H.: *Keramik Teil 1: Allgemeine Grundlagen und wichtige Eigenschaften*, 6th edn. Springer, Berlin (1982). ISBN 3-540-10987-0
- [SAXL97] Saxler, W.: *Erkennung von Schleifbrand durch Schallemissionsanalyse*. Doctoral Thesis at RWTH Aachen University (1997)
- [SCHE73] Scheidemann, H.: *Einfluß der durch Abrichten mit zylindrischen und profilierten Diamantrollen erzeugten Schleifscheiben-Schneidfläche auf den Schleifvorgang*. Doctoral Thesis at TU Braunschweig (1973)

- [SCHH10] Schuh, G., Boos, W., Gaus, F., Ziskove, H.: New business models for tooling companies based on intelligent injection molds. In: Proceedings of the 17th CIRP International Conference on Life Cycle Engineering LCE 2010, Hefei, pp. 175–79, 19–21 May 2010
- [SCHI02] Schmid, H. G.: Lichtblick im Dschungel der Diamant-Sonderprodukte. *Diam. Bus.* 2 (2002)
- [SCHI10] Schilling, R.E.: Choose the right grinding mill. *Chemical Processing* (2010). www.chemicalprocessing.com
- [SCHL04] Schlattmeier, H.: Diskontinuierliches Zahnflankenprofilschleifen mit Korund. Doctoral Thesis at RWTH Aachen University (2004)
- [SCHM68] Schmitt, R.: Abrichten von Schleifscheiben mit diamantebestückten Rollen. Doctoral Thesis at TU Braunschweig (1968)
- [SCHT11] Schmidt Maschinentechnik: Produktinfo - hydraulische Einständerpressen HE. url:<http://www.schmidt-maschinentechnik.de/index6.html>. Accessed 02 Nov 2012
- [SCHÖ03] Schön, J., Buchmüller, K., Dahmen, N., Griesheimer, P., Schwab, P., Wilde, H.: EMSIC- Ein Pfiffiges Verfahren zur Entölung von Metall- und Glas-Schleifschlämmen; Wissenschaftliche Berichte FZKA 6799; Karlsruhe (2003)
- [SCHR71] Schreitmüller, H.: Kinematische Grundlagen für die praktische Anwendung des spitzenlosen Hochleistungsschleifens. Doctoral Thesis at RWTH Aachen University (1971)
- [SCHT81] Schuetz, W.: Schleifen und Schleifmittel. In: Ullmann's Enzyklopaedie der Technischen Chemie, vol. 20, pp. 449–455 (1981). Wiley-VCH Verlag GmbH
- [SCHU96] Schulz, A.: Das Abrichten von keramisch gebundenen CBN-Schleifscheiben mit Formrollen. Doctoral Thesis at RWTH Aachen University (1996)
- [SEAL70] Seal, M., Etched metal coated diamond grains in grinding wheels. Patent US 3,528,788, 15 Sept 1970
- [SEN02] Sen, P.K.: Synthetische Diamant-Abrichtrohlinge für den zukünftigen Industriebedarf. *Industrie Diamanten Rundschau* Ausgabe 2, 153–166 (2002)
- [SEN91] Sen, P. K.: Wheel dressing and natural diamond. *Ind. Diam. Rev.* Band 51, Heft 542, 32–38 (1991)
- [SETH11] Seth, A., Cai, Y., Saint Gobain Abrasives, Inc., Saint Gobain Abrasifs: Hydrophilic and hydrophobic silane surface modification of abrasive grains. Patent US 8,021,449 B2, 20 Sep 2011
- [SEXT82] Sexton, J.S.: Chatter vibrations and their suppression through wheel design. *Ind. Diam. Rev.* 3, 161–170 (1982)
- [SHAW96] Shaw, M.C.: Principles of Abrasive Processing. Clarendon Press, Oxford (1996)
- [SIGM12] Sigma-Aldrich: Material Safety Data Sheet. url:<http://www.sigmaaldrich.com>. Accessed 22 Oct 2012
- [SING12] Singh, R.K., Murty, H.R., Gupta, S.K., Dikshit, A.K.: An overview of sustainability assessment methodologies. *Ecol. Ind.* 15, 281–299 (2012)
- [SINL10] Singh, L., Khangura, S.S., Mishra, P.S.: Performance of abrasives used in magnetically assisted finishing: a state of the art review. *Int. J. Abrasive Technol.* 3(3), 215–227 (2010)
- [SIOU80] Sioui, R.H., Carver, E.B., Norton Company: Magnetic cores for diamond or cubic boron nitride grinding wheels. Patent US 4184854, 22 Jan 1980
- [SPUR89] Spur, G.: *Keramikbearbeitung: Schleifen, Honen, Läppen, Abtragen*, Carl Hanser Verlag München Wien. ISBN 3-446-15620 (1989)

- [STAB81] Stabenow, R.: Einfluss von Schleifscheibenspezifikationen auf das Schleifergebnis, Jahrbuch Schleifen, Honen, Läppen und Polieren, 50. Ausgabe, Hrsg. Saljé, E.; Rohde, G., Vulkan-Verlag, , pp. 237–248 (1981). ISBN 3-8027-2650-2
- [STAD62] Stade, G.: Technologie des Schleifens. Carl Hanser Verlag München (1962)
- [STEF83] Steffens, K.: Thermomechanik des Schleifens. Doctoral Thesis at the RWTH Aachen University (1983)
- [STET74] Stetiu, G., Lal, G.K.: Wear of grinding wheels. *Wear* **30**, 229–236 (1974)
- [STIA07] Stiassnie, E., Shpitalni, M.: Incorporating lifecycle considerations in axiomatic design. *Ann. CIRP* **56**(1/2007), 1–4 (2007)
- [STOC86] Stockwell, B.H.: Die Metallurgie der Metallwerkzeuge. *Industrie Diamanten Rundschau* **1**(86), 31–35 (1986)
- [STRA75] Strachan, P.F.: Bewertung und Analyse von Prüfverfahren für Diamant-Körnungswerkzeuge. *IDR* **9**(4), 204–211 (1975)
- [STUC88] Stuckenholtz, B.: Das Abrichten von CBN-Schleifscheiben mit kleinen Zustellungen. Doctoral Thesis at RWTH Aachen University (1988)
- [STUF96] Stuff, D.: Einsatzvorbereitung keramisch gebundener CBN-Schleifscheiben. Doctoral Thesis at RWTH Aachen University (1996)
- [SUH01] Suh, N.P.: *Axiomatic Design: Advances and Applications*. Oxford University Press, Oxford (2001). ISBN 0-19-513466-4
- [TAWA11] Tawakoli, T., Azarhoushang, B.: Theoretical and experimental investigation of intermittent grinding of SiC with a segmented grinding wheel. *Int. J. Abrasive Technol.* **4**(1), 90–99 (2011)
- [TAWA12] Tawakoli, T., Reinecke, H., Vesali, A.: An experimental study on the dynamic behavior of grinding wheels in high efficiency deep grinding. In: 5th CIRP Conference on High Performance Cutting 2012, *Procedia CIRP* **1**, pp. 382–387 (2012)
- [TELL00] Telling, R.H., Pickard, C.J., Payne, M.C., Field, J.E.: Theoretical strength and cleavage of diamond. *Phys. Rev. Lett* **84**(22), 5160–5163 (2000)
- [TODD94] Todd, R.H., Allen, D.K., Altng, L.: *Fundamental Principles of Manufacturing Processes*. Industrial Press Inc., New York (1994)
- [TOLA68] Tolansky, S.: *The Strategic Diamond*. Oliver and Boyd Ltd., Edinburgh (1968)
- [TOML76] Tomlinson, P.N.: Grundlagen des Schleifens von Hartmetall mit kunstharzgebundenen Diamantscheiben. *Industrie Diamanten Rundschau* **10** (4), 193–200 (1976)
- [TOML78a] Tomlinson, P.N.: Langform-Diamantkorn, das neue Konzept zum erfolgreichen Schleifen von Hartmetall. *Industrie Diamanten Rundschau* **12**(2), 72–79 (1978)
- [TOML78b] Tomlinson, P.N.: CDA-M, eine neue Diamantkörnung zum Trockenschleifen von Hartmetall. *Industrie Diamanten Rundschau* **12**(2), 80–87
- [TÖNS04] Tönshoff, H.K.: *Spanen - Grundlagen*. Springer, Berlin (2004). ISBN 3-540-00588-92004
- [TÖNS92] Tönshoff, H.K., Peters, J., Inasaki, I., Paul, T.: Modelling and simulation of grinding processes. *Ann. CIRP* **41**(2), 677–687 (1992)
- [TOPA10] Topas GmbH: *US-Sedimentometer USS 791*, company brochure (2010)
- [TYRO03] Tyrolit company brochure: *Wie entsteht ein Tyrolit Schleifwerkzeug*, Anhang 1, Anhang 2 (Z1), 2nd edn., Dec 2003

- [TYRO03b] Tyrolit company brochure: Grindology Boxes, Begleitheft zum Koffer “Allgemeine Grundlagen 1”, Accompanying notes to case “General Basics 1”, 2nd edn. (2003)
- [UAMA09] Unified Abrasives Manufacturers’ Association: Introduction to Abrasives, Abrasives Information. url:<http://www.uama.org/>. Last accessed 5 Sept 2012
- [UEDA09] Ueda, K., Takenaka, T., Vancza, J., Monostori, L.: Value creation and decision-making in sustainable society. *Ann. CIRP* **58**(2) (2009)
- [UHLM01a] Uhlmann, E., Brücher, M.: Untersuchungen zum Oxidationsverschleiß von diamantbasierten Schneidstoffen. *Industrie Diamanten Rundschau Ausgabe 2*, 127–133 (2001)
- [UHLM01b] Uhlmann, E., Friemel, J., Brücher, M.: Adhäsiver Verschleiß an CVD-Diamant. *Industrie Diamanten Rundschau Ausgabe 4*, 281–286 (2001)
- [UHLM10] Uhlmann, E., Sammler, C.: Ressourceneffizientes Schleifen - Loesungen und Grenzen, Moderne Schleiftechnologie und Feinstbearbeitung 2010, Vulkan-Verlag (2010). ISBN 978-3-8027-2957-7
- [UHLM97] Uhlmann, E.G., Stark, C.: Potentiale von Schleifwerkzeugen mit mikrokristalliner Aluminiumoxidkörnung. Beitrag 58. Jahrbuch “Schleifen, Honen, Läppen und Polieren”, pp. 281–309 (1997)
- [UMED12] Umeda, Y., Takata, S., Kimura, F., Tomiyama, T., Sutherland, J.W., Kara, S., Herrmann, C., Dufflou, J.R.: Toward integrated product and process life cycle planning—an environmental perspective. *Ann. CIRP* **61**(2), 681–702 (2012)
- [UMER12] Umer, M., Saptaji, K., Subbiah, S.: Study of pressure distribution in compliant coated abrasive tools for robotic polishing. In: Proceedings of the ASME 2012 International Manufacturing Science and Engineering Conference MSEC 2012, Notre Dame, Indiana, USA, 04–08 June 2012
- [UN07] United Nations Committee on Sustainable Development UN-CSD: Indicators of Sustainable Development: Guidelines and Methodologies, 3rd edn. The United Nations, New York (2007). url:<http://www.un.org/esa/sustdev/natlinfo/indicators/guidelines.pdf>
- [UN87] United Nations: Report of the World Commission on Environment and Development: Our Common Future, General Assembly Resolution 42/187, 11 Dec 1987. url:<http://www.un-documents.net/our-common-future.pdf>. Accessed 7 July 2012
- [UNIT09a] United Abrasives Inc.: Material Safety Data Sheet Coated Abrasives. Prepared By IH&SC Inc., Shelton, CT 06484, revised 1 Dec 2009
- [UNIT09b] United Abrasives Inc.: Material Safety Data Sheet Diamond Wheels. Prepared By IH&SC Inc., Shelton, CT 06484, revised 30 Nov 2009
- [UNIT12a] United Abrasives Inc.: Material Safety Data Sheet Resinoid Bonded Abrasives. Prepared By IH&SC Inc., Shelton, CT 06484, revised 24 Aug 2012
- [UNIT12b] United Abrasives Inc.: Material Safety Data Sheet Vitrified Bonded Abrasives. Prepared By IH&SC Inc., Shelton, CT 06484, revised 23 May 2012
- [UPAD09] Upadhyay, R.D., Ramanath, S., Corcoran R.F., Jr., Puthanangady, T., Hall, R.W.J., Harley, L.L., Saint-Gobain Abrasifs: Multifunction abrasive tool with hybrid bond. Patent WO2009075775 (A1), 18 June 2009
- [USGS12a] USGS, Minerals information: Abrasives (manufactured). url:<http://minerals.usgs.gov/minerals/pubs/commodity/abrasives/mcs-2012-abras.pdf>. Last accessed 30 Aug 2012

- [USGS12b] USGS, Minerals information: Diamond (industrial). url:<http://minerals.usgs.gov/minerals/pubs/commodity/diamond/myb1-2010-diamo.pdf>. Last accessed 30 Aug 2012
- [VANP39] Van der Pyl, E., Norton Company: Grinding wheel. Patent US 2150886, 14 Mar 1939
- [VDI04] VDI-Richtlinien, draft of norm VDI 3392 Blatt 1 “Abrichten von Schleifkörpern - Profilieren und Schärfen”, Apr 2004
- [VDI05] VDI-Richtlinien, VDI 2884 Verein Deutscher Ingenieure (VDI), Purchase, Operating and Maintenance of Production Equipment using Life Cycle Costing (2005)
- [VOLK72] Volkmann, C.-U.: Untersuchung der Einspannkraefte an Schleifscheibenaufnahmen. Doctoral Thesis at the TU Hannover (1972)
- [VOLL03a] Vollstädt, H., Hess, K.-U., List, E.: Single particle characterization of abrasives and superabrasives. In: Intertech Conference (2003)
- [VOLL03b] Vollstädt, H., List, E.: Controlling the stability of the properties of superabrasive powders. In: 4th Zhengzhou International Superhard Materials and Related Products Conference (2003)
- [VOLL10] Vollstädt-Diamant GmbH: Operating instruction Shape Sorter, Type 3, company brochure, 1 Jan 2010
- [VOLL11a] Vollstädt-Diamant GmbH: Operating Instruction DiaSusz, Magnetic Susceptibility System for synthetic diamonds, company brochure (2011)
- [VOLL11b] Vollstädt-Diamant GmbH: Operating instruction Magnetic Sorter 3.01, company brochure (2011)
- [VOLL12] Vollstädt-Diamant GmbH: Friability Tester Type ST1/ST4, company brochure. url:http://www.vdiamant.de/Download/data%20sheet_FriaTester_ST1_ST4.pdf. Accessed on 26 Sept 2012
- [VÖLL80] Völler, R.: Abnutzung von Abrichtwerkzeugen, Technische Mitteilungen, 73. Jahrgang, Heft 8, pp. 656–663 (1980)
- [VUCE08] Vucetic, D.: Zerspan- und Verschleißmechanismen beim Verzahnungshonen. Doctoral Thesis at RWTH Aachen Unviersity (2008)
- [WAB09] WAB-Willy A. Bachofen AG - Maschinenfabrik: Turbula_Datenblatt_DE, 2009. url:http://www.wab.ch/fileadmin/redaktion/downloads/Datenblatt_DE_Turbula_Datenblatt.pdf. Accessed 02 Oct 2012
- [WALT12] Walther Trowal: Trowal Mass Finishing-Chips and Compounds, company brochure (2012)
- [WANG12] Wang, X.W., Guo, P.Q., Zhao, H.D., Cao, Y.K.: Review of quick-point grinding technology. Key Eng. Mater. **499**, 295–300 (2012)
- [WARN88] Warnecke, G., Grün, F.J., Geis-Drescher, W.: Anwendung von PKD-Schneidplatten in Abrichtrollen. Industrie Diamanten Rundschau Ausgabe **I**, 25–31 (1988)
- [WASH12] Washington Mills: Company brochure, Washington Mills Recycling Services. url:<http://www.washingtonmills.com/documents/literature/>. Last accessed 4 Sept 2012
- [WASH12b] Washington Mills: Technical Data Sheets. url:<http://www.washington-mills.com/documents/technical-datasheets/>. Last accessed 4 Sept 2012
- [WEBS04] Webster, J., Tricard, M.: Innovations in abrasive products for precision grinding. Keynote paper. Ann. CIRP **53**(2), 597–642 (2004)
- [WECK05] Weck, M.; Brecher, C.: Werkzeugmaschinen 1-Maschinenarten und Anwendungsbereiche. Springer, Berlin (2005). ISBN 9-783-540-225-041
- [WEDL77] Wedlake, R.J.: Diamond synthesis. Ind. Diam. Rev. 196, Ausgabe Juni 1977

- [WEGE11] Wegener, K., Hoffmeister, H.-W., Karpuschewski, B., Kuster, F., Hahmann, W.-C., Rabiey, M.: Conditioning and monitoring of grinding wheels. *Ann. CIRP* **60**(2), 757–777 (2011). doi:10.1016/j.cirp.2011.05.003
- [WEID06] Weidema, B.P.: The integration of economic and social aspects in life cycle impact assessment. *Int. J. Life Cycle Assess.* **11**(Special Issue 1), 89–96 (2006)
- [WEIN76] Weinert, K.: Die zeitliche Änderung des Schleifscheibenzustandes beim Außenrund-Einsteichschleifen. Doctoral Thesis at TU Braunschweig (1976)
- [WEIS08] Weiss, C., Ade, E.: Zweite Generation der Kobaltalternativmaterialien im Markt. *Industrie Diamanten Rundschau*, II, pp. 14–16 (2008)
- [WENT60] Wentorf, R.H., General Electric: Abrasive Material and Preparation Thereof. Patent US 2,947,617, 2 Aug. 1960
- [WENT61] Wentorf, R.H.: Synthesis of the cubic form of boron nitride. *J. Chem. Phys.* **34**(3), 809 ff. (1961)
- [WERN71] Werner, G.: Kinematik und Mechanik des Schleifprozesses. Doctoral Thesis at RWTH Aachen University (1971)
- [WERN73] Werner, G.: Konzept und Technologische Grundlagen zur adaptiven Prozessoptimierung des Aussenrundscheifens, Habilitation at RWTH Aachen University (1973)
- [WHIT72] Whitaker, Noble D.: A method for making thermosetting resinous abrasive tools. Patent US 3661544, 9/5/1972
- [WILK62] Wilks, E.M.: The hardness of diamond. In: *Proceedings of the first international congress on diamonds in industry*, Paris, pp. 283–289 (1962)
- [WILK91] Wilks, J., Wilks, E.: *Properties and Applications of Diamond*. Butterworth-Heinemann Ltd, Oxford (1991)
- [WILL11] Willcock, N.: Managing hand-arm vibration in abrasive processes, *Abrasiveshub*, Feb 2011
- [WIMM95] Wimmer, J.: Konditionieren hochharter Schleifscheiben zum Schleifen von Hochleistungskeramik. Doctoral Thesis at TU Kaiserslautern (1995)
- [WINE12] Winterthur, Company brochure, Handbook Creepfeed. url:http://www.winterthursa.com/osMedia/doc/handbookcreepfeed_1310.pdf. Last accesses: 4 Sept 2012
- [WINE12] Holz, R., Sauren, J.: Schleifen mit Diamant und CBN. In: Ernst Winter & Sohn GmbH & Co (eds.), 2nd edn., *Brendes & Langhans GmbH*, Norderstedt, Aug 1988
- [WITT07] Wittmann, M.: Bedarfsgerechte Kühlschmierung beim Schleifen. Doctoral Thesis at University of Bremen (2007)
- [WOYD87] Woydt, M.: Technisch-physikalische Grundlagen zum tribologischen Verhalten keramischer Werkstoffe, Bundesanstalt für Materialforschung und -prüfung, 133 (1987). ISBN 3-88314-609-9
- [XU07] Xu, H., Kahraman, A., Anderson, N.E., Maddock, D.G.: Prediction of mechanical efficiency of parallel-axis gear pairs. *J. Mech. Des.* **129**, 58–68 (2007)
- [YAMA12] Yamaguchi, H., Srivastava, A.K., Tan, M.A., Riveros, R.E., Hashimoto, F.: Magnetic abrasive finishing of cutting tools for machining of titanium alloys. *Ann. CIRP* **61**(1), 311–314 (2012)
- [YAN12] Yan, B.-H., Lee, S.-M., Hung, J.-C., National Central University, TW: Bamboo charcoal composite abrasive material and method of fabricating the same. Patent US 8,236,075, 07 Aug 2012
- [YARN69] Yarnitsky, Y., Dolev, D.: Porosity - the third phase in grinding wheels. *IDR* **29**(347), 414 f. (1969)

- [YEGE86] Yegenoglu, K.: Berechnung von Topographiekenngößen zur Auslegung von CBN-Schleifprozessen. Doctoral Thesis at RWTH Aachen University (1986)
- [YIN00] Yin, L.W., Zou, Z.D., Li, M.S., Liu, Y.X., Cui, J.J., Hao, Z.Y.: Characteristics of some inclusions contained in synthetic diamond single crystals. *Mater. Sci. Eng.* **293**(1–2), 107–111 (2000)
- [YOUN66] Young, B.: The graphitisation of diamond during the manufacture of diamond tools. *Ind. Diam. Rev.* **26**(312), 483–488 (1966)
- [YU11] Yu, A.B., Wu, L., Gao, B.Y.: Recovery of electroplated diamond tool with thermal shock method. *Key Eng. Mater.* **487**, 215–219 (2011)
- [YUAH10] Yuan, H., Gao, H., Liang, Y.D.: Fabrication of a new-type electroplated wheel with controlled abrasive cluster and its application in dry grinding of CFRP. *Int. J. Abrasive Technol.* **3**(4), 299–315 (2010)
- [YUAN09] Yuan, C., Dornfeld, D.: Human health impact characterization of toxic chemicals for sustainable design and manufacturing. In: Proceedings of IEEE International Symposium on Sustainable Systems and Technology, Phoenix, Arizona, 18–20 May 2009. Retrieved from: <http://www.escholarship.org/uc/item/4dp8x0k3>
- [YUAN12] Yuan, C., Zhai, Q., Dornfeld, D.: A three dimensional system approach for environmentally sustainable manufacturing. *Ann. CIRP* **61**(1), 39–42 (2012)
- [YUAN12] Yuan, Z.J., Yao, Y.X., Zhou, M., Bai, Q.S.: Lapping of single crystal diamond tools. *Ann. CIRP* **52**(1), 285–288 (2003)
- [ZEIN11] Zein, A., Li, W., Herrmann, C., Kara, S.: Energy efficiency measures for the design and operation of machine tools: an axiomatic approach. In: Proceedings of the 18th CIRP Conference on Life Cycle Engineering, Technische Universität Braunschweig, Braunschweig, Germany, pp. 274–279, 2nd–4th May 2011
- [ZEIN11b] Zein, A., Oehlschlaeger, G., Herrmann, C.: Polymer water as optimal cutting fluid - an analysis of environmental advantages. In: Proceedings of the 44th CIRP International Conference on Manufacturing Systems, Madison, WI, USA, 1–3 June 2011
- [ZEPP05] Zeppenfeld, C.: Schnellhubschleifen von γ -Titanaluminiden. Doctoral Thesis at RWTH Aachen University (2005)
- [ZHAG11] Zhang, J.Q., Guan, P., Su, C., Yu, T.B., Wang, W.S.: Simulation of grinding wheel with random three-dimensional abrasive and microporous bond. *Key Eng. Mater.* **487**, 209–214 (2011)
- [ZHAN03] Zhang, C., Shin, Y.C.: Wear of diamond dresser in laser assisted truing and dressing of vitrified CBN wheels. *Int. J. Mach. Tools Manuf.* **43**(1), 41–49 (2003)
- [ZHAT07] Zhang, T.W., Dornfeld, D.: Energy use per worker-hour: evaluating the contribution of labor to manufacturing energy use. In: Advances in Life Cycle Engineering for Sustainable Manufacturing Businesses, Proceedings of the 14th CIRP Conference on Life Cycle Engineering, Waseda University, Tokyo, Japan, pp. 189–193, 11th–13th June 2007
- [ZHEN10] Zheng, L., Fletcher, T., Na, T.K., Sventek, B., Romero, V., Lugg, P.S., Kim, D.: Finishing of display glass for mobile electronics using 3M™ Trizact™ diamond tile abrasive pads. *Proc. SPIE* **7655**, 76550L (2010). doi:[10.1117/12.865606](https://doi.org/10.1117/12.865606)